

# **Cytological profiling of natural product scaffolds libraries for Parkinson's disease**

**Minh Tam Tran Thi**

*B.Sc.*

School of Sciences

Science, Environment, Engineering and Technology

Griffith University

Submitted in fulfillment of the requirements of the degree of

Master of Philosophy

October 2015

## **Abstract**

Parkinson's disease (PD) is a highly debilitating age-related neurodegenerative disorder arising from the prominent loss of dopaminergic nigro-striatal tracts. It affects approximately 2% of the population over 65 years of age. The majority of cases of PD arise from complex interactions between a myriad of risk-associated genes and environmental risk factors. Due to the intricate combination of multiple factors, efforts towards designing therapies for PD have demonstrated limited efficacy. Current drugs mainly relieve symptoms rather than retarding or modifying disease progression. Natural products (NPs) have served as an invaluable source of new drugs for over 25 years. It stands to reason therefore that these bioactive small molecules may themselves become promising therapeutic agents for PD.

Cytological profiling has emerged as a powerful tool to rapidly identify the effects of thousands of small molecules on the biological properties of the cells. This platform employs an automated microscopy system from which images of cells in multi well plate format are obtained. Subsequently the resulting images are segmented and a number of cytological features are quantified based on the amount and location of fluorescence within cells. Together with effective downstream data processing, image-based screening technologies play crucial roles in drug lead discovery and optimization. Notably, among 75 first-in-class small molecule drugs approved by US Food and Drug Administration between 1999 and 2008, 28 were discovered by phenotypic screening.

In this thesis, two different libraries were screened using cytological profiling against a patient-derived PD cellular model, namely human olfactory neuroepithelium derived (hONS) cells which display functional and genetic discrepancies in a disease-specific

manner. The first library was constructed based on different natural product scaffolds that have been previously explored, albeit the activity against PD patient cells has not been previously reported. The second library contains a series of novel compounds designed around naturally occurring 1-azaadamantane scaffold, which is the core structure of pharmacologically important synthetic compounds, especially for central nervous system diseases. Instead of focusing on a particular phenotype, our strategy employed multiple cellular markers targeting several cellular components implicated in PD including mitochondria, lysosomes, endosomes, and autophagosomes. The current cytological profiling approach effectively identified compounds with biological activities in PD cells. In the first library, one hit compound was associated with tubulin depolymerization and enhancement of lysosome activity. In the second screening, three hit compounds displayed significant effects on nuclear and cellular morphology as well as intensity of tubulin, mitochondria, LC3b and lysosome. Examination of bioclusters of screened compounds of both libraries revealed groups of structurally related compounds. This result along with analysis of structure activity relationships showed that chemical similarity led to similar biological activity. However, some compounds with similar structures surprisingly exhibited different biological effects on several cytological features. It indicated that minor differences of chemical structures can render dramatic changes in activity. Overall, the current work demonstrated the potential of cytological profiling as useful tool for early stage of drug discovery.

## Statement of Originality

*This work has not previously been submitted for a degree or diploma in any university.*

*To the best of my knowledge and belief, the thesis contains no material previously published or written by another person except where due reference is made in the thesis itself.*

---

Minh Tam Tran Thi

30/10/2015

---

Date



## **Acknowledgement**

First and foremost, I would like to thank Professor Ronald Quinn who gave me guidance and all supports that I could wish for to complete this project.

I would like to say a heartfelt thank you to Associate Professor Stephen Wood who gave me opportunities to follow my dream and always made his constant help available from the first day I was in Australia.

I want to express my deeply-felt words to Dominique Gorse who was willing to spend hours with me and taught me about data analysis. He also had to deal with my “dumb” questions and enthusiastically found the simplest way to help me to understand. Not all data analysis that applied in my research project could have been possible without his help.

I also want to thank Marie for her help in number of ways of experiment operation.

It is a pleasure to thank members of Eskitis Institute, Ron group and Wood group. Special thanks to all of my friends: Johana, Devarthri, Megha and Mariyam who share with me sad days, happy moments and crazy times. Also I want to thank you...all of you...my friends for your concern, encouragement and valuable help.

## Table of content

<b>Abstract .....</b>	<b>i</b>
<b>Acknowledgement .....</b>	<b>iv</b>
<b>Table of content .....</b>	<b>v</b>
<b>List of Figures and Tables .....</b>	<b>viii</b>
<b>Abbreviations.....</b>	<b>xi</b>
<b>1. INTRODUCTION.....</b>	<b>2</b>
1.1 Natural Products .....	2
1.1.1 Plant-derived Natural Products .....	3
1.1.2 Marine Natural Products .....	5
1.2 Roles of Microorganisms in Drug Discovery .....	7
1.3 The importance of scaffolds embedded into Natural Products .....	11
1.4 Parkinson's disease .....	15
1.4.1 Epidemiology of Parkinson's disease .....	17
1.4.2 Clinical signs and symptoms.....	17
1.4.3 Etiologic factors and molecular pathogenesis .....	25
1.4.4 Environment and PD .....	28
1.4.5 Treatment .....	30
1.4.6 Models of PD .....	36
1.4.7 Therapeutic Perspectives of Natural Products in Parkinson's disease.....	37
1.5 The importance of High Throughput Screening and Statistical analysis in Drug Discovery .....	41
1.5.1 High throughput screening (HTS).....	41
1.6 The importance of statistics in drug discovery .....	46
1.7 Research Objective .....	51
<b>2. MATERIALS AND METHODS .....</b>	<b>54</b>
2.1 Experimental design – Overview .....	54
2.2 Description of hONS cells and their Culture .....	55
2.3 Cytological profiling of natural products on PD patient derived cell line .....	57

2.3.1 Selection of cytological markers .....	57
2.3.2 Preparation of stock solutions .....	59
2.3.3 Compound transfer .....	60
2.3.4 Cell based assay .....	63
2.3.5 Descriptions of cytological features .....	68
2.3.6. Imaging and image evaluation .....	72
<b>3. CYTOLOGICAL PROFILING OF SYNTHETIC COMPOUNDS</b>	
<b>ON PARKINSON'S DISEASE CELLS .....</b>	<b>78</b>
3.1 Introduction.....	78
3.2 Materials and methods .....	79
3.2.1 Compound library .....	79
3.2.2 Compound transfer.....	79
3.2.3 Cell based assay .....	80
3.2.4. Imaging and image evaluation .....	80
3.2.5 Data analysis .....	81
3.3. Results.....	89
3.3.1 Intra-plate Variation .....	89
3.3.2 Chemical Library.....	89
3.3.3 Cytological Profiling Screen .....	90
3.3.4 Examination of the structure activity relationships (SARs).....	119
3.3.5 Examples of structure activity relationships in the first library .....	125
3.3.6 Cytological features of most active "hits" .....	130
3.4 Discussion .....	134
<b>4. OPTIMIZATION OF DATA ANALYSIS METHOD .....</b>	<b>139</b>
4.1 Introduction.....	139
4.2 Optimization of data analysis method .....	139
4.3 Conclusion .....	145
<b>5. CYTOLOGICAL PROFILING OF NATURAL PRODUCTS</b>	
<b>SCAFFOLDS INSPIRED SYNTHETIC COMPOUNDS FOR</b>	
<b>PARKINSON'S DISEASE. ....</b>	<b>147</b>
5.1 Introduction.....	147

5.2 Materials and methods .....	148
5.2.1 Compound purity.....	148
5.2.2 Compound library .....	148
5.2.3 Compound transfer.....	149
5.2.4 Cell based assay .....	150
5.2.5 Imaging and image evaluation. ....	150
5.2.6 Data analysis .....	150
5.3 Results.....	153
5.3.1 Compound library .....	153
5.3.2 Assessment of intra-plate variability and assay reproducibility.....	154
5.3.3 Hierarchical clustering .....	155
5.3.4 Chemical structures of screened compounds .....	160
5.3.5 Exploration of structure and activity relationships (SARs) .....	183
5.3.6 Examples of structure activity relationships in the second library.....	186
5.3.7 Hit identification .....	192
5.4 Discussion .....	196
<b>6. GENERAL DISCUSSION .....</b>	<b>200</b>
<b>7. REFERENCES .....</b>	<b>204</b>

## List of Figures and Tables

### Chapter 1

<b>Figure 1.1</b> Chemical structures of selected plant derived natural products .....	4
<b>Figure 1.2</b> Drugs derived from marine natural products for treatment of cancer.....	7
<b>Figure 1.3</b> Representative examples of natural products based antimicrobial drugs .....	9
<b>Figure 1.4</b> Pathology of Parkinson's disease.....	16
<b>Figure 1.5</b> Motor symptoms of Parkinson's disease.....	20
<b>Figure 1.6</b> An overview of workflows for drug discovery .....	43

### Chapter 2

<b>Figure 2.1</b> General flow of Cytological profiling of small molecules.....	55
<b>Figure 2.2</b> The PD patient derived olfactory neuroepithelium (ONS) cell line C1200080013 at approximately 70% confluence.....	57
<b>Figure 2.3</b> Cytological markers for cytological profiling .....	58
<b>Figure 2.4</b> Examples of positive controls and negative control wells .....	62
<b>Figure 2.5</b> Images of stain set 1 .....	64
<b>Figure 2.6</b> Images of stain set 2 .....	66
<b>Figure 2.7</b> Size and morphology of nuclei and cells .....	71
<b>Figure 2.8</b> General view of image analysis by Harmony 5.0 .....	75
<b>Figure 2.9</b> Overview of cytological approach used in this study .....	76
<b>Table 2.1</b> Reagents for cell culture .....	56
<b>Table 2.2</b> Reagents for cell based assay.....	67
<b>Table 2.3</b> List of investigated cytological features .....	70
<b>Table 2.4</b> General image analysis sequence by Harmony 5.0 .....	74

## Chapter 3

<b>Figure 3.1</b> Plate format for compounds on 384 well plate layout .....	80
<b>Figure 3.2</b> The flow from raw data to reported results in cytological profiling .....	82
<b>Figure 3.3</b> Distribution of Lysosome marker intensity mean parameter .....	84
<b>Figure 3.4</b> Box plot displaying distribution of Lysosome marker texture across plates .....	88
<b>Figure 3.5</b> Hierarchical clustering of cytological profiles using Pearson correlation .....	91
<b>Figure 3.6</b> Example of a compound cytological profile .....	92
<b>Figure 3.7</b> Identification of compounds inducing Weak phenotypes .....	94
<b>Figure 3.8</b> Heat map of 127 compound dose instances .....	96
<b>Figure 3.9</b> Heat map of biocluster 1 .....	98
<b>Figure 3.10</b> Heat map of biocluster 2 .....	99
<b>Figure 3.11</b> Heat map of biocluster 3 .....	100
<b>Figure 3.12</b> Heat map of biocluster 4 .....	101
<b>Figure 3.13</b> Heat map of biocluster 5 .....	102
<b>Figure 3.14</b> Heat map of unclustered compound dose instances.....	103
<b>Figure 3.15</b> Biological profiles and chemical structures of investigated sub-bioclusters .....	121
<b>Figure 3.16</b> Examples of structure activity relationships in the first library .....	128
<b>Figure 3.17</b> Phenotypic changes in PD hONS cells induced by compound 33_1 .....	131
<b>Figure 3.18</b> Cytological features of compound 33_1 at 1 $\mu$ M .....	133
<b>Table 3.1</b> List of parameters required log <sub>2</sub> transformation .....	85
<b>Table 3.2</b> Scaffold information of individual compound dose instances .....	103

## Chapter 4

<b>Figure 4.1</b> Established downstream data processing .....	140
<b>Figure 4.2</b> Correlation matrix using squared Pearson correlation coefficient .....	142
<b>Figure 4.3</b> Volcano plot of nucleus texture .....	144
<b>Table 4.1</b> List of retained cytological features.....	143

## Chapter 5

<b>Figure 5.1</b> Examination of compound purity.....	149
<b>Figure 5.2</b> Plating format for compounds on 384 well plate layout .....	150
<b>Figure 5.3</b> Overview of downstream data processing .....	151
<b>Figure 5.4</b> A scatter plot displays the cytological features scores .....	155
<b>Figure 5.5</b> Heat map of 153 compound dose instances .....	156
<b>Figure 5.6</b> Heat map of biocluster 1 .....	157
<b>Figure 5.7</b> Heat map of biocluster 2 .....	158
<b>Figure 5.8</b> Heat map of biocluster 3 .....	159
<b>Figure 5.9</b> Heat map of biocluster 4 .....	160
<b>Figure 5.10</b> Clustering of chemical structures .....	184
<b>Figure 5.11</b> Exploration of general structure activity relationship in principal component analysis (PCA) .....	185
<b>Figure 5.12</b> Examples of structure activity relationships in the second library.....	191
<b>Figure 5.13</b> A scatter plot for hit identification .....	193
<b>Figure 5.14</b> Biological profiles of three hit compounds .....	195
<b>Table 5.1</b> Structures of natural products and natural product scaffold inspired synthetic compounds.....	160

## Abbreviations

6-OHDA	6-hydroxydomapine
CP	Cytological profiling
CV	Coefficient of variation
DAPI	4',6-diamidino-2-phenylindole
DA	Dopamine
DMEM/F12	Dulbecco's Modified Eagle Medium/ Ham F-12
DMSO	Dimethyl sulfoxide
FBS	Fetal bovine serum
FDA	US Food and Drug Administration
HCS	High content screening
hONS	Human olfactory neuroepithelium cells
HTS	High throughput screening
L-DOPA	L-dihydroxyphenylalanine, levodopa
LB	Lewy body
LC-MS	Liquid chromatography-mass spectrometry
LN	Lewy neuritis
LRRK2	Leucine-rich repeat kinase 2
MAO-B	Monoamine oxidase B
MPP+	1-methyl-4-phenylpyridinium
MPTP	1-methyl-4phenyl-1,2,3,6-tetrahydropyridine
NP	Natural product
PBS	Phosphate buffered saline
PCA	Principal component analysis
PD	Parkinson's disease



PFA	Paraformaldehyde
PINK1	PTEN induced putative kinase 1
SARs	Structure activity relationships
SCNA	Synuclein, alpha
SNpc	Substantia nigra pars compacta

**CHAPTER 1**  
**INTRODUCTION**

# 1. INTRODUCTION

## 1.1 Natural Products

Natural products (NPs) are defined as any biological molecules derived from various natural sources such as plants, microbes and animals. Natural products can constitute an entire organism (e.g. a microorganism, plant or animal), or a part thereof, (e.g. flowers, leaves or isolated animal organ) or an organismal extract (e.g. alkaloid, coumarins, flavonoid, etc.). The vast majority of these molecules may not play any particular role in the growth and development of the organisms and but act as toxins, pheromones, attractants and repellents in ecological interactions with other organisms. Such small molecules (molecular weight < 500 Da) are traditionally referred to as secondary metabolites. Primary metabolites, which include proteins, nucleic acids, amino acids, polysaccharides, etc. on the other hand, participate directly in metabolism that is a fundamental process of life.

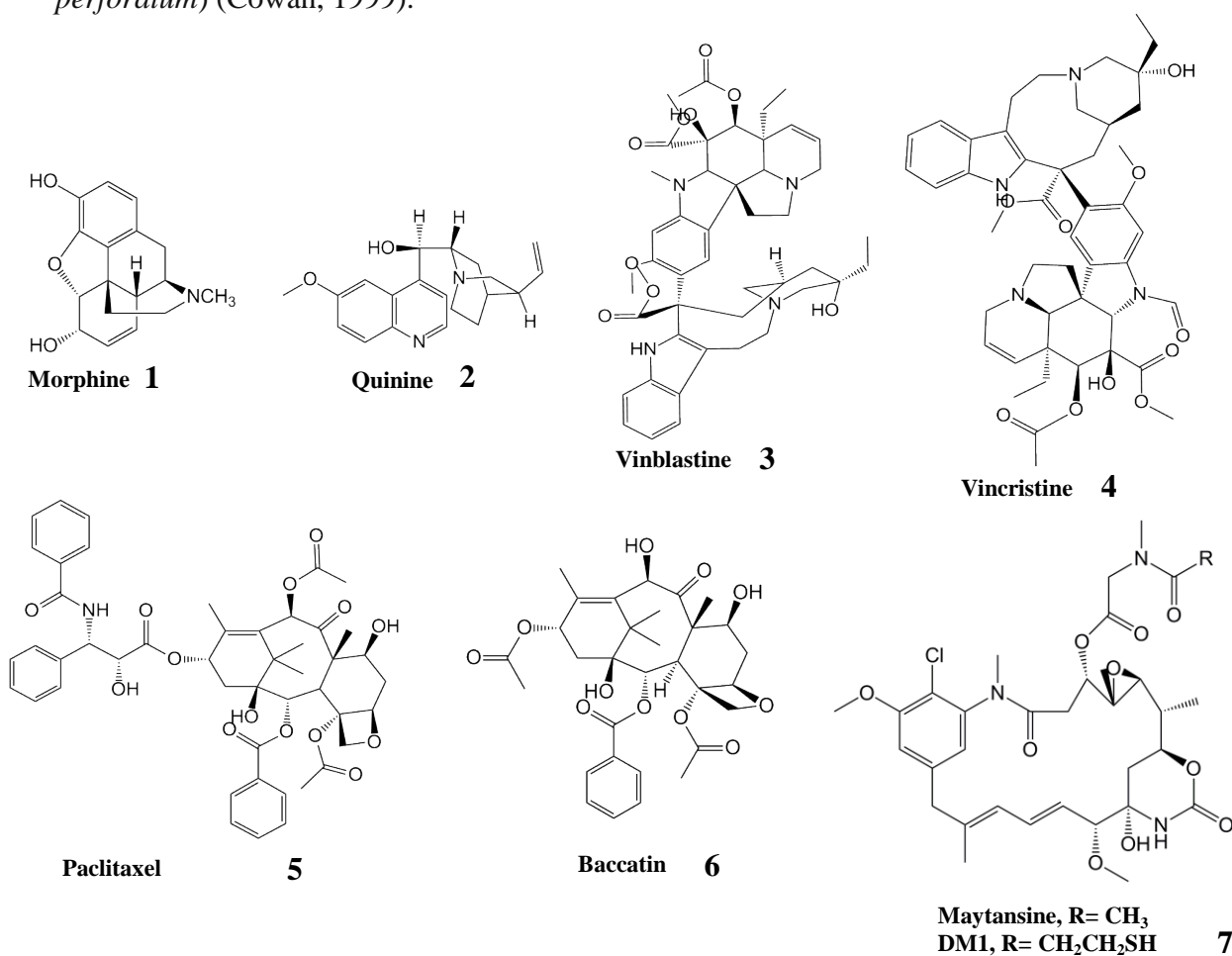
Nature stands for an inexhaustible source of novel chemotypes and pharmacophores, and has served as an invaluable source of medicinal agents for millennia. Indeed, natural products have played a vital role in the empirical treatment of illness in many advanced civilizations. Many hand-written accounts of ancient civilizations, e.g. Chinese, Indians, North Africans, detail the use of natural products, especially plants, in disease treatments. The oldest known medical record was written in clay tablets from ancient Mesopotamia, *circa* 2600 BC. It describes 1000 plants and over 700 plant-based substances, such as oils of *Cupressus sempervirens* (*Cypress*) and the resin of *Commiphora myrrha* (*myrrh*), which remain in use today as cough, cold and inflammation remedies (Cragg and Newman, 2013). Natural product-based medicines

were not only used in Occidental countries but, also flourished in the Orient, as evidenced by the practice of Indian Ayurveda (contains 341 plant derived drugs) and the primitive Chinese book, “Prescription for Fifty Two Diseases” (lists 247 natural agents) (Dias et al., 2012).

### **1.1.1 Plant-derived Natural Products**

Historically, plants have provided a source of inspiration for novel drug compounds, and plant-derived medicines have made large contributions to human health and well-being. Initially dispensed in the form of crude drugs including tinctures, teas, powders, and other mixed herbal formulations, plant-based medical knowledge has been passed down from generation to generation in various parts of the world (Samuelsson, 2004, Balunas and Kinghorn, 2005, Mazumder et al., 2013). Despite the long-term use of these substances, their desired therapeutic effects remained unclear until the eighteenth and nineteenth centuries. Plant-derived NPs have substantially contributed to novel therapeutics. In 1805, with the aid of modern analytical and structural chemistry, morphine (**1**) (**Figure 1.1**), was successfully isolated from *Papaver somniferum* L. (*opium poppy*) (Newman et al., 2000). Extracted from the bark of *Cinchona succirubra* Pav. ex Klotzsch by the French pharmacists, Caventou and Pelletier in 1820, the anti-malaria drug, quinine (**2**), has long been used for the cure of malaria, fever and cancer (Cragg and Newman, 2013). Known as a painkiller, preparations of the *Willow* tree have been used in traditional medicine. The successful isolation of salicin from the bark of the willow tree (*Salix alba*) as the active component followed by acetylation produced the semisynthetic product “Aspirin” commercialized by Bayer in 1899 for the treatment of arthritis and pain (B.Singh, 2012). Other significant drugs developed from traditional medicinal plants include: the antihypertensive agent, reserpine, isolated from

*Rauwolfia serpentina* which was used in Ayurvedic medicine for the treatment of snakebite and other ailments (Kapoor, 1990, Potterat and Hamburger, 2008); ephedrine, from *Ephedra sinica* (Ma Huang), a plant used in traditional Chinese medicine, and the basis for the synthesis of the anti-asthma agents (beta agonists), salbutamol and salmetrol; the muscle relaxant, tubocurarine, isolated from *Chondrodendron* and *Curarea* species used by indigenous groups in the Amazon as the basis for the arrow poison, curare (Buss, 1995); and promising results against HIV from the extracts of many plants including turmeric (*Curcuma longa*) and St. John's wort (*Hypericum perforatum*) (Cowan, 1999).



**Figure 1.1** Chemical structures of selected plant derived natural products

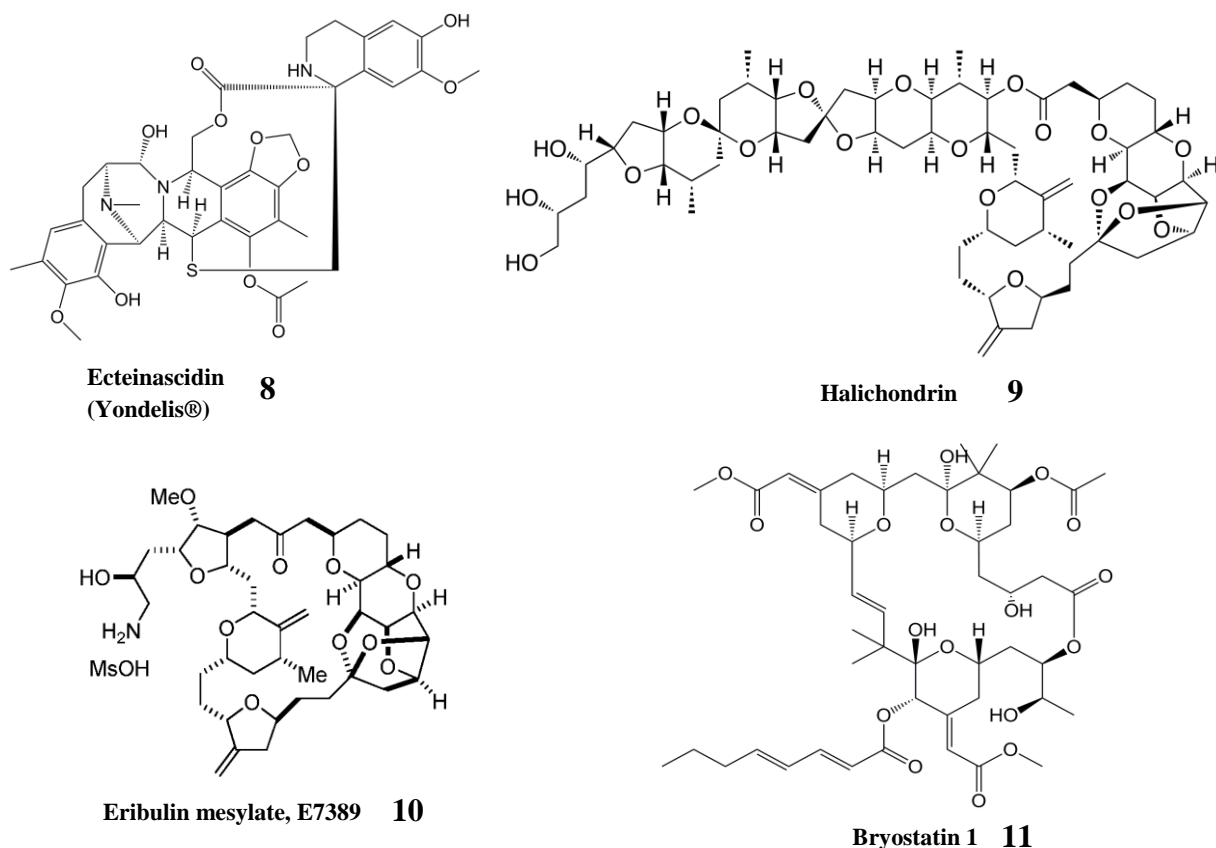
Plants have a long history in the treatment of cancer (Hartwell, 1982). However cancer, as a specific disease entity, was not well-defined in term of traditional medicine, and therefore, the efficacy of such treatments needs to be rigorously investigated (Cragg et al., 1994). Of the plant-derived anticancer drugs in clinical use, the best known are the so-called vinca alkaloids, vinblastine (**3**) and vincristine (**4**). Isolated from the Madagascar periwinkle, *Catharanthus roseus*; etoposide and teniposide which are semisynthetic derivatives of the NP epipodophyllotoxin; paclitaxel (Taxol®) (**5**), which occurs along with several key precursors (the baccatins) (**6**) in the leaves of various *Taxus* species, and the semisynthetic analogue, docetaxel (Taxotere®) (**Figure 1.1**) (Cragg and Newman, 2013).

Despite the recent interest in molecular modelling, combinatorial chemistry, and other synthetic chemistry techniques by pharmaceutical companies, natural products, and particularly medicinal plants, remain an important source of new drugs and drug leads (Butler, 2004). Recently, one of the first plant-derived tubulin interactive compounds has shown promising early clinical results. Maytansine isolated in the early 1970s from the Ethiopian tree *Maytenus serrata*, was effectively granted a new lease of life as antibody-conjugated maytansine derivatives (**7**) (**Figure 1.1**). Ado-trastuzumab emtansine (T-DM1), for instance, the first antibody-directed chemotherapy accepted for solid malignancy, was granted US Food and Drug Administration (FDA) approval in 2013 (Peddi and Hurvitz, 2014).

### 1.1.2 Marine Natural Products

In contrast to plant-based treatments, marine organisms do not have significant history of use in traditional medicine. Despite the fact that the world's oceans cover 70% of the

earth surface, representing enormous resource of bioactive agents, the collection of marine organisms was unattainable until the mid-1970s due to the lack of reliable diving techniques (Dias et al., 2012). The rapidly increasing pace of these investigations over recent decades has established that marine secondary metabolites display unusual structural features, potent biologic activity, many of which cannot be found in terrestrial natural products. Invertebrates, mainly sponges, tunicates, bryozoans or molluscs provide the majority of marine natural products involved in clinical or preclinical trials (D. Alonso, 2003). The first marine-derived product to gain approval as a drug (in 2004) was Ziconotide, a non-narcotic analgesic, that is currently marketed as Prialt® (Wallace, 2006). This compound serves as venom of the tropical cone snail genus *Conus* to stun its prey prior to capture (Bulaj et al., 2003). According to the US National Cancer Institute's preclinical cytotoxicity screening, approximately 1% of the tested marine samples showed anti-tumor potential versus 0.1% of terrestrial samples (Munro et al., 1999). The complex alkaloid ecteinascidin 743 is a noteworthy example. It was isolated from the tunicate *Ecteinascidia turbinata* and launched for the treatment of soft tissue sarcomas in Europe in late 2007 and for the treatment of relapsed ovarian cancer in Europe and the United States in 2009 under the name Yondelis® (**8**) (**Figure 1.2**). It is also in a phase III trial against ovarian cancer in conjunction with liposomal doxorubicin, and in phase II trials for breast, prostate, and pediatric sarcomas (Cragg and Newman, 2009, Cragg et al., 2009, Henriquez, 2005). Further examples of anticancer agents are halichondrin B (**9**) a complex polyether isolated in miniscule yield from several sponge sources along with successful large scale synthesis of its analogue E7389 (Eribulin mesylate, Halaven<sup>TM</sup>) (**10**) which subsequently gained FDA approval in 2010; and bryostatin 1 (**11**), another complex macrolide, originally isolated by Pettit and his collaborators from the bryozoan, *Bugula neritina* (Cragg et al., 2009, Cragg and Newman, 2009, Yu, 2005, Newman, 2005, Newman, 2012, Kollar et al., 2014).



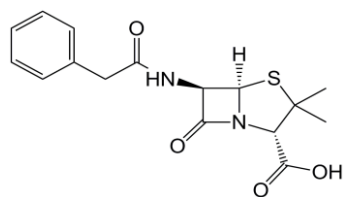
**Figure 1.2** Drugs derived from marine natural products for treatment of cancer

## 1.2 Roles of Microorganisms in Drug Discovery

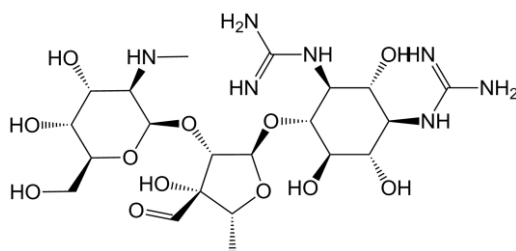
Microorganisms are able to produce natural products with a broad range of pharmacological activities. The greatest attention in the past has been paid to the discovery of penicillin, by Flemming in 1929, from the filamentous fungus, *Penicillium notatum*, which opened the “Golden Age” of antibiotics (1940-1962). Penicillin G (**12**) (**Figure 1.3**) was the first penicillin in clinical use (Singh and Barrett, 2006, Walsh, 2003). Shortly after that, in 1943, the aminoglycoside antibiotic streptomycin (**13**) was isolated from *Streptomyces griseus* and, in addition to being active against *Mycobacterium tuberculosis*, was active against a wide range of other pathogenic



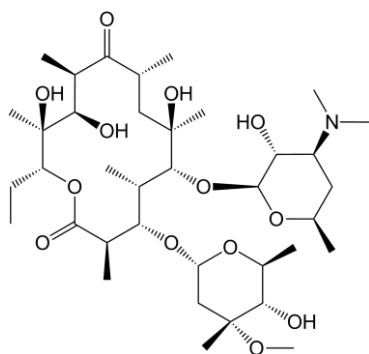
organisms. The macrolide antibiotic, exemplified by erythromycin (**14**), is still prescribed today, particularly for pediatric patients. Many antibiotics currently remain in use, such as aminoglycosides, tetracyclines (**15**) (Buss, 1995), amoxicillin (**16**), cephalexin (**17**) (B.Singh, 2012) and other polyketides of many structural types (from the *Actinomycetales*). Vancomycin (**18**), a glycopeptide produced by *Streptomyces orientalis* discovered in 1954, is a key Gram-positive antibiotic (Walsh, 2003) (Figure 1.3). However, bacteria have rapidly evolved resistance to various classes of antibiotics, which means new generations of antibiotics need to be constantly discovered. A report from the US Centers for Disease Control and Prevention (September 2013) showed that 2 million Americans a year contract bacterial infections that are resistant to existing antibiotics and 23,000 die from these infection (Williams, 2014). In spite of technological breakthroughs progress is slow with only two new antibiotics approved by FDA from 2008 to 2012 (Spellberg, 2013).



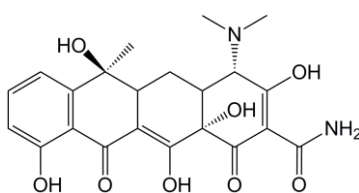
**Penicillin 12**



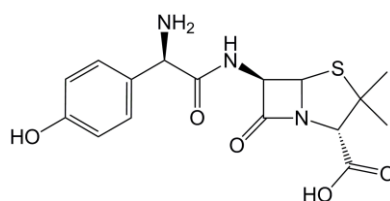
**Streptomycin 13**



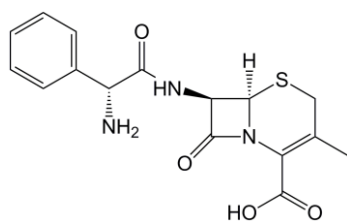
**Erythromycin 14**



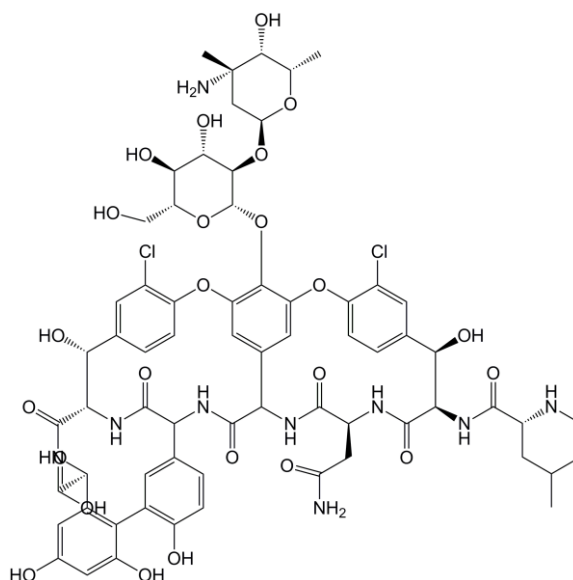
**Tetracycline 15**



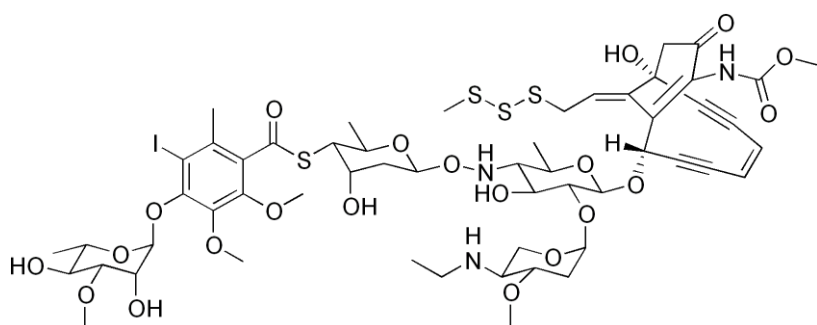
**Amoxicillin 16**



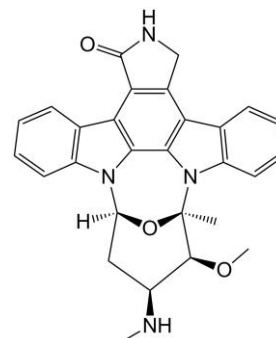
**Cephalexin 17**



**Vancomycin 18**



**Calicheamicin  $\gamma_1$  19**



**Staurosporine 20**

**Figure 1.3** Representative examples of natural products based antimicrobial drugs

Microorganisms, particularly fungi are capable of producing antitumor antibiotics, which have played a much bigger role, perhaps second only to antibacterial agents, either as drugs or lead to drugs. Regarding their antitumor perspective, anthracycline (Arcamone, 2005, Arcamone, 2012), one of the most important chemical classes of compound derived from *Actinomycetales*, along with daunorubicin and its derivative doxorubicin (adriamycin) are still a major component of breast cancer treatment (Swanson et al., 1991, Ackermann et al., 2004). Another important molecule, also from *Actinomycetales*, family of glycopeptide antibiotics, is bleomycin (Hecht, 2005, Hecht, 2012). Bleomycin is currently applied for the treatment of squamous cell carcinomas, germ cell tumors, and select lymphomas. The enediynes are a structurally unique class of antitumor antibiotics, comprising microbial compounds, calicheamicin  $\gamma I_1$  (**19**) (**Figure 1.3**) (Giddings and Newman, 2013, Hamann P.R. et al., 2005, Hamann P.R. et al., 2012). Activation of calicheamicin leads to structural rearrangement of DNA resulting in cleaved double-strand DNA and eventually cell death. In 2000, gemtuzumab ozogamicin, an anti-CD33 humanized antibody linked to a semi-synthetic calicheamicin derivative was approved by the FDA for use against chronic myeloid leukemia and remains the most potent approved antitumor drug to date (Giddings and Newman, 2013). In 1986, the indolocarbazole alkaloid staurosporines (**20**) was discovered as potent inhibitor of protein kinase C (Tamaoki et al., 1986, Prudhomme, 2005). A significant number of staurosporine-like agents were introduced in clinical trials. Reported in 2010, PKC-412 or midostaurin was in phase III clinical trials under Novartis for acute leukemia (AML); and lestaurtinib, also known as CEP-701, was in phase II/III clinical trials for treatment of relapsed AML (Prudhomme, 2005).

### **1.3 The importance of scaffolds embedded into Natural Products**

Natural products represent attractive sources of diverse structures, which play pivotal roles in drug discovery. As secondary metabolites, these substances at least have been synthesized with purposes for the organisms that produced them. Alkaloid has been used by many plants as protectant from animals, especially mammals. Such cases have enabled alkaloids to target mammalian proteins and eventually poison the corresponding organisms. Based on “Dictionary of Alkaloids” and other sources, a total of 53 alkaloids have been used as medicines within the last 50 years including morphine, atropine, colchicine, quinine, strychnine and vinblastine (Amirkia and Heinrich, 2014). Another example needing to be exemplified is the toxin of snakes, scorpions and spiders which commonly interfere with voltage-gated ion channels in mammalian nerve cell membranes leading to muscle and/or respiratory paralysis and ultimately death (Kularatne and Senanayake, 2014). Furthermore, yeast synthesizes a protein that is homologous to a human protein functioning as immunosuppressant. Therefore, it stands to reason that these substances are able to bind human proteins (Breinbauer et al., 2002b). Whereas, there are also several limitations of natural products such as (i) difficulty in access and supply, (ii) complexities of natural products because of their large size and complicated structures which require structural optimization to improve binding affinity and selectivity and, (iii) long development times owing to their presence as mixtures in extracts, which require highly labour intensive and substantially time consuming isolation and structure elucidation compared to synthetic chemicals (Harvey, 2008). Despite the perceived disadvantages, natural products have remained the progenitors of many approved drugs today (Cragg and Newman, 2013).

Combinatorial chemistry, on the other hand, has made significant contributions, since the early 1990s, to the generation of thousands of novel compounds in an effort to more effectively discover new chemical entities (Grabowski et al., 2008). Surprisingly, over the period from 1980 to 2005 only one *de novo* antitumor compound (Sorafenib, Nexavar® from Bayer) was approved by FDA (Newman and Cragg, 2007). This implies that combinatorial chemistry failed to create new chemical skeletons with structural diversity, thus insufficient to complement the wide variety of biomedical targets. This also reflects the fact that we lack the knowledge of essential factors contributing to the physicochemical and biochemical activity of compounds (Grabowski et al., 2008, Wess et al., 2001, Welsch et al., 2010). This demonstrates the need to develop new approaches in natural product research.

To address these limitations, minor alterations of functional groups of natural products were initially applied. For instance, some natural products were converted to esters or ethers, while others were alkylated, hydrolysed, oxidised or reduced. In the late nineteenth century, structural elucidation of alkaloids commenced a new era of analogue synthesis in which core scaffolds, or core structures, of the molecules were retained (Sneader, 2005). There are several ways to characterize the scaffold of a molecule. Bemis and Murcko proposed molecular frameworks which is the union of ring systems and linkers in a molecule or, the exocyclic double bonds and the atom at the exocyclic end (Bemis and Murcko, 1996). Alternatively, using the example of the dopamine D3 receptor antagonist BP-890, a molecular scaffold can be defined as maximum common substructures (MCS) which is the largest fragment or rings (Mcgregor and Willett, 1981); Bemis and Murcko's molecular framework; molecular fragments obtained by Retrosynthetic Combinatorial Analysis Procedure (RECAP) that allows electronical

molecule fragmentation around bonds which are formed by common chemical reactions, followed by identification of common motifs/fragments using databases of biologically active molecules (Lewell et al., 1998, Krier et al., 2006).

Indeed, natural products offer better coverage of chemical space relative to large synthetic compounds (Grabowski et al., 2008). In contrast to synthetic organic chemistry, by which numbers of compounds are achieved by repeating a reliable sequence of chemical reactions time after time with different inputs, Nature rationally partitions its limited building blocks into various pathways to make biologically active molecules with a high degree of diversity. Results of a study in 2009 have shown that 83% (12,977) of core ring scaffolds present in natural products were absent from commercial collections through investigation of the systematic absence in chemical biology as well as screening libraries (Hert et al., 2009). This raises the possibility that libraries comprising compounds containing scaffolds existing in natural products will provide better opportunities to find both screening hits and chemical biology probes. Given the molecular frameworks known for binding to certain protein domains, synthetic chemists can vary appended functional groups to obtain structural diversity conferring selectivity for related targets. As suggested by a study in 2004 -if a natural product is selected for binding to a particular protein domain, then the underlying structural framework can be employed as a biologically validated starting point for focused libraries which provide selectivity to other targets sharing similar protein folds, albeit not necessarily catalysing the same chemical reactions (Breinbauer et al., 2002a). As discussed previously, compared to synthetic molecules, natural products are more similar to endogenous ligands or metabolites, thereby more easily accepted as a substrate by transporters. Therefore, it would be more profitable to utilize the structural

diversity of natural products to facilitate the development of bioactive compounds with novel scaffolds (Ganesan, 2008).

Another concept of scaffolds that has been applied to the planning of natural product-like libraries and associated with computational methods and pharmacophore methods is *privileged scaffolds or privileged structures* (Guo and Hobbs, 2003). This term was first proposed by Evans and colleagues to describe a single molecular framework that can serve as an affinity ligand for various types of protein receptors (Evans et al., 1988). These privileged structures refer to three dimensionally well-defined rigid polyheterocyclic skeletons rather than flexible linear compounds, including benzamidines, biphenyltetrazoles, spiropiperidines, indoles and benzylpiperidines (Mason et al., 1999). These substructures have been found in number of bioactive natural products and pharmaceutically designed agents and have been considered as essential elements for good drug-likeness (Mason et al., 1999, Newman, 2008). The concept of “privileged structure” is highlighted with the example of *Linum album* (Linaceae family), an herbaceous and medicinal plant, which biosynthesizes some important lignans such as podophyllotoxin,  $\alpha$  and  $\beta$  – peltatin, possessing various biological activities such as antitumor, anti-inflammatory and cytotoxicity (Weiss et al., 1975). Similarly, genistein, a component of soy products, known as a protein tyrosine kinase inhibitor also inhibits topoisomerase II and 1-phosphatidylinositol 4-kinase and binds to the estrogen receptor beta with high affinity (Markovits et al., 1994, Wang et al., 1996). It is also extremely useful in early stages of screening when information about targets structure and function is inadequate. Here, on the basis of biological targets, which can contain structurally common small molecule binding sites, all existing ligands that are active on sequentially/structurally related proteins could be screened (Breinbauer et al., 2002b, Leeson et al., 2004). In lead development,

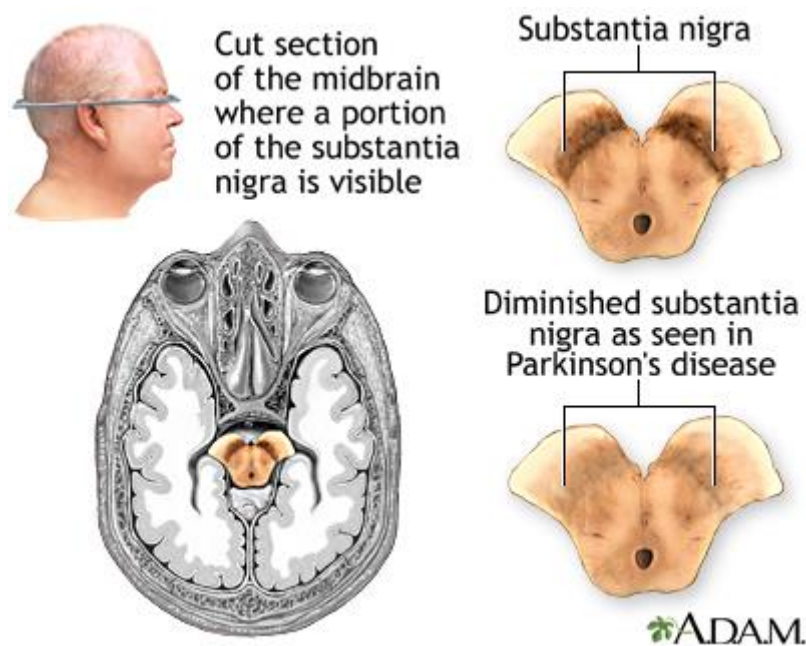
modification of substitution pattern of the backbone attached to privileged structures renders them specific for one or a range of distinct biological targets. These designed privileged structures can be optimized for their binding affinity and selectivity. With aid of privileged structures as chemical “navigators” of biologically relevant chemical space, combinatorial chemistry can prepare diverse libraries of drug-like small molecules which allows faster recognition of novel agonists, antagonists or inhibitors for receptors or enzyme site of known structure; and ultimately shorten and accelerate significantly lead discovery process (Martin et al., 1995, Kim et al., 2014). This concept has been applied for construction of focused libraries in numerous studies (Guo and Hobbs, 2003, Collins and Jones, 2014, Welsch et al., 2010).

#### **1.4 Parkinson’s disease**

Parkinson’s disease (PD) is the second most common neurodegenerative movement disorder, following Alzheimer’s disease, and was first described in a monograph, namely *An Essay on the Shaking Palsy* 1817, by James Parkinson (Goetz, 2011, Massano and Bhatia, 2012). Initially recognized by its clinical symptoms both motor and non-motor features, eventually PD was diagnosed in 1912 by the presence of Lewy bodies (LB) and Lewy neuritis (LN) along with the loss of dopaminergic neurons in the substantia nigra pars compacta (**Figure 1.4**) (Waxman & Giasson, 2009). Despite advances in genetic research over the subsequent years, the pathogenetic mechanism underlying selective dopaminergic cell loss in PD remains unclear. Current thinking is that mitochondrial dysfunction, oxidative stress, and, proteasomal impairment play central roles in PD. Idiopathic PD is considered a complex interaction between non-genetic factors, such as environmental risk factors, and susceptibility genes in patients (Cook et al., 2011). At present, the most effective medication for the disease is the



replacement of dopamine, using either the biosynthetic precursor of dopamine L-dihydroxyphenylalanine (L-DOPA, levodopa) or direct agonists of dopamine receptors. However, long term use of this therapeutic leads to various motor complications including end-of-dose wearing off, dyskinesias and dystonia (Vlaar et al., 2011). To date there is no true cure for PD resulting in an increasing burden on healthcare.



**Figure 1.4** Pathology of Parkinson's disease. Panel depicts human cut section of midbrain to reveal portion of the substantia nigra. It demonstrates normal pigmentation of the substantia nigra pars compacta (SNpc) produced by neuromelanin within the dopaminergic neurons. However, there is significant depletion of dopaminergic neurons in Parkinson's disease in which nigrostriatal pathway degenerates (Campellone, 2014).

### **1.4.1 Epidemiology of Parkinson's disease**

PD affects people all around the world in all ethnic groups (Zhang and Roman, 1993). It was reported that prevalence of PD rises exponentially among people between 65 and 90 years which accounts for 0.3 percent of general population and 3 percent of people 65 years or older have PD (Moghal et al., 1994). Having collected data from 12 US and European studies, a review estimated PD prevalence of over 65 years old population at 950 per 100,000; approximately 349,000 individuals with PD were found in the USA (Wirdefeldt et al., 2011). Another study showed an significant increase in the number of middle age population (over 50 years) affected by PD ranging between 4.1 and 4.6 million in 2005 to between 8.7 to 9.3 million by year 2030 (Dorsey et al., 2007). Gender difference as a risk factor for developing PD has been discussed in many studies. Most report higher PD incidence rates in males, particularly in the oldest age group. However several studies found no gender difference. The neuroprotective effects of female hormones, such as oestrogens, have been proposed to confer the higher risk of PD in men than in women. However, their role is still controversial (Baumann, 2012, de Lau and Breteler, 2006a).

### **1.4.2 Clinical signs and symptoms**

#### *1.4.2.1 Motor symptoms*

Parkinson's disease is clinically characterized by four cardinal features: tremor at rest, rigidity, bradykinesia (or slowing of movement), and postural instability (balance impairment) (Schneider and Obeso, 2014) (**Figure 1.5**).

#### *1.4.2.1.1 Tremor*

With a prevalence of 70% in PD patients, tremor at rest is the most common symptom of the disease. Rest tremor typically disappears with action and during sleep. It also involves tremor of the lips, chin, jaw and legs. The frequency of rest tremor is normally in the range of 3-6 Hz. In addition, many patients with PD also experience postural tremor (re-emergent tremor) that occurs immediately on stretching out the arms. While occurring at disease onset, postural tremor can be seen in action in later stage disease with a short pause in the transition from rest to posture. Unlike rest tremor, postural tremor is faster with range of 6-8 Hz (Jankovic et al., 1999b, Jankovic, 2008, Massano and Bhatia, 2012).

#### *1.4.2.1.2 Rigidity*

Rigidity refers to resistance rising from passive movement that remains unchanged throughout motion of a limb or the neck (flexion, extension or rotation about a joint). In the early stages of disease progression, flexor muscles of the limbs are more affected than extensors. It is noteworthy that although the resistance is escalated by velocity, minimum or no rigidity is observed with higher mobilization speed. In clinical practice, activation of voluntary movement is employed to detect mild rigidity (Rodriguez-Oroz et al., 2009, Jankovic, 2008, Massano and Bhatia, 2012).

#### *1.4.2.1.3 Bradykinesia*

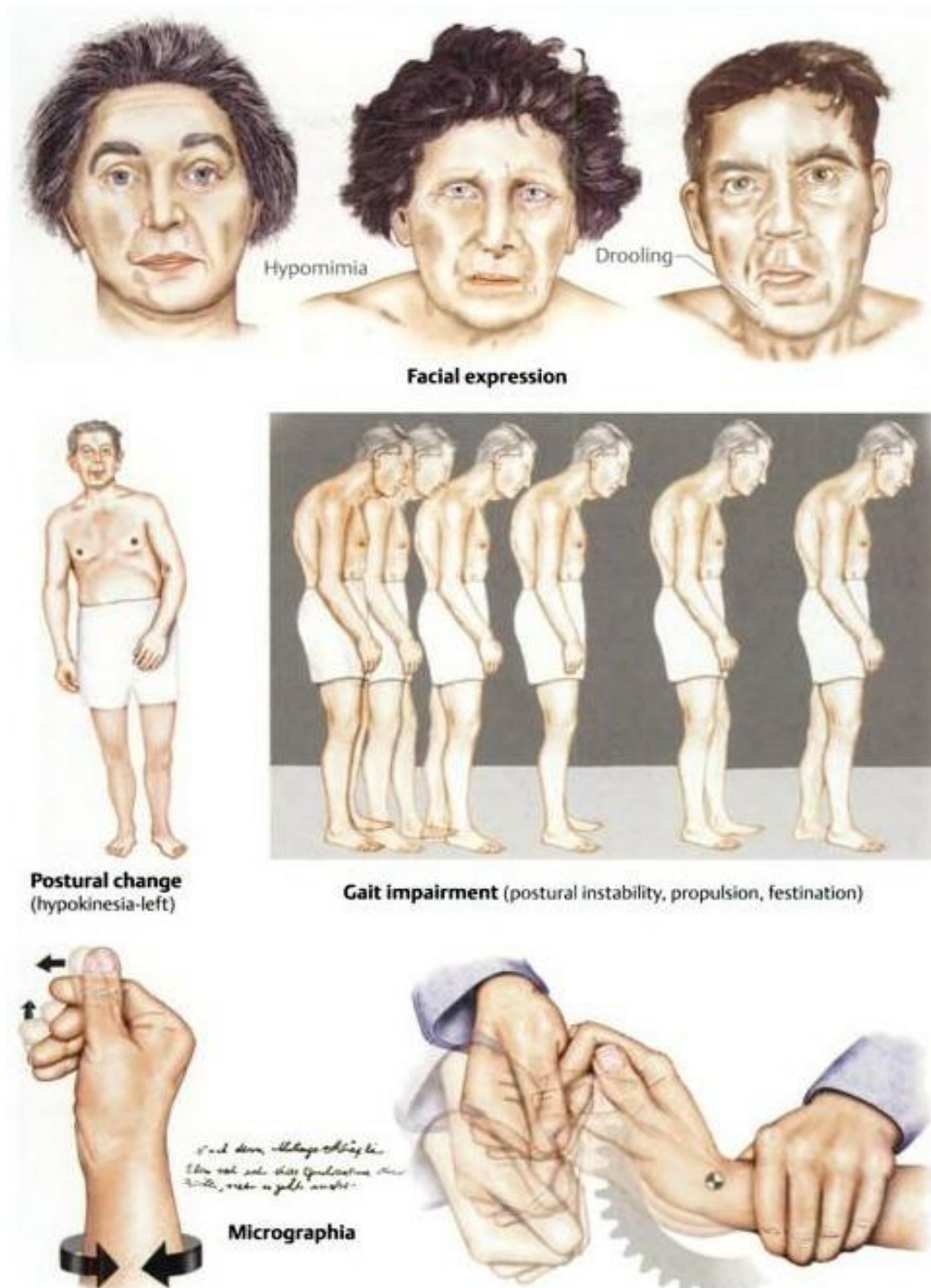
Bradykinesia is the most disabling symptom of early Parkinson's disease and is a hallmark of basal ganglia dysfunction in PD (Jankovic et al., 1999a). This symptom

involves a slowness of movement with difficulties in performing sequential and simultaneous tasks. Initially recognized by loss of speed in carrying out normal daily activities and tasks requiring fine motor control, such as doing up buttons and handwriting, bradykinesia progressively leads to a loss of spontaneous movements and gesturing, loss of facial expression (hypomimia), swallowing impairment, and reduced arm swing while walking (loss of automatic movements). Bradykinesia, similar to other parkinsonian symptoms, is dependent on the emotional state of the patient. With sudden excitement a patient may catch a ball or even make other fast movements. This special phenomenon reveals that motor programs of PD patients are intact, albeit the help of an external trigger is necessary to utilize or access the programs. In order to evaluate bradykinesia, several tests are implemented: finger tapping, forearm pronation and supination, foot tapping, and fist closing and opening (Massano and Bhatia, 2012, Jankovic, 2008).

#### *1.4.2.1.4 Postural instability*

Postural instability defined as loss of balance associated with propulsion and retropulsion, generally occurs in more advance stage of PD, after other clinical features present. Postural instability in PD patients has been found related to reduced or absent vestibular responses (Pollak et al., 2009). Impairment of balance control can be worsened by the fear of falling in PD patients (Adkin et al., 2003). Unsurprisingly, PD patients often suffer from severe fall related injuries due to loss of protective reactions. Significant risk of hip fractures due to false results in postural instability is the most potentially dangerous motor sign. In association with rigidity and bradykinesia, loss of postural reflexes causes patients to collapse into the chair when attempting to sit down. Postural instability can be easily assessed by pulling patients backward or forward to

check for balance recovery. An abnormal postural response is best observed when patients take more than two steps backwards or the absence of any postural response (Massano and Bhatia, 2012, Jankovic, 2008).



**Figure 1.5** Motor symptoms of Parkinson's disease (Bosley)

#### *1.4.2.1 Non-motor symptoms*

When one thinks about Parkinson's disease, motor disorders are its well-known characteristics. Non-motor symptoms, however, are often underappreciated, create bigger demand on clinical resources and are major determinants of disease outcome, worsening disability, and a substantially poorer quality of life (Chaudhuri and Schapira, 2009). Having these features diagnosed at an early stage of the disease may allow for intervention with neuroprotective strategies when they may have the most impact (Poewe, 2008, Chaudhuri and Schapira, 2009, Lim et al., 2009, Gallagher et al., 2010). Non-motor symptoms comprise cognitive abnormalities, sensory dysfunction, sleep disorders, and autonomic disturbances (Massano and Bhatia, 2012).

##### *1.4.2.1.1 Cognitive abnormalities*

Cognitive impairment can be present in early disease stages. According to result of a community-based survey, 36% of patients exhibited cognitive impairment at diagnosis and 10% of patients developed dementia in the follow-up of 3.5 years (Foltynie et al., 2004, Williams-Gray et al., 2007). Another community-based prospective study showed that PD patients had a sixfold increased risk for dementia (Aarsland et al., 2001). PD related dementia is frequently associated with other neuropsychiatric comorbidities such as apathy, hallucinations, bradyphrenia, poor problem solving and fluctuation in attention (Aarsland et al., 2007). Additionally, many patients also demonstrate neurobehavioral abnormalities including craving, binge eating, compulsive foraging, and pathological gambling. These symptoms have been partially dopaminergic drug responsive; however, the mechanism of these aberrant behaviours is unclear (Palmiter, 2007, Miyasaki et al., 2007, Weintraub et al., 2006).

#### *1.4.2.1.2 Sensory dysfunction*

Patients with PD also experience sensory symptoms such as visual change, decreased olfactory function (hyposmia or anosmia) and, pain. Visual acuity, contrast sensitivity, color discrimination and motion perception are reported with PD patients (Diederich et al., 2002, Uc et al., 2005). Loss of the sense of smell is identified in the earliest stage of PD and is not relieved by drug treatment (Katzenschlager et al., 2004). Pain is a common complaint of PD patients ranging from oral pain, shoulder pain to genital pain. Again, these symptoms are difficult to treat. It appears that each PD patient will have different pain thresholds and may require adjusted doses of levodopa (Schestatsky et al., 2007).

#### *1.4.2.1.3 Sleep disorders*

Sleep disorders can occur decades before motor PD symptoms appear. It is estimated that sleep disturbances, including excessive daytime sleepiness, sleep attacks, advanced sleep phase syndrome, early morning awakenings, and rapid eye movement sleep behavior disorder (RBD) (Park and Stacy, 2009) are suffered by approximately 60-98% of patients with PD (Stacy, 2002). As disease advances, sleep abnormalities have been found to co-occur with circadian rhythm disruption. RBD, for example, is characterized by loss of normal atonia of rapid eye movement (REM) sleep. Nearly one third of PD patients are affected by RBD (Gagnon et al., 2002). On the other hand, 40 – 65 % of patients with RBD will go on to develop PD (Iranzo et al., 2006, Postuma et al., 2009, Adler et al., 2011). Most of the sleep symptoms are untreatable and complicated by long-term use of PD medications. Insomnia and sudden sleep attacks are believed to be

^  
a consequence of dopaminergic drugs, particularly dopamine agonists (Alves et al., 2008).

#### *1.4.2.1.4 Autonomic disturbances*

Autonomic illnesses occur commonly in PD and often predate the appearance of other motor features. Failure in autonomic function is caused by dysfunction of the parasympathetic nervous system leading to a variety of symptoms: constipation, orthostatic hypotension, urinary dysfunction and, sweating abnormalities.

Constipation is by far the most frequent sign cited by patients with a prevalence of approximately 59% (Alves et al., 2008, Cersosimo and Benarroch, 2008). In addition, up to 80% of patients complain of lengthening colon transit time (Park and Stacy, 2009). It is suggested that slow colonic transit may be related to pathogenic Lewy bodies in the colonic myenteric plexus. Notably, dopaminergic treatments showed no improvement on gastrointestinal motility proposing a non-dopaminergic mechanism of pathogenesis (Ahlskog, 2005). Insight study has reported that use of intrajejunal infusion of duodopa, compared to oral therapy, is more beneficially effective on constipation and other bowel symptoms in addition to other non-motor symptoms in patients with advanced-stage PD (Honig et al., 2009, Fasano et al., 2012).

Orthostatic hypotension (OH) and post-prandial hypotension refers to a drop of more than 20mmHg systolic pressure or 10mmHg diastolic pressure from lying flat to sitting or standing and can be observed in patients with idiopathic PD (IPD) and atypical parkinsonism (AP) (Freeman et al., 2011, Fereshtehnejad and Lökk, 2014). It is thought to be present in between 9.6% and 58% of patients (Papapetropoulos et al., 2001, Low,



2008, Fereshtehnejad and Lökk, 2014). Some PD patients might have latent OH pathology, whereas others have no obvious features. Estimates of the frequency of asymptomatic OH vary between 20% and 50% (Jamnadas-Khoda et al., 2009). As result of a decline in blood pressure, dizziness, visual disturbances, impaired cognition and fainting take place followed by dysfunction of cerebral perfusion (Ooi et al., 2000). As disease advances, OH can lead to significant disability including wheelchair confinement. Apparently, dopaminergic load complicates OH symptoms as this also affects blood pressure. It is advised that new approaches in lifestyle comprising more physical activities, less carbohydrate based meals, having adequate hydration before initiating pharmacological treatments be employed (Ha et al., 2011, Senard and Pathak, 2010, Lyons and Pahwa, 2011, Perez-Lloret and Rascol, 2010).

Urinary dysfunction is commonly diagnosed with idiopathic PD. With unpleasant symptoms including urinary frequency and urgency, incomplete bladder emptying, double micturition and urge incontinence, it significantly influences the quality of life for PD patients. The prevalence of urinary symptoms has fluctuated from 27% to 64% (Abrams et al., 2002, Winge et al., 2006, Araki and Kuno, 2000, Campos-Sousa et al., 2003, Barone et al., 2009). This is likely due to loss of the normal D1- mediated inhibition of micturition. Currently, anticholinergic medication remains applicable for an overactive bladder, nevertheless, potential adverse effects of such medication make effective management challenging (Blackett et al., 2009, Yeo et al., 2012).

Although sweating abnormalities are less severe than other symptoms from a medical perspective, it can have considerable impact on patients' physical, psychological and social well-being. In many reports, 30-50% of patients with PD experienced sweating disturbances (Hirayama, 2006b, Swinn et al., 2003, Riley and Chelimsky, 2003,

Zakrzewska-Pniewska and Jamrozik, 2003, Raudino, 2001). These symptoms vary from localised sweats (involvement of head, neck and trunk) to whole body or drenching sweats (Hirayama, 2006a). The mainstay treatment for sweating disorders is the administration of levodopa or dopamine agonist (Sage and Mark, 1995).

### **1.4.3 Etiologic factors and molecular pathogenesis**

#### *1.4.3.1 Role of aging*

The appearance of neurodegenerative diseases mainly in the middle-aged and elderly represents a contribution for the aging process in PD (Kempster et al., 2010). As expected, the gradual loss of dopamine (DA) in the substantia nigra pars compacta (SNpc) progressively worsens over time. PD affects 0.3% of the entire population and 1% of people above the age of 60 in industrialized countries and up to 4% in people over 80 years reflecting the aging effect (de Lau and Breteler, 2006b, Dexter and Jenner, 2013). However, it is worth noting that a different pattern of DA neuron loss occurs in PD from that of other disorders and the incidence of only 5% - 10% people of PD being younger than 45 years old (Lees et al., 2009) suggests an indirect effect of age towards the degenerative process.

#### *1.4.3.2 Genetic causes*

Although fewer than 10% of all PD cases result from monogenetic causes, the identification of specific genes obeying Mendellian inheritance patterns has opened up new insights into the pathogenesis of PD. Seven genes have been linked with familial PD. Of these, the five following genes are well characterized.

#### 1.4.3.2.1 *SCNA (PARK1/PARK4)*

Encoded by the *SCNA* gene,  $\alpha$ -synuclein is a neuronal protein localized in presynaptic termini (Benmoyal-Segal and Soreq, 2006). Although the precise physiologic role of  $\alpha$ -synuclein is unclear, it may be involved in neurotransmitter release, vesicle turnover, synaptic plasticity, and intracellular trafficking within the endoplasmic reticulum or Golgi apparatus. The pathologic role of  $\alpha$ -synuclein needs to be defined but it is the predominant component of Lewy bodies that are abundantly found in familial and sporadic PD brain specimens consisting of proteinaceous inclusions along with ubiquitin and several molecular components (Eriksen et al., 2005). Disease causing mutations in  $\alpha$ -synuclein (A53T, A30P and G46L) frequently result in autosomal dominant PD in rare kindreds (Gao and Hong, 2011).

#### 1.4.3.2.2 *LRRK2 (PARK8)*

Under physiological conditions, leucine-rich repeat kinase 2 (*LRRK2*), also named as Dardarin, participates in substrate binding, protein phosphorylation, neuronal outgrowth and attenuates oxidative stress-induced cell death. Multiple mutations of *LRRK2* have been identified (Arg1441Cys, Arg1441Gly, Tyr1699Cys, Gly2019Ser and Ile2020Thr) as disease causing alterations (Gao and Hong, 2011). Of these, the *LRRK2* Gly2019Ser mutation is the most common known cause of familial autosomal dominant and sporadic PD (Di Fonzo et al., 2005). High mutation frequency in *LRRK2* has been reported in 40% of North African Arabs and Ashkenazi Jewish populations (Healy et al., 2008).

#### 1.4.3.2.3 *Parkin* (*PARK2*)

*Parkin* encodes a 465 amino acid protein, which functions as an ubiquitin E3 ligase in the normal cellular protein degradation pathway. In addition, *Parkin* also takes part in mitochondrial maintenance and clearance of dysfunctional mitochondria by autophagy. Mutation of *Parkin* is the most common cause of autosomal recessive early-onset PD. The clinical patterns of *PARK2*-associated PD include a variety of symptoms such as hyperreflexia, prominent dystonia, sensory axonal neuropathy, increased susceptibility to levodopa induced dyskinesias and wearing-off phenomenon (Deng et al., 2006, Wickremaratchi et al., 2009). The more than 100 different mutations identified also account for 20% of sporadic PD with onset less than 20 years and up to 50% of cases of familial PD (Gao and Hong, 2011). Only a few cases of *Parkin* mutations were associated with  $\alpha$ -synuclein positive inclusion while Lewy bodies were not observed in others. This indicates that additional study is required to fully understand whether  $\alpha$ -synuclein and *Parkin* share the same pathogenic pathway.

#### 1.4.3.2.4 *PINK1* (*PARK6*)

PTEN-induced kinase 1 (*PINK1*) is encoded by gene *PINK1* and is localized to mitochondria. *PINK1* has been reported to participate in multiple mitochondrial functions, such as calcium dynamics, trafficking, respiration efficacy, free radical formation, and opening of the mitochondrial permeability transition pore (Gao and Hong, 2011). Mutations of *PINK1* are thought to result in the loss of kinase activity causing autosomal recessive parkinsonism. Clinical symptoms occurring at early onset in most patients include psychiatric disturbances (anxiety, psychosis), hyperreflexia,

dystonia at onset and excellent levodopa sensitivity (Steinlechner et al., 2007, Kasten et al., 2009, Kasten et al., 2010).

#### *1.4.3.2.5 DJ-1 (PARK7)*

DJ-1 is redox-sensitive molecular chaperone, a member of ThiJ/PfpI family, which is encoded by the *DJ-1* gene (Gao and Hong, 2011). DJ-1 is involved in the protein degradation pathway and apoptotic signalling, but also plays a role as an antioxidant and sensor of oxidative stress. Multiple mutations of *DJ-1* have been found in autosomal recessive PD patients. Affected individuals demonstrate disease onset ranging from 20 to 40 years with classical parkinsonian features. PARK7 shares many common clinical features with PARK6 (Annesi et al., 2005, Dekker et al., 2003)

### **1.4.4 Environment and PD**

Unlike familial events, sporadic and idiopathic cases of PD are more complex and have not been fully understood as yet. The emerging picture is that the combination of susceptible genes and environmental factors, such as rural residence, well-water drinking, exposure to agricultural chemicals and certain occupations (e.g., miners, oil well drillers) likely contribute to the prevalence of sporadic PD (Benmoyal-Segal and Soreq, 2006). Inevitably, recognition of these environmental factors may have far-reaching implications including preventive strategies through the elimination or reduction of specific exposure risks.

#### *1.4.4.1 MPTP*

In 1982 it was discovered that 1-methyl-4-phenyl-1,2,3,6-tetrahydropyridine (MPTP), a by-product of illicit heroin, induces parkinsonian syndrome resembling many of the clinical and pathological features of sporadic PD (Langston et al., 1983). Since then it has been valuable for the study of PD and response to treatment in primates, cats, rodents and human (Jenner, 2003, Wichmann and DeLong, 2003, Hamre et al., 1999). Experimentally, MPTP is converted to 1-methyl-4-phenylpyridinium (MPP<sup>+</sup>) by monoamine oxidase B (Singer et al., 1986), the active toxic compound (Langston et al., 1984). Once taken up into mitochondria and in the presence of counterion such as tetraphenylboron (Nicholls and Ferguson, 2014), it blocks electron transport chains, resulting in early energy crisis and oxidative stress due to increased production of reactive oxygen species, particularly superoxide radicals within the neuronal cytosol (Hantraye et al., 1996, Cleeter et al., 1992). These react with nitric oxide to form peroxynitrite (OONO<sup>-</sup>)- one of the most destructive oxidizing molecules (Ischiropoulos and Almelhdi, 1995, Przedborski and Vila, 2003, Przedborski et al., 2000), which can damage lipids, proteins and DNA and ultimately produce cell death (Radi et al., 2002).

#### *1.4.4.2 Rotenone*

Derived from the roots of *Derris* species, rotenone is a widely used domestic garden pesticide. It is known as a specific inhibitor of the mitochondrial complex I (Sherer et al., 2007). A recent study reported that rotenone exposure was associated with a 2.5 times higher risk of developing PD compared with non-exposure (Tanner et al., 2011). Due to its rapid decomposition by light and air within several days, rotenone is unlikely to be retained in the soil, which suggests that it has an indirect causal effect in PD.

Although it remains to be clarified, rotenone has been employed to model PD in animals. In rodent models, temporary exposure to rotenone can cause progressive functional and pathologic changes in the enteric nervous system of rodents (Greene et al., 2009, Pan-Montojo et al., 2010).

#### *1.4.4.3 Paraquat*

Paraquat is used as a herbicide to control weed growth. With remarkable similarity of chemical structure to MPTP, paraquat has been investigated for its potential link to PD. Though it is a relatively weak inhibitor of mitochondrial complex I activity compared to rotenone and MPTP (i.e. paraquat is less potent inhibitor of  $^3\text{H}$ -dihydrorotenone binding to brain mitochondrial complex I (with an  $\text{IC}_{50}$  of 8.1 mM) compared to MPTP and rotenone ( $\text{IC}_{50}$  values of 381  $\mu\text{M}$  and 14 nM, respectively) (Richardson et al., 2005), paraquat has been proven to significantly augment  $\alpha$ -synuclein fibril formation in vitro (Manning-Bog et al., 2002). In addition, paraquat also causes subcellular modification related to PD including increased production of reactive oxygen species, accumulation of alpha synuclein, and selective nigral injury (Kuter et al., 2010).

### **1.4.5 Treatment**

#### *1.4.5.1 Pharmacological treatment*

##### *1.4.5.1.1 Dopamine Replacement Therapeutics*

First introduced in 1960s, the dopamine precursor levodopa (L-dopa) revolutionized the treatment of PD. It continues as the pharmacotherapy of choice for alleviating motor

symptoms, however, as disease progresses L-dopa has failed to tackle complications. In addition, there is debate over the use of L-dopa as it exhibits distinct side effects including motor fluctuations and dyskinesia after chronic administration. Approximately 50% of patients and nearly 100% of early onset PD patients developed motor complications after 5 year administration of L-dopa (Xie et al., 2014). Thus together with delaying L-dopa use, alternative medications, described in the following paragraph, have been employed by many clinicians to deal with advanced PD (Katzenschlager and Lees, 2002).

In this direction, monoamine oxidase type B (MAO-B) inhibitors and dopamine agonists were launched as long-term symptomatic therapy for de novo patients before L-dopa is required. The MAO inhibitors selegiline and rasagiline were believed to prevent MPTP toxicity to nigral dopaminergic neurons. On the other hand, both drugs also showed broad-spectrum of actions such as antiapoptotic ability, antioxidant effects and, antiglutamatergic effects. Gaining access to clinical trials, these drugs have undergone examination on disease modification in humans. Clinical studies suggest that early administration of selegiline (oral, oral disintegrating) can retard disease progress in PD patients (Palhagen et al., 2006). In common with selegiline, rasagiline has been recommended for patients with the highest degree of motor disability (Olanow et al., 2008). Furthermore, a number of currently available therapeutics have potential for disease modification including three active dopamine receptor agonists (pramipexole and ropinirole in oral form; and apomorphine in injectable form) and two peripheral catechol-*O*-methyltransferase (COMT) inhibitors (tolcapone and entacapone) (Gottwald and Aminoff, 2008, Bonifacio et al., 2007). Approved by the Federal Drugs Administration (FDA), MAO B inhibitors were applied for early and advanced PD treatments while apomorphine was accepted for fluctuating PD symptoms (Factor,



2008). Although dopamine agonists provide more specific therapeutic benefits with lower risk of dyskinesias due to their longer half-life, unexpected side effects (sleep attacks, REM sleep disorder, depression, hallucinations, delusions, psychosis) remain unresolved issues for these dopamine related drugs (Wood, 2010). It was speculated that unstable levels of circulating dopaminergic drugs contribute to the development of complications such as dyskinesia (Antonini and Odin, 2009). This prompted research into new delivery technology that minimizes the variability of plasma dopaminergic concentration. There were several approaches to achieve this goal: continuous fusion of short duration responsive dopaminergic receptor agonist via either subcutaneous injection, direct duodenal infusion with surgical placement of a percutaneous enteroduodenal tube or duodenal infusions of drugs in a viscous gel (Duodopa<sup>®</sup>) (Odin et al., 2008). Of these, duodenal infusions of drugs in a viscous gel (Duodopa<sup>®</sup>) have entered phase III clinical trial in the United States (Westin et al., 2011).

#### *1.4.5.1.2 Non-dopaminergic therapies*

Outside of dopaminergic agonists, anticholinergic drugs are the oldest therapeutic agents applied for PD treatment used since the late 1800s. These acted effectively on alleviating rigidity and tremor symptoms (Koller, 1986) and subsequently were used for idiopathic dystonia (Chuang et al., 2002). Nevertheless, a range of adverse side effects such as memory loss, hallucinations, constipation, and blurred vision made them less favoured therapeutic choices. With the breakthrough of pharmacology, potentially new therapeutic drugs including Adenosine A<sub>2A</sub> receptor antagonists (Morelli et al., 2010), metabotropic glutamate receptor ligands: mGluR4 agonists (Niswender and Conn, 2010, Engers et al., 2011), epinephrine precursor L-threo-DOPS (Devos et al., 2010), methylphenidate (Devos et al., 2007), serotonin and serotonin receptors (Di Matteo et

al., 2008, Bara-Jimenez et al., 2005) have recently entered clinical trials for early untreated, as well as advanced PD patients.

#### *1.4.5.2 Therapeutics for non-motor symptoms (NMS) of PD*

Being frequently unrecognized and untreated, there is renewed interest in treatments of non-motor symptoms in recent years. Clozapine has been assessed for psychosis treatment in PD, albeit due to generation of serious risk of agranulocytosis, prescription of this medication should be carefully considered. In common with Clozapine but with a safer profile, Quetiapine is utilized as a first line antipsychotic agent in PD (Smith et al., 2012, Merims et al., 2006). Another example of therapeutic intervention for NMS is Donepezil that showed good efficacy and tolerability for PD patients with dementia without worsening of Unified PD Rating Scale (UPDRS) motor scores. Results from placebo-controlled randomized trial demonstrated that Donepezil significantly improved Mini Mental State Examination (MMSE) scores in patients with PD and mild to moderate dementia (Aarsland et al., 2002). In addition to donepezil, rivastigmine gained FDA approval as the only acetylcholinesterase inhibitor for dementia.

Depression is often associated with approximately 40-70% PD patients (Wood et al., 2010). Tricyclic antidepressants (TCAs) were identified as the second most common therapeutics for PD depression (Richard and Kurlan, 1997). Recently, Pramipexole has been found to be more effective than placebo in treating PD patients with depression in that 124 of 144 Pramipexole recipients, at a mean daily dose of 2.18 mg, exhibited more significant decline in depressive symptoms associated with PD, than 133 of 152 placebo treated patients with dose equivalent to 2.51 mg (Barone et al., 2010).

Clinical features of autonomic dysfunction have been identified including orthostatic hypotension (OH), urinary dysfunction, and constipation. Fludrocortisone and midodrine are the most commonly prescribed medication for OH in PD. Clinical trials have provided strong evidence for the ability of polyethylene glycol in constipation treatment (Zesiewicz et al., 2010) while laxatives are more commonly used agents however without therapeutic trial data.

In PD, the use of levodopa/carbidopa for periodic limb movements in sleep (PLMS) has been confirmed. Clonazepam is considered first line treatment for REM sleep behaviour disorder (RBD). It is efficacious in alleviating aberrant motor activity. Following clonazepam, melatonin intake at night may also be effective for treating insomnia and daytime sleepiness (Chaudhuri and Schapira, 2009, Srinivasan et al., 2011).

#### *1.4.5.3 Surgical treatments*

When medication such as L-dopa ceases to be effective or adverse effects such as motor fluctuations and dyskinesia are intolerable, surgical interventions may be used to control symptoms of PD patients (Goetz, 2011). Radiofrequency (RF) lesioning and deep brain stimulation (DBS) of basal ganglia nuclei are the most common neurosurgical approaches for PD (Strauss et al., 2014). These procedures target nodes of the basal ganglia-thalamo-cortical motor circuit in disease states (Smith et al., 2012). Several randomized clinical trials have reported that unilateral pallidotomy, subthalamic nucleus (STN), and globus pallidus internus (GPi) are the best methods for the motor fluctuations and dyskinesias related with PD (Rodriguez-Oroz et al., 2012). Of these procedures, thalamotomy or thalamic stimulation is highly effective for tremors suppression (Fox et al., 2011). Effects of DBS, moreover, can be seen through

alleviation of parkinsonism motor signs, “off” period reduction and drug-induced dyskinesias and dystonia decline (Bronstein et al., 2011). Significant improvement of motor features coupled with substantial decrease of medication doses have been recorded in advanced PD patients with bilateral STN DBS (Kleiner-Fisman et al., 2006, Moro et al., 2010, Follett et al., 2010). In spite of good efficacy for long-term control of both dopaminergic features of the disease and motor complications of chronic administration of currently available medications, surgical procedures in general cannot completely eradicate PD (Krack et al., 2003, Castrioto et al., 2011). Hence, there is an urgent need to develop new therapies targeting both motor and non-motor symptoms and ultimately eliminating the disease.

#### *1.4.5.4 Other therapeutic approaches*

Besides conventional pharmacologic and surgical treatments, many beneficial therapeutic options are currently being explored for PD patients. One approach is the transplantation of fetal dopamine-rich mesencephalic tissue and other sources of dopamine (DA) neurons (e.g., generated from stem cells or by direct conversion of somatic cells). These have been suggested to induce substantial (at least 50-70%) amelioration of motor symptoms without significant side effects (Lindvall and Bjorklund, 2011). However, although receiving support, this approach also encounters opposition arising from its potential risks including tumour formation, inappropriate stem cell migration, immune rejection of transplanted stem cells, haemorrhage during neurosurgery and postoperative infection that seemingly outweigh potential benefits of relieving parkinsonian symptoms and decreasing doses of parkinsonian drugs (Master et al., 2007, Lindvall and Bjorklund, 2011). Thus, the development of stable, homogenous and reliable cell sources for transplantation, improvement of transplantation procedures

and standardization of their implementation in clinical trials would be a prerequisite for future therapies.

Another avenue of investigation is the gene transfer approach that utilizes the stereotactic injection of viral vectors into deep brain nuclei. In the most recent trials, an adeno associated viral type-2 (AAV2) vector was used containing different genes of interest encoding either trophic factors such as Neurturin for neutralization of the neurodegenerative process, or glutamic acid decarboxylase (GAD), the rate limiting enzyme for GABA production, for modulation of basal ganglia activity. Results from randomized, double-blind clinical trials showed strong evidence of the benefit of gene therapy in PD (LeWitt et al., 2011, Marks et al., 2010).

#### **1.4.6 Models of PD**

Various species have been utilized as models to study the mechanisms of action of the multiple factors that play a role in PD. Transgenic overexpression of mutant autosomal-dominant genes (*SNCA* and *LRRK2*) and knockout/knockdown of autosomal-recessive genes (*Parkin*, *DJ-1*, and *PINK1*) in different organisms, such as mice, *Drosophila* and *C. elegans* have been used to model PD. Animal models using MPTP, rotenone, paraquat have also been extensively exploited to study their proposed effects on mitochondrial complex I activity (Gao and Hong, 2011, Berry et al., 2010).

Furthermore, preclinical studies of therapeutic approaches are frequently conducted in animals before they progress to clinical studies in humans. In primate models of PD, lentiviral-mediated delivery of glial cell line- derived neurotrophic factor (GNDF) was examined for its capability to prevent nigrostriatal degeneration (Kordower et al., 2000). Another approach is transplantation of stem cells, which obtained preliminary

encouraging results from animal models that consequently can be used to help determine improved future treatments (Master et al., 2007).

#### **1.4.7 Therapeutic Perspectives of Natural Products in Parkinson's disease**

At present, most pharmacological therapies in PD are aimed at replacing striatal dopamine and relieving symptoms while avoiding the development of other complications. Thus, ideal drugs should have no, or minimal, side effects even under chronic administration along with the ability to target multiple pathways implicated in PD. In this direction, natural products including natural antioxidants and phytochemicals with neuroprotective properties are being exploited for adjunctive therapy.

##### *1.4.7.1 Curcumin*

Curcumin, the yellow curry spice extracted from the rhizome of turmeric, is a polyphenolic compound with several beneficiary properties in human ailments and has been documented for centuries in Ayurveda (Joe et al., 2004). Many studies have reported that curcumin has been used as an antioxidant, antiseptic, anti-inflammatory, anti-bacteria and anti-tumor agent in various diseases including arthritis, cardiovascular diseases, lung fibrosis, gall stone formation, diabetes, wound healing, Alzheimer's disease and stroke (Sharma et al., 2006, Yang et al., 2005). In addition, curcumin also has special properties that make it a potentially interesting therapeutic molecule for PD. Curcumin possesses the ability to cross the blood brain barrier which is essential for therapeutic action in brain. High doses of curcumin showed minimal toxicity in human subjects (Lao et al., 2006, Bharath et al., 2002). The effectiveness of curcumin on

oxidative stress and apoptosis was shown in a transgenic *Drosophila* brain model. A significant decline in oxidative stress, apoptosis and life span expansion were reported when human alpha synuclein expressing flies were exposed to curcumin (Ramana et al., 2014). Another study showed ROS detoxification, prevention of protein aggregation and neurogenesis of curcumin *in vivo* (Kim et al., 2008). It has also been established that curcumin treatment in the 6-OHDA rat model of PD can protect substantia nigra (SN) neurons, improve striatal dopamine levels and chelate  $\text{Fe}^{2+}$ . Specifically, curcumin inhibits the aggregation of  $\alpha$ -synuclein *in vitro*, and hence enhances solubility of  $\alpha$ -synuclein making it less toxic (Pandey et al., 2008, Wang et al., 2010). In spite of useful medicinal properties, poor bioavailability including insolubility in water, poor absorption, quick gut metabolism and elimination have restricted curcumin's therapeutic applications (Mythri and Bharath, 2012). In a recent study, diester derivatives of curcumin (di-piperoyl, di-valinoyl and di-glutamoyl), which are not degraded by processing in the gastrointestinal tract, were used with a resultant enhanced protection against GSH depletion mediated oxidative stress. Among curcumin derivatives, the di-glutamoyl derivative exhibited advanced protection owing to its de-esterification following absorption thereby rendering glutamate as a precursor for GSH synthesis (Harish et al., 2010, Mythri et al., 2011). These pro-drugs claim to be suitable for cellular uptake processes that favour treatment of neurodegenerative diseases such as PD.

#### 1.4.7.2 Ginger (*Zingiber Officinale Roscoe*)

The ginger plant, *Zingiber officinale*, belongs to the family Zingiberaceae, comprising of different spices such as turmeric, cardamom and galangal. Ginger is well known for its medicinal properties: as an analgesic, antipyretic, sedative, antibacterial activities

and anti-inflammatory *in vivo* (Park et al., 2008, Suekawa et al., 1984). Furthermore, administration of zingerone, an alkaloid extracted from the ginger root, was reported to inhibit 6-hydroxydopamine (6-OHDA) induced dopamine decline in the mouse striatum and increases superoxide scavenging activity in serum (Kabuto et al., 2005).

#### 1.4.7.3 Phytic acid

Increased brain iron level has been implicated as a risk factor for PD pathogenesis through the interaction between iron and  $\alpha$ -synuclein, tyrosine hydroxylase and dopamine that disrupts the function of dopaminergic neurons (Hashimoto et al., 1999, Mythri et al., 2012). Therefore, regulation of iron level has become an important strategy in anti-PD strategies. Abundantly present in plants, mainly in cereals, nuts, oil seed, legumes, pollen and spores (Midorikawa et al., 2001), phytic acid (myo-inositol hexaphosphoric acid or IP6) can inhibit iron catalysed hydroxyl radical formation by iron chelation and lipid peroxidation (Rimbach and Pallauf, 1998). The effect of this compound against 6-hydroxydopamine- (6-OHDA-) induced DNA damage and apoptosis at high level of iron state in order to protect dopaminergic neurons has been speculated (Xu et al., 2008, Xu et al., 2011). In common with curcumin, phytic acid has the ability to cross the blood-brain barrier consistent with its neuroprotective effect *in vivo* (Grases et al., 2001). These results suggest the possible value of using phytic acid in PD management.

#### 1.4.7.4 Danshen

Danshen, one of the most important traditional Chinese medicines, is the dry root and rhizome of *Salvia miltiorrhiza* Bunge. It has been widely used for thousands of years



and is prescribed as a common hemorheologic agent to promote blood circulation in the treatment of cardiovascular disorders and cerebrovascular disease (Hugel and Jackson, 2014). In recent years, danshen has been one of the most prominent drugs in Chinese drug research (Cao et al., 2012). There are 18 bioactive compounds extracted from danshen including non-polar (lipid-soluble) diterpenoidal compounds and water-soluble (hydrophilic) phenolic compounds. Of these, salvianolic acid B (SalB) is a major ingredient and possesses the strongest pharmacological activity of the total phenolic acids of danshen (Tang et al., 2002, Chen et al., 2014). The anticancer effect of danshen in human cancer cell lines, such as glioma U87 cells as well as head and neck squamous cell carcinoma, has been recently recognized (Chen et al., 2014, Zhao et al., 2011, Wang et al., 2013). Furthermore, it was also demonstrated that SalB functions as a protective agent against 1-methyl-4-phenyl-pyridinium ( $\text{MPP}^+$ ) or 6-hydroxydopamine (6-OHDA) induced apoptosis in human SH-SY5Y neuroblastoma cells (Tian et al., 2008, Zeng et al., 2010). Interestingly, using mesencephalic cell cultures and an in vivo PD model, SalB was shown to considerably rescue neuronal injury induced by  $\text{MPP}^+$  and lipopolysaccharide (LPS) and reduced further deterioration of the remaining DA neurons in the SNpc (Zhou et al., 2014). Importantly, salB possesses key properties including minimal toxicity in human subjects, and the ability to cross biological membranes as well as the blood-brain barrier, making it a promising candidate in the battle to beat PD (Chen et al., 2011).

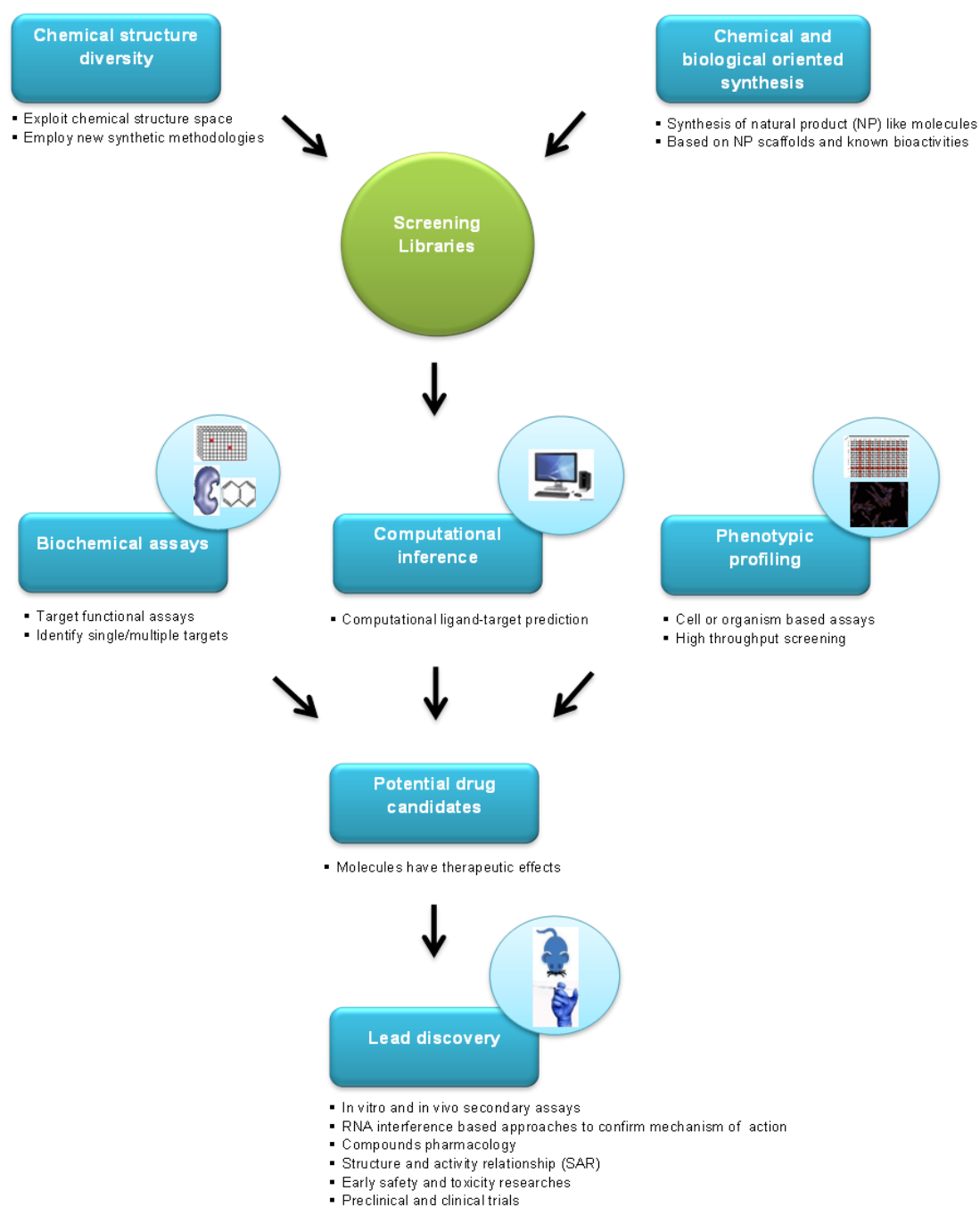
## **1.5 The importance of High Throughput Screening and Statistical analysis in Drug Discovery**

### **1.5.1 High throughput screening (HTS)**

Bioassays play four main roles in small molecule screenings (Suffness & Pezzuto, 1991). These are as prescreens, screens, monitors and secondary testings. In a pre-screen, large numbers of samples are assayed for their bioactivity. Characteristics of such bioassays are their high capacity and low cost, in terms of both time and reagents. Unlike pre-screens and bioassays, monitoring employed to isolate the pure bioactive constituents from initially crude materials are often quick, preferably and of high capacity. The reason to carry out bioassays in a screening is to select pharmacologically active molecules that are subsequently assessed in the secondary testing using multiple models and test conditions to find drug-like small molecules for development towards clinical trial. Such bioassays are relatively expensive, slow, and of low efficiency (Suffness and Pezzuto, 1991).

In drug discovery, in order to exploit compound bioactivities, efforts should be made to carefully design as many screening programmes as possible. To achieve this goal, there is a need for efficient integration of chemical and biological knowledge about a compound. A generalised overview of workflows for drug discovery is shown in **Figure 1.6**. Briefly, a library of small molecules selected based on chemical structure diversity and/or biological oriented synthesis. The next step is target identification that is performed by using a combination of direct biochemical assays, genetic or genomic methods or via computational inference methods. The outcome of this activity is the collection of potential drug candidates for follow-up intensive search of lead discovery

stage. Molecules that meet the requirement of secondary screenings, efficacy and low toxicity will advance to preclinical and if validated, clinical trials and eventually progress to the medicinal market (Schenone et al., 2013).



**Figure 1.6** An overview of workflows for drug discovery

While profiling the chemical structures of compounds has become progressively sophisticated, biological profiling of compounds has encountered difficulties in integrating large data sets of phenotypic profiles, chemical similarity and predicted protein-binding activity of active compounds. During recent decades, with major breakthroughs in technology in the search for novel bioactive compounds, high throughput screening (HTS) and HTS amenable techniques have been developed. Conventionally, a HTS strategy involves measuring a single phenotypic readout induced by large number of compounds under one set of conditions. On the contrary, a more recent technique, namely “cytological profiling” (CP) (Perlman et al., 2004, Mitchison, 2005, Lorang and King, 2005) has been developed to deal with multiple readouts under similar conditions, and binding activities across many proteins (Wagner et al., 2008, Clemons et al., 2010) and even multiple phenotypic readouts against many cell lines. Practically, CP is an unbiased image-based screening in which cells are visualized using biologically relevant markers in multi-well plate format with automated fluorescence microscopy. The resulting images are quantified into various descriptors, including, average value per well (overall fluorescence intensity in one well), distribution of measurement on individual cells (eg. nuclear or cell size) and texture of specific organelle (e.g. morphology of lysosome).

Several factors are crucial to the success of CP. Regardless of in-depth knowledge of underlying biology and chemistry, it begins with the selection of cell lines or tissues and their associated cellular features such as suspension or adherent culture, to fully interpret the phenotypic patterns elicited by small molecules. It is worth highlighting the importance of these confounding factors since they can be sources of variability in data analysis (Basu et al., 2013). This approach has been most evident in a genetic study, where Epstein-Barr virus (EBV) –transformed lymphoblastoid cell lines (LCLs) derived

from human B lymphocytes (International HapMap, 2005) against seven compounds with diverse mechanisms of toxicity resulted in insufficient statistical power due to non-genetic confounders like cell growth rate or EBV concentration for cell transformation. Thus, it became clear that more attention should be focused on the cell source used (Johannessen et al., 2015). Other important considerations of possible sources of noise and variability that can diminish assay performance are the position of individual samples within a plate, plate-to-plate variability, assay-to-assay variability and the edge effect. Artefacts can be generated from the position of individual samples within and across plates. To address this challenge, randomization of the sample placement within a plate in a systematic manner is ideal. Additionally, edge effects arise from quicker evaporation from outer wells allowing them to reach desired incubation temperature faster than the inner wells. One approach to minimize edge effect is the allocation of an equal number of positive and negative controls on each available row and column (the peripheral wells on plate) (Bray and Carpenter, 2004). Plate-to-plate variability often imposes constraints on assay design. To obtain valid results, assay controls should be run on every plate and where possible, both inter- and intra-plate replicate wells should be applied, as replicates reduce the false negative rate without rising incidence of false positives.

Over the past decades, a growing stream of studies focused on profiling has been published. Successful results from previous studies have supported the idea that phenotypic profiling is great tool to identify bioactive compounds against a number of cell lines. Other recent studies exploited profiling for mechanism of action (MOA) based on phenotypic fingerprint of the cells (Woehrmann et al., 2013, Schulze et al., 2013). The majority of studies in the 2000s mainly attempted to discover cell / small molecule interactions, while recent efforts to integrate profiling and human genetics,

particularly in cancer researches, have infused the literature. With the advent of genomic sequencing and genotyping, profiling of NCI-60 collection at transcriptional level across a set of 7000 genes was conducted (Staunton et al., 2001). A more intensive work also examined somatic gene copy number alteration and oncogenic mutations along with annotation of genomes of non-small cell lung cancer cell lines (Sos et al., 2009). Another application of CP has been the identification of resistance mechanisms in cancers. For example, explicit exploitation of malignant melanoma as a model system to study therapeutic resistance (Johannessen et al., 2013) and identification of several kinase mediators of resistance such as human epidermal growth factor 2 (HER2) inhibition (Moody et al., 2014) have demonstrated CP as a powerful tool for uncovering novel molecular drug targets for better cancer treatments.

## **1.6 The importance of statistics in drug discovery**

Approaches to drug discovery fall into two broad, but not mutually exclusive, categories, high throughput screening (HTS) and high content screening (HCS). Although no precise definitions of either are agreed upon, in general HTS was defined as a rapid examination of thousands of small molecules in a variety of *in-vitro* and cell-based assays using simplistic readouts for complex biological processes. Limitations of HTS include that molecular pathways leading to particular cellular phenotypic modifications are unknown. HCS, however, differs from HTS by including the examination multidimensional cytological features yielding more complex biological information, which in turn, provides greater detail of cellular responses to treatments (Varma H et al., 2011).

As technologies in the field of HTS mature, interests is now shifting to cytological profiling of large numbers of compounds in a timely and resource-efficient manner. Such profiling is considered a critical step in drug discovery and is expected to provide high quality data at the primary screening level. HTSs are mostly performed using 96 and 384 well microplate formats. As assay miniaturization technologies for small molecule have advanced, many liquid handling instruments currently used for HTS are now capable of routine handling a 1536 well nanoplate format. Despite their popularity, large data sets from HTS are typically subjected to data variability. Many researchers are struggling with interpretation, integration and decision making based on such data. It is suggested that potential sources of noise and random variability originate from technical or procedure failures such as batch, plate, measurement errors, positional effects and edge effects, and biological aspects such as differential cell growth, uneven cell response across plates. These favor false positives and false negative rates and ultimately lower the accuracy of the entire screening (Macarron et al., 2011, Shun et al., 2011). To address challenges of large, multidimensional datasets, a number of currently available statistical tools are employed. HTS data analysis often includes several steps: evaluation of assay quality, background correction, data normalization and hit detection.

Before any intensive analysis, more caution must be taken to ensure the available data in the study meet quality standards for HTS. In practice, the most widely used measurement to determine assay quality on a plate basis is the Z factor as it is simple and accounts for the variability of both compared groups, i.e. the distribution of sample and control signal at the same time, thus providing better representation of assay quality (Eq.1) (Zhang et al., 1999). The Z factor ranges from 0 to 1, which represents an ideal assay. Acceptable HCS assays for compound screening routinely have a Z factor ranging from 0 to 0.5 while for most HTS the Z factor must be greater than 0.5 (Bray



and Carpenter, 2004). Another accepted statistical coefficient that is utilized to evaluate the quality of HTS is the coefficient of variation (CV) which takes into account the number of wells per tested compound per concentration that are used in assay (Eq.2). The acceptance criteria is such that the CV of each signal must be less than or equal to 20% (Bray and Carpenter, 2004).

$$Z\ factor = 1 - \frac{3\sigma_s + 3\sigma_c}{|\mu_s - \mu_c|} \quad (1)$$

where  $\sigma_s$  and  $\mu_s$  are standard deviation and mean of sample; and  $\sigma_c$  and  $\mu_c$  are standard deviation and mean of controls.

Coefficient of variation is calculated by as follow:

$$CV = \frac{\sigma}{\mu} \times 100 \quad (2)$$

where  $\sigma$  and  $\mu$  are standard deviation and mean of either sample or control.

As cellular features are visualized using fluorescent dyes, the resulting images normally couple with foreground and background intensities. The overall intensity of the subject is defined as foreground, and background fluorescence is generally the ambient signals. The source of this noise primarily involves signals from non-specific hybridization of antibodies or dyes, excessive fluorescence from adjacent subjects, and technical failures such as deposits from incomplete washing steps, and the optical noise of the scanner. Attempts to exclude this non-specific signal are called background correction (BG). Prior to data normalization, unwanted signals is separated from total fluorescence by subtraction that is considered as traditional approach in data preprocessing methodologies (Koooperberg et al., 2002). Whereas, some have suggested that this

method amplifies the variance of expression ratios (Scharpf et al., 2007, Kooperberg et al., 2002), others have proposed different approaches to BG including a Bayesian strategy. In this approach high intensity ratios remain unchanged while decreasing low signal ratios (Kooperberg et al., 2002), variance stabilizing models that integrate additive components to avoid negative intensities (Durbin and Rocke, 2004), spatial smoothing methods by carrying out ordinary kriging (OK) or 2D LOWESS to smooth background values prior to applying a background correction algorithm (Schutzenmeister and Piepho, 2010).

A further step in data processing is the normalization strategy. The purpose of normalization is to remove systematic errors from datasets and to enable combination and comparison of different measurements in a screening. Many methods for normalization have been established (Malo et al., 2006). The percent of control (POC) (Eq.3) is a common approach that aims to resolve plate-to-plate variation by using compound relative to on-plate controls ratio. This method requires a relatively large number of controls and is greatly influenced by control outliers.

$$POC = \frac{x_i}{\mu} \times 100 \quad (3)$$

where  $x_i$  is the raw measurement of  $i^{\text{th}}$  compound and  $\mu$  is mean of all positive control measurements in an antagonist assay.

Another control-based method is normalized percent inhibition (Eq.4), which is calculated by dividing the difference between compound and mean of all positive controls to the difference between the means of positive and negative controls. It is not necessary to obtain many replicates for controls using this strategy.

$$NPI = \frac{\mu_+ - x_i}{\mu_+ - \mu_-} (4)$$

where  $x_i$  is the raw measurement of  $i^{\text{th}}$  compound and  $\mu_+$  and  $\mu_-$  are mean of all positive control measurements and all negative control measurements, accordingly, in an antagonist assay.

Z score (Eq.5), by contrast, does not take any control measurements into account and compound values are rescaled by subtracting the mean of the plate values and dividing the standard deviation of all measurements within plate. Nonetheless, Z score is sensitive to outliers that in view of HTS are potential hits. One way to improve precision is to replace mean and standard deviation in the Z score formula with median and median absolute deviation (Malo et al., 2006).

$$Z = \frac{x_i - \mu}{\sigma_x} (5)$$

where  $x_i$  is the raw measurement of  $i^{\text{th}}$  compound,  $\mu$  and  $\sigma_x$  is mean and standard deviation of all measurements within a plate.

The ultimate goal of any primary HTS is to identify better hits that are significantly different from negative controls. The output of this activity is the selection of active compounds for secondary screening. Despite a number of approaches having been developed, hit detection procedures seem to be influenced by the subjection of screeners rather than being based on formal models in decision of making process (Malo et al., 2006). Perhaps, one sample and multiple sample t-tests are the most common methods for hit detection. Other approaches are also currently in use for RNAi screening

including mean + or – k standard deviations, median + or – kMAD, quartile based selection, SSMD, rank product and Bayesian models (Birmingham et al., 2009).

Many confounding factors can influence the accuracy of HTS data. Various strategies have evolved to address this issue, including integration of replicates in primary screenings to facilitate the sensitivity and specificity of the screening processing and efforts on assay design to avoid plate related bias. However, in context of statistical methods, no single data processing method is effective for all HTS datasets. It is likely to be dependent on the purpose of the screening; a combination of different data analysis approaches may pave an avenue for providing high-quality data and yielding better primary hits.

## **1.7 Research Objective**

The objectives of this thesis are as follows:

- (1) Cytological profiling of the libraries of compounds that were synthesized based on natural products in order to determine if they have biological activities on multiple cellular components implicated in Parkinson's disease.
- (2) Determining if chemical similarity leads to similar biological activity.

To achieve this goal, an unbiased cell-morphology based screen was implemented against a patient-derived cellular model of PD. Specifically, to use human olfactory neuroepithelium derived (hONS) cells that express some functional and genetic discrepancy in a disease specific manner, to profile compounds based on quantifiable phenotypic features. This assay format was used to evaluate libraries of both pure NP and NP scaffold inspired synthetic compounds. Cellular phenotypes induced by each

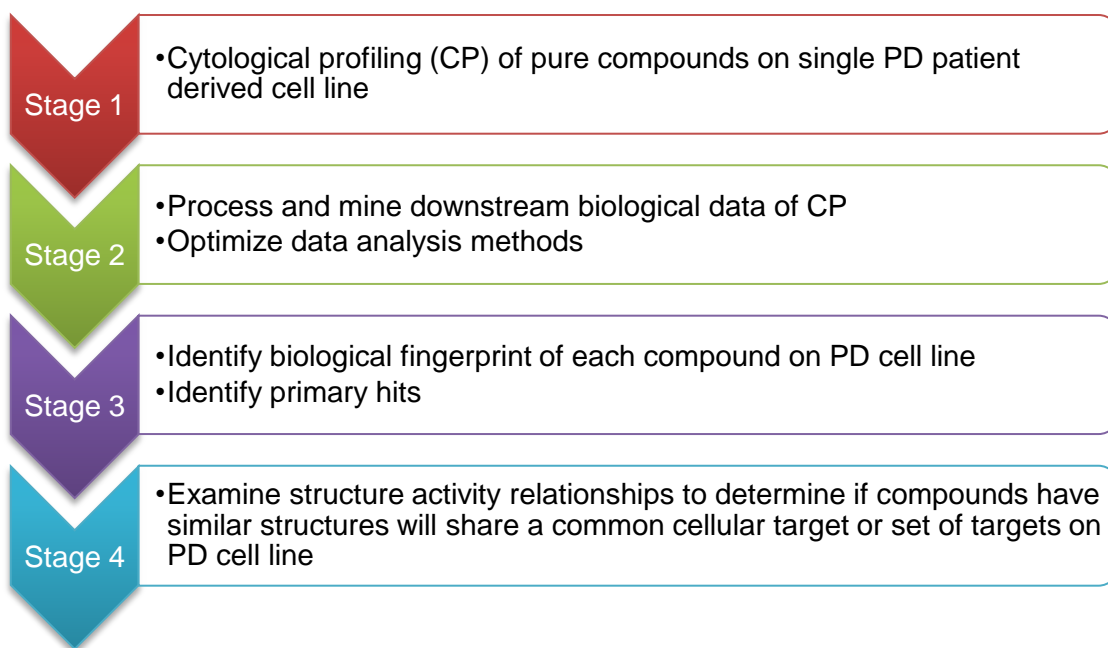
compound were quantified by multivariate statistical analysis of morphology and staining intensity of cells, nuclei, tubulin and autophagy. The screened compounds were then clustered based on their biological profiles. Analysis of structure activity relationship was performed to determine the relevance of biological profiles, if any, to their chemical space.

**CHAPTER 2**  
**MATERIALS AND METHODS**

## 2. MATERIALS AND METHODS

### 2.1 Experimental design – Overview

The general flow of cytological profiling (CP) of small molecules is shown in **Figure 2.1**. Overall, cytological profiling of small molecules was implemented against a single PD patient derived cell line that was established at the Eskitis Institute, Griffith University (Wang et al., 2016). Typically, CP screening generates gigabytes of images from which measurements are performed and numbers are extracted describing cell morphology and cellular components on a cell-to-cell basis. It requires sufficient methods for downstream data processing and mining of biological meaning from the data. Thus, the next step was to optimize data analysis methods that subsequently allow biological interpretation including identification of bioactive molecules on the PD cell line and examination of structure activity relationships for all compounds in the screening, to determine if compounds having similar structures share a common cellular target or set of targets.



**Figure 2.1** General flow of Cytological profiling of small molecules.

## 2.2 Description of hONS cells and their Culture

The olfactory epithelium is the epithelial layer typically located inside nasal cavity consisting of several cell types including olfactory receptor neurons, basal cells and supporting cells. The olfactory receptor neuron is considered as the most important cell type as it maintains the sense of smell. The olfactory receptor neuron is a bipolar cell, extending an unmyelinated neurite, whose apical surface undergoes knoblike protrusion to give rise into olfactory cilia, which extend into the mucus layer covering inner surface of the lumen of nasal cavity. The structures comprising the mucus layer produced by Bowman's glands, olfactory epithelium generated by basal cells and olfactory ensheathing cells supporting axon myelination and regeneration is called the olfactory mucosa (Purves et al., 2001, Mackay-Sim, 2010).

Olfactory receptor neurons are generated, from stem cells throughout life to replace the loss of old or injured neurons (Graziadei, 1973). Moreover, these cells are easily

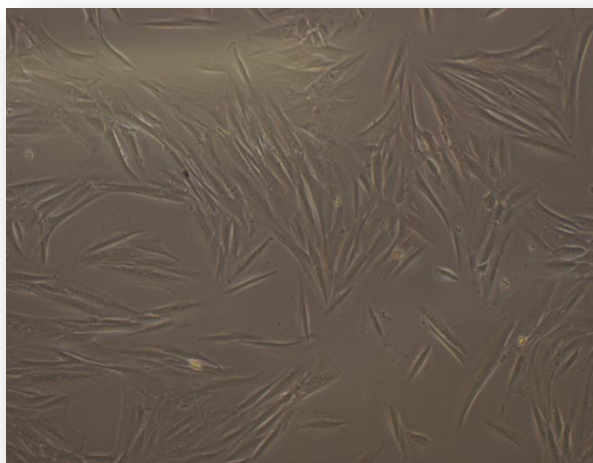


attained from biopsy of the human olfactory mucosa. These properties make olfactory epithelium an attractive source of biological materials for investigation of function in mature central nervous system as well as study of neurodegenerative diseases such as PD (Graziadei, 1973, Feron et al., 1999, Mackay-Sim and Silburn, 2008, Matigian et al., 2010a).

The PD patient derived olfactory neuroepithelium (ONS) cell line C1200080013 (**Figure 2.2**) used in this experiment was established at the Eskitis Institute under a protocol described and characterised previously (Féron et al., 1998, Matigian et al., 2010a). Initially, a frozen vial of adherent cells at passage two was thawed, grown in DMEM:F12 containing 10% FBS at 37°C and 5% CO<sub>2</sub>. At reaching 90% confluence, the cells were expanded sequentially from passage two to passage five. For each passage, the cells were banked down in aliquots after harvest and stored at -80°C in 90% FBS and 10% DMSO (vol/vol) (Refer to **Table 2.1** for information about cell culture reagents). Cells at passage six were used for all experiments in this study.

**Table 2.1** Reagents for cell culture

Reagents	Brand Name
DMEM:Ham F12 (1:1) (1X)	Gibco, Life Technology
FBS	SFBS, Bovogen
TrypLE™ Express (no phenol red)	Gibco, Life Technology
HBSS (1X)	Gibco, Life Technology
DMSO	Ajax Finechem



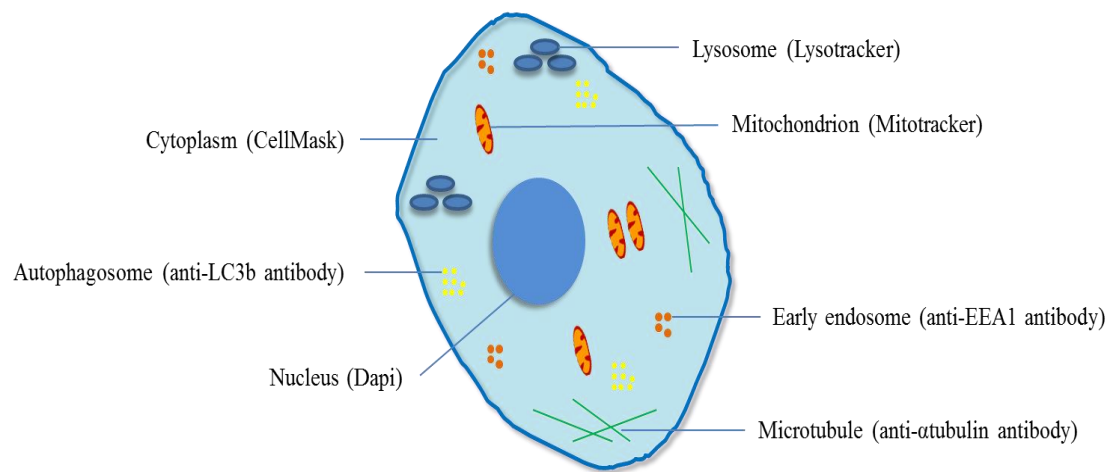
**Figure 2.2** The PD patient derived olfactory neuroepithelium (ONS) cell line C1200080013 at approximately 70% confluence.

### **2.3 Cytological profiling of natural products on PD patient derived cell line**

Cytological profiling of synthesized pure compounds based on several common natural products scaffolds was carried out under established protocol (Vial et al., 2016).

#### **2.3.1 Selection of cytological markers**

Parkinson's disease is a complex disorder that is associated with mitochondrial dysfunction, impairment of lysosomal function, and dysregulation of autophagy system. In order to determine compound induced effect on PD cells, we used cytological markers of these cellular organelles. DAPI and anti  $\alpha$ -tubulin were also employed to provide information about nucleus and cytoskeleton, respectively.



**Figure 2.3** Cytological markers for cytological profiling. There are seven cytological markers utilized in this experiment consisting of the nucleus (DAPI), the mitochondria (Mitotracker), the microtubule (anti- $\alpha$ tubulin antibody), the lysosome (Lysotracker), the early endosome (anti-EEA1 antibody), the autophagosome (anti-LC3b antibody), and the cytoplasm (CellMask).

DAPI preferentially stains AT rich region of double stranded DNA, thus providing information of DNA content and nuclear morphology (Kubista et al., 1987). Mitotracker<sup>®</sup> Orange CMTMRos is used to label active mitochondria in live cells. It accumulates in mitochondrial matrix upon passive diffusion across plasma membrane (Presley et al., 2003). Alpha-tubulin ( $\alpha$ -tubulin) is one of the components of microtubular system which is responsible for intracellular transport, cell division, and cytoskeleton (Bulinski et al., 1988). Lysotracker<sup>®</sup> Red DND-99 is used to label acidic organelles such as lysosome (Fogel et al., 2012). Early endosome antigen 1 is protein involved in endosome fusion (Lawe et al., 2002). Microtubule-associated protein light chain 3 (LC3) is important protein required for formation of autophagosome. It is used as marker to monitor autophagy and autophagy related processes (Schlafli et al., 2016). CellMask<sup>™</sup> Deep Red is commonly used as plasma membrane stain (Fenyvesi et al., 2014).

## **2.3.2 Preparation of stock solutions**

### *2.3.2.1 4% Paraformaldehyde (PFA)*

Fixation is crucial step in immunohistology in which the morphology of cells and cellular components are essential to provide information of interest. Fixation assists in preservation of cellular architecture and biochemical compositions in a life like state that is fundamental for following immunostaining steps. Paraformaldehyde (PFA) is the most widely used fixative (Wang et al., 2016). The molecular mechanism of cell fixation with PFA has not been well documented. It is determined that PFA is able to preserve structure and antigenic determinants of various cellular organelles. The key factor influencing fixation is pH, i.e. low pH solution will cause cell shrinkage while high pH will lead to cell swelling (Howat and Wilson, 2014, Thavarajah et al., 2012).

To prepare a stock solution, 700-800 ml of deionised water was prepared in a chemical baker and heated in microwave to achieve temperature of 55-57<sup>0</sup>C. Inside the fume hood, 40 grams of PFA powder were added into previously prepared warm water followed by addition of NaOH, to increase pH to approximately 8 and, subsequently placed on the heatplate with magnetic stir bar to facilitate dissolution. Until the solution was completely clear and cooled down at room temperature, 5 tablets of PBS (Sigma) were added. Deionised water was further added to make up 1 litre of 4% PFA solution. Solution pH was adjusted to 7.4. The stock was divided into aliquots and stored at -20<sup>0</sup>C for later use.

#### 2.3.2.2 Mitotracker® Orange CMTMRos

To label active mitochondria in live cells, Mitotracker® Orange CMTMRos was employed. This stain is derivative of tetramethylrosamine allowing it to be retained in mitochondria in subsequent processing such as fixation and permeabilization with detergent Triton X-100.

To achieve 1mM of stock solution, 117 µl of DMSO was added to dissolve lyophilized Mitotracker® Orange CMTMRos. Aliquots were prepared by dividing stock solution into eppendorf tubes, frozen at -20<sup>0</sup>C and protected from light. In experiments, 1mM stock solution was diluted to final working concentration in growth medium.

#### 2.3.2.3 DAPI

DAPI is a commonly used dye that specifically stains nucleic acid, particularly dsDNA and emits blue fluorescence. To prepare 5mg/ml stock solution, 10 mg of DAPI was reconstituted in 2 ml of deionized water. For long term storage, stock solution was aliquoted and kept at -20<sup>0</sup>C. DAPI stock solution was diluted in PBS to achieve final working concentration in experiment.

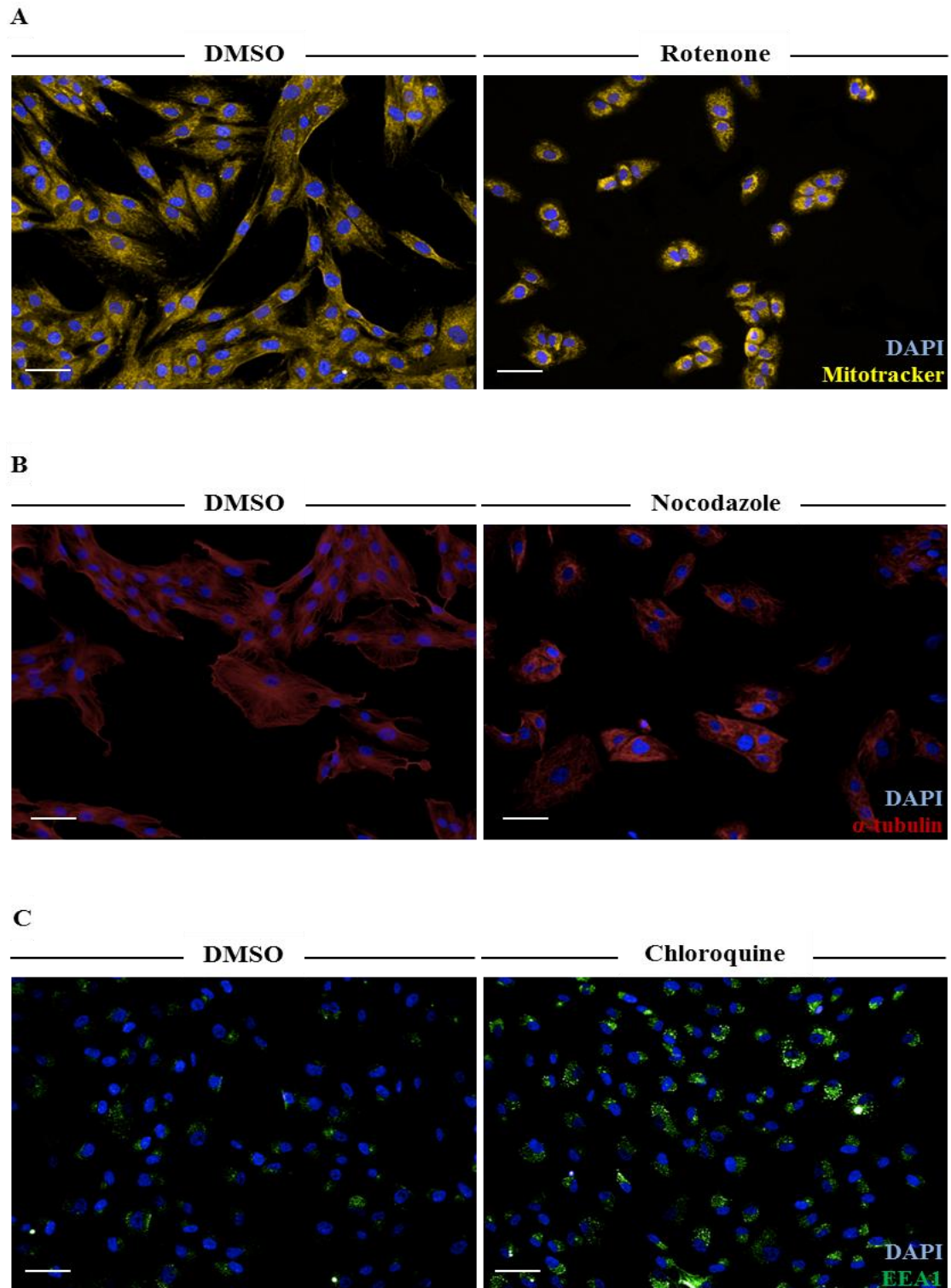
### 2.3.3 Compound transfer

We set out to screen and profile the biological activities of synthesized pure compounds based on several common scaffolds. These compound stocks at 5mM were submitted and stored in Compounds Australia (Eskitis Institute, Griffith University). For

biological assays, Compounds Australia processed and plated compounds at 300, 100, 30 and 10nL per well with all wells being backfilled to 300nL/well with DMSO, into CellCarrier™ 384 well plates (#6007550, PerkinElmer, Waltham, MA). Each plate contained each compound at four different concentrations 30µM, 10µM, 3µM, and 1µM.

Each plate also contained negative and positive controls. DMSO (0.6%) was utilized as negative control. Rotenone (20 µM, 0.6% DMSO), Chloroquine (10 µM, 0.6% DMSO) and Nocodazole (10 µM, 0.6% DMSO) were used as positive controls to ensure that employed stains and antibodies work correctly. Rotenone is botanical pesticide which is known as inhibitor of mitochondrial complex I (Tanner et al., 2011) (**Figure 2.4 A**). Nocodazole interferes with polymerization and function of microtubules (Baudoin et al., 2008) (**Figure 2.4 B**). Chloroquine inhibits the fusion of endosome and lysosome and subsequently disrupts cellular trafficking (Bodenstine et al., 2014) (**Figure 2.4 C**).

Assay layout will be discussed later in chapters 3 and 5.



**Figure 2.4** Examples of positive controls and negative control wells. Panel (A), (B), (C) Cells treated for 24h with Rotenone (20  $\mu$ M, 0.6% DMSO), Nocodazole (10  $\mu$ M, 0.6%), Chloroquine (10  $\mu$ M, 0.6%) and negative control (DMSO, 0.6%), respectively. Cells were then stained with DAPI (blue), Mitotracker (yellow), anti  $\alpha$ -tubulin (red), and anti-EEA1 (green).

### 2.3.4 Cell based assay

PD patient derived hONS cells were plated into 25 cm<sup>2</sup> flasks and cultured in DMEM/Ham F12 supplemented with 10% FBS. When they reached 90% confluence, the cells were harvested using 1 ml TrypLE<sup>TM</sup> Express and resuspended in 4ml of growth medium. Cell counts were performed using a haemocytometer (Blaubrand<sup>®</sup>). Cells were seeded at a density of 1350 cells per well in 50µl of Dulbecco's Modified Eagle Medium/ Ham F-12 (DMEM/F12) (Gibbco, Life Technology), containing 10% Fetal Bovine Serum (Bovogen) to achieve final compound concentrations of 1, 3, 10, and 30 µM, 0.6% DMSO. The cells were allowed to attach at 37<sup>0</sup>C, 5% CO<sub>2</sub> for 24 hours.

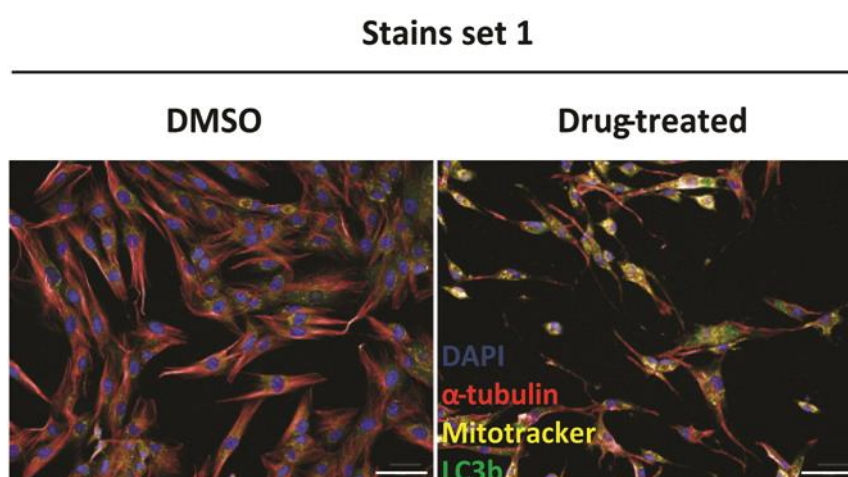
Each compound was subjected to two different sets of stains which are described in details as follows:

#### *2.3.4.1 Mitochondrial marker, α-tubulin and LC3b markers (autophagy markers) (stain set 1)*

Following 24 hours incubation, treatments were aspirated and the cells were stained with the Mitochondrial marker (Mitotracker<sup>®</sup> Orange CMTMRos) diluted in growth medium to 400nM (25µl) for 30 minutes at 37<sup>0</sup>C, 5% CO<sub>2</sub>. Aspiration of Mitotracker was followed by 5 minutes incubation of fixation PFA 4% at room temperature (RT). Two washings in PBS (25µl), 5 minutes for each washing, were carried out and non-specific binding was blocked with blocking solution (25µl) containing 0.2% Triton-X100, 3% Goat serum in PBS for 45 minutes at RT covered by aluminium foil. The next step was to incubate primary antibodies (25µl) (mouse anti- α-tubulin 1:4000,



rabbit anti-LC3b 1:335, 3% goat serum in PBS) for 1 hour at RT covered by aluminium foil. The cells were then washed twice as described above and secondary antibodies (25µl) (Alexa Fluor® 647 Goat anti-mouse IgG, 1:500, Alexa Fluor® 488 Goat anti-rabbit IgG, 1:500; 3% goat serum in PBS) were subsequently dispensed into each well. Following a further 30 minutes light-protected incubation at RT, two washings were conducted. Thereafter, the cells were further stained by addition of 25µl of nucleus marker solution (DAPI 1:5000). After 10 minutes incubation at RT, the cells were washed twice in PBS and ultimately left in 25µl of PBS. The plate was carefully covered by aluminium foil and kept at 4<sup>0</sup>C until imaging. Representative images of stain set 1 are shown in **Figure 2.5**.

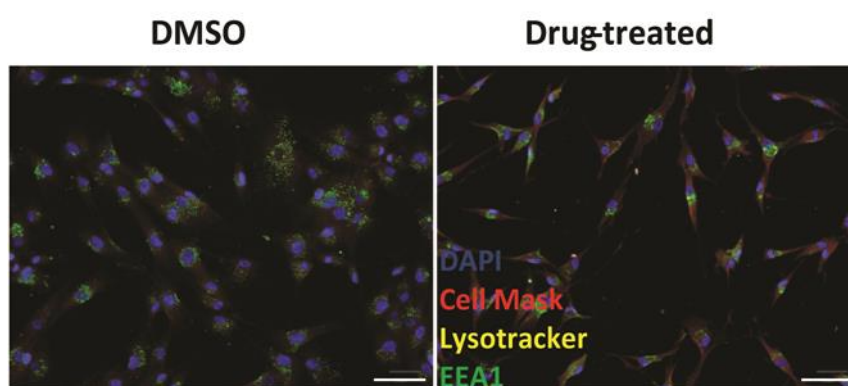


**Figure 2.5 Images of stain set 1.** Stain set 1 consists of cell nuclei marker (4', 6-diamidino-2-phenylindole; DAPI), tubulin stain (anti- $\alpha$  tubulin antibody), mitochondria stain (Mitotracker) and LC3b stain (anti LC3b antibody) which is related to autophagy. Scale bar is 50 µm.

#### 2.3.4.2 Lysosome marker, early endosome (EEA1) marker (stain set 2)

Treatments were removed after 24 hours incubation. Lysosome marker (Lysotracker® Red DND-99) diluted in growth medium to 100nM was transferred into each well (25µl). After 1 hour incubation at 37<sup>0</sup>C, 5% CO<sub>2</sub>, the cells were fixed by paraformaldehyde 4% for 5 minutes at room temperature. Two washings were performed as described above, then 25µl of blocking solution (0.2% Triton X100, 3% Goat serum in PBS) was added to each well and the plate was incubated at RT for 45 minutes, light-protected. A volume of 25µl of primary antibody (mouse anti- EEA1, 1:200 in PBS) was added and maintained for 1 hour at RT, aluminium covered, followed by two PBS washes. Afterwards, 30 minutes incubation of secondary antibody (Alexa Fluor® 488 Goat anti-mouse IgG, 1:500; 3% goat serum diluted in PBS) was conducted at RT, light-protected. Cells were washed twice with PBS before they stained with nucleus and cytoplasm markers (DAPI and Cell Mask, each 1:5000 in PBS) for 10 minutes followed by two additional PBS washes and subsequently coated in 25µl of PBS. The plate was carefully covered by aluminium foil and kept at 4<sup>0</sup>C. Representative images of stain set 2 are displayed in **Figure 2.6**

## Stains set 2



**Figure 2.6 Images of stain set 2.** Stain set 2 contains DAPI, Lysotracker, anti-EEA1 antibody, and cell mask for cell nuclei, lysosomes, early endosomes and plasma membrane, respectively. Scale bar is 50  $\mu\text{m}$ .

For more information about cell based assay reagent, refer to **Table 2.2**.

**Table 2.2** Reagents for cell based assay

	<b>Reagents (Supplier)</b>	<b>Final concentration</b>
<b>Fixation</b>	Paraformaldehyde (ProSciTech)	4%
<b>Washing</b>	Phosphate buffer saline tablet (Sigma)	1X
<b>Permeabilization</b>	Triton X100 (Sigma)	0.2 %
<b>and Blocking</b>	Goat serum (Sigma)	3%
<b>Staining</b>	Mitotracker® Orange CMTMRos (Invitrogen)	400nM
	Lysotracker® Red DND-99 (Invitrogen)	100nM
	Dapi (Invitrogen)	1:5000
	Cell Mask™ Deep Red (Invitrogen)	1:5000
<b>Primary antibodies</b>	Monoclonal mouse anti $\alpha$ -Tubulin (Sigma)	1:4000
	Monoclonal rabbit anti LC3b (Sigma)	1:335
	Monoclonal mouse anti EEA1 (Sigma)	1:200
<b>Secondary Antibodies</b>	Alexa Fluor® 647 Goat anti mouse IgG (Life Technology)	1:500
	Alexa Fluor® 488 Goat anti rabbit IgG (Life Technology)	1:500
	Alexa Fluor® 488 Goat anti mouse IgG (Life Technology)	1:500

### 2.3.5 Descriptions of cytological features

In this study, different cellular compartments were investigated using specific fluorescent probes. Given biological information extracted from segmentation of images obtained from two stain sets, 38 cytological parameters were generated as described in Table 2.3. DAPI was used to measure size and morphology of nuclei including seven parameters as follow: nucleus area, nucleus width, nucleus length, nucleus ratio width to length, nucleus roundness, nucleus texture and nucleus intensity. The cell area parameter was generated from two markers: anti  $\alpha$ -tubulin antibody in stain set 1 and CellMask in stain set 2. Other four parameters describing cellular morphology containing cell roundness, cell width, cell length, and cell ratio width to length were also obtained from anti  $\alpha$ -tubulin antibody. In addition, this marker was also used to identify other five parameters, *i.e.* tubulin marker texture, tubulin marker intensity, tubulin marker intensity in cytoplasm, tubulin marker intensity in outer region of cytoplasm and tubulin marker intensity in inner region of cytoplasm. Mitotracker® Orange CMTMRos was applied to characterize mitochondria properties comprising four parameters: mitochondria marker texture, mitochondria marker intensity, mitochondria marker intensity in outer region of cytoplasm, mitochondria in inner region of cytoplasm. From anti-LC3b antibody, four parameters was identified, namely LC3b marker texture, LC3b marker intensity, LC3b marker intensity in outer region of cytoplasm, LC3b in inner region of cytoplasm. Lysotracker® Red DND-99 was utilized to characterize four lysosome properties including lysosome marker texture, lysosome marker intensity, lysosome marker intensity in outer region of cytoplasm, lysosome in inner region of cytoplasm. The anti-EEA1 antibody generated ten parameters encompassing EEA1 marker texture, EEA1 spot signal in cytoplasm, EEA1 spot signal in outer region of cytoplasm, EEA1 spot signal in inner region of cytoplasm, number of

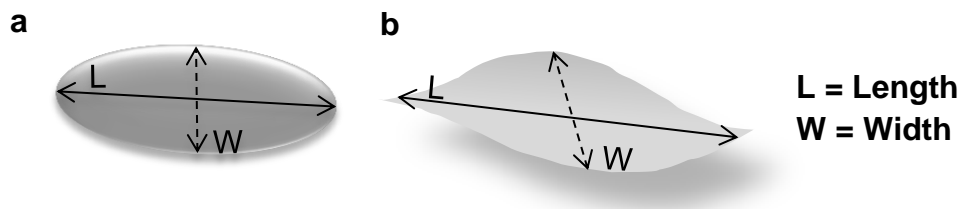
EEA1 spots in cytoplasm, number of EEA1 spots in outer region of cytoplasm, number of EEA1 spots in inner region of cytoplasm, number of EEA1 spots per area of cytoplasm, number of EEA1 spots per area of outer region, number of EEA1 spots per area of inner region.

**Table 2.3** List of investigated cytological features

#	Stains/Antibodies	Cytological features
1	DAPI	Nucleus texture
2		Nucleus intensity
3		Nucleus area ( $\mu\text{m}^2$ )
4		Nucleus morphology roundness
5		Nucleus morphology width ( $\mu\text{m}$ )
6		Nucleus morphology length ( $\mu\text{m}$ )
7		Nucleus morphology ratio width to length
8	Anti- $\alpha$ tubulin antibody	Cell area ( $\mu\text{m}^2$ )
9		Cell morphology roundness
10		Cell morphology width
11		Cell morphology length
12		Cell morphology ratio width to length
13		Tubulin texture
14		Tubulin intensity in cytoplasm region
15		Tubulin intensity in outer region
16		Tubulin intensity in inner region
17	Mitotracker <sup>®</sup> Orange CMTMRos	Mitochondria texture
18		Mitochondria intensity in cytoplasm region
19		Mitochondria intensity in outer region
20		Mitochondria intensity in inner region
21	Anti-LC3b antibody	LC3b texture
22		LC3b intensity in cytoplasm region
23		LC3b intensity in outer region
24		LC3b intensity in inner region
25	Anti-EEA1 antibody	EEA1 texture
26		EEA1 Marker Intensity in cytoplasm region
27		EEA1 Marker Intensity in outer region
28		EEA1 Marker Intensity in inner region
29		Number of EEA1 spots in cytoplasm region
30		Number of EEA1 spots per area of cytoplasm
31		Number of EEA1 spots in outer region
32		Number of EEA1 spots per area of outer region
33		Number of EEA1 spots in inner region
34		Number of EEA1 spots per area of inner region
35	Lysotracker <sup>®</sup> Red DND-99	Lysosome texture
36		Lysosome intensity in cytoplasm
37		Lysosome intensity in outer region
38		Lysosome intensity in inner region

### 2.3.5.1 Size and morphology of nuclei and cells

As listed in **Table 2.3**, these indexes are pixel areas that are reported by using specific fluorescent probes including DAPI, CellMask and  $\alpha$ -Tubulin. It is important to recognize size and shape of nuclei and cells that enable differentiation between healthy cells and diseased cells. Cell shape changes not only relate to specialized functions such as cell division and differentiation (Sheu et al., 2000), but also reflect cell behaviour in disease such as apoptosis (DeCoster et al., 2010). They are associated with measurements like area, roundness, width, length and ratio width to length (**Figure 2.7**).



**Figure 2.7** Size and morphology of nuclei and cells. Panels a and b show length and width of nucleus and cell respectively. Length feature is defined by the longest distance going from one end to the other end inside the cell. Similarly, width property is described by circle with largest diameter that fully fits into the cell.

### 2.3.5.2 Intensity of cellular components

Intensity is the amount of fluorescence accumulated in regions of interest inside the cells. Intensity descriptor is employed to reveal cellular states. For instance, intensity of nucleus is directly associated with cellular DNA content that is useful for cell cycle studies (Darzynkiewicz, 2011). Another example is intensity of LC3b protein that primarily reflects autophagy activity in which the formation of autolysosomes resulted from fusion of autophagosomes and lysosomes affects LC3b content (Mizushima et al.,



2010). Common measurements of intensity statistically consist of sum and mean of fluorescence containing area.

#### *2.3.5.3 Texture of cellular components*

Along with alteration of morphology and intensity, texture modification is also good indicator of biological effects of treatment. There is no strict definition of texture. Texture is a visual property of intensity distribution of an object, which normally involves in smoothness, coarseness, regularity, granulation, or spot (Gonzalez and Woods, 1992).

### **2.3.6. Imaging and image evaluation**

#### *2.3.6.1 Imaging*

Plates were automatically imaged using a 20X objective on the PerkinElmer Operetta® High Content Imaging System (PerkinElmer). Six images per well were captured for each staining and the properties of individual cells were measured on Mitotracker® Orange CMTMRos, Lysotracker® Red DND-99,  $\alpha$ -tubulin marker, LC3b marker, EEA1 marker, DAPI and CellMask.

#### *2.3.6.2 Image evaluation and data analysis*

Images were analyzed using Harmony 5.0 software by setting up analysis sequences that quantitatively measured and extracted biological features of cells and cellular

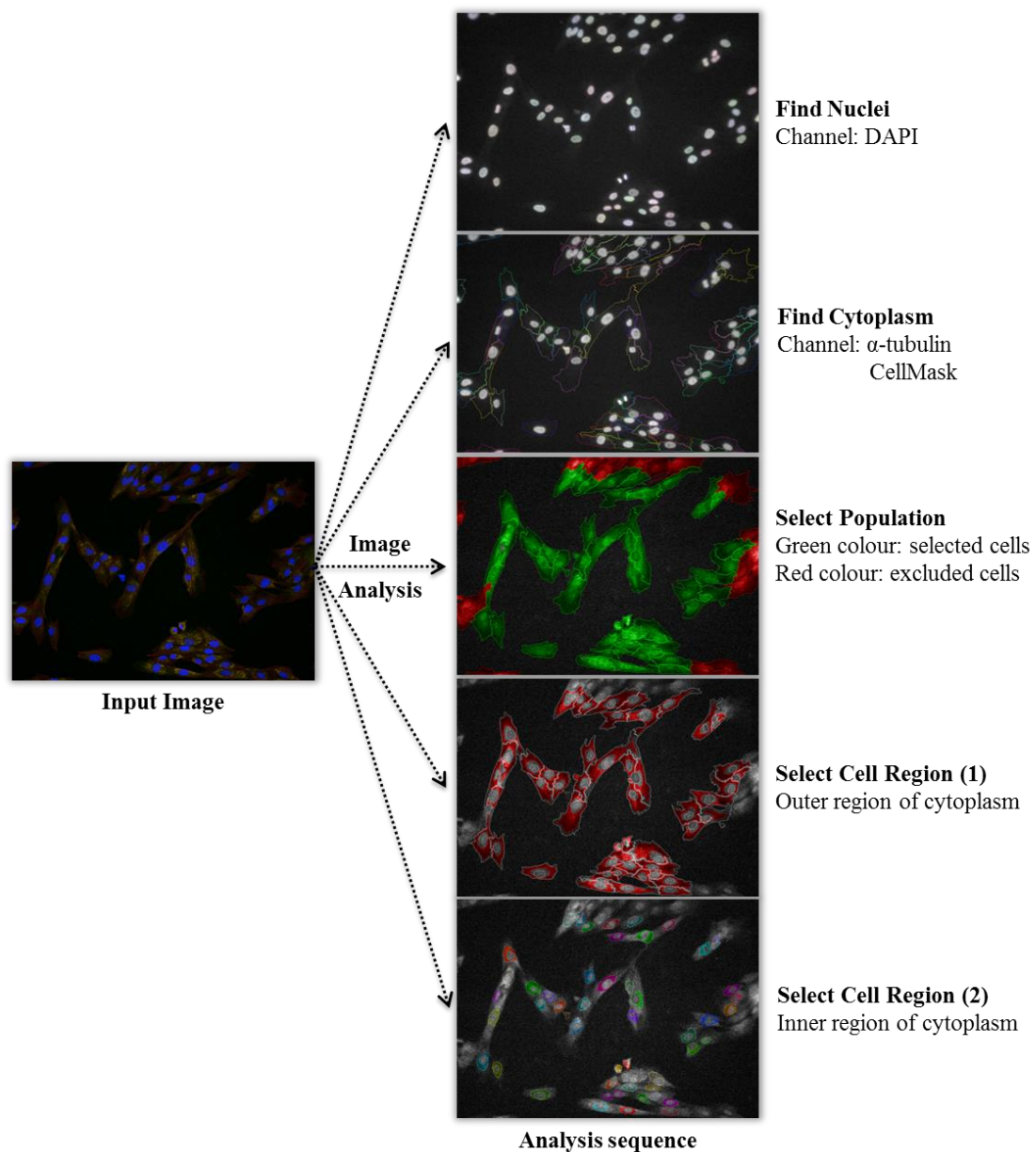
components following the size and shape of nuclei and cells, texture and intensity of nuclei, mitochondria, lysosome, tubulin, early endosome and autophagy protein LC3.

There are five analysis sequences were used for image evaluation. Three analysis sequences, *i.e.* nuclear and cellular analysis, texture analysis and intensity analysis were applied for stain set 1. Two analysis sequences including lysosome analysis and EEA1 analysis were employed for stain set 2. General analysis sequence is described in **Table 2.4**. Building blocks including Input Image, Find Nuclei, Find Cytoplasm, Select Cytoplasm, Select Population, Select Cell Region (1), Selected Cell Region (2), Calculate Morphologies Properties, Calculate Texture Properties, Calculate Intensity Properties were selected based on experimental requirement. Average of individual cells properties were exported as results of image analysis which subsequently entered downstream data processing. Examples of individual cell properties identified and analysed using building blocks are shown in **Figure 2.8**.

Data analysis process will be discussed in details in chapter 3 and chapter 5.

**Table 2.4** General image analysis sequence by Harmony 5.0.

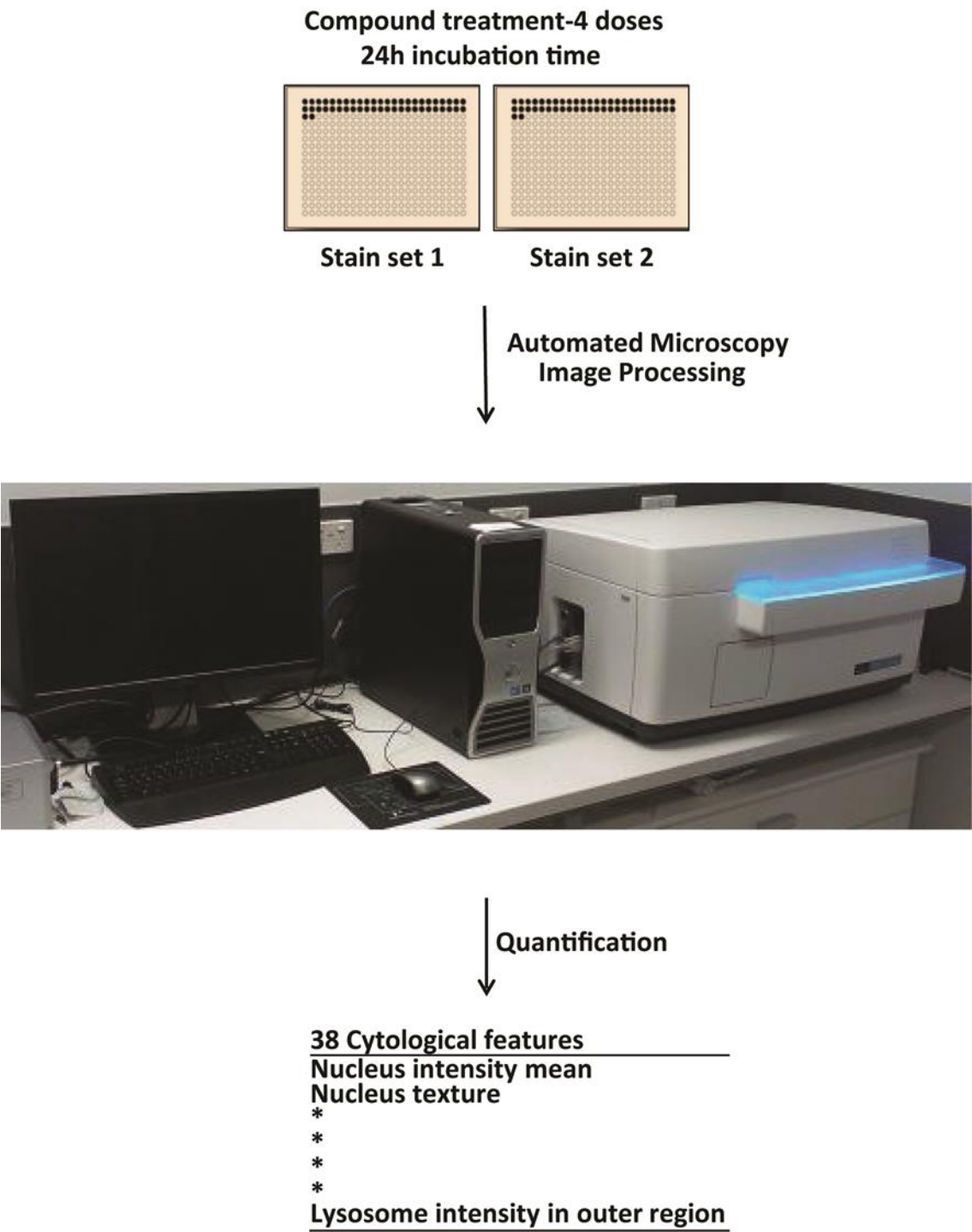
Input Image	
Stack Processing	Individual Plane
Flatfield Correction	Basic
Find Nuclei	
Channel	DAPI
Method	B
Common Threshold	0.65
Output Population	All nuclei
Find Cytoplasm	
Channel	AlexaFluor 647 ( $\alpha$ -tubulin and CellMask)
Population	All nuclei
Method	D
Individual Threshold	0.12
Select Population	
Population	All cells
Method	Common filters: remove border objects
Output Population	All cells selected
Select Cell Region (1)	
Population	All Cells Selected
Method	Resize Region (%)
Region Type	Cytoplasm Region
Outer Border	5%
Inner Border	25 %
Output Region	Outer Region
Selected Cell Region (2)	
Population	All Cells Selected
Method	Resized Region (%)
Region Type	Cytoplasm Region
Outer Border	25 %
Inner Border	50 %
Output Region	Inner Region
Calculate Morphology Properties	
Population	Nuclei or Cells Selected
Region	Nucleus or Cells
Method	Standard: area, roundness, width, length, ratio width to length
Calculate Texture Properties	
Population	Nuclei Selected
Region	Nucleus or Cytoplasm
Method	SER Spot 1 px
Calculate Intensity Properties	
Population	Nuclei Selected
Region	Nucleus or Cytoplasm
Method	Standard: Mean



**Figure 2.8** General view of image analysis by Harmony 5.0. Six images per well were captured by an automated microscope. Individual cells were segmented and analysed by using building blocks listed in Table 2.4 to identify nuclei, cytoplasm and different regions of cytoplasm. Cells at field or well boundaries (red colour) were excluded and cells in green were kept for further analysis. Consequently, 38 cytological features were generated for each cell. Scale bar is 50  $\mu$ m.

2.3.6 Overview of cytological profiling approach

Cytological profiling approach used in this study is generally described in Figure 2.9.



**Figure 2.9** Overview of cytological approach used in this study.

**CHAPTER 3**

**CYTOLOGICAL PROFILING OF SYNTHETIC COMPOUNDS ON  
PARKINSON'S DISEASE CELLS**

### **3. CYTOLOGICAL PROFILING OF SYNTHETIC COMPOUNDS ON PARKINSON'S DISEASE CELLS**

#### **3.1 Introduction**

Parkinson's disease (PD) is the second most common neurodegenerative movement disorder, affecting approximately 3 % of the over 65 years old population (Moghal et al., 1994). However, no disease modifying therapeutics has been effective and, current drugs only temporarily relieve symptom severity. Although these medications effectively ameliorate symptoms at early stages, long term treatment does not halt disease progression and commonly promotes the development of other complications (Vlaar et al., 2011). Due to the complexity of this disease etiology, it is crucial to develop innovative approaches, which are capable of identifying new chemical entities for managing disease and/or reversing damage associated with PD.

High throughput screening (HTS) has emerged as rapid and powerful tool for classifying large numbers of chemicals and their biological activities as potential candidates for follow-up pharmacological validation. Notably, the majority of current HTS are cell based assays. Approaches combines HTS technologies and modern automated microscopy systems, namely cytological profiling, have allowed screens using multi-well plate formats, analysis of multiple cellular components simultaneously and automated imaging microscopy. Subsequently, image based quantification is performed on a cell-to-cell basis in order to identify changes in cytological features based on the quantity of fluorescence as well as morphology. In this study, a library of 193 synthetic compounds (Krasavin, 2013, Krasavin, 2012, Taheri et al., 2014) was

screened using a patient-derived PD cellular model to determine compounds induced biological effects on cellular compartments implicated in PD. Furthermore, biological profiles of active molecules were explored to determine their relevance, if any, to their chemical space.

## **3.2 Materials and methods**

### **3.2.1 Compound library**

We screened and profiled 193 synthetic compounds. All compounds were determined by LC/MS to be at least 90% pure. Compounds were dissolved in DMSO to generate a stock concentration of 5mM. These compounds were submitted and stored in micro-tubes the Compounds Australia (Griffith University, Nathan).

### **3.2.2 Compound transfer**

Refer to **Section 2.3.3** in **Chapter 2**

Assay layout is shown in **Figure 3.1** with column 1, 2, 23 and 24 containing negative and positive controls.



	1	2	3	4	5	6	7	8	9	10	11	12	13	14	15	16	17	18	19	20	21	22	23	24
A	DMSO 0.6 %	Rot	Sample 1 (30,10,3,1 uM)				Sample 17 (30,10,3,1 uM)				Sample 33 (30,10,3,1 uM)				Sample 49 (30,10,3,1 uM)				Sample 65 (30,10,3,1 uM)				DMSO 0.6 %	Rot
B	DMSO 0.6 %	Rot	Sample 2 (30,10,3,1 uM)				Sample 18 (30,10,3,1 uM)				Sample 34 (30,10,3,1 uM)				Sample 50 (30,10,3,1 uM)				Sample 66 (30,10,3,1 uM)				DMSO 0.6 %	Rot
C	DMSO 0.6 %	Rot	Sample 3 (30,10,3,1 uM)				Sample 19 (30,10,3,1 uM)				Sample 35 (30,10,3,1 uM)				Sample 51 (30,10,3,1 uM)				Sample 67 (30,10,3,1 uM)				DMSO 0.6 %	Rot
D	Rot	DMSO 0.6 %	Sample 4 (30,10,3,1 uM)				Sample 20 (30,10,3,1 uM)				Sample 36 (30,10,3,1 uM)				Sample 52 (30,10,3,1 uM)				Sample 68 (30,10,3,1 uM)				Rot	DMSO 0.6 %
E	Rot	DMSO 0.6 %	Sample 5 (30,10,3,1 uM)				Sample 21 (30,10,3,1 uM)				Sample 37 (30,10,3,1 uM)				Sample 53 (30,10,3,1 uM)				Sample 69 (30,10,3,1 uM)				Rot	DMSO 0.6 %
F	Rot	DMSO 0.6 %	Sample 6 (30,10,3,1 uM)				Sample 22 (30,10,3,1 uM)				Sample 38 (30,10,3,1 uM)				Sample 54 (30,10,3,1 uM)				Sample 70 (30,10,3,1 uM)				Rot	DMSO 0.6 %
G	Chlor	Noco	Sample 7 (30,10,3,1 uM)				Sample 23 (30,10,3,1 uM)				Sample 39 (30,10,3,1 uM)				Sample 55 (30,10,3,1 uM)				Sample 71 (30,10,3,1 uM)				Chlor	Noco
H	Chlor	Noco	Sample 8 (30,10,3,1 uM)				Sample 24 (30,10,3,1 uM)				Sample 40 (30,10,3,1 uM)				Sample 56 (30,10,3,1 uM)				Sample 72 (30,10,3,1 uM)				Chlor	Noco
I	Chlor	Noco	Sample 9 (30,10,3,1 uM)				Sample 25 (30,10,3,1 uM)				Sample 41 (30,10,3,1 uM)				Sample 57 (30,10,3,1 uM)				Sample 73 (30,10,3,1 uM)				Chlor	Noco
J	Noco	DMSO 0.6 %	Sample 10 (30,10,3,1 uM)				Sample 26 (30,10,3,1 uM)				Sample 42 (30,10,3,1 uM)				Sample 58 (30,10,3,1 uM)				Sample 74 (30,10,3,1 uM)				Noco	DMSO 0.6 %
K	Noco	DMSO 0.6 %	Sample 11 (30,10,3,1 uM)				Sample 27 (30,10,3,1 uM)				Sample 43 (30,10,3,1 uM)				Sample 59 (30,10,3,1 uM)				Sample 75 (30,10,3,1 uM)				Noco	DMSO 0.6 %
L	Noco	DMSO 0.6 %	Sample 12 (30,10,3,1 uM)				Sample 28 (30,10,3,1 uM)				Sample 44 (30,10,3,1 uM)				Sample 60 (30,10,3,1 uM)				Sample 76 (30,10,3,1 uM)				Noco	DMSO 0.6 %
M	DMSO 0.6 %	Chlor	Sample 13 (30,10,3,1 uM)				Sample 29 (30,10,3,1 uM)				Sample 45 (30,10,3,1 uM)				Sample 61 (30,10,3,1 uM)				Sample 77 (30,10,3,1 uM)				DMSO 0.6 %	Chlor
N	DMSO 0.6 %	Chlor	Sample 14 (30,10,3,1 uM)				Sample 30 (30,10,3,1 uM)				Sample 46 (30,10,3,1 uM)				Sample 62 (30,10,3,1 uM)				Sample 78 (30,10,3,1 uM)				DMSO 0.6 %	Chlor
O	DMSO 0.6 %	Chlor	Sample 15 (30,10,3,1 uM)				Sample 31 (30,10,3,1 uM)				Sample 47 (30,10,3,1 uM)				Sample 63 (30,10,3,1 uM)				Sample 79 (30,10,3,1 uM)				DMSO 0.6 %	Chlor
P			Sample 16 (30,10,3,1 uM)				Sample 32 (30,10,3,1 uM)				Sample 48 (30,10,3,1 uM)				Sample 64 (30,10,3,1 uM)				Sample 80 (30,10,3,1 uM)					

**Figure 3.1** Plate format for compounds on 384 well plate. Negative control (DMSO, 0.6%) and positive controls including Rotenone (Rot), Chloroquine (Chlor), and Nocodazole (Noco) were included on each plate.

### 3.2.3 Cell based assay

Refer to **Section 2.3.4** in **Chapter 2**

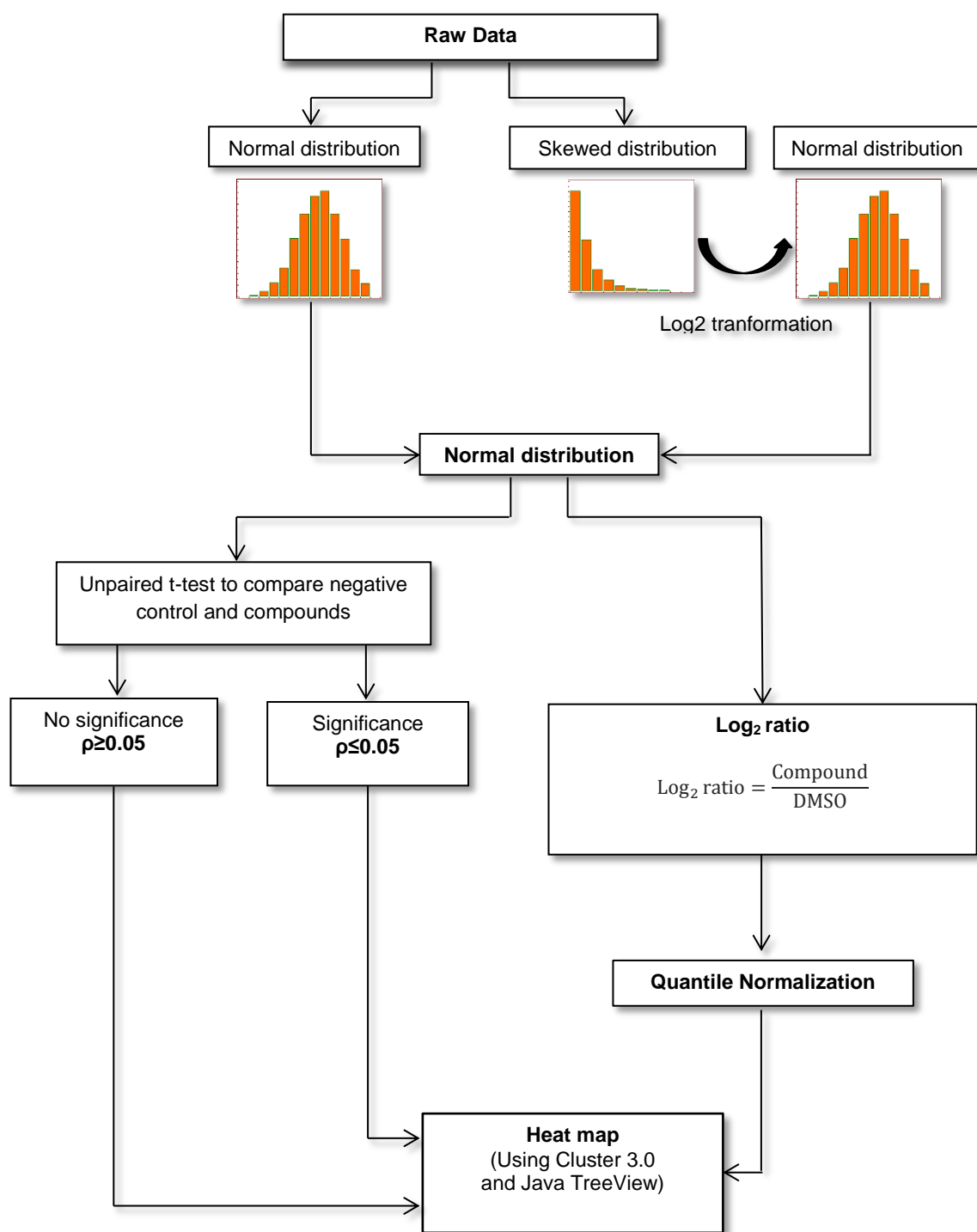
### 3.2.4. Imaging and image evaluation

Refer to **Section 2.3.6** in **Chapter 2**

### 3.2.5 Data analysis

#### *3.2.5.1 Overview of data analysis process*

Overview of data analysis process is shown in **Figure 3.2**. Briefly, distribution of each cytological feature's raw data was explored and cytological features with skewed distributions were transformed to obtain normal distributions, which are required for subsequent stages of analysis. Downstream data processing involved the following steps: 1. Unpaired t-test was performed to compare which compound-treated samples were significantly different from negative controls. 2. Concurrently, computation of the  $\log_2$  ratio of compound relative to negative control. 3. Hierarchical clustering of biological responses and generation of heat map to visualize biological profiles of compounds.



**Figure 3.2** The flow from raw data to reported results in cytological profiling.

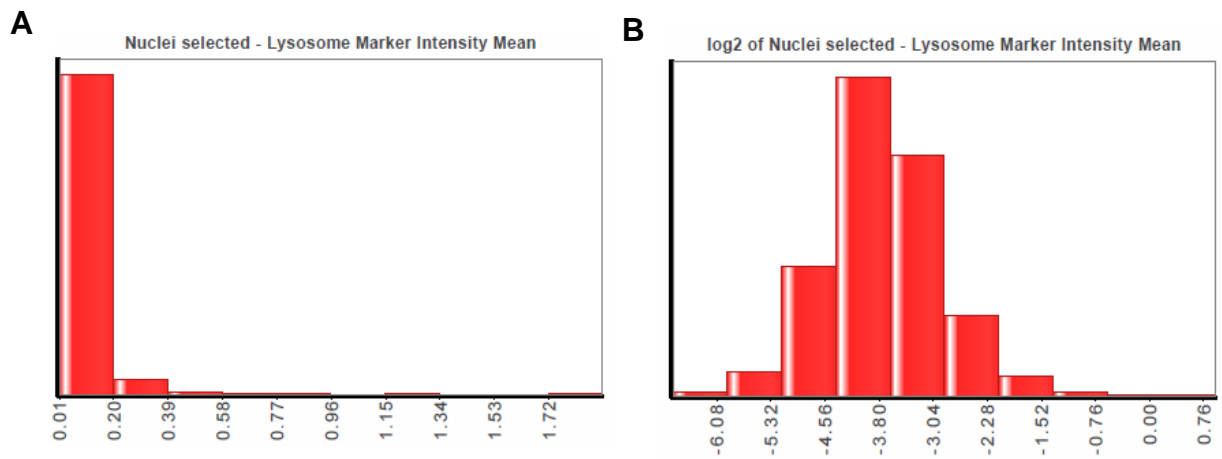
### 3.2.5.2 Normalization of raw cytological scores for a single cell

Depending on the cell area, the raw intensity for each cell will fluctuate. Therefore, it is necessary to normalize raw intensity of a single cell, **I**, for its morphological area. Normalized intensity, **Z**, is expressed as:

$$\mathbf{Z} = \frac{\mathbf{I}}{\text{Cell Area } (\mu\text{m}^2)}$$

### 3.2.5.3 Transformation of raw data

Generally, cytological profiling of compounds is based on an integrated set of morphological features of many individual cells. Given the non-parametric nature of profiles obtained from these features, quantitatively different data type' analysis requires a strategy that enables comparison of changes in cytological features among compounds. Moreover, with this data type, it can be reliable on p-Values computed from two sample t-test for meaningful evaluations that is designed for Normal distribution. For these purposes, distribution of each feature was examined and binary transformations (log base 2) were performed for non-parametric features, **T**, with  $\mathbf{T} = \log_2(\mathbf{Z}^{\text{np}})$  and np denotes non-parametric feature. An example of the distribution of lysosome marker intensity mean before transformation and after transformation is shown **Figure 3.3**. Parameters required log<sub>2</sub> transformation after examination for normality is shown in **Table 3.1**.



**Figure 3.3** Distribution of Lysosome marker intensity mean parameter. (A) Distribution of raw data is non-parametric. (B) In order to correctly perform downstream data processing, raw data is transformed using binary logarithm.

**Table 3.1** List of parameters required log<sub>2</sub> transformation

No.	Parameters
1	Nucleus Marker Texture
2	Nucleus Area ( $\mu\text{m}^2$ )
3	Nucleus Roundness
4	Cell Roundness
5	Cell Ratio Width to Length
6	Tubulin Marker Texture
7	Tubulin Marker Intensity in Cytoplasm
8	Tubulin Marker Intensity in Outer Region
9	Tubulin Marker Intensity in Inner Region
10	Mitochondria Marker Texture
11	Mitochondria Marker Intensity in Cytoplasm
12	Mitochondria Marker Intensity in Outer Region
13	Mitochondria Marker Intensity in Inner Region
14	LC3b Marker Texture
15	LC3b Marker Intensity in Cytoplasm
16	LC3b Marker Intensity in Outer Region
17	LC3b Marker Intensity in Inner Region
18	Lysosome Marker Texture
19	Lysosome Marker Intensity in Cytoplasm
20	Lysosome Marker Intensity in Outer Region
21	Lysosome Marker Intensity in Inner Region
22	EEA1 Marker Texture
23	EEA1 Marker Intensity in Cytoplasm
24	EEA1 Marker Intensity in Outer Region
25	EEA1 Marker Intensity in Inner Region
26	Number of EEA1 Marker Spots per area of Cytoplasm
27	Number of EEA1 Marker Spots per area of Outer Region
28	Number of EEA1 Marker Spots per area of Inner Region

#### *3.2.5.4 Raw cytological values for a single well*

For each feature, the raw cytological value  $\mu_m$  was calculated as the average of all individual cell values in  $m$ , where  $m$  is a single well.

The intra-plate variability of the assay was assessed by computing percentage of coefficient of variation (%CV) of 24 negative control wells (DMSO controls).

#### 3.2.5.6 Comparison between well scores and negative control

193 compounds were screened over 6 different plates. Negative control (DMSO) wells were present in each plate. We denote  $\mu_{\text{DMSO}}$  as the average of all individual cell values in DMSO. To biological effects of compounds in comparison with negative control (DMSO control),  $\log_2$  of compound to DMSO ratio was performed,  $C_1$  for every cytological feature was calculated using Equation.1, apart from those which required transformation (See **Table 3.1**) in the previous step were calculated as  $C_2$  (Equation 2).

$$C_1 = \log_2 \left( \frac{\text{compound}}{\text{DMSO}} \right) = \log_2 \left( \frac{\mu_m}{\mu_{\text{DMSO}}} \right) \text{ (Eq. 1)}$$

$$C_2 = \log_2(\mu_m^T) - \log_2(\mu_{\text{DMSO}}^T) \text{ (Eq. 2)}$$

#### 3.2.5.7 Two sample unpaired t-test

To test for statistically significant differences between negative control DMSO and compound phenotypes, two sample unpaired t-tests were employed.

**Null hypothesis  $H_0$ :  $\mu_W = \mu_{\text{DMSO}}$ ;**

The null hypothesis claims that the mean of compound treated cell population of values is not significantly different from the mean of control cell population of values ( $p > 0.05$ ).

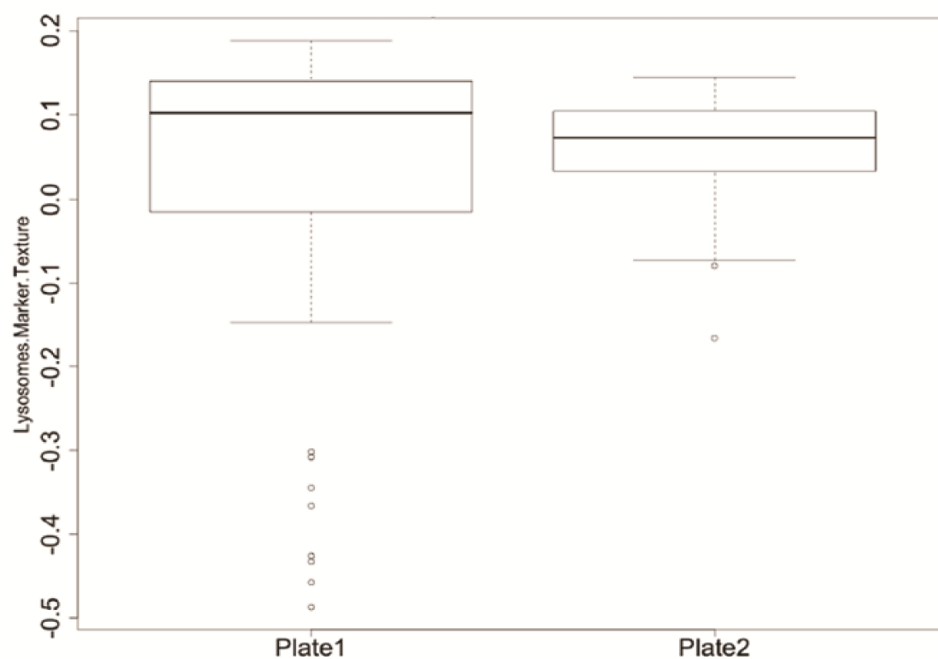
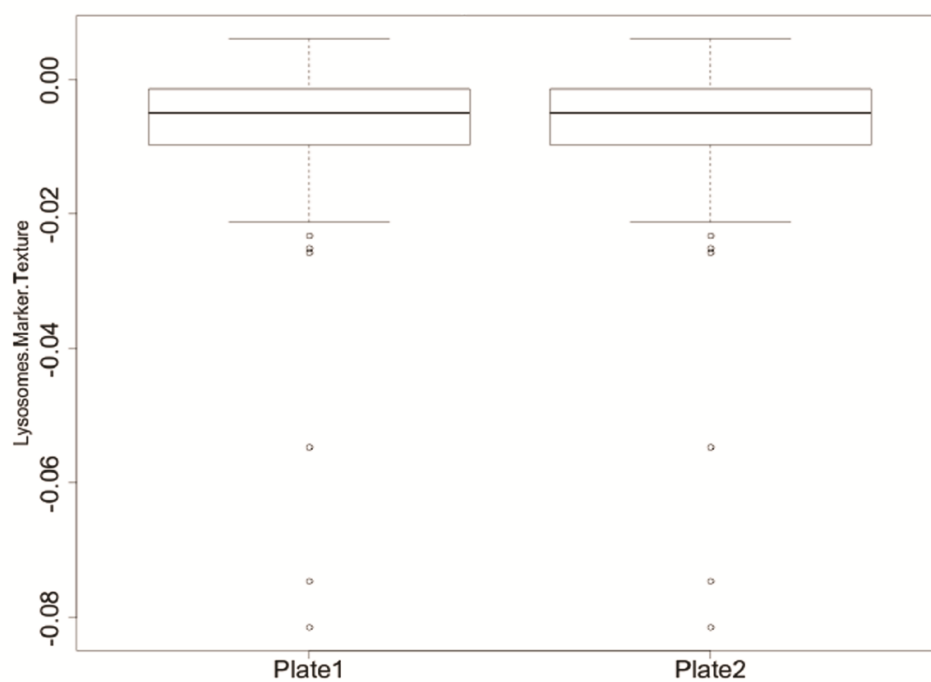
### **Alternative hypothesis $H_a$ : $\mu_W \neq \mu_{DMSO}$**

In the alternative hypothesis, when undergoing compound treatments, cells exhibit significantly different phenotypes from cells in control. A p-Value is used to measure the strength of the evidence against null hypothesis. The null hypothesis is rejected if p-Value is less than or equal to 0.05.

#### *3.2.5.8. Quantile normalization for inter-plate comparison*

We applied quantile normalization for our downstream data processing to make distribution of cytological feature in different plates within the experiment the same. This method is based on the assumption that cytological feature distributions are expected to remain constant across plates (Bolstad et al., 2003). Moreover, it also can be used to effectively remove plate effects. As shown in **Figure. 3.4**, there is great variation across compound dose instances for lysosome marker texture between plate 1 and 2 before normalization while the distributions are identical following quantile normalization. This technique was performed for all cytological features in order to facilitate data comparison across plates.



**A****B**

**Figure 3.4** Box plot displaying distribution of Lysosome marker texture across plates. Data are represented as logarithm base 2 ratio of compound relative to DMSO. Panels (A) and (B) are distributions of lysosome marker texture before and after quantile normalization, respectively.

#### 3.2.5.9 Hierarchical clustering

Hierarchical clustering was performed using Cluster 3.0 (centroid linkage and uncentered Pearson correlation coefficient) and Java<sup>TM</sup> TreeView. Clusters were defined by identifying nodes at which the Pearson correlation coefficient was greater than 0.6 (indicating similarity of biological profiles).

Data analysis was performed using Pipeline Pilot (version 9.1), R studio (version 3.0), GraphPad Prism (version 6.0), Cluster 3.0 and Java<sup>TM</sup> TreeView.

### 3.3. Results

#### 3.3.1 Intra-plate Variation

Coefficient of variation (CV) between the negative control wells (DMSO control) was used to measure intra-plate variation.

In our instance, 193 compounds were screened across 6 different plates. Compounds showed CV greater than 20% (33 compounds) were eliminated from further analysis. The remaining 160 compounds were kept for hierarchical clustering.

#### 3.3.2 Chemical Library

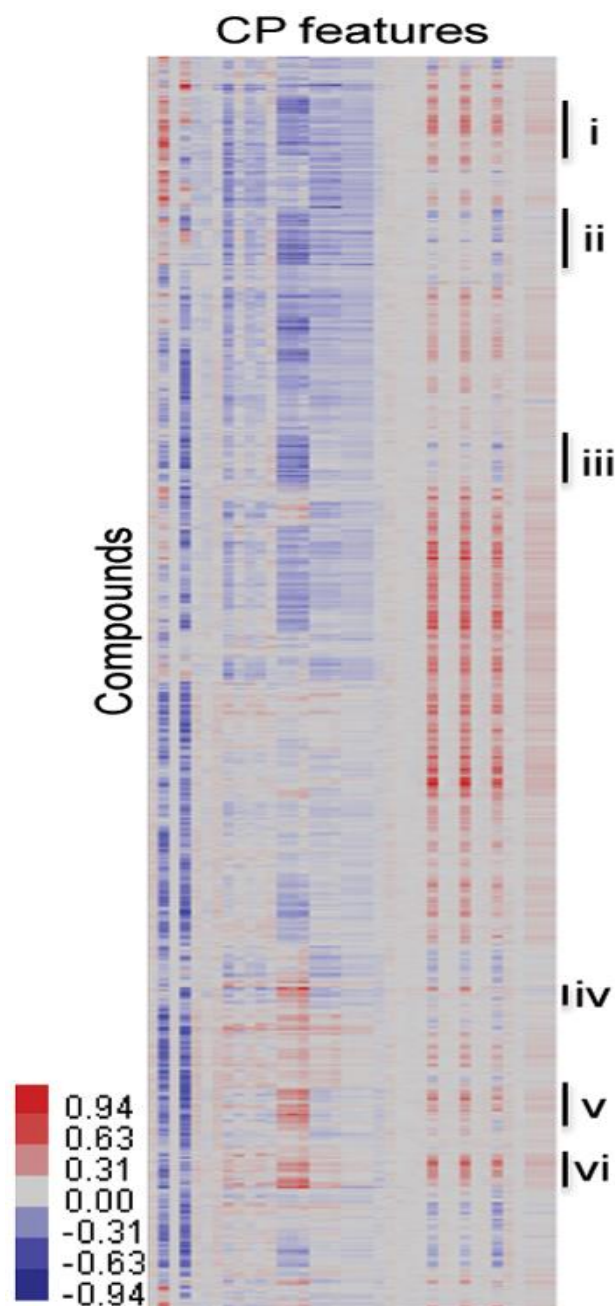
A library of 160 synthetic compounds, that are close structural analogs, were screened for biological activity profiles. The synthetic compound collection offers the advantage of reducing the false negative rate since compounds were derived from a limited number of basic scaffolds. Thus, potential non-identification of an active compound (false-negative) was minimized if other, related compounds were determined

(Rydzewski, 2008). More importantly, the use of structurally related compounds offers the advantages of acquisition of structure-activity relationship directly from primary screening supporting the development of new synthetic methodologies for improving selectivity of addressable biological targets in future library design.

### 3.3.3 Cytological Profiling Screen

#### 3.3.3.1 Hierarchical clustering of 160 compounds

Hierarchical clustering of biological activity profiles of 160 compounds at four concentrations was performed using centroid linkage. The dendrogram revealed six prominent bioclusters exhibiting strong phenotypes (strong negative or positive deviation from DMSO control) (**Figure 3.5**). Example of a compound cytological profile is shown in **Figure 3.6**. Compound is active if its cytological features are significantly different that of DMSO control ( $p < 0.05$ ). Notably, there were two distinctive morphology spaces (*i.e* negative deviation from controls in bioclusters i, ii, iii while positive deviation was observed in bioclusters iv, v, vi for tubulin intensity).



**Figure 3.5** Hierarchical clustering of cytological profiles using Pearson correlation Heat map displays 160 compounds at four concentrations each, with individual compounds on the y axis and individual cytological features on x axis. Red features indicate positive deviation from control (positive values from zero), blue features indicate negative deviation from control (negative values from zero), and grey features show no difference with control (values equal zero).



**Figure 3.6** Example of a compound cytological profile. Each cytological profile contains information about individual cell properties (*i.e.* 38 parameters generated from image segmentation and analysis).

One of the most noticeable bioclusters was biocluster i. This biocluster showed positive deviation from control wells for nucleus intensity, nucleus roundness and the number of spots of early endosomes in different regions of cytoplasm and also strongly negative deviation for cell area, tubulin intensity while weakly negative effect on mitochondria and LC3b intensity. Although sharing the similar morphology space to biocluster i, compounds in biocluster ii had only a minor or no effect on cell area and early endosomes. Biocluster iii contained compounds that predominantly induced reduction of nucleus intensity, nucleus roundness and tubulin intensity.

Generally, bioclusters iv, v, vi were phenotypically similar to each other, with the exception of several features that described cell morphology including cell area, roundness, width, length and ratio width to length. Moreover, these clusters exhibited

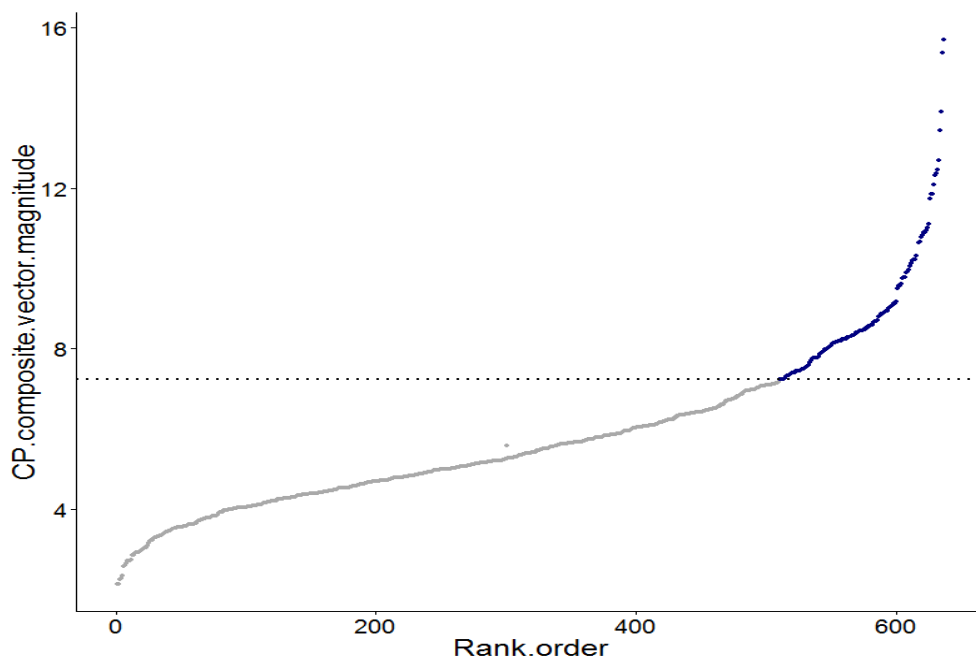
opposite effects on tubulin intensity and nucleus intensity and roundness. Biocluster iv displayed a positive deviation for tubulin intensity and also negative deviation for nucleus roundness and cell morphology. Compounds in biocluster v and vi caused increased number of spot in different regions of early endosome and cell morphology but decreased nucleus intensity.

In addition, weak phenotypes inducing compounds were identified in the heat map (**Figure 3.5**). In this study, we focused only on compounds exhibiting strong phenotypes, therefore weak phenotypes were excluded in the next section (**Section 3.3.3.2**).

#### *3.3.3.2 Weak phenotype removal*

In this study, we focused only on compounds exhibiting strong phenotypes, therefore weak phenotypes were excluded using a method as previously described (Woehrmann et al., 2013). This technique computes the distance between negative controls and each compound dose instance (each compound was tested at four doses, each dose is called compound dose instance), thereby, providing effective measurement of compound overall effects across multidimensional cytological features and facilitating the identification of potent compounds. As a result, only the strong compound dose instances (top 20% with cytological profiling (CP) vector magnitudes  $\geq 7.23$ ) were retained in our analysis (**Figure 3.7**). To confirm discarded compound dose instances were weak phenotypes, we compared the above results with biological profiles in the heat map (**Figure 3.5**). We found that those biological profiles belonged to grey, light pink and light blue coloured regions of the heat map, indicating weak biological activity. In addition, toxic samples identified by low cell count (less than 20% of initial

cell number) after treatment were discarded. This resulted in the further elimination of 3 toxic compounds (compound 26\_1, 22\_1 and 55\_2) at their highest concentration (30  $\mu$ M). Overall, we focused our analysis on 127 compound dose instances (95 compounds) accounting for 59% of the library

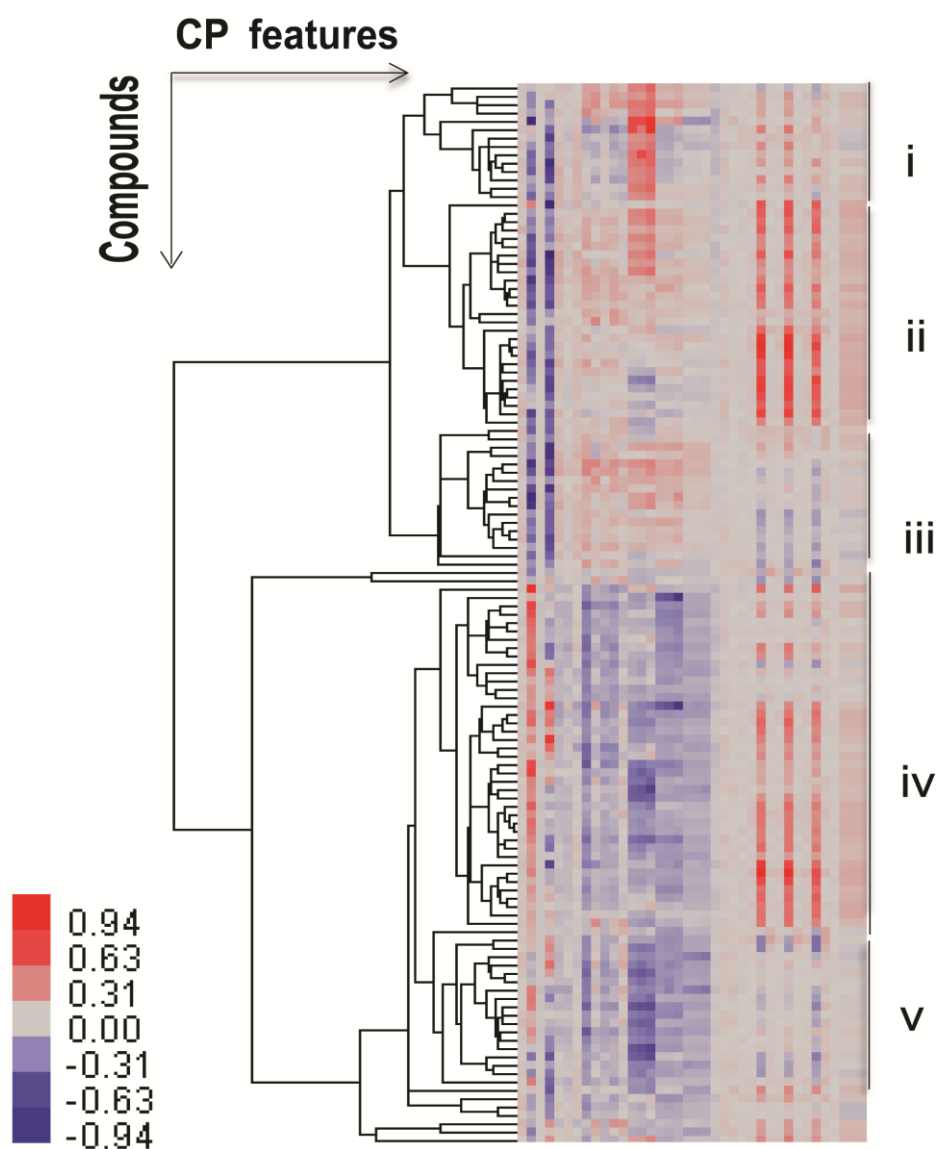


**Figure 3.7** Identification of compounds inducing weak phenotypes. Compound dose instances below cutoff (grey colour) were excluded from further analysis. Compound dose instances were non-toxic and above the cutoff (blue colour) were retained.

#### *3.3.3.3 Hierarchical clustering of 127 compound dose instances*

After weak and toxic phenotypes were removed, hierarchical clustering of 127 compound dose instances was again performed and heat map was generated (**Figure 3.8**).



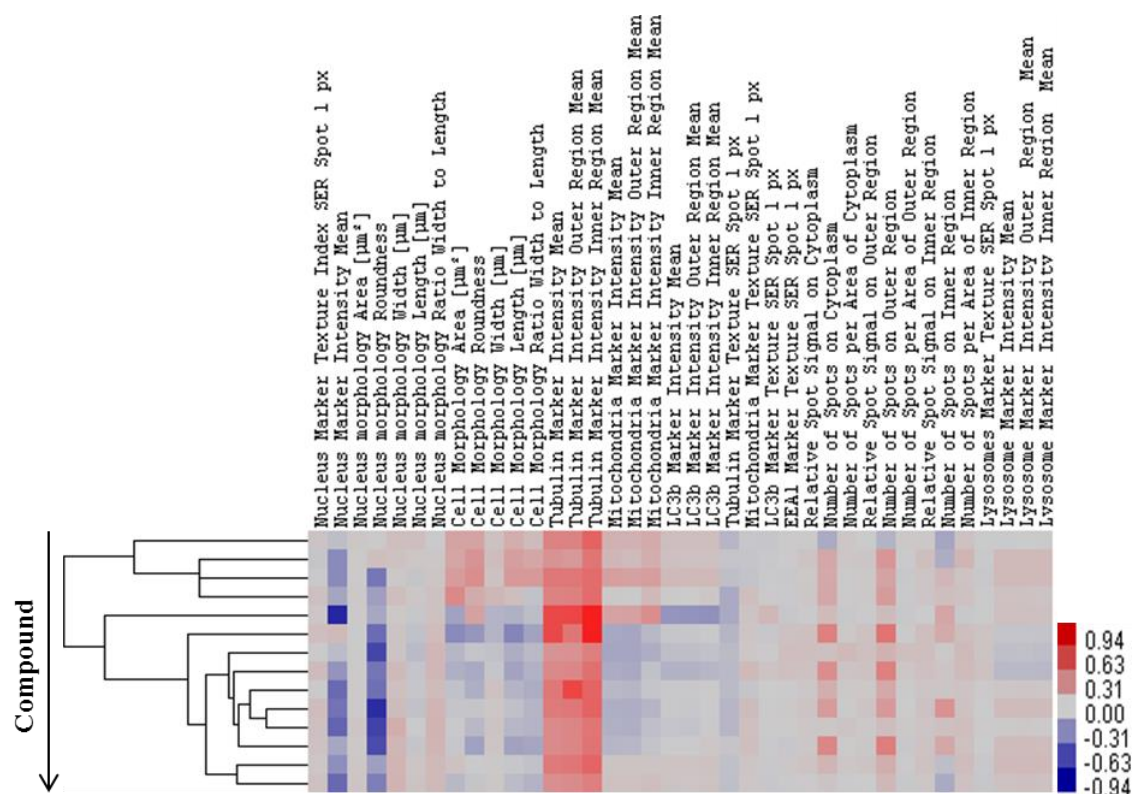


**Figure 3.8** Heat map of 127 compound dose instances plotted on the y axis and 38 cytological features on x axis. Cytological features and their arrangement are the same as described in Figure 3.6. Red features indicate positive deviation from control, blue features indicate negative deviation from control, and grey features show no difference with control.

In the above heat map, two dominant response patterns of screened compounds were readily identifiable. Bioclusters i, ii and iii had distinguishable phenotypes resulting from changes in nucleus morphology (*i.e.* nucleus intensity and roundness; negative deviation from DMSO control) and tubulin intensity (positive deviation). In addition, these bioclusters showed negative deviations in nucleus intensity and roundness while positive deviations in tubulin intensity. On the other hand, opposite patterns were observed in bioclusters iv and v which exhibited positive deviations in nucleus intensity and negative deviations in majority of cytological features. Interestingly, biocluster iii phenotypically contrasted to biocluster v, with the exception of features that describe the number of spots in early endosome and lysosome intensity. Detail of each biocluster is described as follows:

### **Biocluster 1**

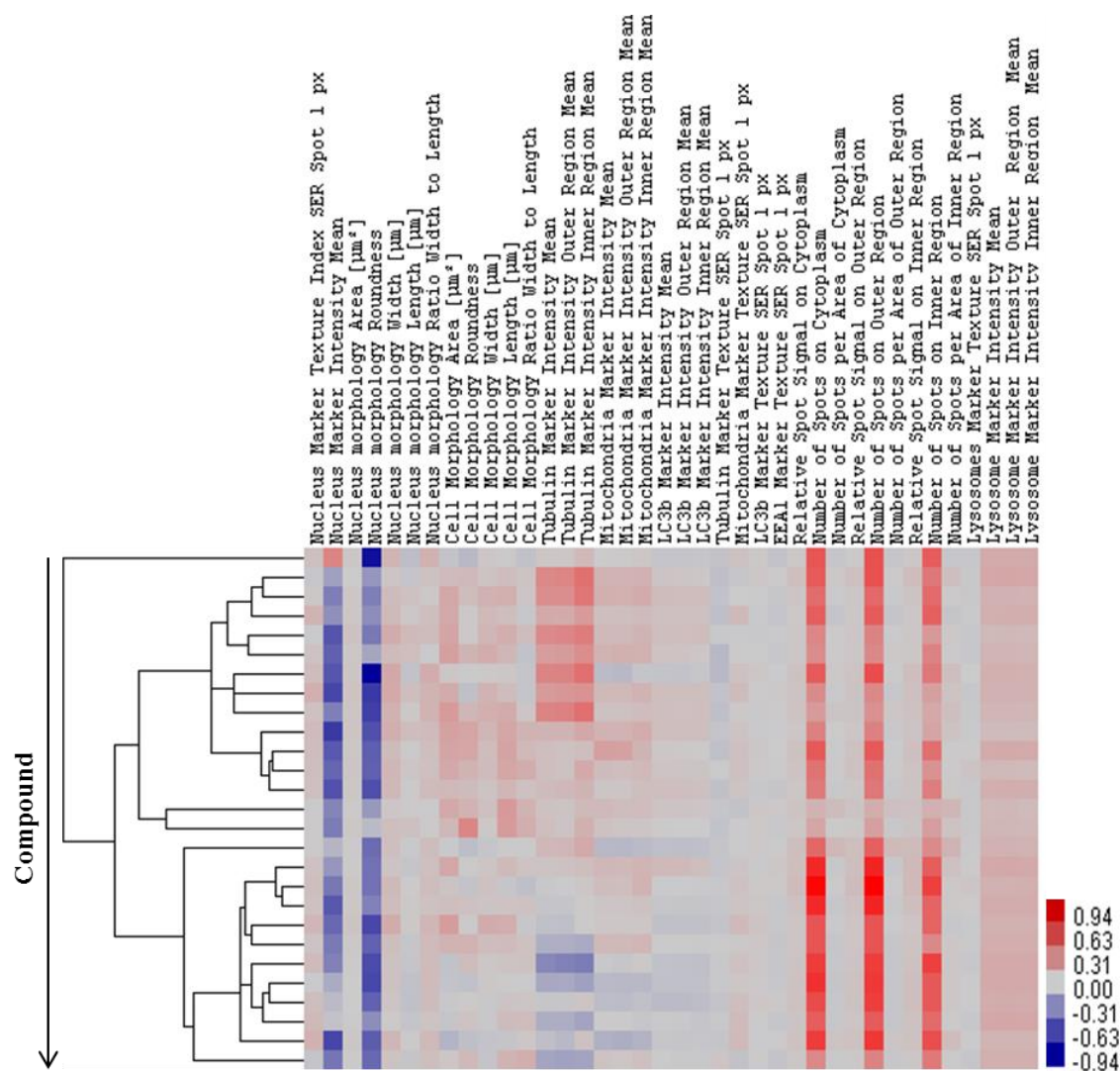
Biocluster 1 contained 14 compound dose instances, which predominantly displayed negative deviation from DMSO control in nucleus texture and nucleus roundness; and positive deviation in tubulin intensity in cytoplasm, tubulin intensity in outer region and tubulin intensity in inner region (**Figure 3.9**).



**Figure 3.9** Heat map of biocluster 1. Heat map depicting cytological profiles of compound dose instances located in biocluster 1 with compounds on y axis and cytological features on x axis.

## Biocluster 2

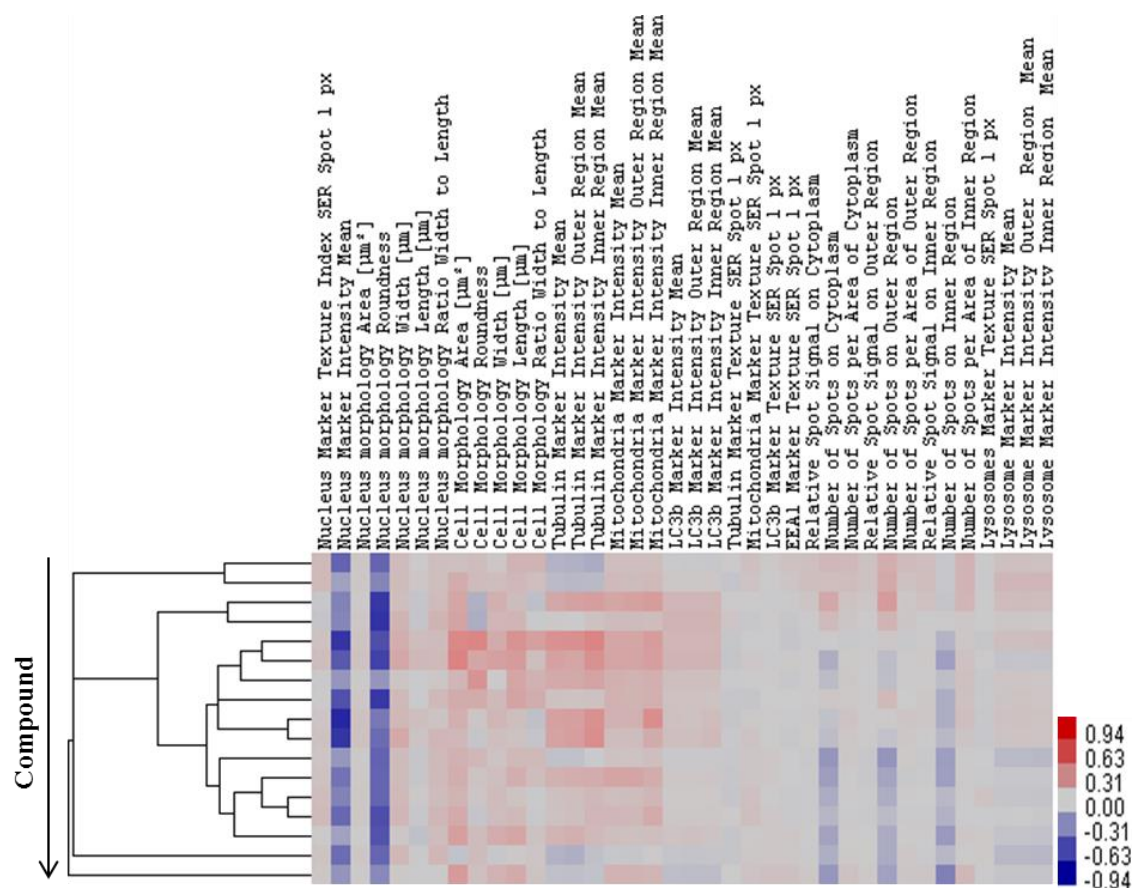
Biocluster 2 consisted of 27 compound dose instances which exhibited negative deviation in nucleus texture, nucleus roundness. These compounds were also associated with positive deviation in number of EEA1 spots in cytoplasm and different regions of cytoplasm (**Figure 3.10**)



**Figure 3.10** Heat map of biocluster 2. Heat map depicting cytological profiles of compound dose instances located in biocluster 2 with compounds on y axis and cytological features on x axis.

### Biocluster 3

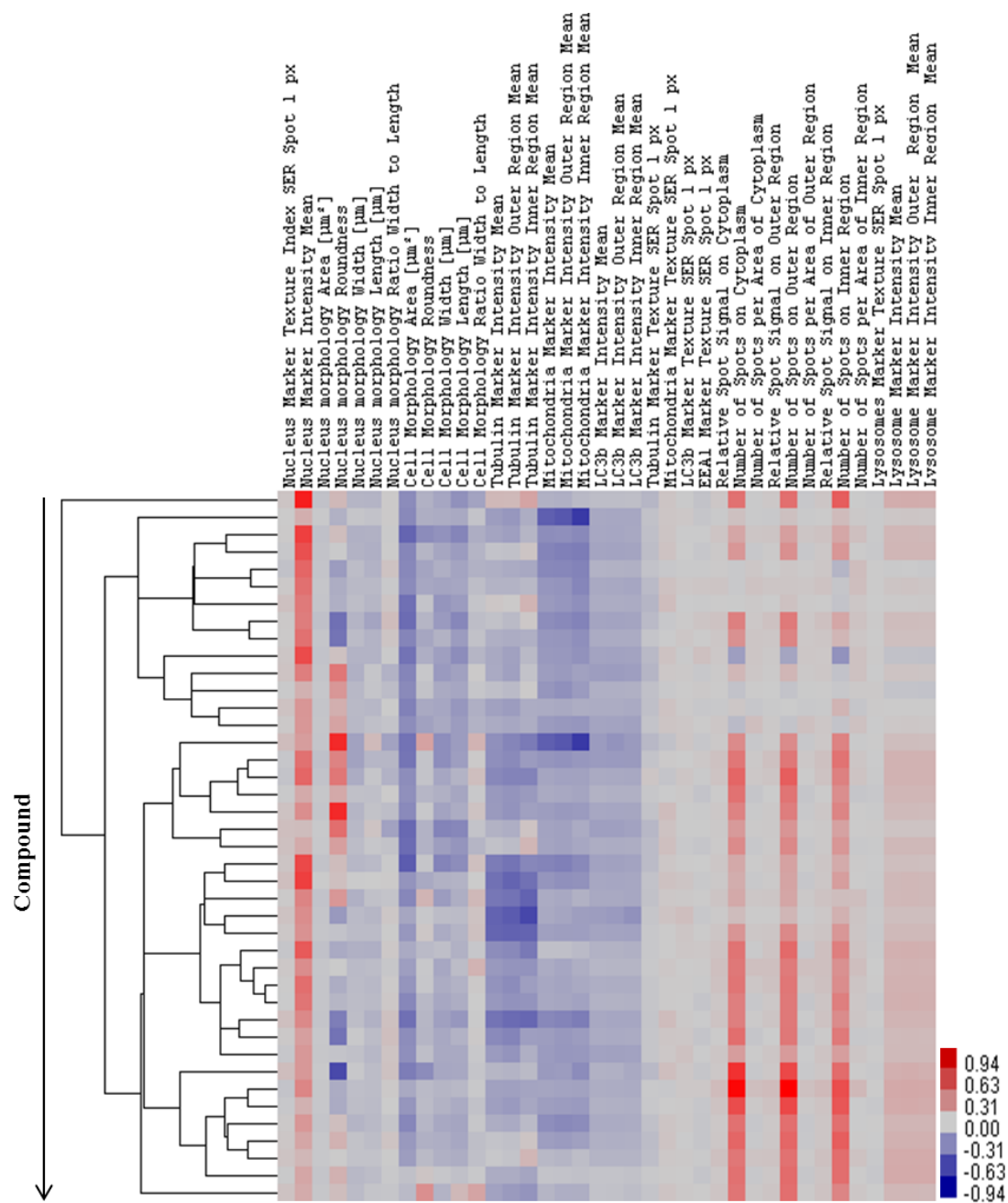
Biocluster 3 comprised of 17 compound dose instances which predominantly produced negative deviation in nucleus texture and nucleus roundness (**Figure 3.11**).



**Figure 3.11** Heat map of biocluster 3. Heat map depicting cytological profiles of compound dose instances located in biocluster 3 with compounds on y axis and cytological features on x axis.

#### Biocluster 4

41 compound dose instances were grouped into biocluster 4, which induced positive deviation in nucleus intensity and number of EEA1 spots in cytoplasm and different regions of cytoplasm while giving effects on cell morphology and intensity of tubulin, mitochondria and LC3b in cytoplasm and different regions of cytoplasm in negative direction (**Figure 3.12**).

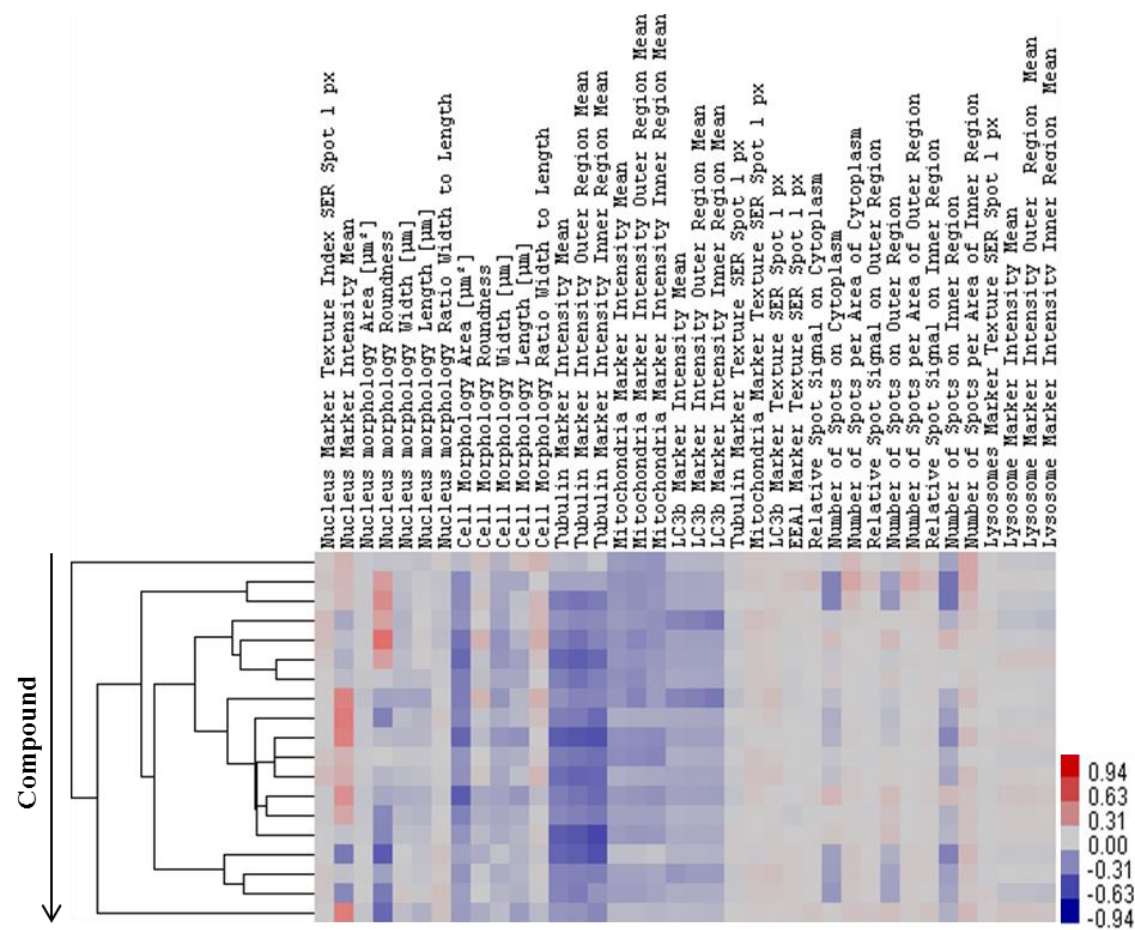


**Figure 3.12** Heat map of biocluster 4. Heat map depicting cytological profiles of compound dose instances located in biocluster 4 with compounds on y axis and cytological features on x axis.



**Biocluster 5**

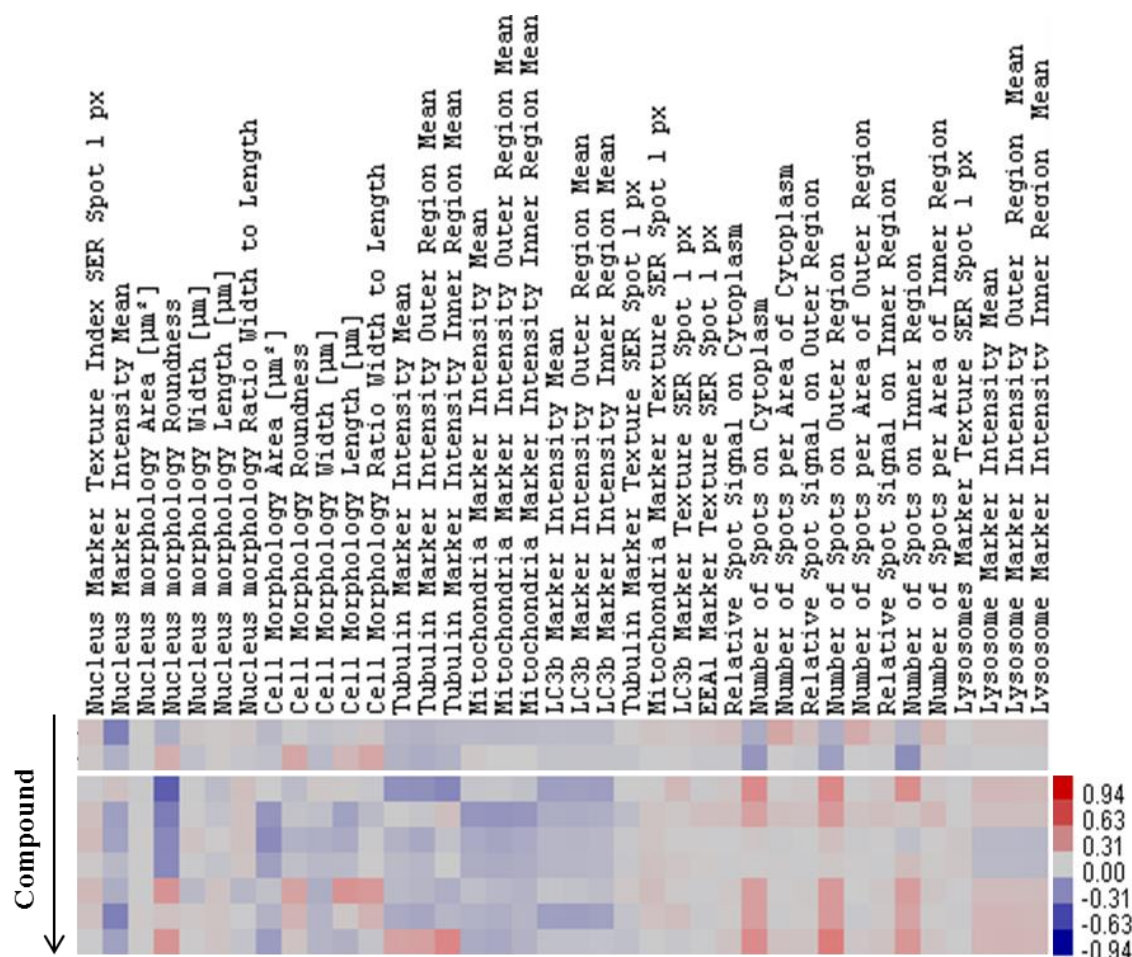
Biocluster 5 contained 19 compound dose instances, which showed negative deviation in intensity of tubulin, mitochondria and LC3b in cytoplasm and different regions of cytoplasm (**Figure 3.13**).



**Figure 3.13** Heat map of biocluster 5. Heat map depicting cytological profiles of compound dose instances located in biocluster 5 with compounds on y axis and cytological features on x axis.

**Unclustered compound dose instances**

There were nine unclustered compound dose instances which exhibited distinct effects on investigated cytological features (**Figure 3.14**).



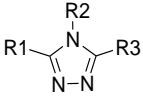
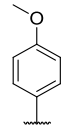
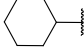
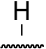

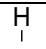
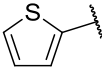

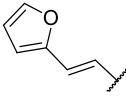
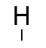
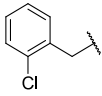
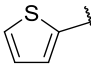
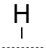
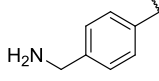
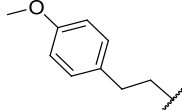
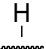
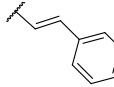
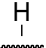
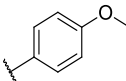
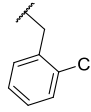
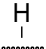
**Figure 3.14** Heat map of unclustered compound dose instances. Heat map depicting cytological profiles of unclustered compound dose instances with compounds on y axis and cytological features on x axis.

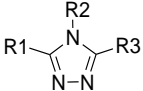
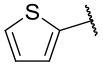
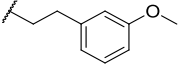

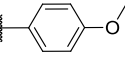
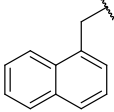
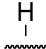
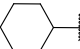
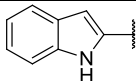

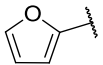
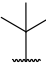
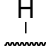
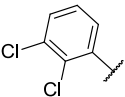
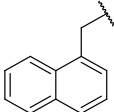
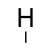
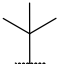
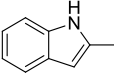

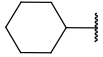
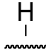
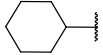
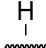
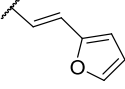
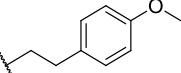
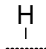
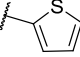
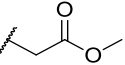
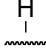
### 3.3.3.4 Chemical structures of 127 compound dose instances

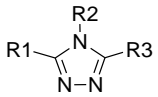
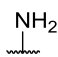
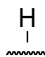
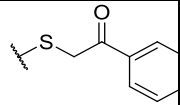
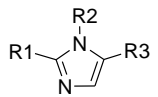
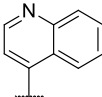
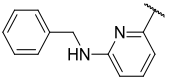
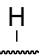
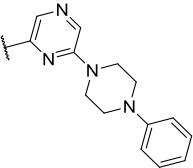
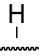
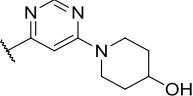
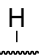
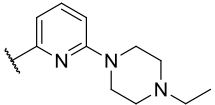
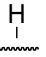
Information about scaffolds of 127 compound dose instances and their bioclusters are represented in **Table 3.2**.

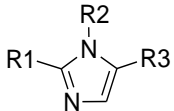
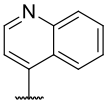
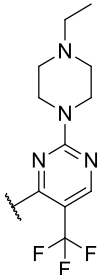
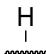
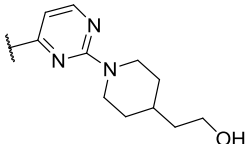
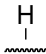
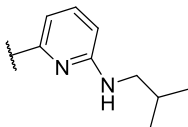
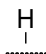
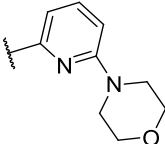
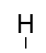
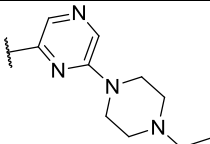
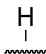
**Table 3.2** Table displaying scaffold information of individual compound dose instances.


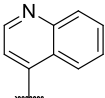
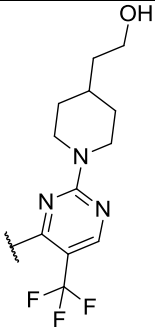
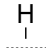
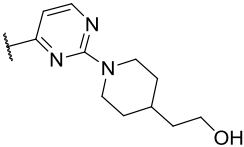
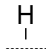
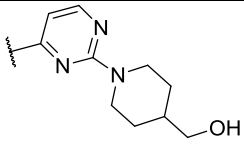
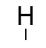
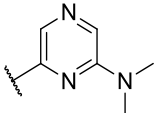
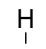
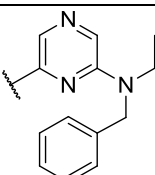
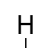
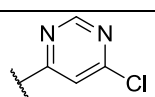
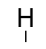


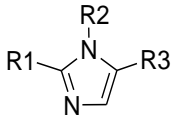
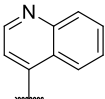
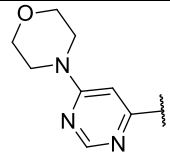
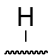
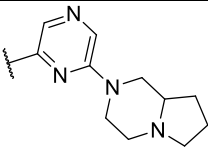

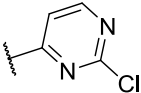
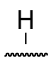
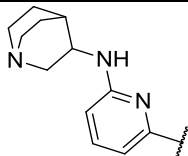
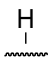
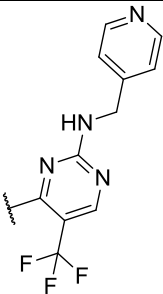
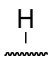
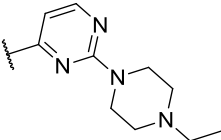

#	Compound	Scaffold	R <sup>1</sup>	R <sup>2</sup>	R <sup>3</sup>	Concentration (μM)	Biocluster
1	24_2					30	i
2	24_2					10	ii
3	24_2					1	iv
4	33_2					3	iii
5	36_2					1	iv
6	32_2					3	ii
7	42_2					30	iv
8	44_2					30	iv
9	31_2					10	iv

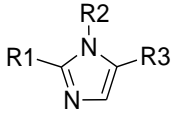
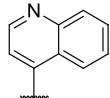
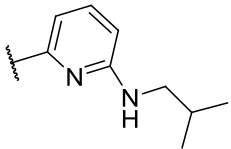
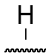
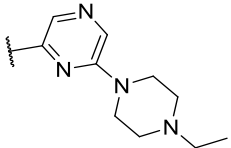
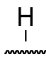
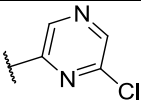
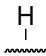
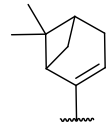
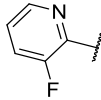

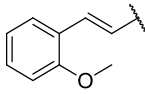
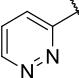
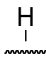
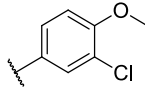
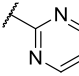
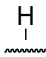
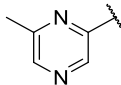
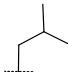
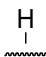
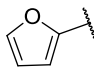
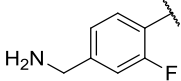
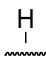
10	39_2					30	iv
11	29_2					30	iv
12	22_2					1	iv
13	21_2					1	iv
14	45_2					30	iv
15	23_2					3	iv
16	26_2					30	iv
17	22_2					30	ii
18	43_2					30	v
19	34_2					30	Unclustered

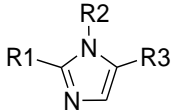
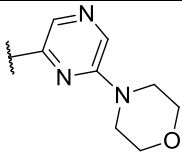
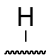
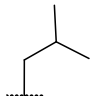
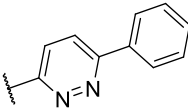
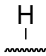
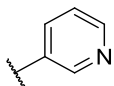
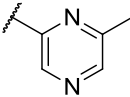
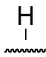
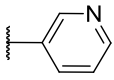
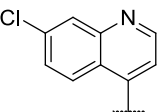
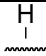
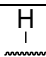
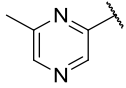
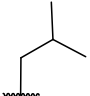
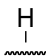
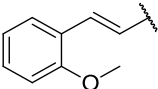
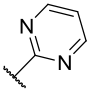
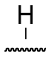
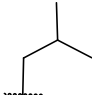
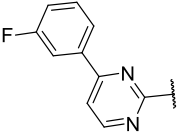
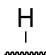
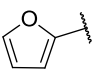
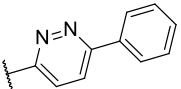
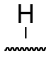
20	69_2					30	iv
21	65_1					30	i
22	65_1					1	i
23	65_1					10	i
24	65_1					3	i
25	49_1					3	i
26	49_1					1	i
27	33_1					30	i
28	33_1					10	ii
29	33_1					1	iv
30	66_1					1	i

31	39_1					30	ii
32	56_1					30	ii
33	64_1					3	ii
34	62_1					1	ii
35	47_1					3	ii

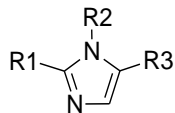
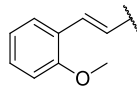
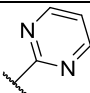
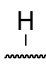
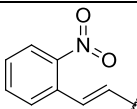
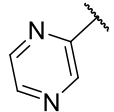
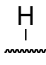
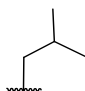

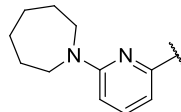
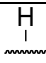


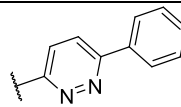
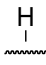

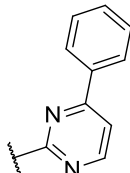
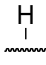
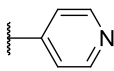
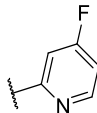

36	44_1					30	ii
37	56_1					10	iii
38	55_1					3	iii
39	48_1					30	iii
40	60_1					30	iii
41	58_1					3	Unclustered

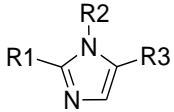
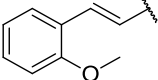
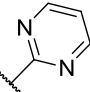
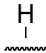
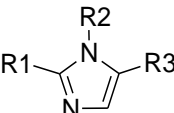
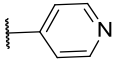


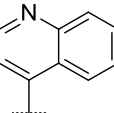

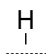
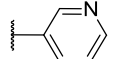


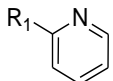
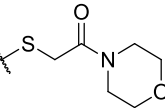
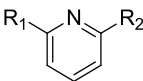
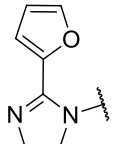
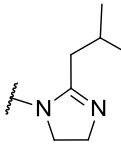
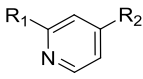
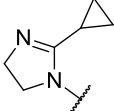
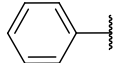
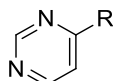
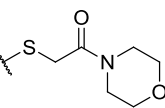
42	36_1					3	iv
43	46_1					30	iv
44	61_1					30	iv
45	63_1					30	iv
46	45_1					10	iv
47	53_1					3	v

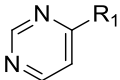
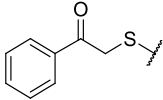
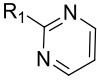
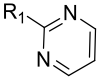
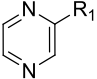
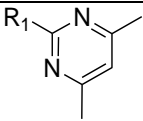
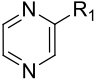
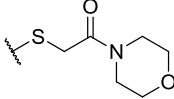
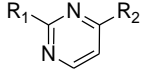
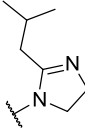
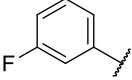
48	64_1					30	v
49	47_1					10	Unclustered
50	51_1					3	Unclustered
51	23_1					1	ii
52	9_1					30	ii
53	8_1					1	ii
54	2_1					1	ii
55	24_1					30	iii

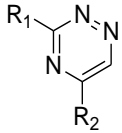
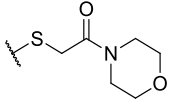
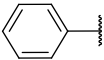
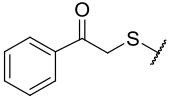
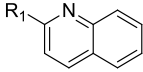
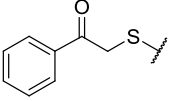
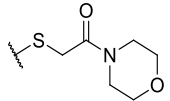
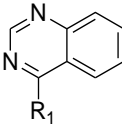
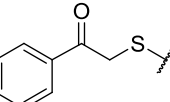
56	57_1					30	iii
57	7_1					10	iii
58	5_1					1	Unclustered
59	13_2					10	iv
60	13_2					30	iv
61	2_1					30	iv
62	22_1					1	iv
63	20_1					3	iv
64	3_1					30	iv

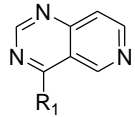
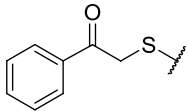
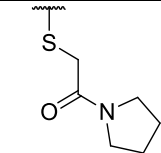
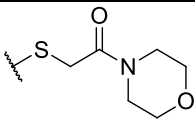
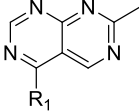
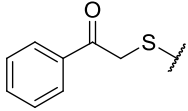
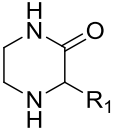
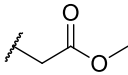
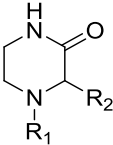
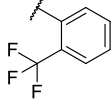
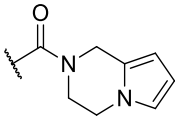


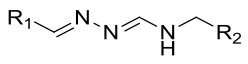
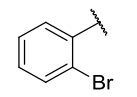
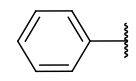
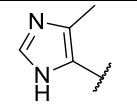
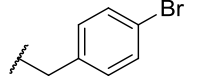
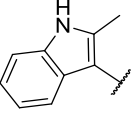
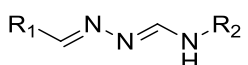
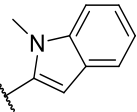
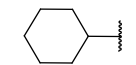
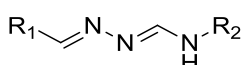
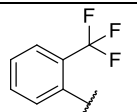
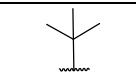
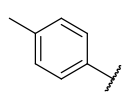
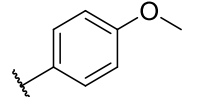
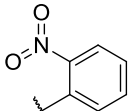
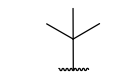
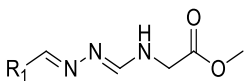
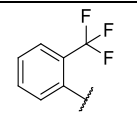
65	22_1					3	iv
66	26_1					10	iv
67	4_1					10	v
68	18_1					30	v
69	18_1					10	v
70	18_1					1	Unclustered
71	7_1				30	v	
72	6_1					30	v
73	1_1				3	Unclustered	

74	22_1					10	Unclustered
75	27_1					10	v
76	70_1					3	iii
77	28_1					10	iv
78	48_2					1	ii
79	17_1					30	iv
80	25_1					30	iv
81	55_2					3	ii
82	55_2					10	ii

83	60_2					30	v
84	50_2					30	iii
85	50_2					10	iii
86	52_2					30	v
87	51_2					3	Unclustered
88	53_2					30	iv
89	20_1					30	v

90	63_2					1	ii
91	63_2					3	ii
92	63_2					10	ii
93	62_2					10	ii
94	58_2					30	i
95	58_2					3	ii
96	58_2					10	iii
97	59_2					30	iv
98	54_2					30	i
99	54_2					3	i
100	54_2					1	i
101	54_2					10	ii

102	64_2					30	ii
103	73_2					30	iii
104	65_2					10	v
105	57_2					10	iv
106	77_2					3	v
107	77_2					30	v
108	79_1					1	ii
109	79_1					30	iii

110	16_2					3	i
111	16_2					10	iv
112	76_2					3	ii
113	75_2					30	iii
114	7_2					10	iv
115	10_2					10	ii
116	8_2					30	iii
117	1_2					10	iv
118	12_2					10	iv

119	18_2					1	iv
120	18_2					30	iv
121	79_2					1	v
122	78_1					10	iv
123	76_1					30	v
124	2_2					3	iv
125	15_2					3	iii
126	17_2					10	v
127	72_2					30	v

### 3.3.4 Examination of the structure activity relationships (SARs)

In medicinal chemistry, the central principle is that structurally similar molecules have similar biological activities. The concept of similarity has been particularly favored in drug discovery. We closely examined this screening set to address the molecular similarity principle. We have selected different biological sub-bioclusters to study SARs in more details. Chemical structures of representative compound dose instances and their biological profiles are shown in **Figure 3.15**.

A sub-biocluster belonging to biocluster i showed strongly negative deviation in nuclear roundness and intensity as well as positive deviations from the negative controls in tubulin intensity. This sub-biocluster showed both strong phenotypic similarity (similarity > 0.8) (**Figure. 3.15 A**). Interestingly, compound dose instance 33\_1 generated the strongest phenotypic signature at 1  $\mu$ M rather than 30  $\mu$ M. Analysis of compound structures in this sub-biocluster revealed that they share the same scaffold with different substitutions.

Unlike compounds in biocluster i, the sub-biocluster within biocluster ii exhibited low structural convergence (**Figure. 3.15 B**). This sub-biocluster was defined by strong negative deviation in nucleus roundness and intensity but positive deviation in tubulin intensity and strongly positive deviation in the number of early endosome spots. It contained 7 compound dose instances based on 6 different scaffolds.

Another phenotypic sub-biocluster within biocluster iii showed various effects on the nucleus and mitochondria, tubulin and autophagy features (strongly negative deviation from controls in nucleus intensity and roundness and weakly positive deviation in mitochondria, tubulin

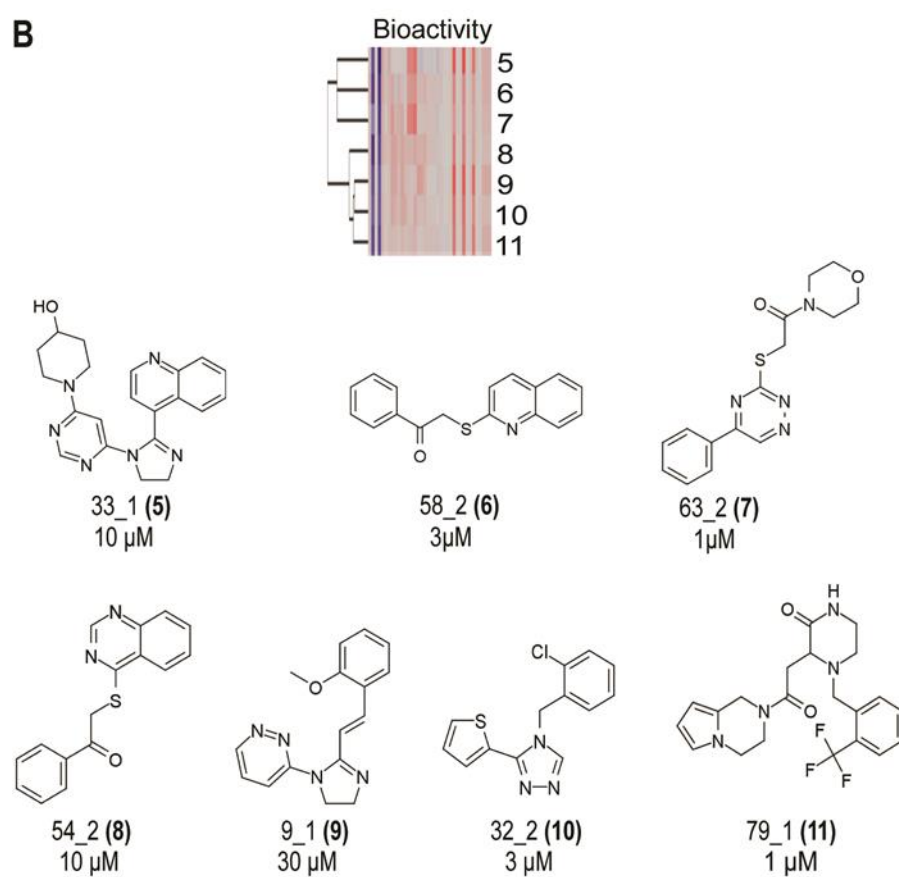
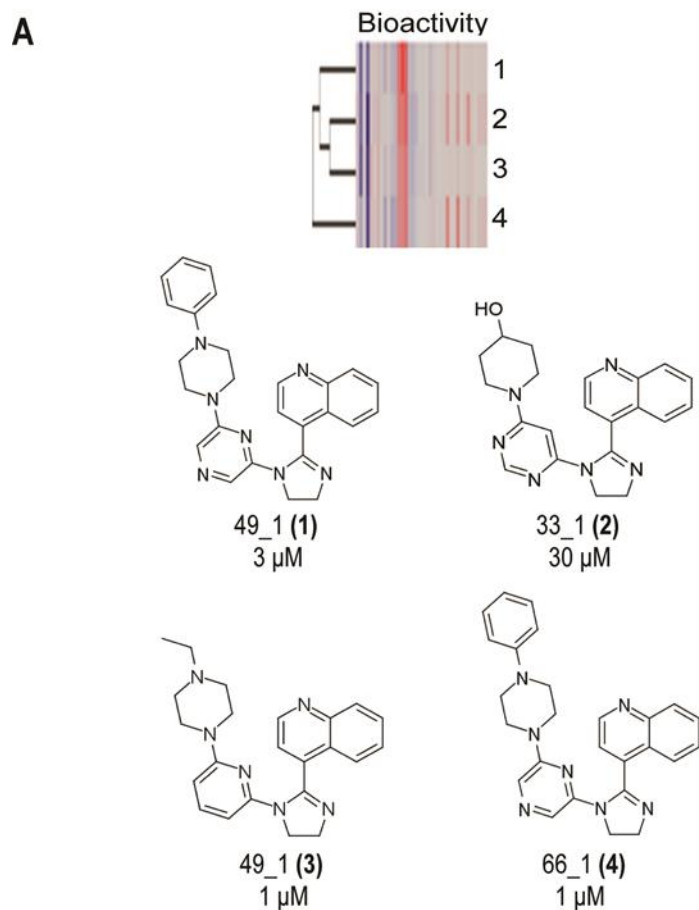


and LC3b) (**Figure. 3.15 C**). In this sub-biocluster, we found three groups of structurally distinct compound dose instances.

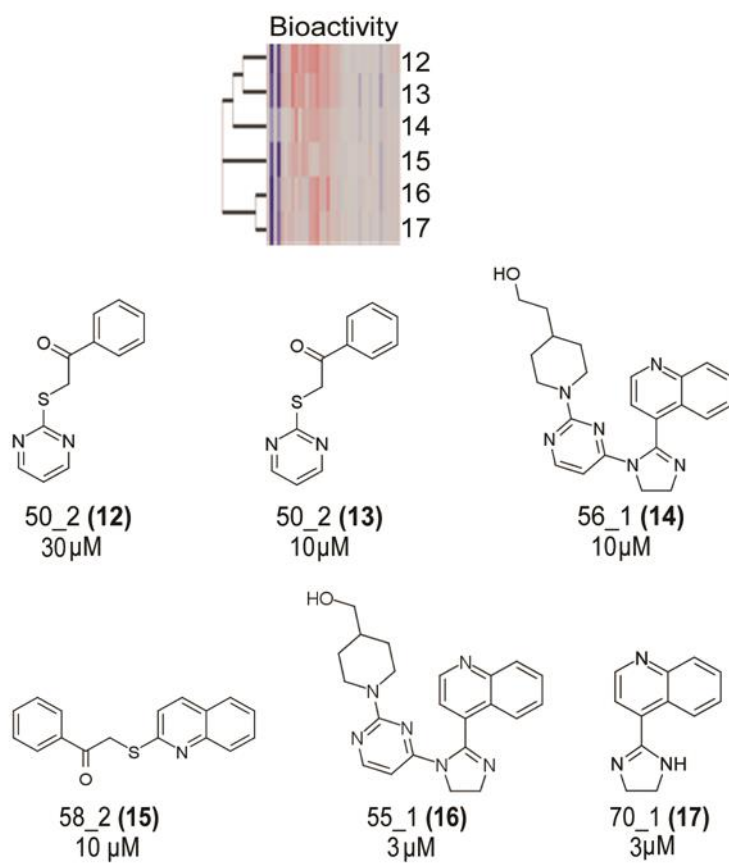
A sub-biocluster within biocluster iv contained compounds with high structural convergence including four compounds with significant structural similarity separated by only one structural dissimilar compound (**Figure. 3.15 D**). These compounds exhibited strongly positive deviation from control wells in nucleus intensity and strongly negative deviation in tubulin features (tubulin intensity in cytoplasm, in inner region of cytoplasm and in outer region of cytoplasm) while relatively weak negative deviation in mitochondria and LC3b features.

Unlike other sub-bioclusters, the second sub-biocluster derived from biocluster iv had strong effects on early endosome features (strong deviation from the average for control wells in the number of spots on early endosome in cytoplasm, inner region of cytoplasm and outer region of cytoplasm), but relatively weak effects on other investigated cellular components. Overall, this sub-biocluster comprises of compound dose instances with four different scaffolds (**Figure. 3.15 E**).

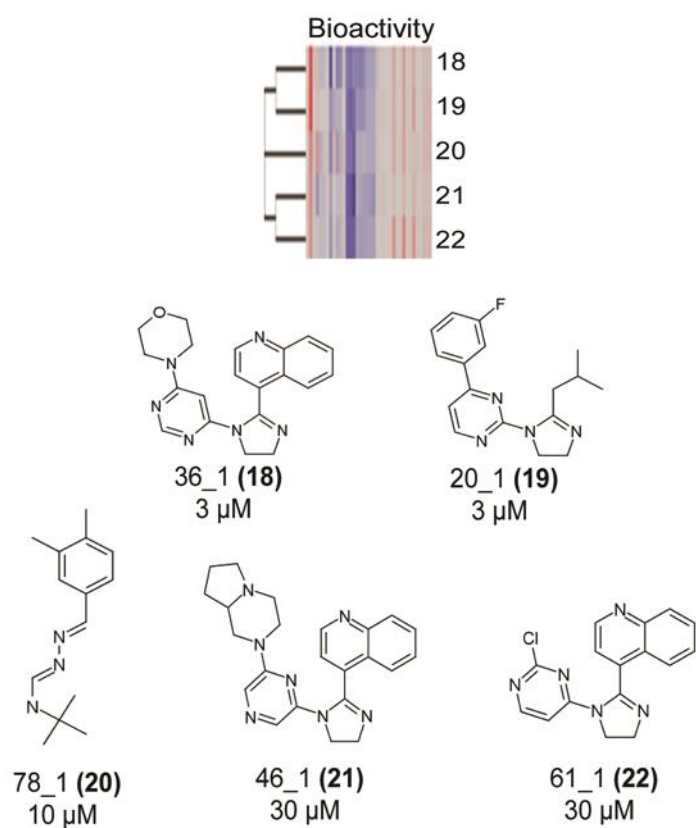
Within biocluster v, a sub-biocluster exhibited strongly negative deviation from controls in tubulin intensity but weakly deviation in mitochondria and LC3b intensity. In addition, three (7\_1, 76\_1, 72\_2) of 7 compound dose instances showed strongly positive deviation in nucleus intensity (**Figure 3.15 F**). Examination of this sub-biocluster revealed that the presence of structurally dissimilar compound dose instances including five different scaffolds (**Figure. 3.15 F**). Such non-structurally related compounds surprisingly generated substantially phenotypic convergence.



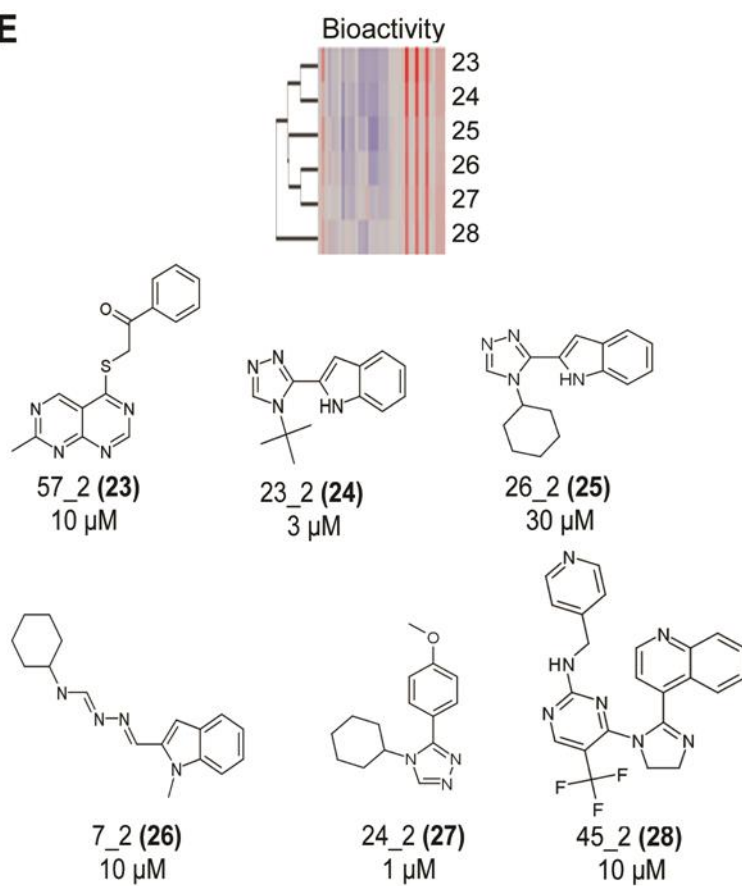
**C**



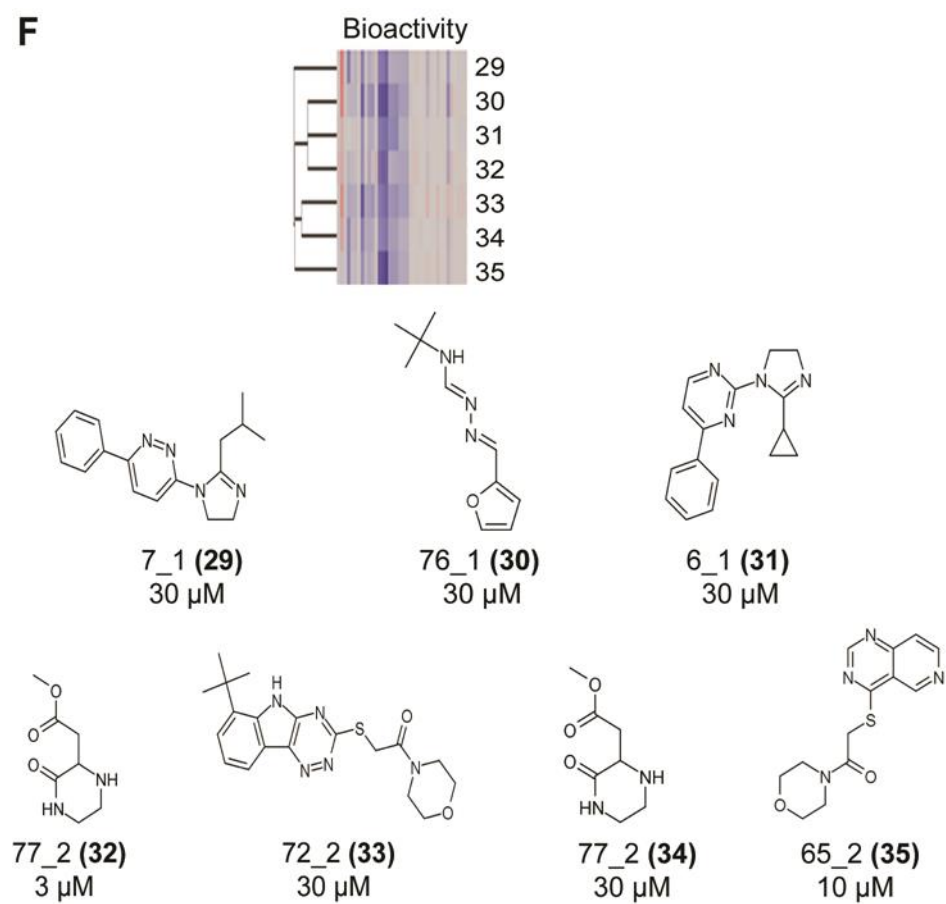
**D**



**E**



**F**



**Figure 3.15** Biological profiles and chemical structures of investigated sub-bioclusters. **(A)** A sub-biocluster characterized by positive deviation in tubulin intensity as well as negative deviation in nucleus intensity and roundness. This sub-biocluster consists of structurally related compounds sharing one common scaffold. **(B)** A sub-biocluster containing compounds producing strongly negative deviation in nucleus roundness and intensity but positive deviation in tubulin intensity and strongly positive deviation in number of early endosome spots. The sub-biocluster included compounds based on six different scaffolds. **(C)** Sub-biocluster showed various effects on nucleus and mitochondria, tubulin and autophagy features (strongly negative deviation from controls in nucleus intensity and roundness and weakly positive deviation in mitochondria, tubulin and LC3b). There were three groups of structurally distinct compound dose instances including three different scaffolds. **(D)** A sub-biocluster within biocluster iv containing compounds having 2 scaffolds. These compounds exhibited strongly positive deviation from control wells in nucleus intensity and strongly negative deviation in tubulin feature (tubulin intensity in cytoplasm, in inner region of cytoplasm and in outer region of cytoplasm) while relatively weak negative deviation in mitochondria and LC3b features. **(E)** The second sub-biocluster derived from biocluster iv had strong effects on early endosome features but relatively weak effects on other investigated cellular components. This sub-biocluster comprised of compound dose instances with four distinctive scaffolds. **(F)** Within biocluster v, a sub-biocluster exhibited strong negative deviation from controls in tubulin intensity but weak deviation in mitochondria and LC3b intensity. This sub-biocluster comprised of five different scaffolds.

### 3.3.5 Examples of structure activity relationships in the first library

Three compounds (49\_1, 36\_1, 53\_1) at 3  $\mu$ M were chosen to investigate how changes in chemical structure affect biological activity. To address this aspect, we compared chemical structures of three representative compounds with their biological responses. As shown in **Figure 3.16 A**, these compounds share the same scaffold, imidazole, with the same substituents at positions R<sub>1</sub> (4-quinoline) and R<sub>3</sub> (hydrogen). However, they have different substituents at position R<sub>2</sub> as follows: 6-(4-phenylpiperazin-1-yl)pyrazine (compound 49\_1), 4-(pyrimidin-4-yl)morpholine (compound 36\_1), and 2-(4-ethylpiperazin-1-yl)pyrimidine (compound 53\_1) (Refer **Table 3.2** for more information about chemical structures). Their biological functions were investigated using both heat map and bar chart. The generation of the heat map was described extensively in section 3.3.3 and it indicated that the compounds (49\_1, 36\_1, 53\_1) did not cluster together but separated into bioclusters i, iv and v, respectively (**Figure 3.8**). Cytological features used to generate the above heat map were then plotted in a bar chart to better understand the impact of the compounds on the cells (**Figure 3.16 B**).

The chemical difference between compounds 36\_1 and 53\_1 is that 4-(pyrimidin-4-yl)morpholine was substituted for 2-(4-ethylpiperazin-1-yl)pyrimidine. It induced an opposite effect on nucleus intensity (**Figure 3.16 B, cytological feature 2**), that is a strong positive deviation from DMSO control (compound 36\_1) and weak negative deviation (compound 53\_1). The 4-(pyrimidin-4-yl)morpholine substituent also induced an opposite effect on the above property compared to 6-(4-phenylpiperazin-1-yl)pyrazine (compound 49\_1). However, when the 2-(4-ethylpiperazin-1-yl)pyrimidine substituent (compound

53\_1) was changed to 6-(4-phenylpiperazin-1-yl)pyrazine (compound 49\_1), a similar effect (negative deviation), albeit greater, on nucleus intensity was observed.

With respect to nucleus roundness (**Figure 3.16 B, cytological feature 4**), both 4-(pyrimidin-4-yl)morpholine and 2-(4-ethylpiperazin-1-yl)pyrimidine substituents produced indistinguishable effects (positive deviation from DMSO control). However, 4-(pyrimidin-4-yl)morpholine produced a minor effect compared to 2-(4-ethylpiperazin-1-yl)pyrimidine. On the other hand, replacement of the above substituent with 6-(4-phenylpiperazin-1-yl)pyrazine caused a larger effect and in the negative direction. Indeed, 6-(4-phenylpiperazin-1-yl)pyrazine showed greatest effect in the opposite direction compared to 4-(pyrimidin-4-yl)morpholine and 2-(4-ethylpiperazin-1-yl)pyrimidine.

Examination of tubulin intensity in the cytoplasm and different regions of cytoplasm (**Figure 3.16 B, cytological features 13, 14, and 15**) revealed that replacement of 4-(pyrimidin-4-yl)morpholine with 6-(4-phenylpiperazin-1-yl)pyrazine induced a reversed effect (negative deviation and positive deviation, accordingly). Substitution of (4-ethylpiperazin-1-yl)pyrimidine for 6-(4-phenylpiperazin-1-yl)pyrazine also showed an opposite effect (negative deviation and positive deviation, respectively). Whereas, a change from 4-(pyrimidin-4-yl)morpholine to (4-ethylpiperazin-1-yl)pyrimidine resulted in comparable effects in the negative direction.

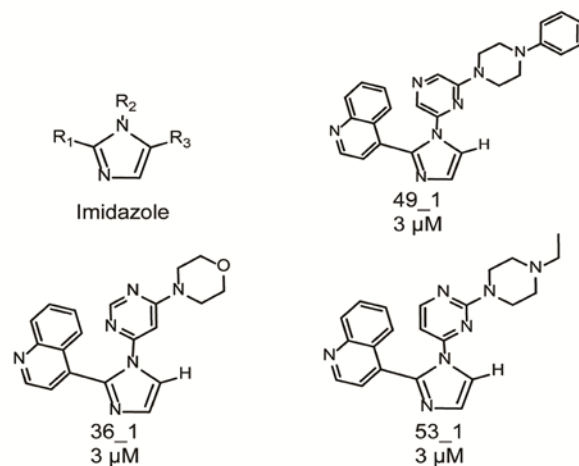
In summary, compound 49\_1 with 6-(4-phenylpiperazin-1-yl)pyrazine substituent from biocluster i displayed significantly different effects across three investigated cytological features compared to both compounds 36\_1 with 4-(pyrimidin-4-yl)morpholine substituent and 53\_1 with 2-(4-ethylpiperazin-1-yl)pyrimidine substituent from bioclusters iv and v,

respectively. In particular, the 6-(4-phenylpiperazin-1-yl)pyrazine substituent induced reversed effects on nucleus roundness, and tubulin intensity in cytoplasm and different regions of cytoplasm compared to the other two substituents. In addition, 6-(4-phenylpiperazin-1-yl)pyrazine substituent caused a similar effect, albeit more significant, on nucleus intensity compared to 2-(4-ethylpiperazin-1-yl)pyrimidine; and produced an opposite effect compared to 4-(pyrimidin-4-yl)morpholine on the same cytological feature.

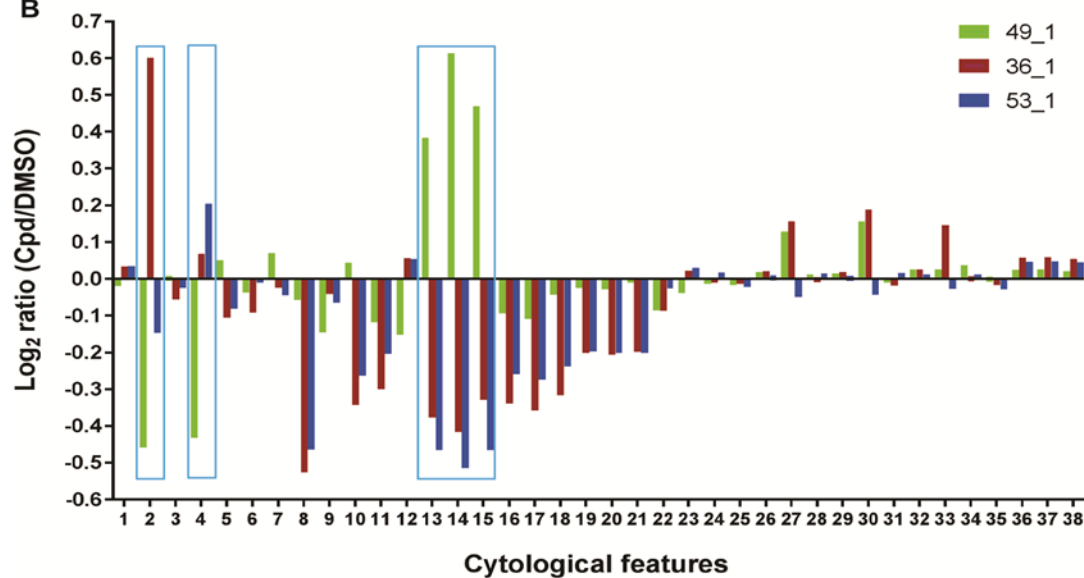
Examination of biological profiles of three representative compounds suggested that the substitution alteration led to changes in certain cytological features, especially nucleus intensity, nucleus roundness and tubulin intensity in the cytoplasm. The mechanisms underlying these alterations and their impact on the cellular functions need to be further pursued.



**A**



**B**

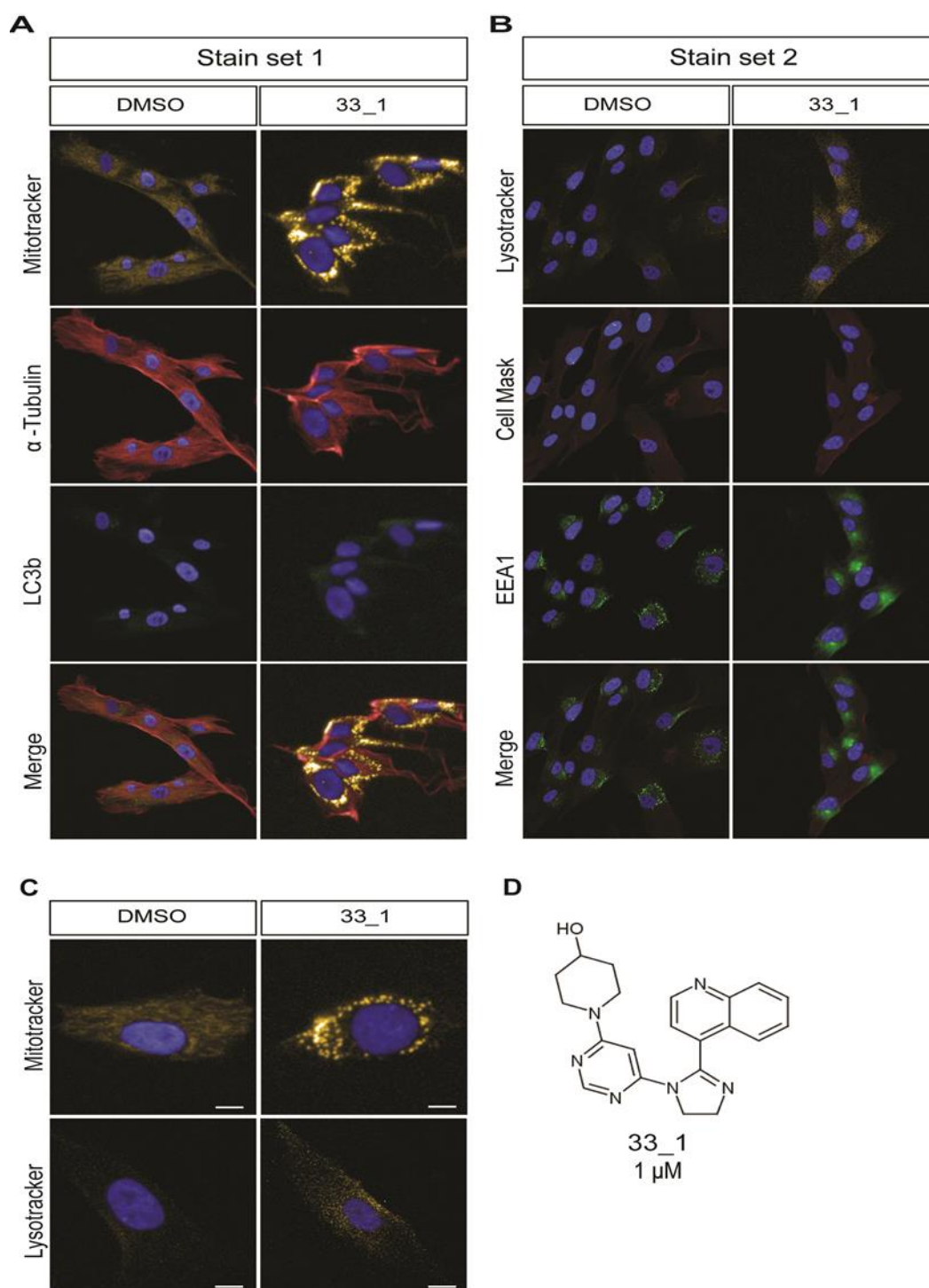


1. Nucleus marker texture
2. Nucleus marker intensity
3. Nucleus area [ $\mu$ m<sup>2</sup>]
4. Nucleus roundness
5. Nucleus width [ $\mu$ m]
6. Nucleus length [ $\mu$ m]
7. Nucleus ratio width to length
8. Cell area [ $\mu$ m<sup>2</sup>]
9. Cell roundness
10. Cell width [ $\mu$ m]
11. Cell length [ $\mu$ m]
12. Cell ratio width to length
13. Tubulin marker intensity
14. Tubulin marker intensity outer region
15. Tubulin marker intensity inner region
16. Mitochondria marker intensity
17. Mitochondria marker intensity outer region
18. Mitochondria marker intensity inner region
19. LC3b marker intensity
20. LC3b marker intensity outer region
21. LC3b marker intensity inner region
22. Tubulin marker texture
23. Mitochondria marker texture
24. LC3b marker texture
25. EEA1 marker texture
26. Relative EEA1 spot signal on cytoplasm
27. Number of EEA1 spots on cytoplasm
28. Number of EEA1 spots per area of cytoplasm
29. Relative EEA1 spot signal on outer region
30. Number of EEA1 spots on outer region
31. Number of EEA1 spots per area of outer region
32. Relative EEA1 spot signal on inner region
33. Number of EEA1 spots on inner region
34. Number of EEA1 spots per area of inner region
35. Lysosomes marker texture
36. Lysosome marker intensity
37. Lysosome marker intensity outer region
38. Lysosome marker intensity inner region

**Figure 3.16** Examples of structure activity relationships. **Panel (A)** Scaffold imidazole and chemical structures of three imidazole containing compounds. **Panel (B)** The two dimensional plot describes biological responses of three imidazole containing compounds (compound 49\_1: green colour, compound 36\_1: maroon colour, compound 53\_1: petrol blue colour) at 3  $\mu$ M with x axis as 38 cytological features and y axis as logarithm base 2 of the ratio of compound and DMSO. Blue rectangular boxes indicate investigated cytological features.

### 3.3.6 Cytological features of most active “hits”

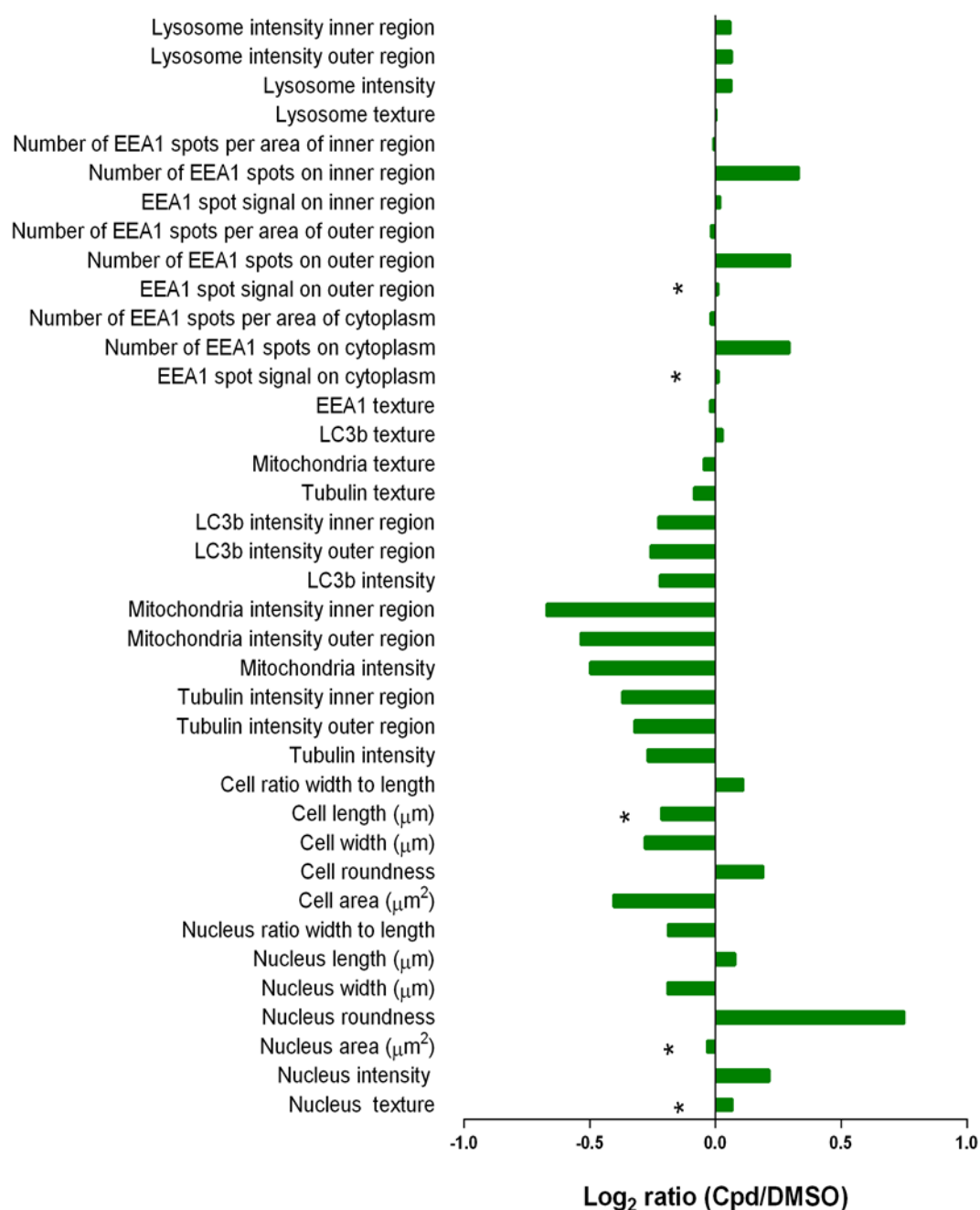
Based on cytological features scores computed in **Section 3.3.3.2**, compound 33\_1 at 1  $\mu\text{M}$  with approximately 60% of initial cell number (200 cells) remained after treatment was the strongest hit in our screen while it was inactive at 3  $\mu\text{M}$ , thus being excluded as a weak phenotype. At 10  $\mu\text{M}$  and 30  $\mu\text{M}$ , it exhibited moderate effects. Biological profiles of this compound at 1, 10 and 30  $\mu\text{M}$  were separated into bioclusters 4, 2, and 1, respectively. Treatment of PD hONS cells with this compound resulted in changes in nuclear and cell sizes and shapes, interference with tubulin formation, mitochondrial rearrangement, and aberrant autophagy. Visual inspection of the captured images showed that this molecule induced nuclei rounder than that of control cells. In addition, compound treated cells became smaller and also rounder (**Figure. 3.17 A and B**). Furthermore, as observed in **Figure 3.17 C**, this compound caused changes on lysosome by increasing the number of lysosome compared to DMSO control. Indeed, 33\_1 had great effects on the intensity indexes of tubulin, mitochondria and lysosome. Chemical structure of compound 33\_1 is shown in **Figure 3.17 D**.



**Figure 3.17** Phenotypic changes in PD hONS cells induced by compound 33\_1. **(A)** Stain set 1 consists of cell nuclei marker (4', 6-diamidino-2-phenylindole; DAPI, blue), tubulin stain (anti- $\alpha$  tubulin antibody), mitochondria stain (Mitotracker) and LC3b stain (anti LC3b antibody) which is related to autophagy pathway. **(B)** Stain set 2 contains DAPI, Lysotracker, EEA1 marker (anti-EEA1 antibody), and cell mask for cell nuclei, lysosomes, early endosomes and plasma membrane, respectively. **(C)** Influence of

compound 33\_1 on mitochondria and lysosome in compared to DMSO as controls. Images were obtained with 20 x objective. Scale bar is 50  $\mu$ m. **(D)** Chemical structure of compound 33\_1.

DeCoster et al. proposed that nuclear area and cell area factors can be used as indicators of apoptosis. Cells that are normally non-rounded tend to become rounder as they undergo apoptosis (DeCoster, 2007). In our case, nuclear area remained unchanged ( $p > 0.05$ ) while nucleus intensity was significantly different from DMSO treated cells ( $p < 0.05$ ). Decreased cell area was observed in treated compared to untreated cells ( $p < 0.05$ ). This might correspond to the DeCoster et al study since PD hONS cells are typically longer than wide. In addition, the study in 2010 also reported that roundness ( $\text{perimeter}^2 / (4 \times \text{pix area})$ ) is also a useful descriptor for apoptosis (Mark A. DeCoster et al., 2010). In this study, we employed both roundness and ratio of width to length descriptors to describe nucleus and cell morphologies with 1.0 indicating a perfect circular object and either greater or lesser than indicating non-round objects. Examination of individual cytological features showed that both nucleus and cell roundness were significantly increased compared to controls ( $p < 0.05$ ) (**Figure. 3.18**). Taken together, we suggest that 33\_1 affects cell morphology leading to changes of other organelles intensity as well as tubulin structure and lysosome intensity.



**Figure 3.18** Cytological features of compound 33\_1 at 1  $\mu\text{M}$ . Data are presented as logarithm base 2 ratio of compound relative to DMSO controls. The \* indicates no significant difference ( $p > 0.05$ ) compared with DMSO.

### 3.4 Discussion

In 1998, Marton et al developed yeast mutant strains which were exposed to drug collections using DNA microarrays. They proved that the employed method was useful for identification of drug-induced modification in gene expression that are regulated by different molecular pathways rather than expected mechanisms (Marton et al., 1998). Through evolution of technologies, such profiling was performed using human cell based assays and images of individual cells obtained from automated microscopy. This approach provides valuable information of overall cellular morphology and organelles that involve fundamental biological processes. However, previous studies only applied single readout cell based assays or measured limited numbers of biological responses leading to missing of potential molecules. It is noteworthy that some morphological modifications are dose dependent. Therefore, studies examining a single concentration might fail to identify mechanisms of drug action involving the binding of multiple targets with different affinity (Marton et al., 1998, Perlman et al., 2004, Young et al., 2008).

Here, our study demonstrated the power of cytological profiling for the discovery of potent, novel compounds. Unlike previous studies mainly utilizing cancer cell lines, we developed a PD cellular model derived from patient mucosa biopsy, which is able to capture genetic and functional discrepancies in a disease-specific manner. Furthermore, we attempted to cover a range of biological target space implicated in PD to be sampled in a single screen, with a limited collection of 193 small molecules of limited chemical diversity at four concentrations (1, 3, 10, 30  $\mu$ M). In addition, our approach allowed fast and inexpensive collection of biological responses for each compound per concentration. The goals of this study were to identify bioactive molecules on PD

patient derived cells and to investigate compound structure activity relationships by comparing biological profiles obtained from morphology based screen with structural information of compounds. This approach allowed us to generate 38 cytological features providing useful biological information that could have been missed if screens focusing on a specific phenotype were implemented. We identified that the current focused collection contains potent small molecules sharing common scaffolds. Two distinctive groups of biological clusters of compounds were identified in the heat map (**Figure 3.8**) (termed group 1 and group 2). Group 1 includes cluster i, ii, iii, which displayed positive deviation from control wells in tubulin intensity while group 2 consists compounds from cluster iv, v with negative deviation in intensity of tubulin, mitochondria and LC3b. This biological distinction between two groups might be attributed to dominant presence of 1,3-imidazole scaffold in group 1. The screen also led to the identification of compound 33\_1, which exhibited a multi-dimensional morphological signature distinct from other compounds. An important morphological change induced by this compound requiring consideration is that of mitochondrial shape, which reflects different cellular states during cell cycle (Chan, 2006). Mitochondrial morphologies diverge widely depending on cell types, including as long filaments in fibroblasts or sphere or ovoid in hepatocytes (Youle and van der Bliek, 2012). During apoptosis, the tubular mitochondrial network is disintegrated resulting in formation of punctiform and fragmented phenotypes (Arnoult, 2007). A growing body of evidence confirms morphological changes in mitochondria during the progression of apoptosis and these are likely contributors to cancer and neurodegeneration. Additionally, a study in 2013 has found that stress conditions associated with enhanced mitochondrial reactive oxygen species, such as exposure to toxic agents, induced the development of bold or donut shaped mitochondria in contrast to tubular form detected in healthy cells. It was also reported that increased cytoplasmic calcium level and



escalating calcium uptake in mitochondria is a key mediator of morphological changes of mitochondria (Ahmad et al., 2013). Such mitochondrial morphology in bold shape was clearly observed with cells treated with compound 33\_1 (**Figure 3.17 C**). Furthermore, compound 33\_1 induced the increase of intensity of lysosome (**Figure 3.17 B and C**). Lysosomal accumulation of protein aggregates is a hallmark of PD and enhancing their degradation could be neuroprotective. Nevertheless, in the current screen, it remains unclear if increased number of lysosome could be an indicator of lysosome activity enhancement (Wu et al., 2015). It would be exciting to carry out additional experiments to determine if the molecule could increase lysosome function. If proven the compound could be potential novel drug useful for PD. Taken together, the data suggest that compound 33\_1 at 1  $\mu$ M induced morphological modification of cells and nuclei as well as reorganization of tubulin and change on lysosome intensity.

We profiled a library of compound sharing several common scaffolds, therefore we anticipated that structurally related compounds would fall in the same phenotypic clusters. However, low convergence between biological signatures and chemical structures was observed in all clusters with exception of cluster i where we detected a small group of structurally related compounds. This observation together with analysis of structure activity relationships (**Sections 3.3.4 and 3.3.5**) suggested that common scaffold with different substituents could lead to changes in biological effects.

Cytological profiling offers a useful tool for classifying the functions of novel compounds by quantification of observable effects at cellular level. This technology also allows the identification of correlation between phenotypes and structures in primary screening. However, it is unable to generate comprehensive readouts of specific molecular targets and further biochemical experiments need to be carried out in order to

interpret molecular targets for a given compound. For subsequent follow-ups, prediction of specific targets by combination of cytological features of compounds into computational biomodeling and exploration of the mechanisms of action of these compounds would be an interesting approach. As an expansion to this study, we could envisage the establishment of chemical probes sets that allow visualization of compound influence on specific cellular apparatuses. More broadly, we could construct customized biomarker panels that could be employed for diagnosis of Parkinson's disease as well as evaluation and monitor of novel therapeutics for PD.

**CHAPTER 4**

**OPTIMIZATION OF DATA ANALYSIS METHOD**

## **4. OPTIMIZATION OF DATA ANALYSIS METHOD**

### **4.1 Introduction**

Cytological profiling is useful tool for early stage of drug discovery. It facilitates the identification of putative hits with novel biological activities from focused compound libraries. Normally, this automated image based screening generates numerous images from which many biological descriptors are extracted depicting cellular compartments such as sizes and amount of accumulated fluorescence on cell basis. Herein, 38 cytological descriptors were utilized to describe morphological changes of cellular organelles between treated and untreated cells. These descriptors cannot provide useful biological information unless suitable downstream data processing is carried out. A number of statistical tools have been developed to assist in the detection of hits with high degree of confidence. Depending on biological questions and properties of compound collection, a method or combination of different approaches can be applied.

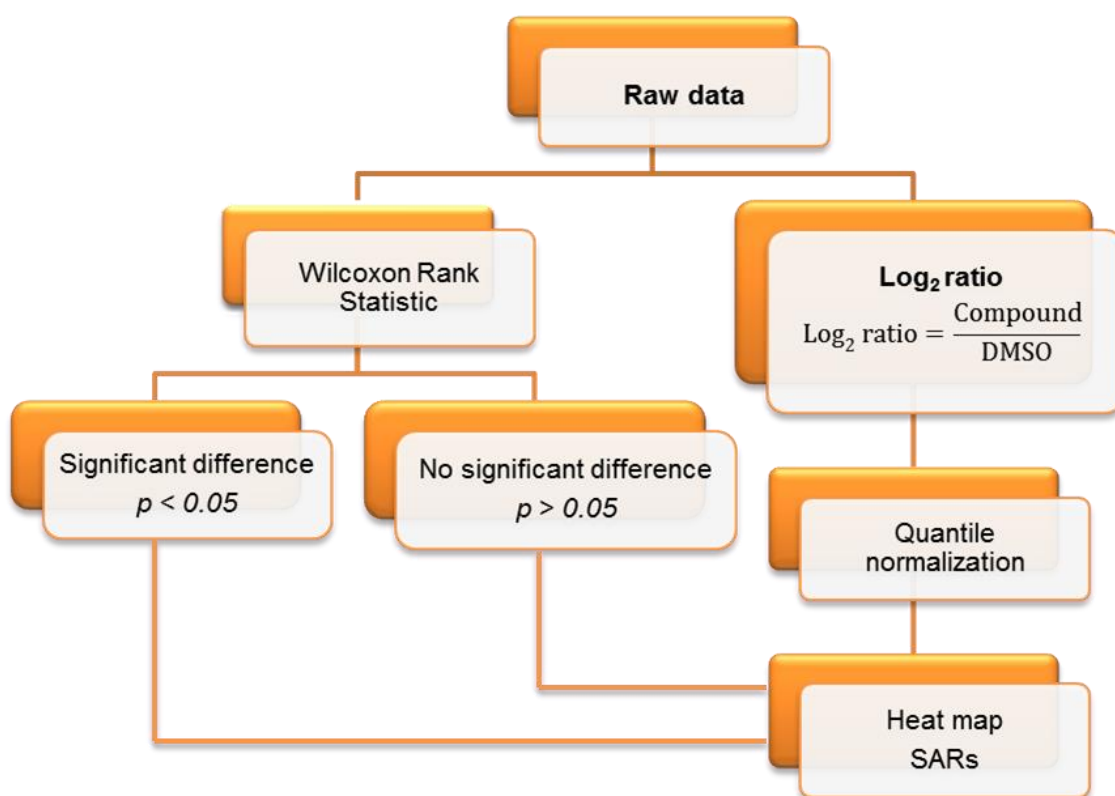
This chapter focuses on the optimization of data analysis method previously used in chapter 3 in order to establish appropriate strategy for mining data of the second library.

### **4.2 Optimization of data analysis method**

Unlike the previous screening in **Chapter 3**, the screening in **Chapter 5** was performed with both biological and technical replicates (three replicates) in order to quantify the variability and increase the possibility to identify true hits. Median was used to compute average values in a single well followed by mean of triplicates. Single well estimates

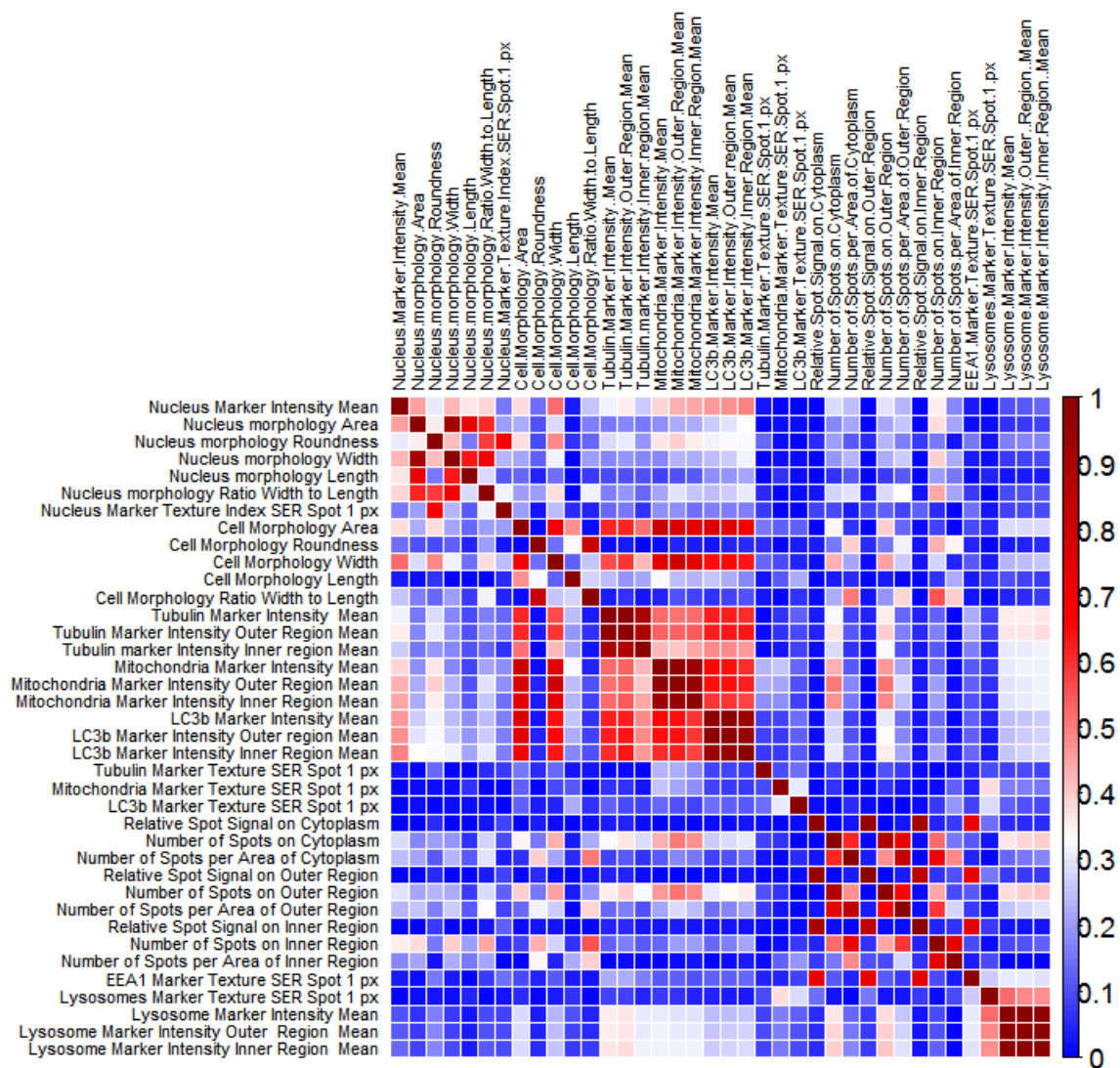
based on median are less variable since it is more resistant to outliers or extreme values than the mean, thereby more accurate estimates were produced.

As noticed in previous screening, exploration of data distribution and implementation of  $\log_2$  transformation were a time-consuming process. Hence, different approach was employed to mine datasets. Wilcoxon Rank statistic is common non-parametric test (equivalent to t-test), which pertains to the comparison of two independent samples and also generates p-Value (Rosner et al., 2006). Wilcoxon statistic provides alternative way to compare untreated and treated samples. By applying this method, downstream data processing was shortened as there is no required transformation of data. An overview of established downstream data processing is shown in **Figure.4.1**.



**Figure 4.1** Established downstream data processing.

Examination of individual cytological features of random compound dose instances revealed that some cytological features follow the same trend. For instance, tubulin marker intensity mean, tubulin marker intensity outer region mean and tubulin marker intensity inner region mean displayed either positive deviation or negative deviation from DMSO controls concurrently. Therefore, a correlation matrix was implemented to investigate the relationship among these parameters by using squared Pearson correlation coefficient. Using this coefficient obtained positive correlation (high correlation  $\geq 0.8$ , dark red colour). The correlation matrix showed that some biological descriptors are highly correlated with each other (**Figure.4.2**). As a result, 20 out of 38 features were retained due to their low correlation with each other and useful biological information content. These 20 cytological features will be utilized for image analysis in **Chapter 5**. List of retained cytological features is represented in **Table 4.1**.



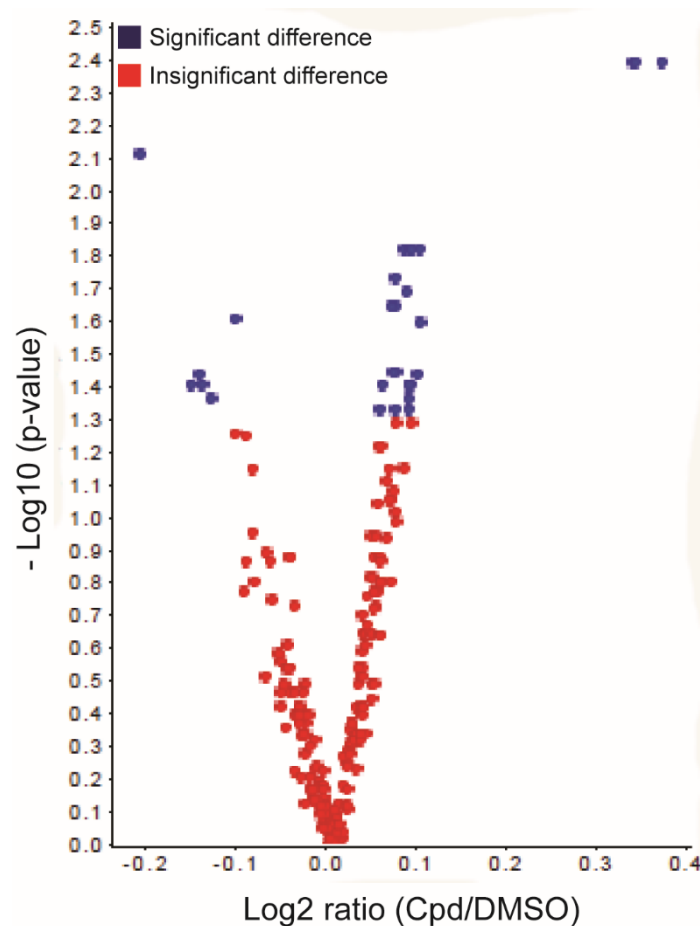
**Figure 4.2** Correlation matrix using squared Pearson correlation coefficient to investigate relationship among biological descriptors. High correlation is indicated by coefficient  $\geq 0.8$  (dark red colour). 20 out of 38 features were retained for their low correlation with each other and useful biological information content.

**Table 4.1** List of retained cytological features

No.	Retained Cytological Features
1	Nucleus Marker Texture
2	Nucleus Marker Intensity
3	Nucleus Area ( $\mu\text{m}^2$ )
4	Nucleus Roundness
5	Nucleus Ratio Width to Length
6	Cell Area ( $\mu\text{m}^2$ )
7	Cell Roundness
8	Cell Ratio Width to Length
9	Tubulin Marker Intensity in Cytoplasm
10	Mitochondria Marker Intensity in Cytoplasm
11	LC3b Marker Intensity in Cytoplasm
12	Tubulin Marker Texture
13	Mitochondria Marker Texture
14	LC3b Marker Texture
15	EEA1 Marker Texture
16	EEA1 Marker Intensity in Cytoplasm
17	Number of EEA1 Spots of Cytoplasm
18	Number of EEA1 Spots per area of Cytoplasm
19	Lysosome Marker Texture
20	Lysosome Marker Intensity in Cytoplasm



Finally, volcano plot with logarithm base 2 ratio between compound and DMSO on x-axis and logarithm base 10 of p-Value on y-axis was utilized for rapid visualization of cytological features that showed statistically significant differences from DMSO (**Figure 4.3**).



**Figure 4.3** Volcano plot of nucleus texture. Each point is single compound at certain concentration. Compounds with significant effects on nucleus texture are colored in blue and those with insignificant effects are in red color.

### 4.3 Conclusion

This chapter detailed the optimization of data analysis method used in **Chapter 3** for establishing new method to better mine the biological activities of novel compounds and to effectively identify more accurate hits in **Chapter 5**.

We used median for single well estimates since it is resistant to outliers and thus providing more accurate values. Parametric test was replaced with non-parametric test to reduce time for examination of data distribution. We observed high correlation among investigated cytological features. Consequently, highly correlated cytological features were excluded. The volcano plot has enabled rapid visualization of cytological features that are statistically significant and insignificant different from negative control (DMSO). Overall, the new downstream data processing improved result accuracy in a time-efficient manner.

**CHAPTER 5**

**CYTOLOGICAL PROFILING OF NATURAL PRODUCTS**

**SCAFFOLDS INSPIRED SYNTHETIC COMPOUNDS FOR**

**PARKINSON'S DISEASE**

## **5. CYTOLOGICAL PROFILING OF NATURAL PRODUCTS SCAFFOLDS INSPIRED SYNTHETIC COMPOUNDS FOR PARKINSON'S DISEASE**

### **5.1 Introduction**

With substantial effort, medicinal chemists have conducted intensive research in the natural product chemistry space aiming to find novel agents to manage Parkinson's disease. By studying heterocyclic scaffolds which occur in currently used drugs or drug candidates, 1-azaadamantane moiety was identified as core structure in Daphniphyllum alkaloids such as dapholdamine B (Zhang et al., 2009b) and daphnezomines A and B (Zhang et al., 2009a). It has been recognized that 1-azaadamantanes containing synthetic compounds have great impact on central nervous system diseases such as Pfizer's 5-HT<sub>4</sub> receptor agonist SC-54750 that prevents cisplatin-induced emesis (Becker et al., 2004), and 1-azaadamantane derivatives that acts as modulators of neuronal nicotinic acetylcholine receptors (Taheri et al., 2014). The pharmacological importance of such molecular frameworks prompted advanced synthetic approaches to improve chemical diversity of the library of 1-azaadamantane embedded compounds. In this direction, Taheri et al has synthesized a library containing 35, 1-azaadamantane embedded compounds (Taheri et al., 2014), which was screened in this chapter. To effectively test the effect of these compounds on PD cells, daphnezomines A, dapholdamine B and its analogues were also included in the current screen.

Here, we performed cytological profiling of 39 compounds (35, 1-azaadamantane embedded compounds and 4 natural products) against a patient-derived PD cellular model, namely human olfactory neuroepithelium derived (hONS) cells which display

functional and genetic discrepancies in a disease-specific manner (Matigian et al., 2010b). Each of the 39 compounds was screened at four concentrations (1, 3, 10, and 30  $\mu$ M), generating 156 compound dose instances. The hierarchical clustering was then carried out to classify compounds based on their biological profiles. As a result, we identified four bioclusters which contain several bioactive molecules. Furthermore, we investigated relationship between biological effects and common scaffold sharing structures.

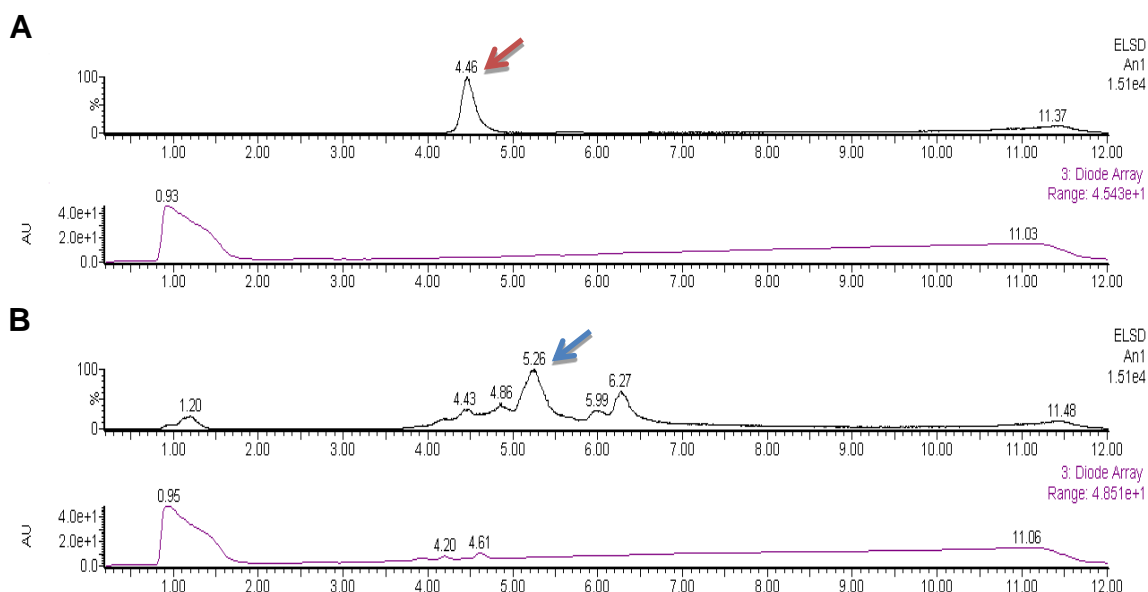
## **5.2 Materials and methods**

### **5.2.1 Compound purity**

The purity of all compounds was examined by Liquid chromatography mass spectrometry (LC-MS). This method employs UV detector and Evaporate Light Scattering detector (ELSD) to provide relative purity of compounds based on peak areas in UV (Diode array) and ELSD chromatograms (Fang et al., 2000). Examples of pure and impure compounds are shown in **Figure 5.1**.

### **5.2.2 Compound library**

We screened and profiled 39 compounds (35 synthetic compounds and 4 natural products). Only compounds determined by LC-MS to be at least 90% pure were included in this screen. Compounds were dissolved in DMSO (Ajax Finechem) for a stock concentration of 5mM. These compounds were submitted and stored in the Compounds Australia (Eskitis Institute, Griffith University).



**Figure 5.1** Examination of compound purity. Panel A are chromatograms of pure compound with single ELSD peak (red arrow) and no peak observed in UV array. Panel B is chromatogram of impure compound with multiple peaks indicating mixture of compound of interest (blue arrow) and other substances.

### 5.2.3 Compound transfer

Refer to **section 2.3.3** in **Chapter 2**

The assays were conducted with two biological replicates, each one with three technical replicates. Assay layout is shown in **Figure 5.2** with column 1, 24 containing positive controls (Rotenone, Chloroquine, and Nocodazole); column 2, 23 containing negative controls (DMSO).

	1	2	3	4	5	6	7	8	9	10	11	12	13	14	15	16	17	18	19	20	21	22	23	24
A	DMSO 0.6 %																							
B	Rot			Sample 1				Sample 6				Sample 11				Sample 16				Sample 21				Rot
C	Rot			Sample 1				Sample 6				Sample 11				Sample 16				Sample 21				Rot
D	Rot			Sample 1				Sample 6				Sample 11				Sample 16				Sample 21				Rot
E	Rot			Sample 2				Sample 7				Sample 12				Sample 17				Sample 22				Rot
F	Rot			Sample 2				Sample 7				Sample 12				Sample 17				Sample 22				Rot
G	Chlor			Sample 2				Sample 7				Sample 12				Sample 17				Sample 22				Chlor
H	Chlor			Sample 3				Sample 8				Sample 13				Sample 18				Sample 23				Chlor
I	Chlor			Sample 3				Sample 8				Sample 13				Sample 18				Sample 23				Chlor
J	Chlor			Sample 3				Sample 8				Sample 13				Sample 18				Sample 23				Chlor
K	Chlor			Sample 4				Sample 9				Sample 14				Sample 19				Sample 24				Chlor
L	Noco			Sample 4				Sample 9				Sample 14				Sample 19				Sample 24				Noco
M	Noco			Sample 4				Sample 9				Sample 14				Sample 19				Sample 24				Noco
N	Noco			Sample 5				Sample 10				Sample 15				Sample 20				Sample 25				Noco
O	Noco			Sample 5				Sample 10				Sample 15				Sample 20				Sample 25				Noco
P	Noco			Sample 5				Sample 10				Sample 15				Sample 20				Sample 25				Noco

**Figure 5.2** Plate format for compounds on 384 well plate layout. Several compounds known to affect staining parameters were included as positive controls on each plate. These were Rotenone (Rot) affects mitotracker, Chloroquine (Chlor) affects lysotracker, and Nocodazole (Noco) affects  $\alpha$ -tubulin.

## 5.2.4 Cell based assay

Refer to **Section 2.3.4** in **Chapter 2**

## 5.2.5 Imaging and image evaluation.

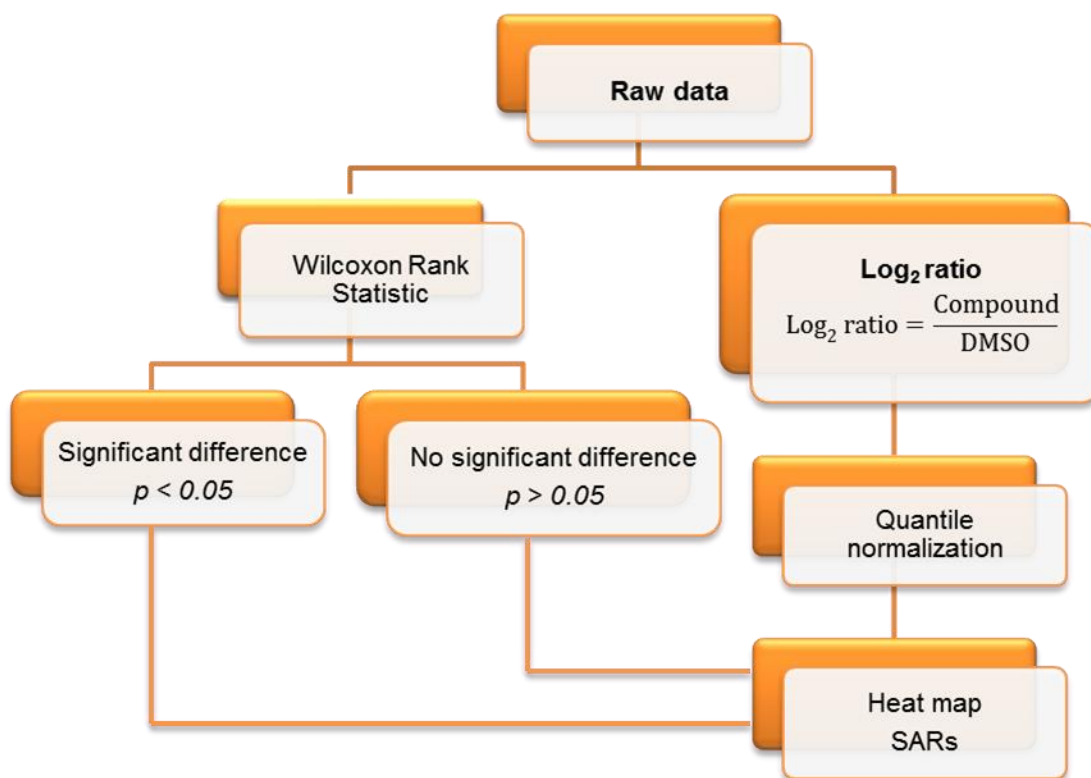
Refer to **Section 2.3.6** in **Chapter 2**

## 5.2.6 Data analysis

### 5.2.6.1 Overview of data analysis process

Data analysis method used in this chapter was based on optimized method described in **Chapter 4**. Briefly, downstream data processing involves the following steps: 1. Wilcoxon Rank Statistic was performed to compare which compound treated samples

are significantly different from negative controls. 2. Concurrently, compute  $\log_2$  ratio of compound relative to negative control. 3. Hierarchically cluster biological responses and generate heat map to visualize biological profiles of compounds (**Figure 5.3**).



**Figure 5.3** Overview of downstream data processing.

#### 5.2.6.2 Raw cytological value for a single well

For each feature, raw cytological value  $\mu_m$  is average of all individual cell value in a single well **m**.

#### 5.2.6.3 Comparison between well values and negative control

39 Compounds were screened in triplicates into 4 different plates. Negative control (DMSO control) was included in each plate. We denote  $\mu_{\text{DMSO}}$  as average of all



individual cell values in DMSO. To quantify biological effects of compounds in comparison with negative control (DMSO control),  $\log_2$  of compound to DMSO ratio (C) was performed for every cytological feature using Equation below.

$$C = \log_2 \left( \frac{\text{compound}}{\text{DMSO}} \right) = \log_2 \left( \frac{\mu_m}{\mu_{\text{DMSO}}} \right)$$

#### 5.2.6.4 Wilcoxon Rank Statistic

To test for statistically significant difference between negative control DMSO and compound phenotypes, Wilcoxon Rank Statistic were employed.

**Null hypothesis  $H_0$ :  $\mu_W = \mu_{\text{DMSO}}$**

The null hypothesis claims that the mean of compound treated cell population of values is not significantly different from the mean of control cell population of values ( $p > 0.05$ ).

**Alternative hypothesis  $H_a$ :  $\mu_W \neq \mu_{\text{DMSO}}$**

In the alternative hypothesis, when undergoing compound treatments, cells exhibit significantly different phenotypes from cells in control. The null hypothesis is rejected if p-Value is less than or equal 0.05.

#### *5.2.6.5 Quantile normalization for inter-plate comparison*

We applied it for our downstream data processing to make distribution of cytological feature in different plates within the experiment the same. This method is based on the assumption that cytological feature distributions that are expected to remain constant across plates (Bolstad et al., 2003). Moreover, it also can be used to effectively remove plate effects. This technique was performed for all cytological features in order to make the data across plates comparable.

#### *5.2.6.6 Hierarchical clustering*

In our instance, 39 compounds were screened into 4 different plates against PD hONS cells. Hierarchical clustering was implemented using Ward's method.

Data analysis was performed using Pipeline Pilot (version 9.1), R studio (version 3.0), GraphPad Prism 6<sup>TM</sup> (San Diego, CA).

### **5.3 Results**

#### **5.3.1 Compound library**

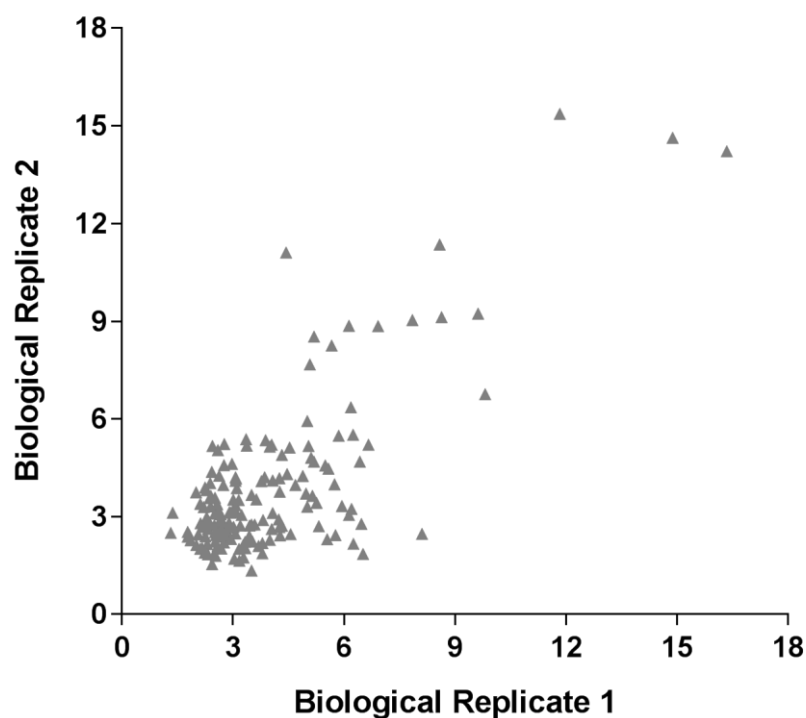
We screened 39 compounds including 4 natural products and 35 natural product scaffold inspired synthetic compounds. The synthetic compound collection has enabled us to decrease the false negative rate since they were synthesized basing on a natural product scaffold. Thus, potential non-identification of an active compound (false-negative) was minimized if other, related compounds were determined (Rydzewski,

2008). In addition, known natural products from which the scaffold was selected for chemical synthesis were screened together with synthetic compounds in order to determine differences in biological activities observed among them.

### **5.3.2 Assessment of intra-plate variability and assay reproducibility**

Coefficient of variation (CV) was used to measure intra-plate variation in 54 technical replicates of negative control (DMSO) and in three technical replicates of all compounds. Our results showed that %CV of three technical replicates of all compounds was less than 20%. However, we observed high %CV in several negative control wells regarding two parameters: tubulin intensity and lysosome intensity. We eliminated negative controls with CV larger than 20%.

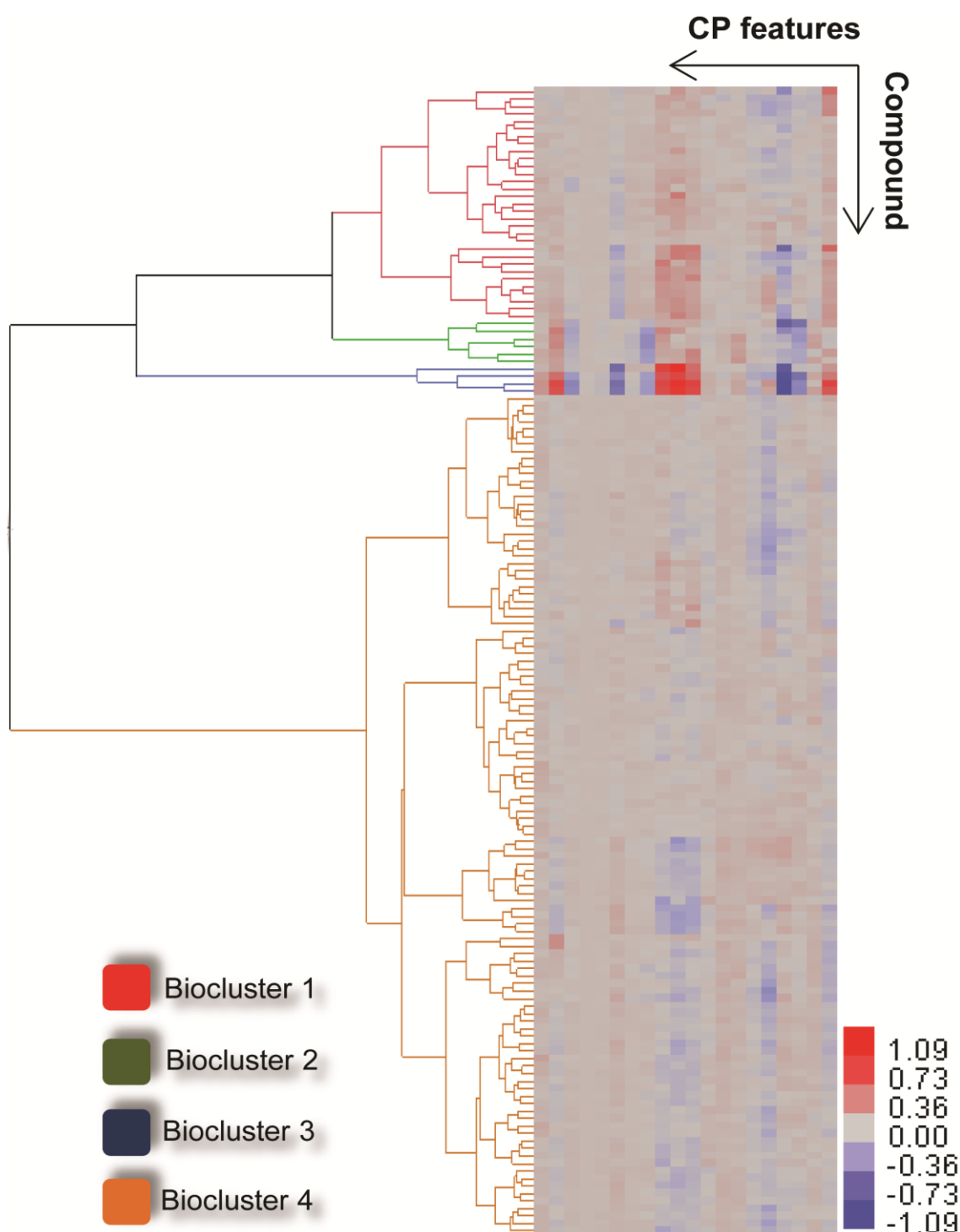
Assay reproducibility was determined by using a method previously published (Woehrmann et al., 2013) that is capable of compacting multidimensional phenotypic responses into a single vector. This method generated cytological features score for each compound across 20 cytological features (See **Section 4.2** and **Table 4.1** in **Chapter 4** for more information about cytological features). The cytological features scores of all compounds in two biological replicates were plotted in scatter plot to determine assay reproducibility (**Figure 5.4**). We observed good linear relationship between two biological replicates.



**Figure 5.4** A scatter plot displays the cytological features scores of all compounds between two replicate experiments. A good linear relationship between two biological replicates was observed.

### 5.3.3 Hierarchical clustering

We profiled 39 compounds at four concentrations, generating 156 compound dose instances. Three toxic compounds (15\_1, 17\_2, 18\_2) at 30  $\mu$ M were eliminated (no viable cell observed after 24h treatment). As a result, the remaining 153 compound dose instances were further analysed. Clustering of biological profiles revealed four bioclusters, of which three bioclusters showed dominant effects on the cells. Heat map of 153 compound dose instances is shown in (**Figure 5.5**).

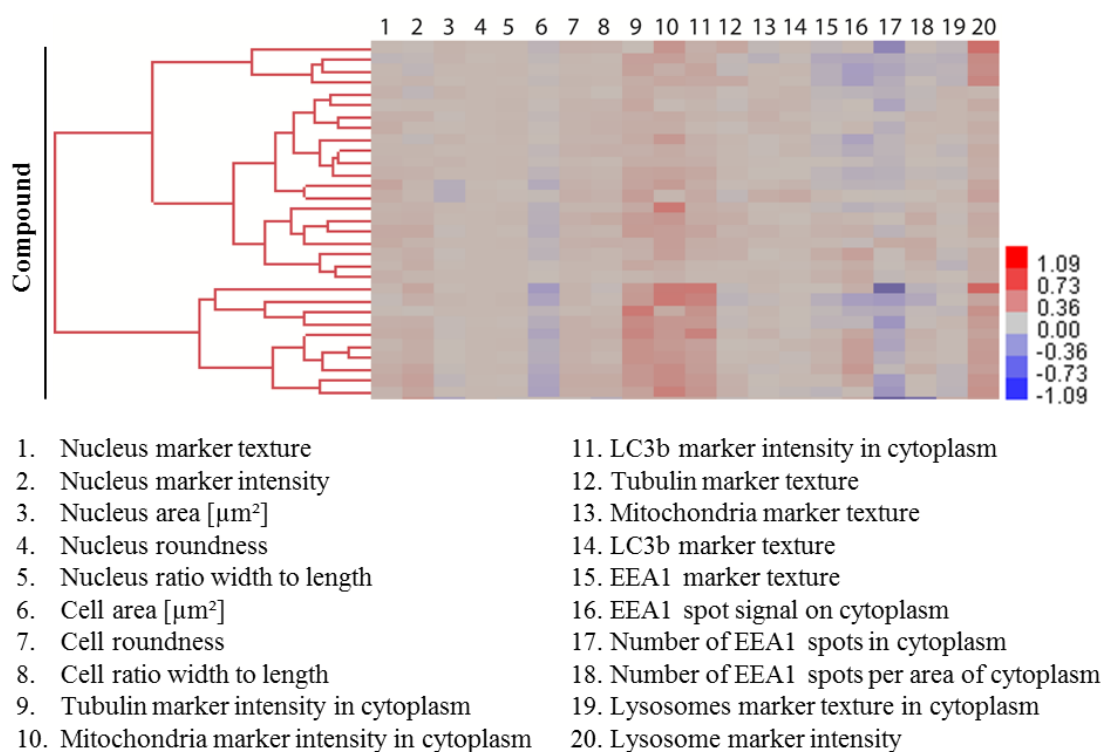


**Figure 5.5** Heat map of 153 compound dose instances plotted on the y axis and 20 cytological features on x axis. Red features indicate positive deviation from control, blue features indicate negative deviation from control, and grey features show no difference with control.

Details of each biocluster is discussed as follows:

## Biocluster 1

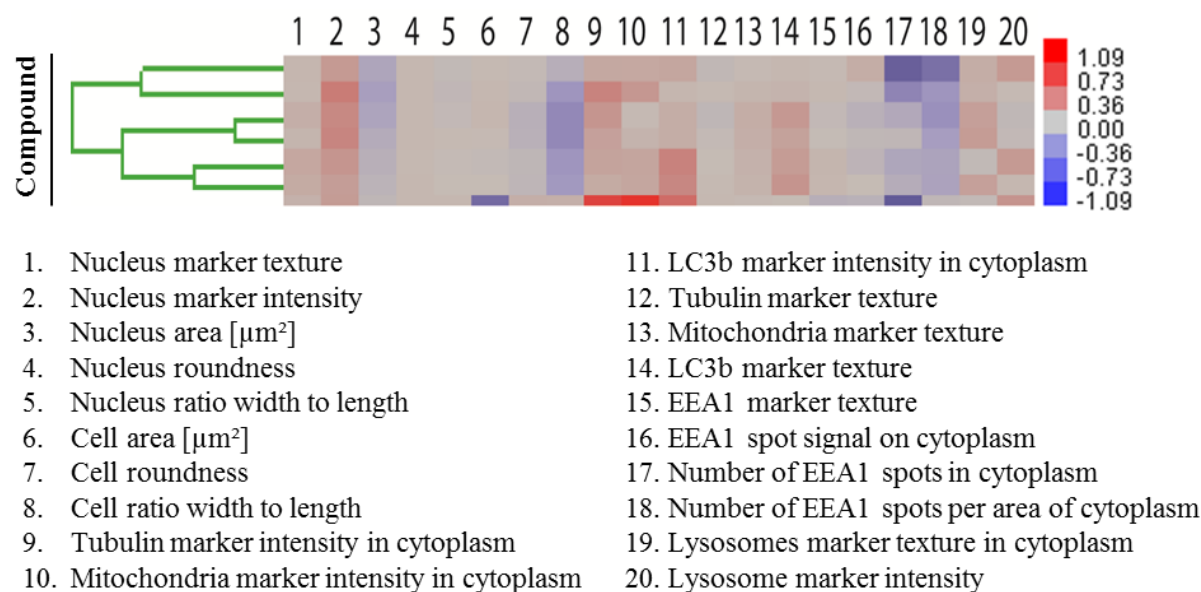
Biocluster 1 contains 31 compound dose instances which showed positive deviation from negative control (DMSO) in intensity of mitochondria, tubulin, LC3b and lysosome and negative deviation in number of early endosome in cytoplasm (**Figure 5.6**).



**Figure 5.6** Heat map of biocluster 1. Heat map depicting cytological profiles of compound dose instances located in biocluster 1 with compounds on y axis and cytological features on x axis.

## Biocluster 2

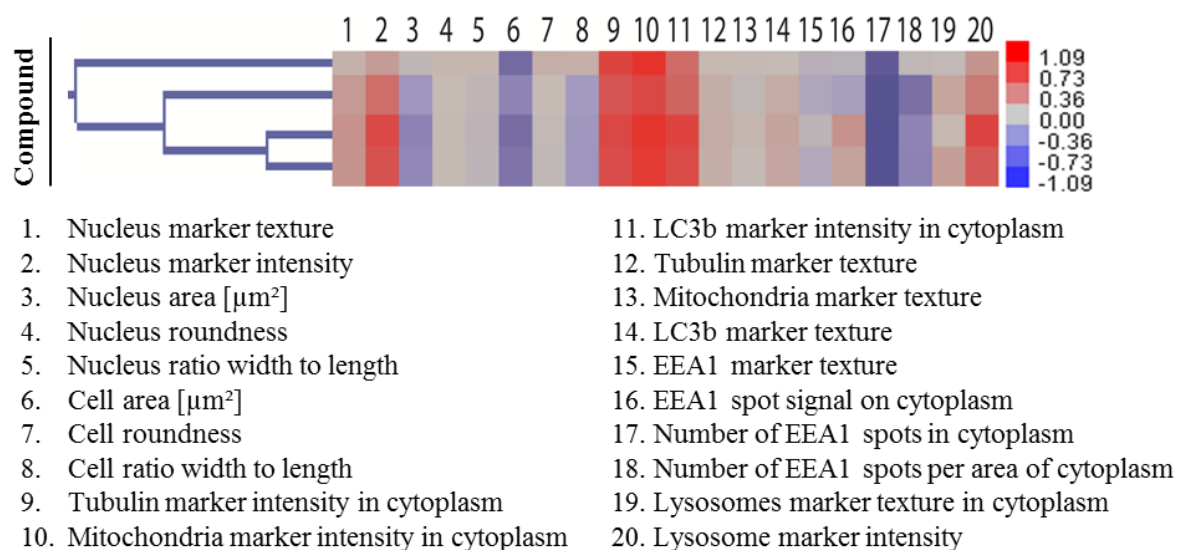
Biocluster 2 consists of 6 compound dose instances which showed positive deviation in intensity of nucleus staining while negative deviation in nucleus area and cell ratio width to length (**Figure 5.7**).



**Figure 5.7** Heat map of biocluster 2. Heat map depicting cytological profiles of compound dose instances located in biocluster 2 with compounds on y axis and cytological features on x axis.

### Biocluster 3

Biocluster 3 contains 4 compound dose instances. Three of them (14\_2 and 15\_2 at 30  $\mu\text{M}$ , and 18\_2 at 10  $\mu\text{M}$ ) exhibited the most potent effect on intensity of tubulin, mitochondria and LC3b (positive deviation), and the number of early endosome in the cytoplasm (negative deviation) (**Figure 5.8**).

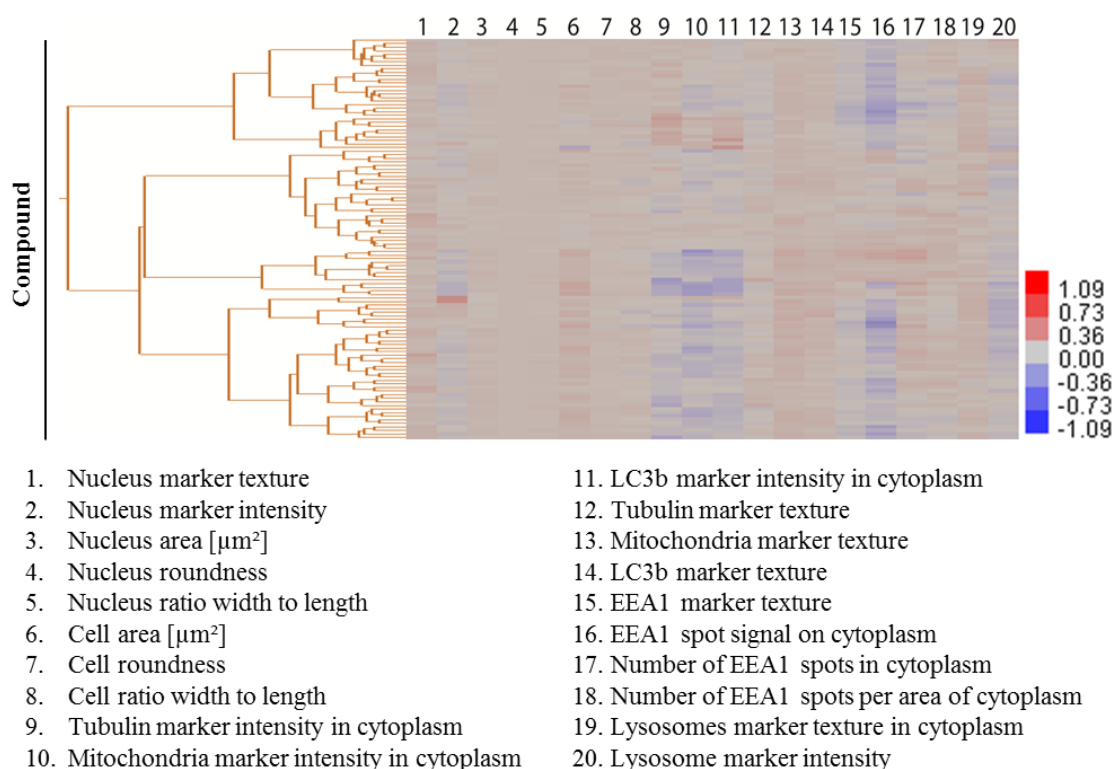


**Figure 5.8** Heat map of biocluster 3. Heat map depicting cytological profiles of compound dose instances located in biocluster 3 with compounds on y axis and cytological features on x axis.

#### Biocluster 4

Biocluster 4 comprises of 112 compound dose instances which showed relatively weak biological effects across 20 cytological features compared to other bioclusters (**Figure 5.9**).



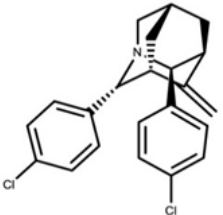
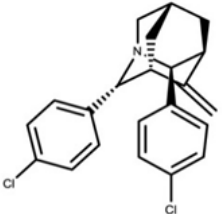
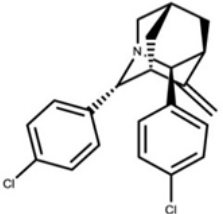
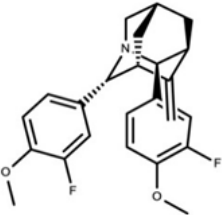
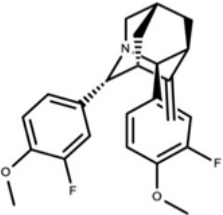
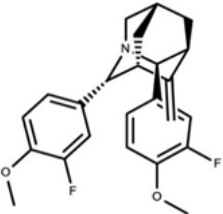
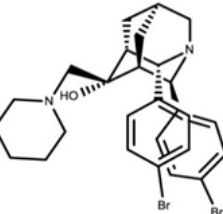


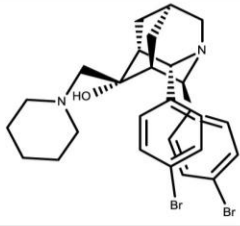
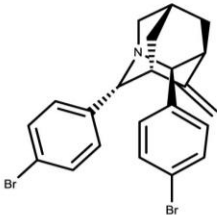
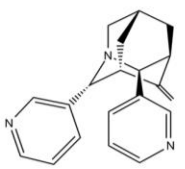
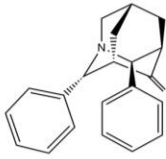
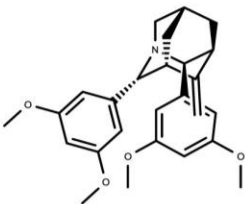
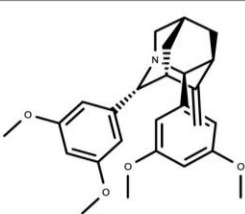
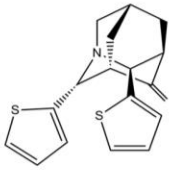
**Figure 5.9** Heat map of biocluster 4. Heat map depicting cytological profiles of compound dose instances located in biocluster 4 with compounds on y axis and cytological features on x axis.

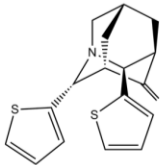
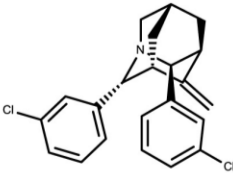
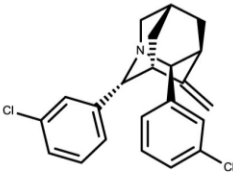
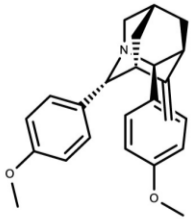
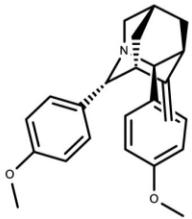
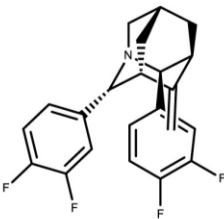
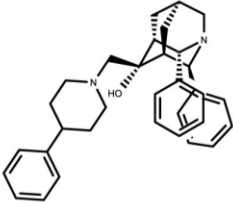
### 5.3.4 Chemical structures of screened compounds

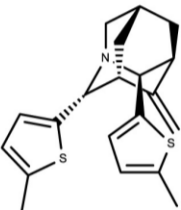
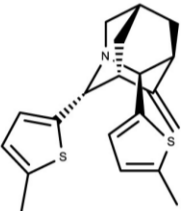
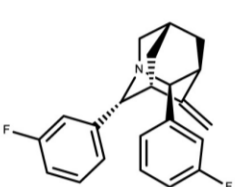
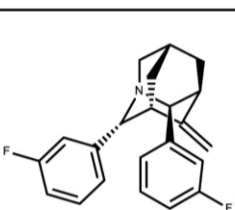
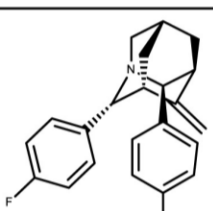
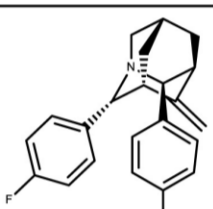
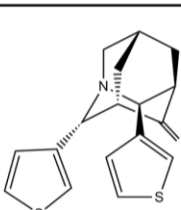
Chemical structures of 35 synthetic compounds and four natural products, and their bioclusters are shown in **Table 5.1**

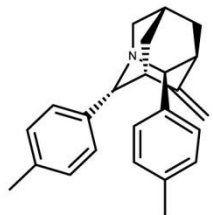
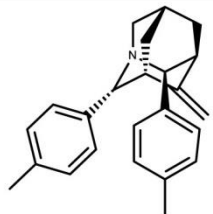
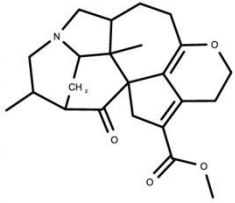
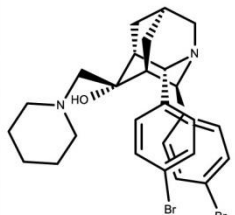
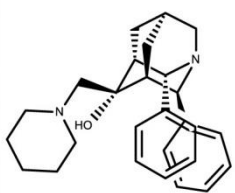
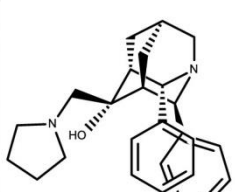
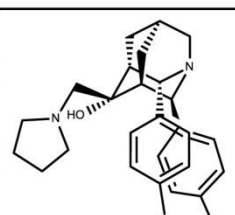
**Table 5.1** Table displays structures of natural products and natural product scaffold inspired synthetic compounds, testing concentration ( $\mu\text{M}$ ), biological clusters and chemical clusters.

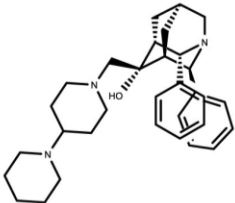
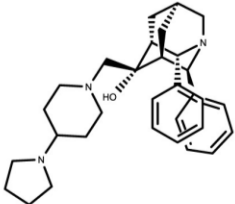
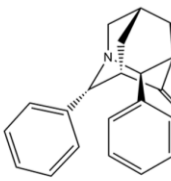
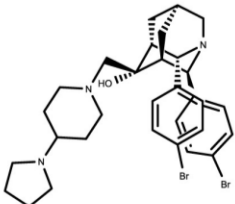
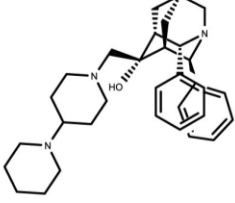
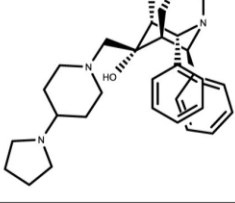
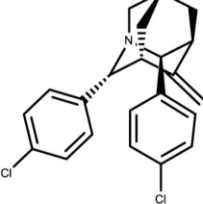
CdId	Structure	Compound	Testing concentration	BioCluster	ChemCluster
1		1_1	30	1	4
2		1_1	10	1	4
3		1_1	1	1	4
4		6_1	30	1	4
5		6_1	10	1	4
6		6_1	3	1	4
7		16_1	3	1	1

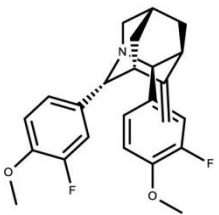
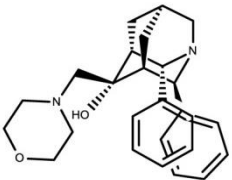
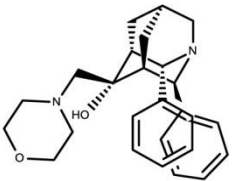
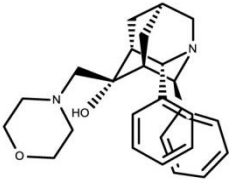
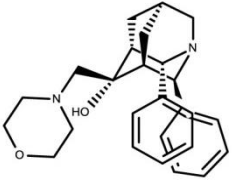
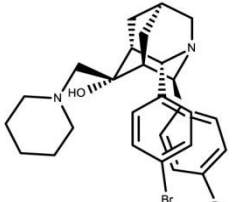
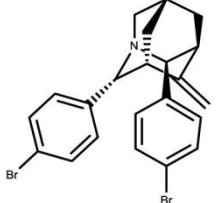
CdId	Structure	Compound	Testing concentration	BioCluster	ChemCluster
8		16_1	1	1	1
9		2_1	30	1	4
10		7_1	30	1	4
11		3_1	10	1	4
12		4_1	30	1	4
13		4_1	10	1	4
14		9_1	30	1	4

CdId	Structure	Compound	Testing concentration	BioCluster	ChemCluster
15		9_1	10	1	4
16		5_1	30	1	4
17		5_1	10	1	4
18		1_2	30	1	4
19		1_2	10	1	4
20		6_2	30	1	4
21		16_2	3	1	1

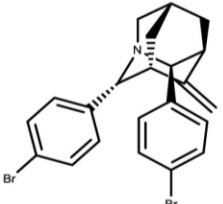
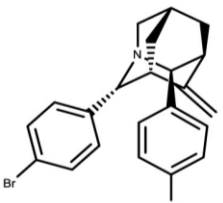
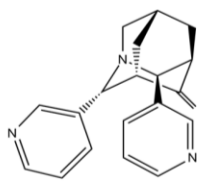
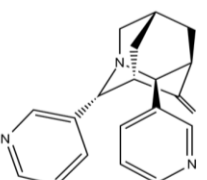
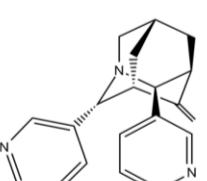
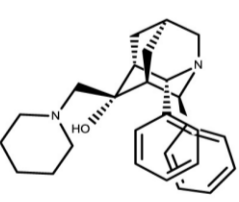
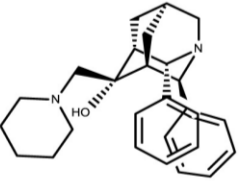
CdId	Structure	Compound	Testing concentration	BioCluster	ChemCluster
22		7_2	30	1	4
23		7_2	10	1	4
24		3_2	30	1	4
25		3_2	10	1	4
26		4_2	30	1	4
27		4_2	10	1	4
28		9_2	30	1	4

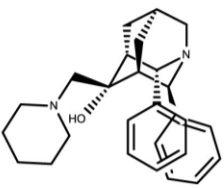
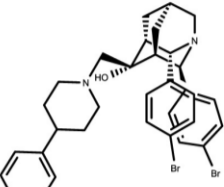
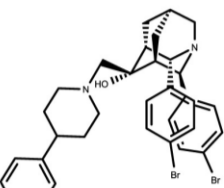
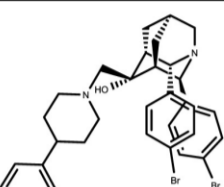
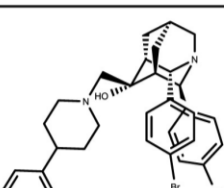
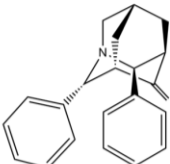
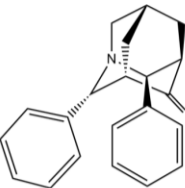
CdId	Structure	Compound	Testing concentration	BioCluster	ChemCluster
29		10_2	30	1	4
30		10_2	10	1	4
31		20_1	30	1	3
32		16_1	30	2	1
33		12_1	30	2	1
34		13_1	30	2	1
35		15_1	10	2	1

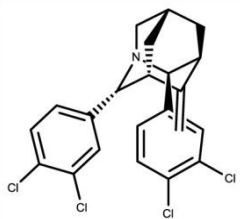
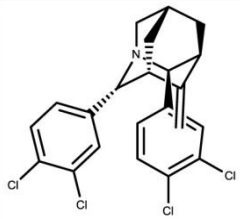
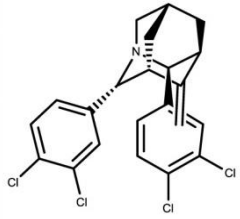
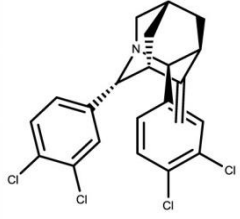
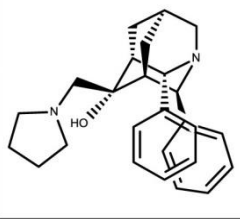
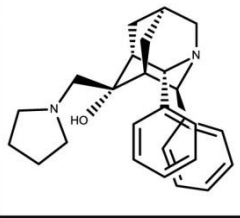
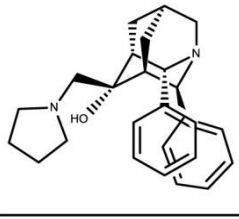
CdId	Structure	Compound	Testing concentration	BioCluster	ChemCluster
36		14_2	10	2	1
37		15_2	10	2	1
38		3_1	30	3	4
39		18_2	10	3	1
40		14_2	30	3	1
41		15_2	30	3	1
42		1_1	3	4	4

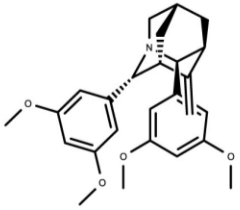
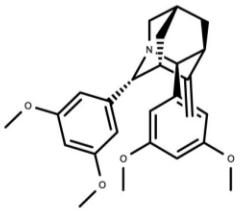
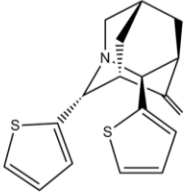
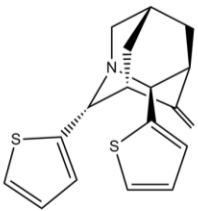
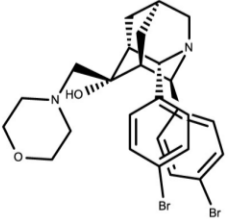
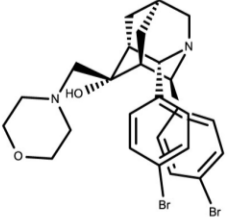
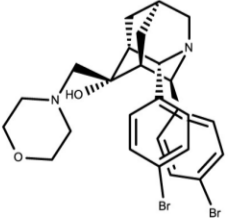
CdId	Structure	Compound	Testing concentration	BioCluster	ChemCluster
43		6_1	1	4	4
44		11_1	30	4	1
45		11_1	10	4	1
46		11_1	3	4	1
47		11_1	1	4	1
48		16_1	10	4	1
49		2_1	10	4	4

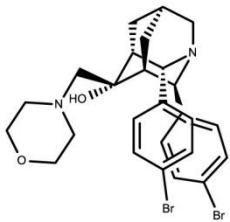
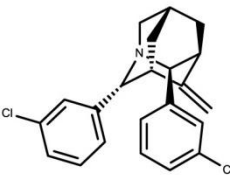
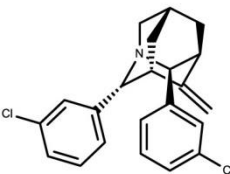
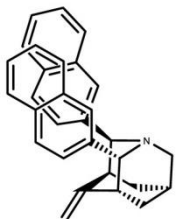
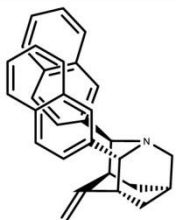
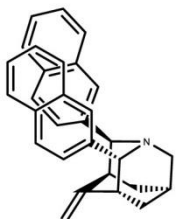
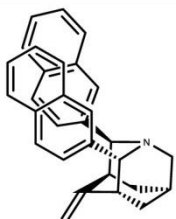


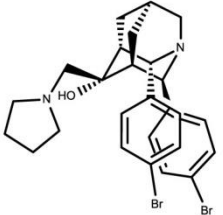
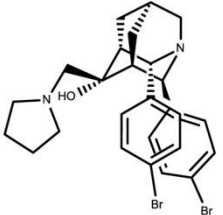
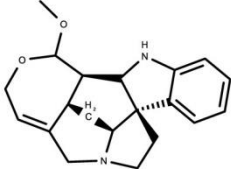
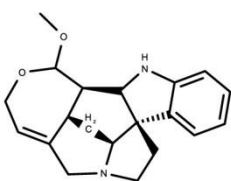
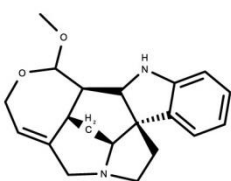
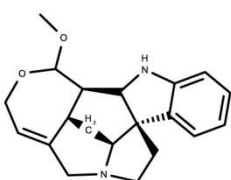
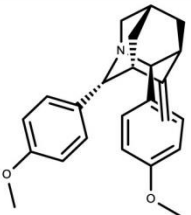
CdId	Structure	Compound	Testing concentration	BioCluster	ChemCluster
50		2_1	3	4	4
51		2_1	1	4	4
52		7_1	10	4	4
53		7_1	3	4	4
54		7_1	1	4	4
55		12_1	10	4	1
56		12_1	3	4	1

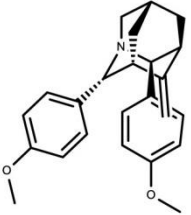
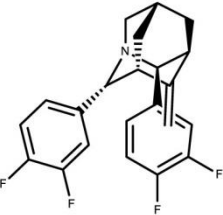
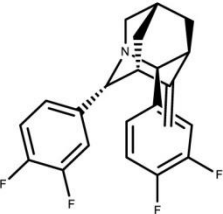
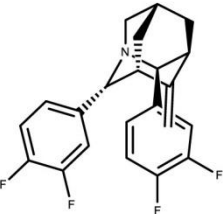
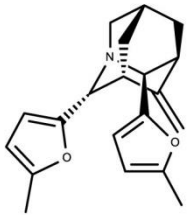
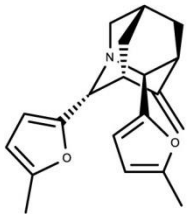
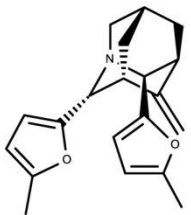
CddId	Structure	Compound	Testing concentration	BioCluster	ChemCluster
57		12_1	1	4	1
58		17_1	30	4	1
59		17_1	10	4	1
60		17_1	3	4	1
61		17_1	1	4	1
62		3_1	3	4	4
63		3_1	1	4	4

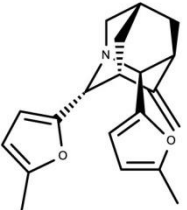
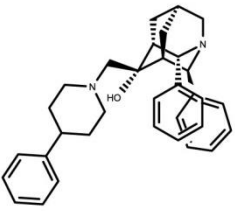
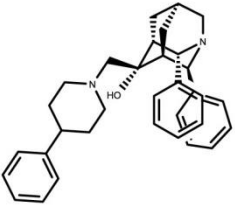
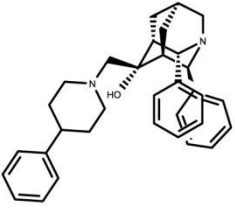
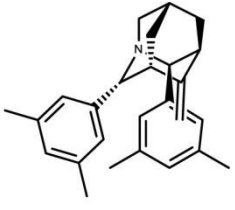
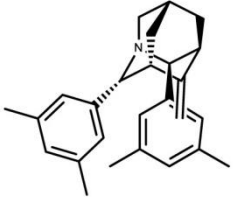
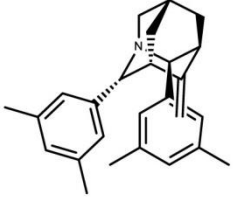
CdId	Structure	Compound	Testing concentration	BioCluster	ChemCluster
64		8_1	30	4	4
65		8_1	10	4	4
66		8_1	3	4	4
67		8_1	1	4	4
68		13_1	10	4	1
69		13_1	3	4	1
70		13_1	1	4	1

CdId	Structure	Compound	Testing concentration	BioCluster	ChemCluster
71		4_1	3	4	4
72		4_1	1	4	4
73		9_1	3	4	4
74		9_1	1	4	4
75		14_1	30	4	1
76		14_1	10	4	1
77		14_1	3	4	1

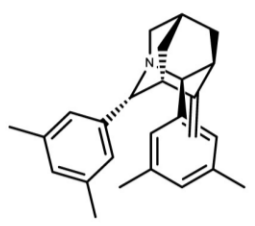
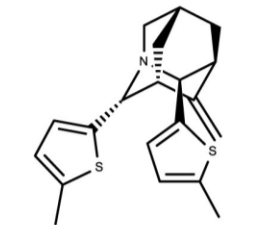
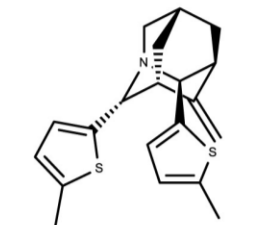
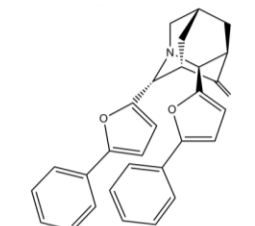
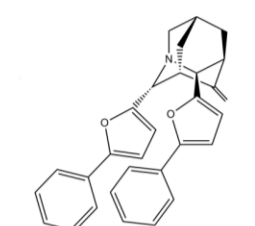
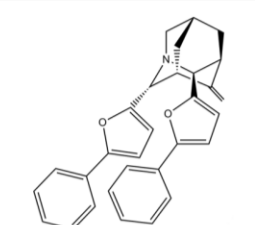
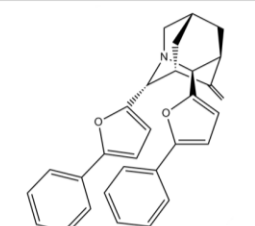
Cdd	Structure	Compound	Testing concentration	BioCluster	ChemCluster
78		14_1	1	4	1
79		5_1	3	4	4
80		5_1	1	4	4
81		10_1	30	4	4
82		10_1	10	4	4
83		10_1	3	4	4
84		10_1	1	4	4

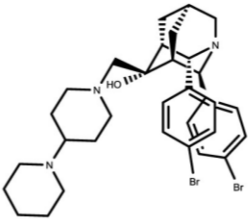
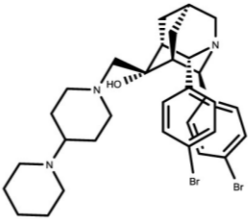
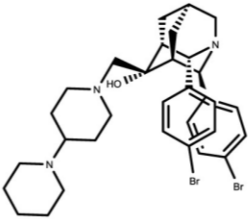
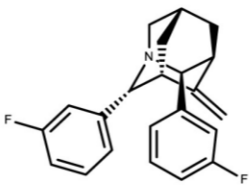
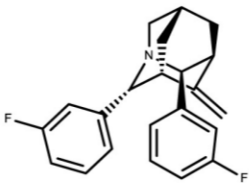
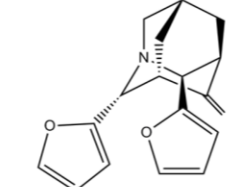
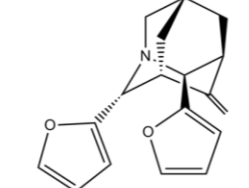
CdId	Structure	Compound	Testing concentration	BioCluster	ChemCluster
85		15_1	3	4	1
86		15_1	1	4	1
87		25_1	30	4	2
88		25_1	10	4	2
89		25_1	3	4	2
90		25_1	1	4	2
91		1_2	3	4	4

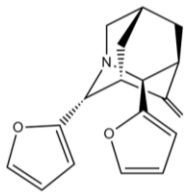
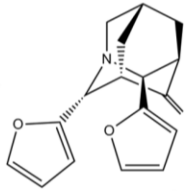
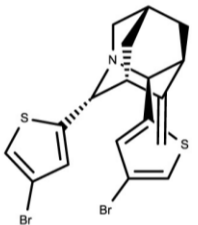
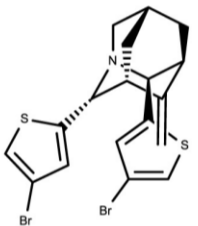
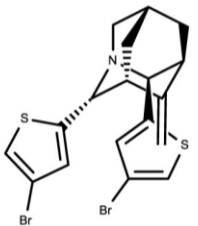
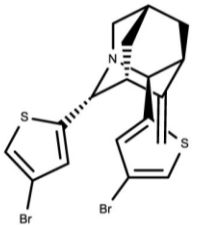
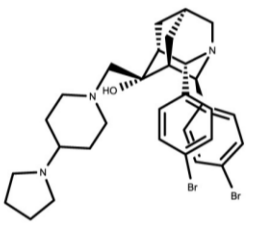
CdId	Structure	Compound	Testing concentration	BioCluster	ChemCluster
92		1_2	1	4	4
93		6_2	10	4	4
94		6_2	3	4	4
95		6_2	1	4	4
96		11_2	30	4	4
97		11_2	10	4	4
98		11_2	3	4	4

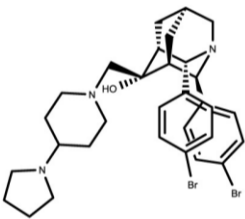
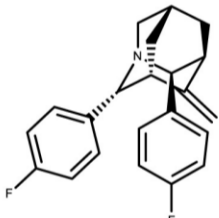
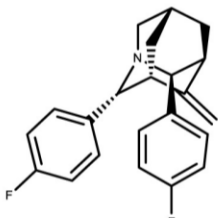
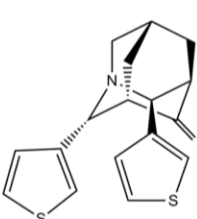
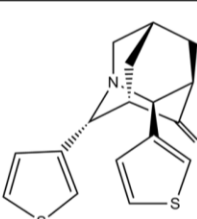
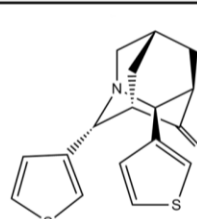
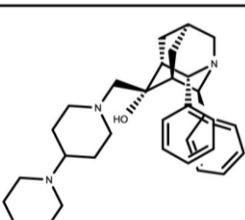
CdId	Structure	Compound	Testing concentration	BioCluster	ChemCluster
99		11_2	1	4	4
100		16_2	30	4	1
101		16_2	10	4	1
102		16_2	1	4	1
103		2_2	30	4	4
104		2_2	10	4	4
105		2_2	3	4	4

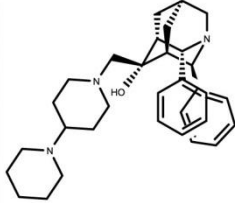
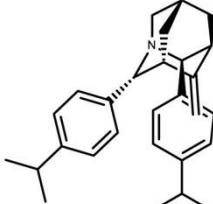
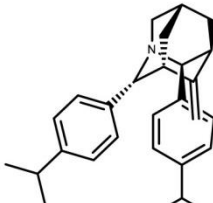
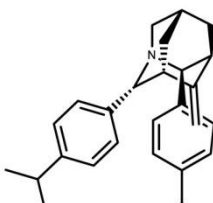
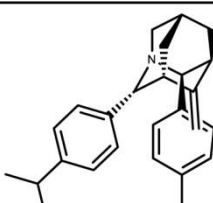
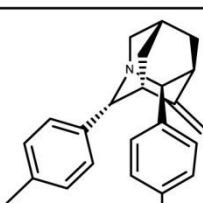
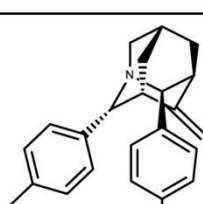


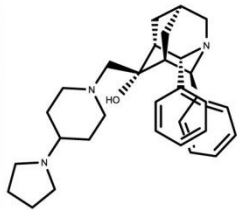
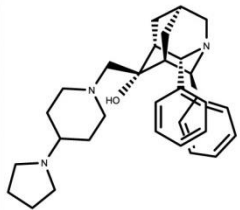
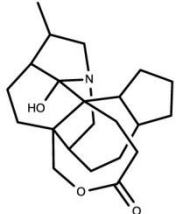
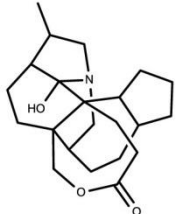
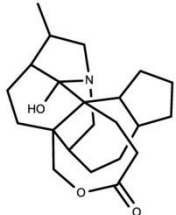
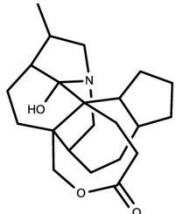
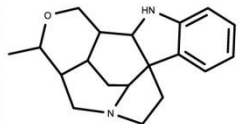
CdId	Structure	Compound	Testing concentration	BioCluster	ChemCluster
106		2_2	1	4	4
107		7_2	3	4	4
108		7_2	1	4	4
109		12_2	30	4	4
110		12_2	10	4	4
111		12_2	3	4	4
112		12_2	1	4	4

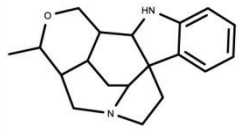
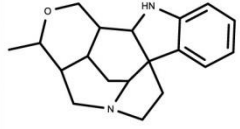
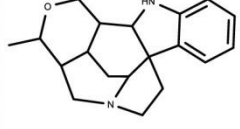
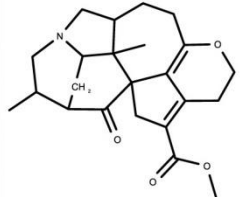
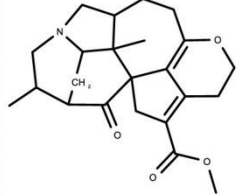
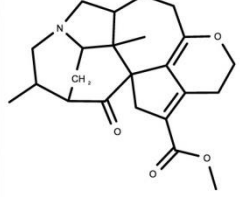
CdId	Structure	Compound	Testing concentration	BioCluster	ChemCluster
113		17_2	10	4	1
114		17_2	3	4	1
115		17_2	1	4	1
116		3_2	3	4	4
117		3_2	1	4	4
118		8_2	30	4	4
119		8_2	10	4	4

CdId	Structure	Compound	Testing concentration	BioCluster	ChemCluster
120		8_2	3	4	4
121		8_2	1	4	4
122		13_2	30	4	4
123		13_2	10	4	4
124		13_2	3	4	4
125		13_2	1	4	4
126		18_2	3	4	1

CdId	Structure	Compound	Testing concentration	BioCluster	ChemCluster
127		18_2	1	4	1
128		4_2	3	4	4
129		4_2	1	4	4
130		9_2	10	4	4
131		9_2	3	4	4
132		9_2	1	4	4
133		14_2	3	4	1

Cdid	Structure	Compound	Testing concentration	BioCluster	ChemCluster
134		14_2	1	4	1
135		5_2	30	4	4
136		5_2	10	4	4
137		5_2	3	4	4
138		5_2	1	4	4
139		10_2	3	4	4
140		10_2	1	4	4

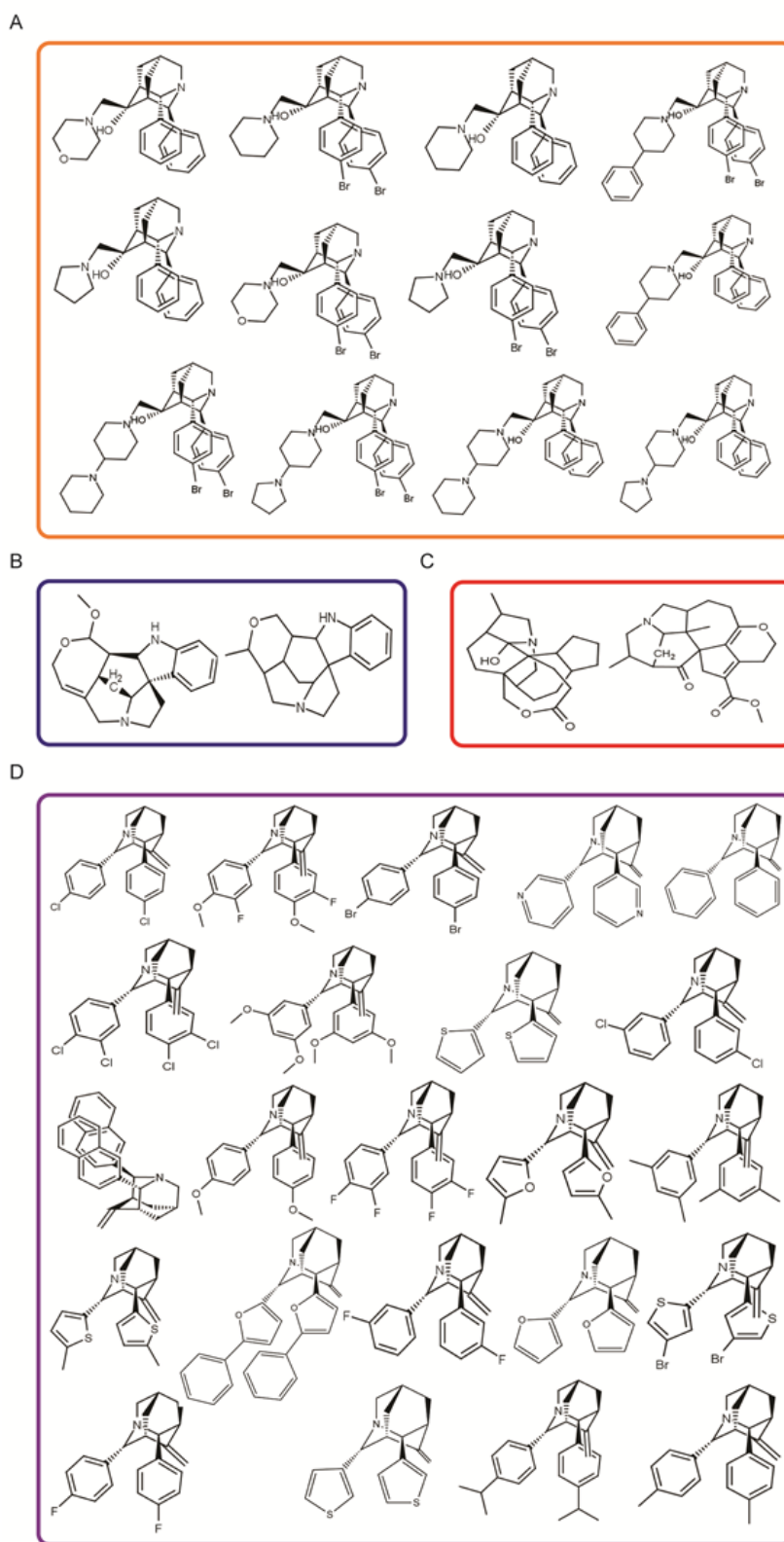
CdId	Structure	Compound	Testing concentration	BioCluster	ChemCluster
141		15_2	3	4	1
142		15_2	1	4	1
143		21_1	30	4	3
144		21_1	10	4	3
145		21_1	3	4	3
146		21_1	1	4	3
147		23_1	30	4	2

CdId	Structure	Compound	Testing concentration	BioCluster	ChemCluster
148		23_1	10	4	2
149		23_1	3	4	2
150		23_1	1	4	2
151		20_1	10	4	3
152		20_1	3	4	3
153		20_1	1	4	3

### 5.3.5 Exploration of structure and activity relationships (SARs)

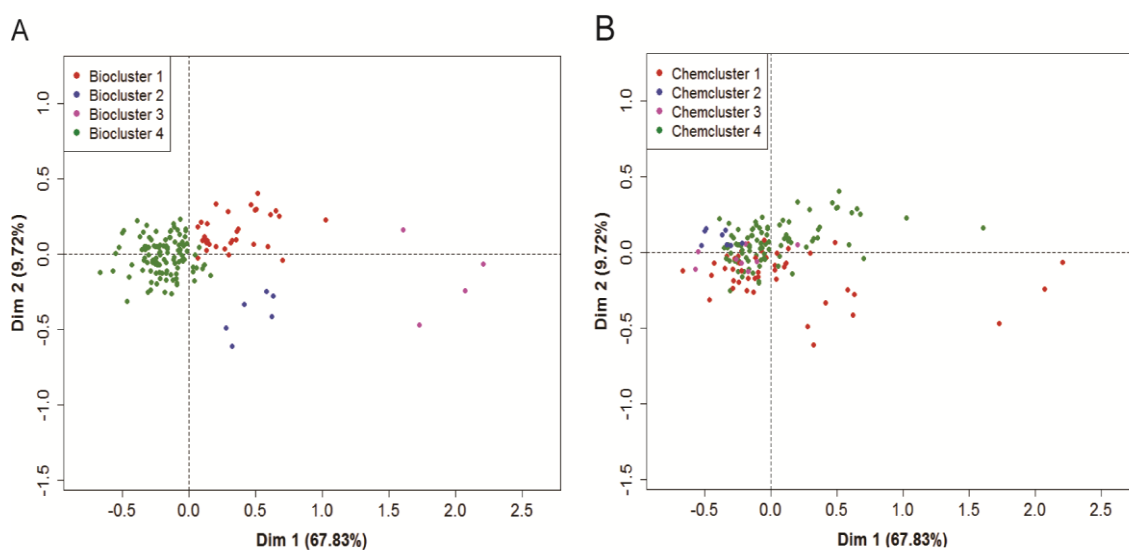
We closely examined this screening set to address chemical similarity. In order to measure structural fingerprints, we employed ECFP\_4 (Extended Connectivity FingerPrint with the largest possible fragment having a width of 4 bonds) which is specifically designed to account for molecular features in relation to biological functions as well as for pharmacological activity prediction (Rogers and Hahn, 2010). The ECFP\_4 fingerprints were then compared using Tanimoto coefficient which is the most often applied to quantify fingerprint overlap (Hu et al., 2009). Taken ECFP\_4 fingerprints and Tanimoto coefficient together, we clustered chemical structures of screened compounds into four chemical clusters (**Figure. 5.10**).





**Figure 5.10** Clustering of chemical structures based on ECFP<sub>4</sub> fingerprints and Tanimoto coefficient. Panels (A), (B), (C) and (D) are chemical clusters 1, 2, 3, 4, respectively.

In medicinal chemistry, the central principle is that structurally similar molecules have similar biological activities. The concept of similarity has been particularly favored in drug discovery. We used principal component analysis (PCA) to explore general structure and activity relationships (**Figure.5.11**). Each colored point represents a single compound at one concentration. Compounds are colored based on biological clusters (bioclusters) (**Figure.5.11 A**) or chemical clusters (chemclusters) (**Figure.5.11 B**). We found that there are three phenotypic clusters displaying high structural convergence: biocluster 1 containing mostly compounds derived from chemcluster 4, biocluster 2 enriching by compounds from chemcluster 1 and biocluster 3 consisting of molecules from chemcluster 1. Unlike other phenotypic clusters, biocluster 4 is enriched with compounds from the four chemclusters.



**Figure 5.11** Exploration of general structure activity relationship in principal component analysis (PCA). Each colored point represents a single compound at one concentration. PCA shows principal component 1 (PC1 or Dim 1) (67.83%) and principal component 2 (PC2 or Dim 2) (9.72%). (A) PCA displays distribution of compounds in biological space. Compounds were colored based on their bioclusters. (B) PCA also gives information about compounds distribution in biological space, however, compounds were colored according to their chemclusters.

### 5.3.6 Examples of structure activity relationships in the second library

In order to determine the extent to which cytological phenotypes are related to changes in chemical structures, we analysed six representative compounds, 1\_1, 2\_1, 3\_1, 14\_2, 15\_2 (each at 30  $\mu$ M) and 18\_2 (at 10  $\mu$ M) by comparing chemical structures with biological profiles. These compounds share the same core structure 1-azaadamantanes, however, possess different substituents. Chemical structures of six representative compounds are shown in **Figure 5.12 A**. Their biological profiles were examined by both heat map and bar chart. As shown in the heat map (**Figure 5.5**), compounds were grouped into different bioclusters: compound 1\_1, 2\_1 belonged to biocluster 1, and compound 3\_1, 14\_2, 15\_2, and 18\_2 belonged to biocluster 3. Bar charts were plotted and six of the cytological features, *i.e.* nucleus intensity, cell area, tubulin intensity, mitochondria intensity, LC3b intensity and lysosome intensity were investigated (**Figure 5.12 B**, blue rectangular boxes).

The difference between compound 1\_1 and 2\_1 is that chlorine was substituted for bromide. These substituents induced the least effect in negative direction on nucleus intensity as compared with other four compounds (**Figure 5.12 B, cytological feature 2**). Compound 3\_1 that displays high structural similarity with 1\_1 and 2\_1 and lacks substituent on the phenyl ring, showed a reversed effect on the same cytological feature. Compounds 14\_2 and 15\_2 are structurally related with different substituents on a six membered ring; the former contains an additional six membered ring whereas the latter has an additional five membered ring. This difference did not induce any significant change in nucleus intensity; both compounds displayed positive deviation from the DMSO control. Notably, compound 18\_2 was cytotoxic at 30  $\mu$ M (no viable cell observed after 24h treatment). The cytotoxicity was potentially due to the additional a -

Br moiety on the phenyl ring which at 10  $\mu$ M rendered 18\_2 a lesser effect than 15\_2 at 30  $\mu$ M on nucleus intensity. Three compounds including 14\_2, 15\_2, and 18\_2 exhibited comparable effects, whereas 14\_2 with 1,4'-bipiperidine and additional a -OH moiety was likely to induce greater effect than 15\_2 with 4-(pyrrolidine-1-yl)piperidine and additional a -OH moiety, and 18\_2 with 4-(pyrrolidine-1-yl)piperidine, -OH and -Br moieties. Compound 3\_1 displayed the least effect as compared with 14\_2, 15\_2 and 18\_2, potentially due to lack of soluble groups. Likewise, compound 2\_1 that lacks soluble group showed minimal effect in negative direction compared to 18\_2.

Investigation of cell area (**Figure 5.12 B, cytological feature 6**) revealed that the six representative compounds showed similar activity in the negative direction. The additional -Cl and -Br moieties significantly decreased activity, rendering 1\_1 and 2\_1 the least effect on cell area (-Cl substituent had slightly greater effect than -Br) among six compounds. The absence of substituents in compound 3\_1 conferred on it the most potent effect on cell area compared to the other five compounds while the presence of substituents including six membered ring with -OH moiety, five membered ring with -OH moiety, and five membered ring, -OH and -Br moieties did not enhance the activity; instead they slightly reduced the effect of 14\_2, 15\_2, 18\_2 as compared with 3\_1. The presence of additional -Br moiety rendered compound 18\_2 less effective than 15\_2. In contrast, the addition of the five membered ring, -OH and -Br moieties in compound 18\_2 substantially increased the effect in the same direction compared to the sole occurrence of -Br moiety in compound 2\_1.

The additional -Cl substituent (compound 1\_1) resulted in a reversed effect, on tubulin intensity (**Figure 5.12 B, cytological feature 9**) as compared with -Br substituent (compound 2\_1) (compound 1\_1: negative deviation, compound 2\_1: positive

deviation). Moreover, -Br substituent had marginally greater effect in opposite direction compared to -Cl substituent.

Similar to the effect pattern observed on cell area, the addition of 4'-bipiperidine with -OH moiety, 4-(pyrrolidine-1-yl)piperidine with -OH moiety, and 4-(pyrrolidine-1-yl)piperidine with -OH and -Br moieties in compounds 14\_2, 15\_2, and 18\_2, respectively, did not significantly increase the activity associated with tubulin intensity. Similarly, the absence of the above substituents in compound 3\_1 did not have any substantial effect, but rather a slight increase in the positive direction in direct comparison to the three compounds above. Nevertheless, the lack of 4-(pyrrolidine-1-yl)piperidine and -OH substituents in compound 2\_1 considerably diminished the effect on tubulin intensity in the same direction as compared with 18\_2. In comparison to 3\_1, and the presence of -Br substituent led to considerable reduction in the positive direction on the above property in compound 2\_1. Markedly, the presence of the -Cl substituent dramatically diminished and reversed the effect of compound 1\_1 as compared with 3\_1.

Regarding mitochondria intensity (**Figure 5.12 B, cytological feature 10**), the six representative compounds showed a similar pattern in cell area features (**Figure 5.12 B, cytological feature 6**), however in the opposite direction (positive deviation). It is worth noting that the absence of any substituent induced the most potent effect on mitochondria intensity (compound 3\_1). The addition of soluble groups could potentially enhance activity on the above property. Evidently, compounds 14\_2, 15\_2, 3\_1 exhibited significantly greater effect than 1\_1 and 2\_1.

A similar effect pattern to that observed for mitochondria intensity (**Figure 5.12 B, cytological feature 10**) was also observed with LC3b intensity (**Figure 5.12 B, cytological feature 11**), apart from compound 3\_1 that lacks any substituent on phenyl ring which showed less effect compared to 14\_2, 15\_2 and 18\_2. In this particular feature, addition of soluble groups potentially improved activity.

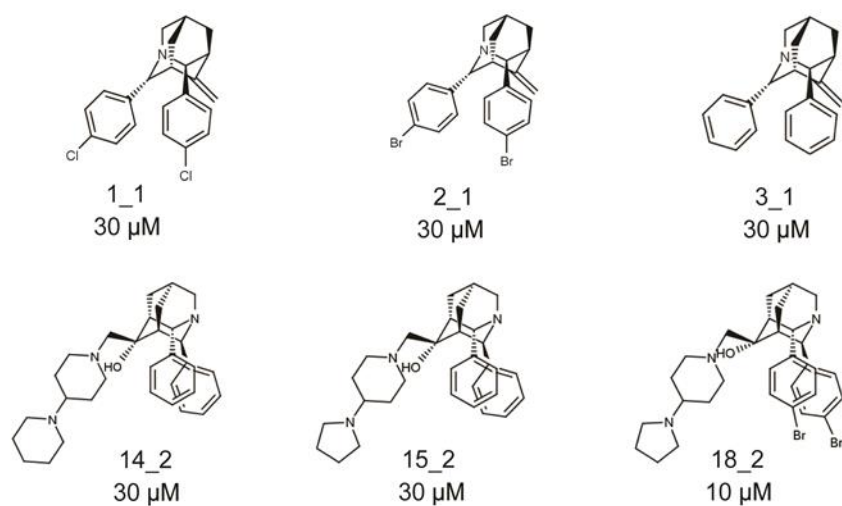
Examination of lysosome intensity (**Figure 5.12 B, cytological feature 20**) showed that compounds 14\_2, 15\_2, 18\_2 exhibited similar effects, with the most potent being 14\_2 and the least potent being 18\_2. In addition, 2\_1 remained the compound with the least effect among six representative compounds. Noticeably, a -Cl substituent (compound 1\_1) induced substantially greater effect on lysosome intensity as compared with -H (compound 3\_1). Likewise, -Cl substituent exhibited more potent effect than five membered ring, -OH and -Br substituents (compound 18\_2). The lack of any substituent in compound 3\_1 resulted in significant reduction of effect on lysosome intensity compared to five membered ring and -Br substituent in compound 18\_2.

In summary, the -Cl and -Br substituents induced minor effects on five investigated cytological features; except for lysosome intensity in cytoplasm (**cytological feature 20**) where -Br moiety is more potent than -Cl, -H and 4-(pyrrolidine-1-yl)piperidine and -Br substituents. In the absence of any substituent, compound 3\_1 exhibited the most potent effect on cell area (**cytological feature 6**), tubulin intensity (**cytological feature 9**) and mitochondria intensity (**cytological feature 10**) among six compounds. In comparison compounds 14\_2, 15\_2 and 18\_2, 4'-bipiperidine with -OH substituent (compound 14\_2) produced more potent effect than 4-(pyrrolidine-1-yl)piperidine with -OH substituent (compound 15\_2) which induced greater effect than 4-(pyrrolidine-1-

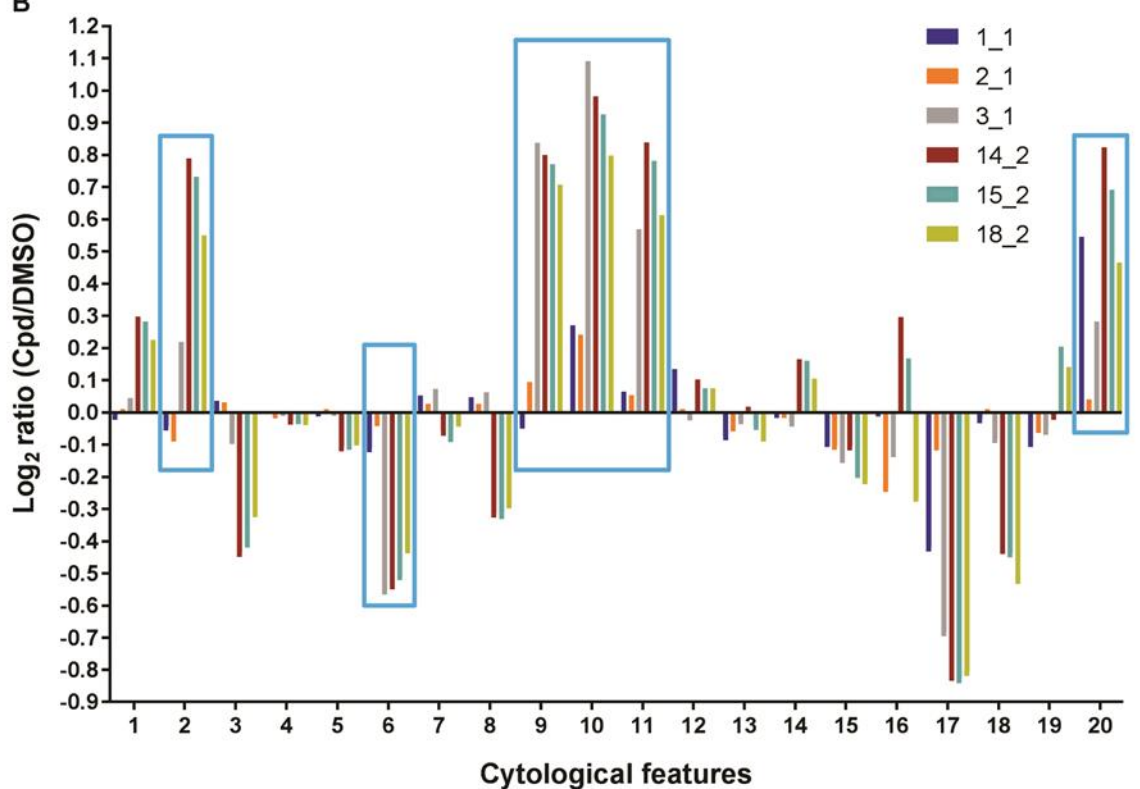
yl)piperidine with -Br and -OH substituents (compound 18\_2), across six investigated cytological features (**blue rectangular boxes**) regardless of the direction of the effect.

The results suggested that different decorations of a common scaffold confer compounds different biological activities evident in varying cellular phenotypes, particularly in nuclear intensity, cell area, and tubulin intensity, mitochondria, LC3b and lysosome. The possible mechanistic explanations for these alterations of biological activity remained to be clarified but cytological profiling offers a sensitive and multiparameter platform on which to assay chemical libraries.

**A**



**B**



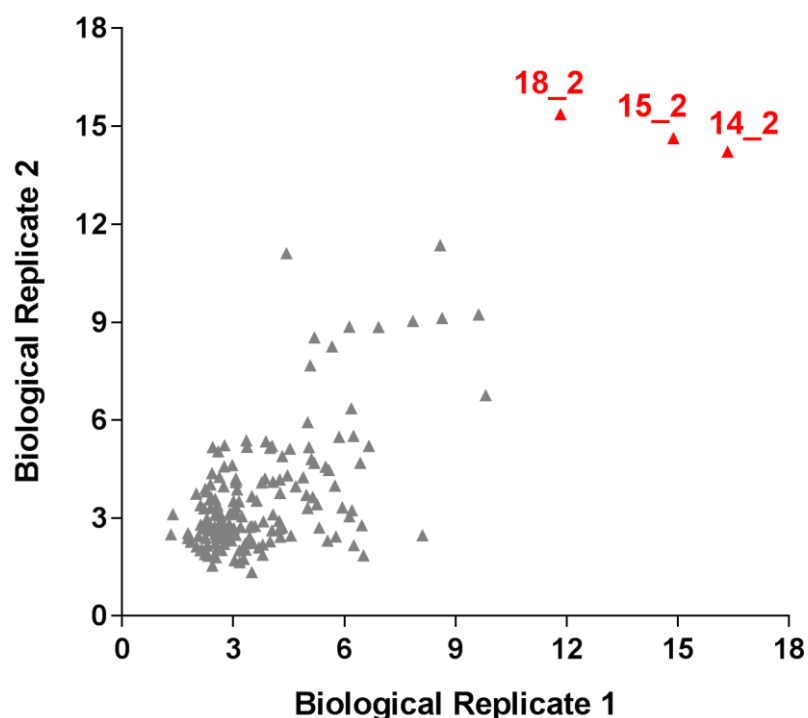
- |  |  |
|--|--|
| 1. Nucleus marker texture                      | 11. LC3b marker intensity in cytoplasm         |
| 2. Nucleus marker intensity                    | 12. Tubulin marker texture                     |
| 3. Nucleus area [ $\mu\text{m}^2$ ]            | 13. Mitochondria marker texture                |
| 4. Nucleus roundness                           | 14. LC3b marker texture                        |
| 5. Nucleus ratio width to length               | 15. EEA1 marker texture                        |
| 6. Cell area [ $\mu\text{m}^2$ ]               | 16. EEA1 spot intensity in cytoplasm           |
| 7. Cell roundness                              | 17. Number of EEA1 spots in cytoplasm          |
| 8. Cell ratio width to length                  | 18. Number of EEA1 spots per area of cytoplasm |
| 9. Tubulin marker intensity in cytoplasm       | 19. Lysosomes marker texture                   |
| 10. Mitochondria marker intensity in cytoplasm | 20. Lysosome marker intensity in cytoplasm     |



**Figure 5.12** Examples of structure activity relationships. **Panel (A)** Scaffold imidazole and chemical structures of six 1- azaadamantanes containing compounds. **Panel (B)** The bar chart describes biological responses of six 1- zaadamantanes containing compounds (compound 1\_1: dark blue colour, compound 2\_1: orange colour, compound 3\_1: grey colour, compound 14\_2: maroon colour, compound 15\_2: petrol blue colour) at 30  $\mu$ M and (18\_2: mustard colour) at 10  $\mu$ M with x axis as 20 cytological features and y axis as logarithm base 2 of the ratio of compound and DMSO. Blue rectangular boxes indicate investigated cytological features.

### 5.3.7 Hit identification

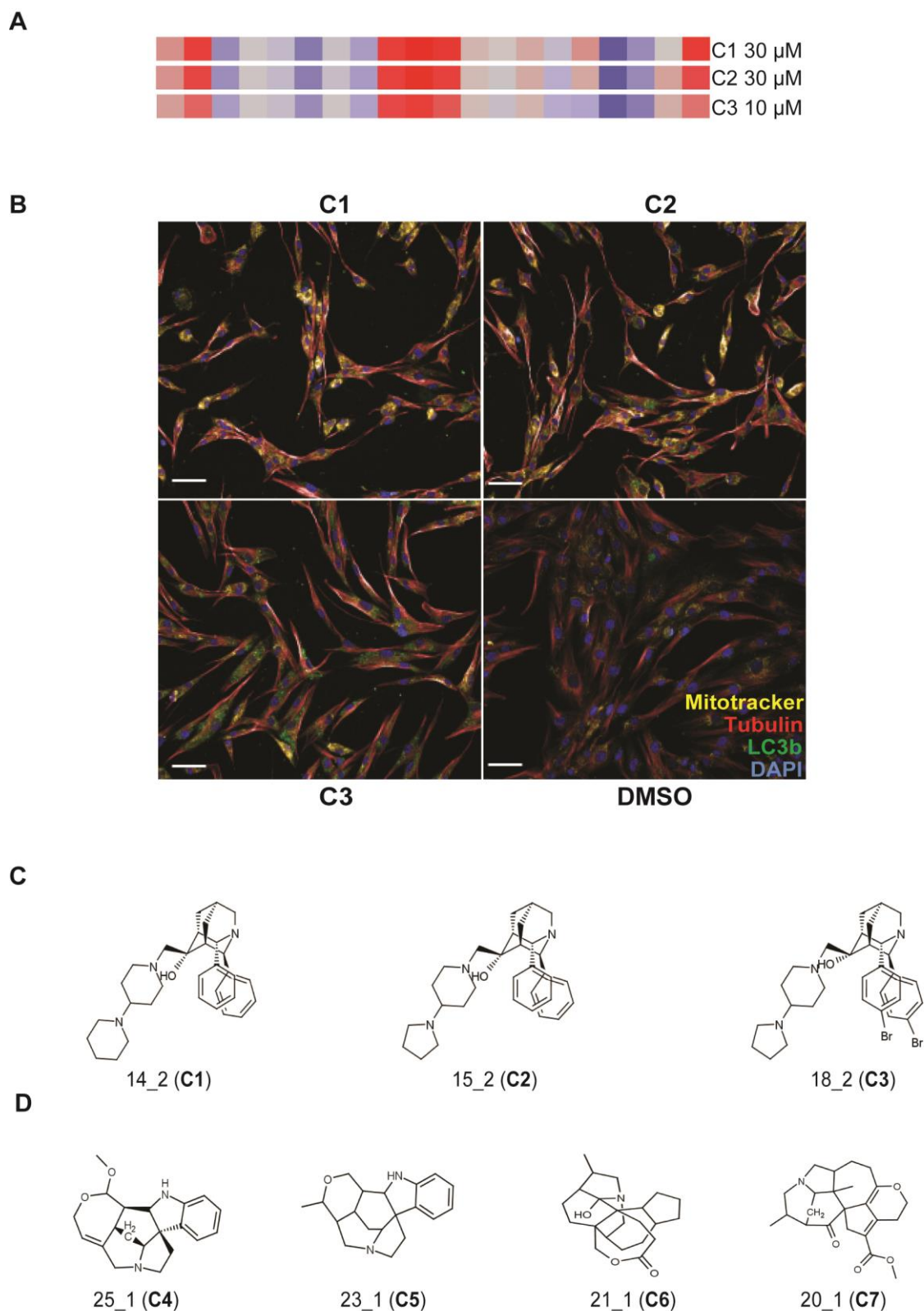
The scatter plot used to assess assay reproducibility in **Section 5.3.2** was again utilized for hit identification. We considered the most active compounds as the ones with highest cytological feature scores in two biological replicates. As a result, we identified 3 hits (14\_2, 15\_2, and 18\_2), that is approximately 8% of the screen set (**Figure 5.13**).



**Figure 5.13** A scatter plot for hit identification. A scatter plot displays the cytological features scores of compounds between two biological replicates. The most active compounds were colored in red (~8%) and non-hit compounds were colored in gray.

The results for the three most potent synthetic compounds have been found to be consistent in two biological replicates. These hits (compounds 14\_2, 15\_2 and 18\_2) exhibited highly similar effects on PD hONS cells, which were observed through their cytological profiles from heat map (**Figure. 5.14 A**). They were associated with biocluster 3 which exhibited strongly positive deviations from control wells in intensity of nucleus, mitochondria, tubulin, LC3b and lysosome while negative deviations in nucleus area, cell area and number of early endosome per area of cytoplasm and strongly negative deviations in number of early endosome on cytoplasm ( $p < 0.05$ ). As shown in **Figure 5.14 B**, treatment with these compounds on cells resulted in changes in nucleus and cell sizes and shapes, and changes on intensity of tubulin and mitochondria. Cells exposed to these molecules also showed smaller nuclei which were less rounded

than in control cells. In addition, compound treated cells became elongated, bipolar and spindle shaped. This biological effect might be the reason driving phenotypic differences of other investigated organelles between control and treated cells. Indeed, they had great effects on intensity indexes of tubulin, mitochondria and lysosome. Despite the high similarity in their chemical structures (**Figure 5.14 C**), two compounds (14\_2 and 15\_2) had strong biological activities at 30  $\mu$ M while 18\_2 at 30  $\mu$ M caused cell death (no viable cells were observed after 24h treatment). The results suggested that minor variation of the structure, such as bromine element addition might lead to toxic activity at high concentration.



**Figure 5.14** Biological profiles of three hit compounds. **(A)** Cytological profiles of the best responses in the screen. **(B)** Phenotypic changes in PD hONS cells that were treated with three synthetic compounds 14\_2 (C1), 15\_2 (C2), 18\_2 (C3) and DMSO as control for 24h. Stain set includes cell nuclei marker (DAPI, blue), tubulin stain (anti  $\alpha$ -tubulin

antibody, red), mitochondria stain (Mitotracker, yellow), autophagosomal marker LC3b (anti-LC3b antibody, green). Scale bars: 50  $\mu$ m. (C) Chemical structures of three compound hits. (D) Chemical structures of natural products.

## 5.4 Discussion

This study presents an effective cytological profiling approach employed on patient derived PD cellular model. Here, we reported here for the first time the use of PD patient cells as meaningful cellular model that is capable of capturing genetic and functional discrepancy in disease specific manner in response to novel small molecules. Unlike other studies examining single doses that might fail to identify mechanism of drug action (Marton et al., 1998, Perlman et al., 2004, Young et al., 2008), we investigated compound effects on multiple cellular organelles implicated in PD at different concentrations. Furthermore, we established downstream data processing that effectively facilitates hit identification and investigation of general structure activity relationships at a primary screening stage.

The compound collection was synthesized based on single natural product scaffold, thus we expected convergence of structure and activity in our screen (*i.e.* clusters of compounds that are related by phenotypes and chemical structures). We compared biological responses with structures in each cluster. The analysis revealed that of the phenotypic similar compound dose instances, only 27% (42 compound dose instances from bioclusters 1, 2, and 3) showed structural convergence (*i.e.* structurally related compounds have similar function). On the other hand, approximately 73% (112 compound dose instances from biocluster 4) showed structural divergence (*i.e.* structurally dissimilar compounds can produce similar phenotypes). These represented majority of cases. This finding could be explained by compounds binding to the same or

different binding sites on common cellular targets or by compounds targeting distinctive parts of common cellular pathways. However, to attest this possibility, further work need to be implemented.

The most readily identifiable biocluster in the heat map was biocluster 3 (**Figure 5.5**). This phenotypic cluster contains 4 structurally similar compounds that exhibited significant effects on the intensity of mitochondria, tubulin, LC3b staining and number of early endosome in the cytoplasm. In this biocluster, three compounds 14\_2, 15\_2, and 18\_2 were considered as the best responses in current screen. Visual inspection of individual images revealed that these molecules caused considerable changes on nucleus area and cell area (**Figure 5.14 B**). There are two possibilities explaining these changes: either compounds cause apoptosis or compounds promote cell differentiation. Regarding the first possibility, sizes of nucleus and cells are useful indicator for apoptosis and are expected to be decreased during apoptosis (Mark A. DeCoster et al., 2010). Examination of individual cytological features showed that both nucleus and cell areas were significantly smaller compared to controls ( $p < 0.05$ ). Hence, it suggests that compounds may induce apoptosis in cells. Relating to the second possibility (differentiated cell morphology), treated cells became more elongated, lost their round shape, which is glial-like morphology (Inuernicia et al., 2008, Andres et al., 2013). Further investigations are required to confirm which of these two possibilities is produced as result of the compound effect.

Analysis of structure activity relationships (**Sections 5.3.5 and 5.3.6**) showed that substitution of six membered ring to five membered ring did not induce significant difference in biological effect between 14\_2 and 15\_2. However, addition of -Br substituent led to significantly different effect between 15\_2 and 18\_2 at 30  $\mu$ M, with

the former being one of the most potent compound and the latter being cytotoxic (no viable cells were observed). (See **Table 5.1** for more information about compound series). To this end, minor changes in structures could lead to changes on biological effects either greater or weaker or inactive. More importantly, our results showed that CP strategy can distinguish subtle phenotypic differences among compounds with substantial effect resemblance. This highlights potential capability of CP in effort of identifying new chemical entities for human diseases.

The most noteworthy limitation of CP, despite many advantages, is that it cannot determine mechanism of action or accurate molecular targets for compounds. Newly identified compounds will require additional experiments to elucidate and validate their targets. Herein, we envisage the construction of customized biomarker panel for visualization of cellular organelles induced by compound treatments, diagnosis of PD, evaluation and monitoring of novel molecules for PD.

**CHAPTER 6**  
**GENERAL DISCUSSION**



## 6. GENERAL DISCUSSION

Natural products have served as invaluable source of new small molecule drugs to treat human diseases for thousands of years. Therefore natural products receive particular attention from medicinal chemists and many drug-like-libraries have been designed around naturally occurring structures. Nevertheless, despite the great value of natural products, the number of new innovative medicines introduced into market has decreased. This has been attributed, in part, to a lack of appropriate screening strategies. Indeed, conventional screenings based on a single readout or single compound concentration, have been unable to sufficiently capture compound activities thereby overlooking potential drug candidates. Nowadays, great efforts have been made to develop screening approaches capable of targeting multi-cellular components in response to drug treatments.

The current study described an advanced cytological profiling approach based on automated microscopy and downstream data processing for the rapid identification of bioactive small molecules for Parkinson's disease in two different natural product scaffold based libraries. In contrast to target-based approaches, cytological profiling does not require prior knowledge of targets. The approach used PD patient derived cells, thereby, results potentially reflect compound treatment induced disease specific changes. Additionally, considerable ability to distinguish subtle phenotypic distinction among compounds confirms the sensitivity of this approach and the effectiveness of downstream data mining.

The goal of this study was to identify biologically active molecules on primary PD patient cells, particularly based on changes in morphology of whole cell and/or cellular organelles; and to determine if chemical similarity leads to similar biological activity.

**Chapter 3** focused on the cytological profiling of 193 synthetic compounds containing a number of basic scaffolds, each compound was screened at four concentrations, against a single PD cell line. However, analysis was performed for only 160 compounds (33 compounds were excluded from analysis due to CV greater than 20%). The clustering of biological profiles of compounds identified five bioclusters. Bioclusters i, ii and iii showed negative deviation from DMSO control in nucleus intensity and roundness, and positive deviation in tubulin intensity. On the other hand, opposite patterns were observed in bioclusters iv and v which exhibited positive deviations in nucleus intensity and negative deviations in majority of cytological features. Low convergence between biological signatures and chemical structures was observed in all bioclusters with exception of cluster i where we detected a small group of structurally related compounds. In addition, we identified **one hit compound** (33\_1) at 1  $\mu$ M which induced morphological modification of cells and nuclei as well as reorganization of tubulin and change on lysosome intensity. The possible mechanism of action behind the compound effect remained to be clarified.

**Chapter 4** detailed the optimization of data analysis method used in **Chapter 3** to establish new method that offered more precise analysis of biological activities of the novel compounds and allowed effectively identify more accurate hits. This new method was applied in **Chapter 5**.

**Chapter 5** focused on the cytological profiling of 35 synthetic compounds embedded with 1-azaadamantanes scaffold and 4 natural products, each compound was screened at four concentrations, against a single PD cell line. The hierarchical clustering of their biological profiles revealed four bioclusters, of which three bioclusters (1, 2 and 3) showed dominant effects on the cells. Additionally, we identified **three hit compounds** including compounds 14\_2 and 15\_2 at 30  $\mu$ M, and 18\_2 at 10  $\mu$ M. These compounds are structurally related. Based on analysis of structure activity relationship, the 1,4'-bipiperidine substituent (compound 14\_2, 30  $\mu$ M) conferred it greater effects than the 4-(pyrrolidin-1-yl)piperidine substituent (compound 15\_2, 30  $\mu$ M), and the 4-(pyrrolidin-1-yl)piperidine and -Br substituents (compound 18\_2, 10  $\mu$ M). It appeared that addition of -Br moiety might be responsible for cytotoxicity of 18\_2 at 30  $\mu$ M. The results suggested that the substitution alteration led to changes in biological effect. The mechanisms underlying these alterations and their impact on the cellular functions need to be further pursued.

The most significant limitation in cytological profiling is that it provides insufficient information regarding the mechanism of action or precise molecular targets for given compounds. Therefore, further experiments will be required to determine and validate identified compound targets.

In both screenings, hit compounds induced changes in tubulin, mitochondria, autophagosome and lysosomes were identified. It would be exciting to carry out additional experiments to determine if these molecules could increase these organelles functions. If proven, these compounds could be pursued as potential novel drug leads useful for treatment of PD.

**CHAPTER 7**  
**REFERENCES**

## 7. REFERENCES

- AARSLAND, D., ANDERSEN, K., LARSEN, J. P., LOLK, A., NIELSEN, H. & KRAGH-SORENSEN, P. 2001. Risk of dementia in Parkinson's disease: a community-based, prospective study. *Neurology*, 56, 730-6.
- AARSLAND, D., BRONNICK, K., EHRT, U., DE DEYN, P. P., TEKIN, S., EMRE, M. & CUMMINGS, J. L. 2007. Neuropsychiatric symptoms in patients with Parkinson's disease and dementia: frequency, profile and associated care giver stress. *J Neurol Neurosurg Psychiatry*, 78, 36-42.
- AARSLAND, D., LAAKE, K., LARSEN, J. P. & JANVIN, C. 2002. Donepezil for cognitive impairment in Parkinson's disease: a randomised controlled study. *J Neurol Neurosurg Psychiatry*, 72, 708-12.
- ABRAMS, P., CARDOZO, L., FALL, M., GRIFFITHS, D., ROSIER, P., ULMSTEN, U., VAN KERREBROECK, P., VICTOR, A., WEIN, A. & STANDARDISATION SUB-COMMITTEE OF THE INTERNATIONAL CONTINENCE, S. 2002. The standardisation of terminology of lower urinary tract function: report from the Standardisation Sub-committee of the International Continence Society. *Neurourol Urodyn*, 21, 167-78.
- ACKERMANN, G., LOFFLER, B., ADLER, D. & RODLOFF, A. C. 2004. In vitro activity of OPT-80 against *Clostridium difficile*. *Antimicrob Agents Chemother*, 48, 2280-2.
- ADKIN, A. L., FRANK, J. S. & JOG, M. S. 2003. Fear of falling and postural control in Parkinson's disease. *Mov Disord*, 18, 496-502.
- ADLER, C. H., HENTZ, J. G., SHILL, H. A., SABBAGH, M. N., DRIVER-DUNCKLEY, E., EVIDENTE, V. G., JACOBSON, S. A., BEACH, T. G., BOEVE, B. & CAVINESS, J. N. 2011. Probable RBD is increased in

- Parkinson's disease but not in essential tremor or restless legs syndrome.  
*Parkinsonism Relat Disord*, 17, 456-8.
- AHLSSKOG, J. E. 2005. Challenging conventional wisdom: the etiologic role of dopamine oxidative stress in Parkinson's disease. *Mov Disord*, 20, 271-82.
- AHMAD, T., AGGARWAL, K., PATTNAIK, B., MUKHERJEE, S., SETHI, T., TIWARI, B. K., KUMAR, M., MICHEAL, A., MABALIRAJAN, U., GHOSH, B., SINHA ROY, S. & AGRAWAL, A. 2013. Computational classification of mitochondrial shapes reflects stress and redox state. *Cell Death Dis*, 4, e461.
- ALVES, G., FORSAA, E. B., PEDERSEN, K. F., DREETZ GJERSTAD, M. & LARSEN, J. P. 2008. Epidemiology of Parkinson's disease. *J Neurol*, 255 Suppl 5, 18-32.
- AMIRKIA, V. & HEINRICH, M. 2014. Alkaloids as drug leads - A predictive structural and biodiversity-based analysis. *Phytochemistry Letters*, 10, XLVIII-liii.
- ANDRES, D., KEYSER, B. M., PETRALI, J., BENTON, B., HUBBARD, K. S., MCNUTT, P. M. & RAY, R. 2013. Morphological and functional differentiation in BE (2)-M17 human neuroblastoma cells by treatment with Trans-retinoic acid. *Bmc Neuroscience*, 14.
- ANNESI, G., SAVETTIERI, G., PUGLIESE, P., D'AMELIO, M., TARANTINO, P., RAGONESE, P., LA BELLA, V., PICCOLI, T., CIVITELLI, D., ANNESI, F., FIERRO, B., PICCOLI, F., ARABIA, G., CARACCIOLO, M., CANDIANO, I. C. C. & QUATTRONE, A. 2005. DJ-1 mutations and parkinsonism-dementia-amyotrophic lateral sclerosis complex. *Annals of Neurology*, 58, 803-807.
- ANTONINI, A. & ODIN, P. 2009. Pros and cons of apomorphine and L-dopa continuous infusion in advanced Parkinson's disease. *Parkinsonism Relat Disord*, 15 Suppl 4, S97-100.

- ARAKI, I. & KUNO, S. 2000. Assessment of voiding dysfunction in Parkinson's disease by the international prostate symptom score. *J Neurol Neurosurg Psychiatry*, 68, 429-33.
- ARCAMONE, F. M. 2005. Anthracyclines. In: CRAGG G.M., KINGSTON D.G.I. & NEWMAN D.J. (eds.) *Anticancer agents from natural products*. Boca Raton, FL: Taylor and Francis.
- ARCAMONE, F. M. 2012. Anthracyclines. In: CRAGG G.M., KINGSTON D.G.I. & NEWMAN D.J. (eds.) *Anticancer agents from natural products*. 2 ed. Boca Raton, FL: Taylor and Francis.
- ARNOULT, D. 2007. Mitochondrial fragmentation in apoptosis. *Trends Cell Biol*, 17, 6-12.
- B.SINGH, S. 2012. Pharmaceuticals: Natural Products And Natural Product Models. In: CIVJAN, N. (ed.) *Natural Products in Chemical Biology*. 1 ed. Somerset, NJ, USA: Wiley.
- BALUNAS, M. J. & KINGHORN, A. D. 2005. Drug discovery from medicinal plants. *Life Sci*, 78, 431-41.
- BARA-JIMENEZ, W., BIBBIANI, F., MORRIS, M. J., DIMITROVA, T., SHERZAI, A., MOURADIAN, M. M. & CHASE, T. N. 2005. Effects of serotonin 5-HT<sub>1A</sub> agonist in advanced Parkinson's disease. *Mov Disord*, 20, 932-6.
- BARONE, P., ANTONINI, A., COLOSIMO, C., MARCONI, R., MORGANTE, L., AVARELLO, T. P., BOTTACCHI, E., CANNAS, A., CERAVOLO, G., CERAVOLO, R., CICARELLI, G., GAGLIO, R. M., GIGLIA, R. M., IEMOLO, F., MANFREDI, M., MECO, G., NICOLETTI, A., PEDERZOLI, M., PETRONE, A., PISANI, A., PONTIERI, F. E., QUATRALE, R., RAMAT, S., SCALA, R., VOLPE, G., ZAPPULLA, S., BENTIVOGLIO, A. R., STOCCHI, F., TRIANNI, G., DOTTO, P. D. & GROUP, P. S. 2009. The

- PRIAMO study: A multicenter assessment of nonmotor symptoms and their impact on quality of life in Parkinson's disease. *Mov Disord*, 24, 1641-9.
- BARONE, P., POEWE, W., ALBRECHT, S., DEBIEUVRE, C., MASSEY, D., RASCOL, O., TOLOSA, E. & WEINTRAUB, D. 2010. Pramipexole for the treatment of depressive symptoms in patients with Parkinson's disease: a randomised, double-blind, placebo-controlled trial. *Lancet Neurol*, 9, 573-80.
- BASU, A., BODYCOMBE, N. E., CHEAH, J. H., PRICE, E. V., LIU, K., SCHAEFER, G. I., EBRIGHT, R. Y., STEWART, M. L., ITO, D., WANG, S., BRACHA, A. L., LIEFELD, T., WAWER, M., GILBERT, J. C., WILSON, A. J., STRANSKY, N., KRYUKOV, G. V., DANKIK, V., BARRETINA, J., GARRAWAY, L. A., HON, C. S. Y., MUNOZ, B., BITTKER, J. A., STOCKWELL, B. R., KHABELE, D., STERN, A. M., CLEMONS, P. A., SHAMJI, A. F. & SCHREIBER, S. L. 2013. An Interactive Resource to Identify Cancer Genetic and Lineage Dependencies Targeted by Small Molecules. *Cell*, 154, 1151-1161.
- BAUDOIN, J. P., ALVAREZ, C., GASPARD, P. & METIN, C. 2008. Nocodazole-induced changes in microtubule dynamics impair the morphology and directionality of migrating medial ganglionic eminence cells. *Dev Neurosci*, 30, 132-43.
- BAUMANN, C. R. 2012. Epidemiology, diagnosis and differential diagnosis in Parkinson's disease tremor. *Parkinsonism Relat Disord*, 18 Suppl 1, S90-2.
- BECKER, D. P., FLYNN, D. L., SHONE, R. L. & GULLIKSON, G. 2004. Azaadamantane benzamide 5-HT<sub>4</sub> agonists: gastrointestinal prokinetic SC-54750. *Bioorg Med Chem Lett*, 14, 5509-12.
- BEMIS, G. W. & MURCKO, M. A. 1996. The properties of known drugs. 1. Molecular frameworks. *J Med Chem*, 39, 2887-93.



- BENMOYAL-SEGAL, L. & SOREQ, H. 2006. Gene-environment interactions in sporadic Parkinson's disease. *J Neurochem*, 97, 1740-55.
- BERRY, C., LA VECCHIA, C. & NICOTERA, P. 2010. Paraquat and Parkinson's disease. *Cell Death Differ*, 17, 1115-25.
- BHARATH, S., HSU, M., KAUR, D., RAJAGOPALAN, S. & ANDERSEN, J. K. 2002. Glutathione, iron and Parkinson's disease. *Biochem Pharmacol*, 64, 1037-48.
- BIRMINGHAM, A., SELFORS, L. M., FORSTER, T., WROBEL, D., KENNEDY, C. J., SHANKS, E., SANTOYO-LOPEZ, J., DUNICAN, D. J., LONG, A., KELLEHER, D., SMITH, Q., BEIJERSBERGEN, R. L., GHAZAL, P. & SHAMU, C. E. 2009. Statistical methods for analysis of high-throughput RNA interference screens. *Nature Methods*, 6, 569-575.
- BLACKETT, H., WALKER, R. & WOOD, B. 2009. Urinary dysfunction in Parkinson's disease: a review. *Parkinsonism Relat Disord*, 15, 81-7.
- BODENSTINE, T. M., SEFTOR, R. E., SEFTOR, E. A., KHALKHALI-ELLIS, Z., SAMII, N. A., MONARREZ, J. C., CHANDLER, G. S., PEMBERTON, P. A. & HENDRIX, M. J. 2014. Internalization by multiple endocytic pathways and lysosomal processing impact maspin-based therapeutics. *Mol Cancer Res*, 12, 1480-91.
- BOLSTAD, B. M., IRIZARRY, R. A., ASTRAND, M. & SPEED, T. P. 2003. A comparison of normalization methods for high density oligonucleotide array data based on variance and bias. *Bioinformatics*, 19, 185-193.
- BONIFACIO, M. J., PALMA, P. N., ALMEIDA, L. & SOARES-DA-SILVA, P. 2007. Catechol-O-methyltransferase and its inhibitors in Parkinson's disease. *CNS Drug Rev*, 13, 352-79.

BOSLEY, S. Parkinson's disease - Clinical features. Retrieved 20 July 2015

<https://www.pinterest.com/pin/109564203409960752/>

BRAY, M. A. & CARPENTER, A. 2004. Advanced Assay Development Guidelines for Image-Based High Content Screening and Analysis. *In*: SITTAMPALAM, G. S., COUSSENS, N. P., NELSON, H., ARKIN, M., AULD, D., AUSTIN, C., BEJCEK, B., GLICKSMAN, M., INGLESE, J., IVERSEN, P. W., LI, Z., MCGEE, J., MCMANUS, O., MINOR, L., NAPPER, A., PELTIER, J. M., RISS, T., TRASK, O. J., JR. & WEIDNER, J. (eds.) *Assay Guidance Manual*. Bethesda (MD).

BREINBAUER, R., VETTER, I. R. & WALDMANN, H. 2002a. From protein domains to drug candidates-natural products as guiding principles in the design and synthesis of compound libraries. *Angew Chem Int Ed Engl*, 41, 2879-90.

BREINBAUER, R., VETTER, I. R. & WALDMANN, H. 2002b. From protein domains to drug candidates - Natural products as guiding principles in the design and synthesis of compound libraries. *Angewandte Chemie-International Edition*, 41, 2879-2890.

BRONSTEIN, J. M., TAGLIATI, M., ALTERMAN, R. L., LOZANO, A. M., VOLKMANN, J., STEFANI, A., HORAK, F. B., OKUN, M. S., FOOTE, K. D., KRACK, P., PAHWA, R., HENDERSON, J. M., HARIZ, M. I., BAKAY, R. A., REZAI, A., MARKS, W. J., JR., MORO, E., VITEK, J. L., WEAVER, F. M., GROSS, R. E. & DELONG, M. R. 2011. Deep brain stimulation for Parkinson disease: an expert consensus and review of key issues. *Arch Neurol*, 68, 165.

BULAJ, G., BUCZEK, O., GOODSSELL, I., JIMENEZ, E. C., KRANSKI, J., NIELSEN, J. S., GARRETT, J. E. & OLIVERA, B. M. 2003. Efficient oxidative

- folding of conotoxins and the radiation of venomous cone snails. *Proc Natl Acad Sci U S A*, 100 Suppl 2, 14562-8.
- BULINSKI, J. C., RICHARDS, J. E. & PIPERNO, G. 1988. Posttranslational Modifications of Alpha-Tubulin - Detyrosination and Acetylation Differentiate Populations of Interphase Microtubules in Cultured-Cells. *Journal of Cell Biology*, 106, 1213-1220.
- BUSS, A. D., WAIGH, R.D. 1995. Natural products as leads for new pharmaceuticals. In: WOLFF, M. E. (ed.) *Burger's Medicinal Chemistry and Drug Discovery. Principles and Practice*. 5 ed. New York: John Wiley & Sons, Inc.
- BUTLER, M. S. 2004. The role of natural product chemistry in drug discovery. *J Nat Prod*, 67, 2141-53.
- CAMPELLONE, J. V. 2014. Substantia nigra and Parkinson's disease. 27 July 2014 ed. Retrieved 20 July 2015  
<http://www.nlm.nih.gov/medlineplus/ency/imagepages/19515.htm>
- CAMPOS-SOUSA, R. N., QUAGLIATO, E., DA SILVA, B. B., DE CARVALHO, R. M., RIBEIRO, S. C. & DE CARVALHO, D. F. M. 2003. Urinary symptoms in Parkinson's disease - Prevalence and associated factors. *Arquivos De Neuro-Psiquiatria*, 61, 359-363.
- CAO, W., GUO, X. W., ZHENG, H. Z., LI, D. P., JIA, G. B. & WANG, J. 2012. Current progress of research on pharmacologic actions of salvianolic acid B. *Chin J Integr Med*, 18, 316-20.
- CASTRIOTO, A., LOZANO, A. M., POON, Y. Y., LANG, A. E., FALLIS, M. & MORO, E. 2011. Ten-year outcome of subthalamic stimulation in Parkinson disease: a blinded evaluation. *Arch Neurol*, 68, 1550-6.

- CERSOSIMO, M. G. & BENARROCH, E. E. 2008. Neural control of the gastrointestinal tract: implications for Parkinson disease. *Mov Disord*, 23, 1065-75.
- CHAN, D. C. 2006. Mitochondria: dynamic organelles in disease, aging, and development. *Cell*, 125, 1241-52.
- CHAUDHURI, K. R. & SCHAPIRA, A. H. 2009. Non-motor symptoms of Parkinson's disease: dopaminergic pathophysiology and treatment. *Lancet Neurol*, 8, 464-74.
- CHEN, T., LIU, W., CHAO, X., ZHANG, L., QU, Y., HUO, J. & FEI, Z. 2011. Salvianolic acid B attenuates brain damage and inflammation after traumatic brain injury in mice. *Brain Res Bull*, 84, 163-8.
- CHEN, X., GUO, J., BAO, J., LU, J. & WANG, Y. 2014. The anticancer properties of salvia miltiorrhiza Bunge (Danshen): a systematic review. *Med Res Rev*, 34, 768-94.
- CHUANG, C., FAHN, S. & FRUCHT, S. J. 2002. The natural history and treatment of acquired hemidystonia: report of 33 cases and review of the literature. *J Neurol Neurosurg Psychiatry*, 72, 59-67.
- CLEETER, M. W. J., COOPER, J. M. & SCHAPIRA, A. H. V. 1992. Irreversible Inhibition of Mitochondrial Complex-I by 1-Methyl-4-Phenylpyridinium - Evidence for Free-Radical Involvement. *Journal of Neurochemistry*, 58, 786-789.
- CLEMONS, P. A., BODYCOMBE, N. E., CARRINSKI, H. A., WILSON, J. A., SHAMJI, A. F., WAGNER, B. K., KOEHLER, A. N. & SCHREIBER, S. L. 2010. Small molecules of different origins have distinct distributions of structural complexity that correlate with protein-binding profiles. *Proceedings of the National Academy of Sciences of the United States of America*, 107, 18787-18792.

- COLLINS, I. & JONES, A. M. 2014. Diversity-oriented synthetic strategies applied to cancer chemical biology and drug discovery. *Molecules*, 19, 17221-55.
- COOK, A. L., VITALE, A. M., RAVISHANKAR, S., MATIGIAN, N., SUTHERLAND, G. T., SHAN, J., SUTHARSAN, R., PERRY, C., SILBURN, P. A., MELLICK, G. D., WHITELAW, M. L., WELLS, C. A., MACKAY-SIM, A. & WOOD, S. A. 2011. NRF2 activation restores disease related metabolic deficiencies in olfactory neurosphere-derived cells from patients with sporadic Parkinson's disease. *PLoS One*, 6, e21907.
- COWAN, M. M. 1999. Plant Products as Antimicrobial Agents. *Clinical Microbiology Reviews*, 12, 564–582.
- CRAGG, G. M., BOYD, M. R., CARDELLINA, J. H., 2ND, NEWMAN, D. J., SNADER, K. M. & MCCLOUD, T. G. 1994. Ethnobotany and drug discovery: the experience of the US National Cancer Institute. *Ciba Found Symp*, 185, 178-90; discussion 190-6.
- CRAGG, G. M., GROTHAUS, P. G. & NEWMAN, D. J. 2009. Impact of Natural Products on Developing New Anti-Cancer Agents. *Chemical Reviews*, 109, 3012-3043.
- CRAGG, G. M. & NEWMAN, D. J. 2009. Nature: a vital source of leads for anticancer drug development. *Phytochemistry Reviews*, 8, 313-331.
- CRAGG, G. M. & NEWMAN, D. J. 2013. Natural products: a continuing source of novel drug leads. *Biochim Biophys Acta*, 1830, 3670-95.
- D. ALONSO, Z. KHALILB, N. SATKUNANTHAN AND B.G. LIVETT 2003. Drugs From the Sea: Conotoxins as Drug Leads for Neuropathic Pain and Other Neurological Conditions. *Mini Reviews in Medicinal Chemistry*, 3, 785-787.
- DARZYNKIEWICZ, Z. 2011. Critical aspects in analysis of cellular DNA content. *Curr Protoc Cytom*, Chapter 7, Unit 7 2.

- DE LAU, L. M. & BRETELER, M. M. 2006a. Epidemiology of Parkinson's disease. *Lancet Neurol*, 5, 525-35.
- DE LAU, L. M. L. & BRETELER, M. M. B. 2006b. Epidemiology of Parkinson's disease. *The Lancet Neurology*, 5, 525-535.
- DECOSTER, M. A. 2007. The Nuclear Area Factor (NAF) a measure for cell apoptosis. *Modern Research and Educational Topics in Microscopy*.
- DECOSTER, M. A., MADDI, S., DUTTA, V. & MCNAMARA, J. 2010. Microscopy and image analysis of individual and group cell shape changes during apoptosis. *Microscopy: Science, Technology, Applications and Education*, 836-843.
- DEKKER, M., BONIFATI, V., VAN SWIETEN, J., LEENDERS, N., GALJAARD, R. J., SNIJDERS, P., HORSTINK, M., HEUTINK, P., OOSTRA, B. & VAN DUIJN, C. 2003. Clinical features and neuroimaging of PARK7-linked parkinsonism. *Mov Disord*, 18, 751-7.
- DENG, H., LE, W., GUO, Y., HUNTER, C. B., XIE, W., HUANG, M. & JANKOVIC, J. 2006. Genetic analysis of LRRK2 mutations in patients with Parkinson disease. *J Neurol Sci*, 251, 102-6.
- DEVOS, D., DEFEBVRE, L. & BORDET, R. 2010. Dopaminergic and non-dopaminergic pharmacological hypotheses for gait disorders in Parkinson's disease. *Fundam Clin Pharmacol*, 24, 407-21.
- DEVOS, D., KRYSTKOWIAK, P., CLEMENT, F., DUJARDIN, K., COTTENCIN, O., WAUCQUIER, N., AJEBBAR, K., THIELEMANS, B., KROUMOVA, M., DUHAMEL, A., DESTEE, A., BORDET, R. & DEFEBVRE, L. 2007. Improvement of gait by chronic, high doses of methylphenidate in patients with advanced Parkinson's disease. *J Neurol Neurosurg Psychiatry*, 78, 470-5.
- DEXTER, D. T. & JENNER, P. 2013. Parkinson disease: from pathology to molecular disease mechanisms. *Free Radic Biol Med*, 62, 132-44.

- DI FONZO, A., ROHE, C. F., FERREIRA, J., CHIEN, H. F., VACCA, L., STOCCHI, F., GUEDES, L., FABRIZIO, E., MANFREDI, M., VANACORE, N., GOLDWURM, S., BREEDVELD, G., SAMPAIO, C., MECO, G., BARBOSA, E., OOSTRA, B. A., BONIFATI, V. & ITALIAN PARKINSON GENETICS, N. 2005. A frequent LRRK2 gene mutation associated with autosomal dominant Parkinson's disease. *Lancet*, 365, 412-5.
- DI MATTEO, V., PIERUCCI, M., ESPOSITO, E., CRESCIMANNO, G., BENIGNO, A. & DI GIOVANNI, G. 2008. Serotonin modulation of the basal ganglia circuitry: therapeutic implication for Parkinson's disease and other motor disorders. *Prog Brain Res*, 172, 423-63.
- DIAS, D. A., URBAN, S. & ROESSNER, U. 2012. A Historical Overview of Natural Products in Drug Discovery. *Metabolites*, 2, 303-336.
- DIEDERICH, N. J., RAMAN, R., LEURGANS, S. & GOETZ, C. G. 2002. Progressive worsening of spatial and chromatic processing deficits in Parkinson disease. *Arch Neurol*, 59, 1249-52.
- DORSEY, E. R., CONSTANTINESCU, R., THOMPSON, J. P., BIGLAN, K. M., HOLLOWAY, R. G., KIEBURTZ, K., MARSHALL, F. J., RAVINA, B. M., SCHIFITTO, G., SIDEROWF, A. & TANNER, C. M. 2007. Projected number of people with Parkinson disease in the most populous nations, 2005 through 2030. *Neurology*, 68, 384-386.
- DURBIN, B. P. & ROCKE, D. M. 2004. Variance-stabilizing transformations for two-color microarrays. *Bioinformatics*, 20, 660-7.
- ENGERS, D. W., FIELD, J. R., LE, U., ZHOU, Y., BOLINGER, J. D., ZAMORANO, R., BLOBAUM, A. L., JONES, C. K., JADHAV, S., WEAVER, C. D., CONN, P. J., LINDSLEY, C. W., NISWENDER, C. M. & HOPKINS, C. R. 2011. Discovery, Synthesis, and Structure-Activity Relationship Development of a

- Series of N-(4-Acetamido)phenylpicolinamides as Positive Allosteric Modulators of Metabotropic Glutamate Receptor 4 (mGlu(4)) with CNS Exposure in Rats. *Journal of Medicinal Chemistry*, 54, 1106-1110.
- ERIKSEN, J. L., WSZOLEK, Z. & PETRUCCELLI, L. 2005. Molecular pathogenesis of Parkinson disease. *Arch Neurol*, 62, 353-7.
- EVANS, B. E., RITTLE, K. E., BOCK, M. G., DIPARDO, R. M., FREIDINGER, R. M., WHITTER, W. L., LUNDELL, G. F., VEBER, D. F., ANDERSON, P. S., CHANG, R. S. & ET AL. 1988. Methods for drug discovery: development of potent, selective, orally effective cholecystokinin antagonists. *J Med Chem*, 31, 2235-46.
- FACTOR, S. A. 2008. Current status of symptomatic medical therapy in Parkinson's disease. *Neurotherapeutics*, 5, 164-80.
- FANG, L. L., PAN, J. M. & YAN, B. 2000. High-throughput determination of identity, purity, and quantity of combinatorial library members using LC/MS/UV/ELSD. *Biotechnology and Bioengineering*, 71, 162-171.
- FASANO, A., RICCIARDI, L., LENA, F., BENTIVOGLIO, A. R. & MODUGNO, N. 2012. Intrajejunal levodopa infusion in advanced Parkinson's disease: long-term effects on motor and non-motor symptoms and impact on patient's and caregiver's quality of life. *Eur Rev Med Pharmacol Sci*, 16, 79-89.
- FENYVESI, F., RETI-NAGY, K., BACSO, Z., GUTAY-TOTH, Z., MALANGA, M., FENYVESI, E., SZENTE, L., VARADI, J., UJHELYI, Z., FEHER, P., SZABO, G., VECSENYI, M. & BACSKAY, I. 2014. Fluorescently Labeled Methyl-Beta-Cyclodextrin Enters Intestinal Epithelial Caco-2 Cells by Fluid-Phase Endocytosis. *Plos One*, 9.



- FERESHTEHNEJAD, S. M. & LOKK, J. 2014. Orthostatic hypotension in patients with Parkinson's disease and atypical parkinsonism. *Parkinsons Dis*, 2014, 475854.
- FERON, F., PERRY, C., HIRNING, M. H., MCGRATH, J. & MACKAY-SIM, A. 1999. Altered adhesion, proliferation and death in neural cultures from adults with schizophrenia. *Schizophr Res*, 40, 211-8.
- FÉRON, F., PERRY, C., MCGRATH, J. J. & MACKAY-SIM, A. 1998. New techniques to biospy and culture human olfactory epithelial neurons. *Arch Otolaryngol Head Neck Surg*, 124, 861-866.
- FOGEL, J. L., THEIN, T. Z. T. & MARIANI, F. V. 2012. Use of LysoTracker to Detect Programmed Cell Death in Embryos and Differentiating Embryonic Stem Cells. *Jove-Journal of Visualized Experiments*.
- FOLLETT, K. A., WEAVER, F. M., STERN, M., HUR, K., HARRIS, C. L., LUO, P., MARKS, W. J., JR., ROTHLIND, J., SAGHER, O., MOY, C., PAHWA, R., BURCHIEL, K., HOGARTH, P., LAI, E. C., DUDA, J. E., HOLLOWAY, K., SAMII, A., HORN, S., BRONSTEIN, J. M., STONER, G., STARR, P. A., SIMPSON, R., BALTUCH, G., DE SALLES, A., HUANG, G. D., REDA, D. J. & GROUP, C. S. P. S. 2010. Pallidal versus subthalamic deep-brain stimulation for Parkinson's disease. *N Engl J Med*, 362, 2077-91.
- FOLTYNIE, T., BRAYNE, C. E., ROBBINS, T. W. & BARKER, R. A. 2004. The cognitive ability of an incident cohort of Parkinson's patients in the UK. The CamPaIGN study. *Brain*, 127, 550-60.
- FOX, S. H., KATZENSCHLAGER, R., LIM, S. Y., RAVINA, B., SEPPI, K., COELHO, M., POEWE, W., RASCOL, O., GOETZ, C. G. & SAMPAIO, C. 2011. The Movement Disorder Society Evidence-Based Medicine Review

- Update: Treatments for the motor symptoms of Parkinson's disease. *Mov Disord*, 26 Suppl 3, S2-41.
- FREEMAN, R., WIELING, W., AXELROD, F. B., BENDITT, D. G., BENARROCH, E., BIAGGIONI, I., CHESHIRE, W. P., CHELIMSKY, T., CORTELLI, P., GIBBONS, C. H., GOLDSTEIN, D. S., HAINSWORTH, R., HILZ, M. J., JACOB, G., KAUFMANN, H., JORDAN, J., LIPSITZ, L. A., LEVINE, B. D., LOW, P. A., MATHIAS, C., RAJ, S. R., ROBERTSON, D., SANDRONI, P., SCHATZ, I. J., SCHONDORF, R., STEWART, J. M. & VAN DIJK, J. G. 2011. Consensus statement on the definition of orthostatic hypotension, neurally mediated syncope and the postural tachycardia syndrome. *Auton Neurosci*, 161, 46-8.
- GAGNON, J. F., BEDARD, M. A., FANTINI, M. L., PETIT, D., PANISSET, M., ROMPRE, S., CARRIER, J. & MONTPLAISIR, J. 2002. REM sleep behavior disorder and REM sleep without atonia in Parkinson's disease. *Neurology*, 59, 585-9.
- GALLAGHER, D. A., LEES, A. J. & SCHRAG, A. 2010. What are the most important nonmotor symptoms in patients with Parkinson's disease and are we missing them? *Mov Disord*, 25, 2493-500.
- GANESAN, A. 2008. The impact of natural products upon modern drug discovery. *Current Opinion in Chemical Biology*, 12, 306-317.
- GAO, H. M. & HONG, J. S. 2011. Gene-environment interactions: key to unraveling the mystery of Parkinson's disease. *Prog Neurobiol*, 94, 1-19.
- GIDDINGS, L.-A. & NEWMAN, D. J. 2013. Microbial natural products: molecular blueprints for antitumor drugs. *Journal of Industrial Microbiology & Biotechnology*, 40, 1181-1210.

- GOETZ, C. G. 2011. The history of Parkinson's disease: early clinical descriptions and neurological therapies. *Cold Spring Harb Perspect Med*, 1, a008862.
- GONZALEZ, R. C. & WOODS, R. E. 1992. *Digital Image Processing*, Reading, MA, Addison-Wesley.
- GOTTWALD, M. D. & AMINOFF, M. J. 2008. New frontiers in the pharmacological management of Parkinson's disease. *Drugs Today (Barc)*, 44, 531-45.
- GRABOWSKI, K., BARINGHAUS, K. H. & SCHNEIDER, G. 2008. Scaffold diversity of natural products: inspiration for combinatorial library design. *Nat Prod Rep*, 25, 892-904.
- GRASES, F., SIMONET, B. M., PRIETO, R. M. & MARCH, J. G. 2001. Phytate levels in diverse rat tissues: influence of dietary phytate. *Br J Nutr*, 86, 225-31.
- GRAZIADEI, P. P. 1973. Cell dynamics in the olfactory mucosa. *Tissue Cell*, 5, 113-31.
- GREENE, J. G., NOORIAN, A. R. & SRINIVASAN, S. 2009. Delayed gastric emptying and enteric nervous system dysfunction in the rotenone model of Parkinson's disease. *Exp Neurol*, 218, 154-61.
- GUO, T. & HOBBS, D. W. 2003. Privileged structure-based combinatorial libraries targeting G protein-coupled receptors. *Assay Drug Dev Technol*, 1, 579-92.
- HA, A. D., BROWN, C. H., YORK, M. K. & JANKOVIC, J. 2011. The prevalence of symptomatic orthostatic hypotension in patients with Parkinson's disease and atypical parkinsonism. *Parkinsonism Relat Disord*, 17, 625-8.
- HAMANN P.R., UPESLACIS J. & BORDERS D.B. 2005. Eneidiynes. In: CRAGG G.M., KINGSTON D.G.I. & NEWMAN D.J. (eds.) *Anticancer agents from natural products*.

- HAMANN P.R., UPESLACIS J. & BORDERS D.B. 2012. Eneidiynes. *In*: CRAGG G.M., KINGSTON D.G.I. & NEWMAN D.J. (eds.) *Anticancer agents from natural products*. 2 ed. Boca Raton, FL: Taylor and Francis.
- HAMRE, K., THARP, R., POON, K., XIONG, X. & SMEYNE, R. J. 1999. Differential strain susceptibility following 1-methyl-4-phenyl-1,2,3,6-tetrahydropyridine (MPTP) administration acts in an autosomal dominant fashion: quantitative analysis in seven strains of *Mus musculus*. *Brain Res*, 828, 91-103.
- HANTRAYE, P., BROUILLET, E., FERRANTE, R., PALFI, S., DOLAN, R., MATTHEWS, R. T. & BEAL, M. F. 1996. Inhibition of neuronal nitric oxide synthase prevents MPTP-induced parkinsonism in baboons. *Nature Medicine*, 2, 1017-1021.
- HARISH, G., VENKATESHAPPA, C., MYTHRI, R. B., DUBEY, S. K., MISHRA, K., SINGH, N., VALI, S. & BHARATH, M. M. 2010. Bioconjugates of curcumin display improved protection against glutathione depletion mediated oxidative stress in a dopaminergic neuronal cell line: Implications for Parkinson's disease. *Bioorg Med Chem*, 18, 2631-8.
- HARTWELL, J. L. 1982. Plants used against cancer, Quarterman, Lawrence, MA.
- HARVEY, A. L. 2008. Natural products in drug discovery. *Drug Discov Today*, 13, 894-901.
- HASHIMOTO, M., HSU, L. J., XIA, Y., TAKEDA, A., SISK, A., SUNDSMO, M. & MASLIAH, E. 1999. Oxidative stress induces amyloid-like aggregate formation of NACP/alpha-synuclein in vitro. *Neuroreport*, 10, 717-21.
- HEALY, D. G., FALCHI, M., O'SULLIVAN, S. S., BONIFATI, V., DURR, A., BRESSMAN, S., BRICE, A., AASLY, J., ZABETIAN, C. P., GOLDWURM, S., FERREIRA, J. J., TOLOSA, E., KAY, D. M., KLEIN, C., WILLIAMS, D. R., MARRAS, C., LANG, A. E., WSZOLEK, Z. K., BERCIANO, J.,

- SCHAPIRA, A. H., LYNCH, T., BHATIA, K. P., GASSER, T., LEES, A. J., WOOD, N. W. & INTERNATIONAL, L. C. 2008. Phenotype, genotype, and worldwide genetic penetrance of LRRK2-associated Parkinson's disease: a case-control study. *Lancet Neurol*, 7, 583-90.
- HECHT, S. M. 2005. Bleomycin group antitumor agents,. *In*: CRAGG G.M., KINGSTON D.G.I. & NEWMAN D.J. (eds.) *Anticancer agents from natural products*. Boca Raton, FL: Taylor and Francis.
- HECHT, S. M. 2012. Bleomycin group antitumor agents. *In*: CRAGG G.M., KINGSTON D.G.I. & NEWMAN D.J. (eds.) *Antitumor agents from natural products*. Boca Raton, FL: Taylor and Francis.
- HENRIQUEZ, R., FAIRCLOTH,G.,CUEVAS,C. 2005. Ecteinascidin743(ET743),Yondelis<sup>TM</sup>; Aplidine, and Kahalalide F. *In*: CRAGG, G. M., KINGSTON, D.G.I., AND NEWMAN,D.J. (ed.) *Anticancer Agents from Natural Products*. Boca Raton, FL: CRC Press.
- HERT, J., IRWIN, J. J., LAGGNER, C., KEISER, M. J. & SHOICHET, B. K. 2009. Quantifying biogenic bias in screening libraries. *Nature Chemical Biology*, 5, 479 - 483.
- HIRAYAMA, M. 2006a. Sweating dysfunctions in Parkinson's disease. *Journal of Neurology*, 253, 42-47.
- HIRAYAMA, M. 2006b. Sweating dysfunctions in Parkinson's disease. *J Neurol*, 253 Suppl 7, VII42-47.
- HONIG, H., ANTONINI, A., MARTINEZ-MARTIN, P., FORGACS, I., FAYE, G. C., FOX, T., FOX, K., MANCINI, F., CANESI, M., ODIN, P. & CHAUDHURI, K. R. 2009. Intrajejunal levodopa infusion in Parkinson's disease: a pilot multicenter study of effects on nonmotor symptoms and quality of life. *Mov Disord*, 24, 1468-74.

- HOWAT, W. J. & WILSON, B. A. 2014. Tissue fixation and the effect of molecular fixatives on downstream staining procedures. *Methods*, 70, 12-9.
- HU, Y., LOUNKINE, E. & BAJORATH, J. 2009. Improving the Search Performance of Extended Connectivity Fingerprints through Activity-Oriented Feature Filtering and Application of a Bit-Density-Dependent Similarity Function. *Chemmedchem*, 4, 540-548.
- HUGEL, H. M. & JACKSON, N. 2014. Danshen diversity defeating dementia. *Bioorg Med Chem Lett*, 24, 708-16.
- INTERNATIONAL HAPMAP, C. 2005. A haplotype map of the human genome. *Nature*, 437, 1299-320.
- INUERNICIA, G., CRISTINI, S., MADEDDU, P., BROCK, S., SPILLMANN, F., BERNASCONI, P., CAPPELLETTI, C., CALATOZZOLO, C., FASCIO, U., BISLERI, G., MUNERETTO, C., ALESSANDRI, G. & PARATI, E. A. 2008. Human adult skeletal muscle stem cells differentiate into cardiomyocyte phenotype in vitro. *Experimental Cell Research*, 314, 366-376.
- IRANZO, A., MOLINUEVO, J. L., SANTAMARIA, J., SERRADELL, M., MARTI, M. J., VALLDEORIOLA, F. & TOLOSA, E. 2006. Rapid-eye-movement sleep behaviour disorder as an early marker for a neurodegenerative disorder: a descriptive study. *Lancet Neurol*, 5, 572-7.
- ISCHIROPOULOS, H. & ALMEHDI, A. B. 1995. Peroxynitrite-Mediated Oxidative Protein Modifications. *Febs Letters*, 364, 279-282.
- JAMNADAS-KHODA, J., KOSHY, S., MATHIAS, C. J., MUTHANE, U. B., RAGOTHAMAN, M. & DODABALLAPUR, S. K. 2009. Are current recommendations to diagnose orthostatic hypotension in Parkinson's disease satisfactory? *Mov Disord*, 24, 1747-51.

- JANKOVIC, J. 2008. Parkinson's disease: clinical features and diagnosis. *J Neurol Neurosurg Psychiatry*, 79, 368-76.
- JANKOVIC, J., BEN-ARIE, L., SCHWARTZ, K., CHEN, K., KHAN, M., LAI, E. C., KRAUSS, J. K. & GROSSMAN, R. 1999a. Movement and reaction times and fine coordination tasks following pallidotomy. *Mov Disord*, 14, 57-62.
- JANKOVIC, J., SCHWARTZ, K. S. & ONDO, W. 1999b. Re-emergent tremor of Parkinson's disease. *J Neurol Neurosurg Psychiatry*, 67, 646-50.
- JENNER, P. 2003. The contribution of the MPTP-treated primate model to the development of new treatment strategies for Parkinson's disease. *Parkinsonism Relat Disord*, 9, 131-7.
- JOE, B., VIJAYKUMAR, M. & LOKESH, B. R. 2004. Biological properties of curcumin-cellular and molecular mechanisms of action. *Critical Reviews in Food Science and Nutrition*, 44, 97-111.
- JOHANNESSEN, C. M., CLEMONS, P. A. & WAGNER, B. K. 2015. Integrating phenotypic small-molecule profiling and human genetics: the next phase in drug discovery. *Trends Genet*, 31, 16-23.
- JOHANNESSEN, C. M., JOHNSON, L. A., PICCIONI, F., TOWNES, A., FREDERICK, D. T., DONAHUE, M. K., NARAYAN, R., FLAHERTY, K. T., WARGO, J. A., ROOT, D. E. & GARRAWAY, L. A. 2013. A melanocyte lineage program confers resistance to MAP kinase pathway inhibition. *Nature*, 504, 138-42.
- KABUTO, H., NISHIZAWA, M., TADA, M., HIGASHIO, C., SHISHIBORI, T. & KOHNO, M. 2005. Zingerone [4-(4-hydroxy-3-methoxyphenyl)-2-butanone] prevents 6-hydroxydopamine-induced dopamine depression in mouse striatum and increases superoxide scavenging activity in serum. *Neurochem Res*, 30, 325-32.

- KAPOOR, L. D. 1990. *CRC Handbook of Ayurvedic Medicinal Plants*, Boca Raton, FL, CRC Press.
- KASTEN, M., KERTELGE, L., BRAGGEMANN, N., VAN DER VEGT, J., SCHMIDT, A., TADIC, V., BUHMANN, C., STEINLECHNER, S., BEHRENS, M. I., RAMIREZ, A., BINKOFSKI, F., SIEBNER, H., RASPE, H., HAGENAH, J., LENCER, R. & KLEIN, C. 2010. Nonmotor Symptoms in Genetic Parkinson Disease. *Archives of Neurology*, 67, 670-676.
- KASTEN, M., KERTELGE, L., BRUGGEMANN, N., HAGENAH, J., SCHMIDT, A., TADIC, V., STEINLECHNER, S., BEHRENS, M. I., RAMIREZ, A., RASPE, H., LENCER, R. & KLEIN, C. 2009. Non-Motor Symptoms in Genetic Forms of Parkinson Disease. *Neurology*, 72, A390-A390.
- KATZENSCHLAGER, R. & LEES, A. J. 2002. Treatment of Parkinson's disease: levodopa as the first choice. *J Neurol*, 249 Suppl 2, II19-24.
- KATZENSCHLAGER, R., ZIJLMANS, J., EVANS, A., WATT, H. & LEES, A. J. 2004. Olfactory function distinguishes vascular parkinsonism from Parkinson's disease. *J Neurol Neurosurg Psychiatry*, 75, 1749-52.
- KEMPSTER, P. A., O'SULLIVAN, S. S., HOLTON, J. L., REVESZ, T. & LEES, A. J. 2010. Relationships between age and late progression of Parkinson's disease: a clinico-pathological study. *Brain*, 133, 1755-62.
- KIM, J., KIM, H. & PARK, S. B. 2014. Privileged structures: efficient chemical "navigators" toward unexplored biologically relevant chemical spaces. *J Am Chem Soc*, 136, 14629-38.
- KIM, S. J., SON, T. G., PARK, H. R., PARK, M., KIM, M. S., KIM, H. S., CHUNG, H. Y., MATTSON, M. P. & LEE, J. 2008. Curcumin stimulates proliferation of embryonic neural progenitor cells and neurogenesis in the adult hippocampus. *J Biol Chem*, 283, 14497-505.



- KLEINER-FISMAN, G., HERZOG, J., FISMAN, D. N., TAMMA, F., LYONS, K. E., PAHWA, R., LANG, A. E. & DEUSCHL, G. 2006. Subthalamic nucleus deep brain stimulation: summary and meta-analysis of outcomes. *Mov Disord*, 21 Suppl 14, S290-304.
- KOLLAR, P., RAJCHARD, J., BALOUNOVA, Z. & PAZOUREK, J. 2014. Marine natural products: bryostatins in preclinical and clinical studies. *Pharm Biol*, 52, 237-42.
- KOLLER, W. C. 1986. Pharmacologic treatment of parkinsonian tremor. *Arch Neurol*, 43, 126-7.
- KOOPERBERG, C., FAZZIO, T. G., DELROW, J. J. & TSUKIYAMA, T. 2002. Improved background correction for spotted DNA microarrays. *J Comput Biol*, 9, 55-66.
- KORDOWER, J. H., EMBORG, M. E., BLOCH, J., MA, S. Y., CHU, Y., LEVENTHAL, L., MCBRIDE, J., CHEN, E. Y., PALFI, S., ROITBERG, B. Z., BROWN, W. D., HOLDEN, J. E., PYZALSKI, R., TAYLOR, M. D., CARVEY, P., LING, Z., TRONO, D., HANTRAYE, P., DEGLON, N. & AEBISCHER, P. 2000. Neurodegeneration prevented by lentiviral vector delivery of GDNF in primate models of Parkinson's disease. *Science*, 290, 767-73.
- KRACK, P., BATIR, A., VAN BLERCOM, N., CHABARDES, S., FRAIX, V., ARDOUIN, C., KOUDSIE, A., LIMOUSIN, P. D., BENAZZOUZ, A., LEBAS, J. F., BENABID, A. L. & POLLAK, P. 2003. Five-year follow-up of bilateral stimulation of the subthalamic nucleus in advanced Parkinson's disease. *N Engl J Med*, 349, 1925-34.
- KRASAVIN, M. 2012. Novel diversely substituted 1-heteroaryl-2-imidazolines for fragment-based drug discovery. *Tetrahedron Letters*, 53, 2876-2880.

- KRASAVIN, M. 2013. Pd-Catalyzed N-arylation of 2-imidazolines Provides Convenient Access to Selective Cyclooxygenase-2 Inhibitors. *Letters in Organic Chemistry*, 10, 235-239.
- KRIER, M., BRET, G. & ROGNAN, D. 2006. Assessing the scaffold diversity of screening libraries. *J Chem Inf Model*, 46, 512-24.
- KUBISTA, M., AKERMAN, B. & NORDEN, B. 1987. Characterization of Interaction between DNA and 4',6-Diamidino-2-Phenylindole by Optical Spectroscopy. *Biochemistry*, 26, 4545-4553.
- KULARATNE, S. A. & SENANAYAKE, N. 2014. Venomous snake bites, scorpions, and spiders. *Handb Clin Neurol*, 120, 987-1001.
- KUTER, K., NOWAK, P., GOLEMBIOWSKA, K. & OSSOWSKA, K. 2010. Increased reactive oxygen species production in the brain after repeated low-dose pesticide paraquat exposure in rats. A comparison with peripheral tissues. *Neurochem Res*, 35, 1121-30.
- LANGSTON, J. W., BALLARD, P., TETRUD, J. W. & IRWIN, I. 1983. Chronic Parkinsonism in Humans Due to a Product of Meperidine-Analog Synthesis. *Science*, 219, 979-980.
- LANGSTON, J. W., LANGSTON, E. B. & IRWIN, I. 1984. MPTP-induced parkinsonism in human and non-human primates--clinical and experimental aspects. *Acta Neurol Scand Suppl*, 100, 49-54.
- LAO, C. D., RUFFIN, M. T. T., NORMOLLE, D., HEATH, D. D., MURRAY, S. I., BAILEY, J. M., BOGGS, M. E., CROWELL, J., ROCK, C. L. & BRENNER, D. E. 2006. Dose escalation of a curcuminoid formulation. *BMC Complement Altern Med*, 6, 10.
- LAW, D. C., CHAWLA, A., MERITHEW, E., DUMAS, J., CARRINGTON, W., FOGARTY, K., LIFSHITZ, L., TUFT, R., LAMBRIGHT, D. & CORVERA, S.

2002. Sequential roles for phosphatidylinositol 3-phosphate and Rab5 in tethering and fusion of early endosomes via their interaction with EEA1. *Journal of Biological Chemistry*, 277, 8611-8617.
- LEES, A. J., HARDY, J. & REVESZ, T. 2009. Parkinson's disease. *Lancet*, 373, 2055-66.
- LEESON, P. D., DAVIS, A. M. & STEELE, J. 2004. Drug-like properties: guiding principles for design - or chemical prejudice? *Drug Discov Today Technol*, 1, 189-95.
- LEWELL, X. Q., JUDD, D. B., WATSON, S. P. & HANN, M. M. 1998. RECAP - Retrosynthetic combinatorial analysis procedure: A powerful new technique for identifying privileged molecular fragments with useful applications in combinatorial chemistry. *Journal of Chemical Information and Computer Sciences*, 38, 511-522.
- LEWITT, P. A., REZAI, A. R., LEEHEY, M. A., OJEMANN, S. G., FLAHERTY, A. W., ESKANDAR, E. N., KOSTYK, S. K., THOMAS, K., SARKAR, A., SIDDIQUI, M. S., TATTER, S. B., SCHWALB, J. M., POSTON, K. L., HENDERSON, J. M., KURLAN, R. M., RICHARD, I. H., VAN METER, L., SAPAN, C. V., DURING, M. J., KAPLITT, M. G. & FEIGIN, A. 2011. AAV2-GAD gene therapy for advanced Parkinson's disease: a double-blind, sham-surgery controlled, randomised trial. *Lancet Neurol*, 10, 309-19.
- LIM, S. Y., FOX, S. H. & LANG, A. E. 2009. Overview of the extranigral aspects of Parkinson disease. *Arch Neurol*, 66, 167-72.
- LINDVALL, O. & BJORKLUND, A. 2011. Cell therapeutics in Parkinson's disease. *Neurotherapeutics*, 8, 539-48.
- LORANG, J. & KING, R. W. 2005. Cytological profiling: providing more haystacks for chemists' needles. *Genome Biol*, 6, 228.

- LOW, P. A. 2008. Prevalence of orthostatic hypotension. *Clin Auton Res*, 18 Suppl 1, 8-13.
- LYONS, K. E. & PAHWA, R. 2011. The impact and management of nonmotor symptoms of Parkinson's disease. *Am J Manag Care*, 17 Suppl 12, S308-14.
- MACARRON, R., BANKS, M. N., BOJANIC, D., BURNS, D. J., CIROVIC, D. A., GARYANTES, T., GREEN, D. V., HERTZBERG, R. P., JANZEN, W. P., PASLAY, J. W., SCHOPFER, U. & SITTAMPALAM, G. S. 2011. Impact of high-throughput screening in biomedical research. *Nat Rev Drug Discov*, 10, 188-95.
- MACKAY-SIM, A. 2010. Stem cells and their niche in the adult olfactory mucosa. *Archives Italiennes De Biologie*, 148, 47-58.
- MACKAY-SIM, A. & SILBURN, P. 2008. Stem cells and genetic disease. *Cell Prolif*, 41 Suppl 1, 85-93.
- MALO, N., HANLEY, J. A., CERQUOZZI, S., PELLETIER, J. & NADON, R. 2006. Statistical practice in high-throughput screening data analysis. *Nature Biotechnology*, 24, 167-175.
- MANNING-BOG, A. B., MCCORMACK, A. L., LI, J., UVERSKY, V. N., FINK, A. L. & DI MONTE, D. A. 2002. The herbicide paraquat causes up-regulation and aggregation of alpha-synuclein in mice: paraquat and alpha-synuclein. *J Biol Chem*, 277, 1641-4.
- MARK A. DECOSTER, SOWGANDHI MADDI & MCNAMARA, V. D. A. J. 2010. Microscopy and image analysis of individual and group cell shape changes during apoptosis. *Microscopy: Science, Technology, Applications and Education*.
- MARKOVITS, J., LARSEN, A. K., SEGAL-BENDIRDJIAN, E., FOSSE, P., SAUCIER, J. M., GAZIT, A., LEVITZKI, A., UMEZAWA, K. &

- JACQUEMIN-SABLON, A. 1994. Inhibition of DNA topoisomerases I and II and induction of apoptosis by erbstatin and tyrphostin derivatives. *Biochem Pharmacol*, 48, 549-60.
- MARKS, W. J., JR., BARTUS, R. T., SIFFERT, J., DAVIS, C. S., LOZANO, A., BOULIS, N., VITEK, J., STACY, M., TURNER, D., VERHAGEN, L., BAKAY, R., WATTS, R., GUTHRIE, B., JANKOVIC, J., SIMPSON, R., TAGLIATI, M., ALTERMAN, R., STERN, M., BALTUCH, G., STARR, P. A., LARSON, P. S., OSTREM, J. L., NUTT, J., KIEBURTZ, K., KORDOWER, J. H. & OLANOW, C. W. 2010. Gene delivery of AAV2-neurturin for Parkinson's disease: a double-blind, randomised, controlled trial. *Lancet Neurol*, 9, 1164-72.
- MARTIN, E. J., BLANEY, J. M., SIANI, M. A., SPELLMEYER, D. C., WONG, A. K. & MOOS, W. H. 1995. Measuring diversity: experimental design of combinatorial libraries for drug discovery. *J Med Chem*, 38, 1431-6.
- MARTON, M. J., DERISI, J. L., BENNETT, H. A., IYER, V. R., MEYER, M. R., ROBERTS, C. J., STOUGHTON, R., BURCHARD, J., SLADE, D., DAI, H. Y., BASSETT, D. E., HARTWELL, L. H., BROWN, P. O. & FRIEND, S. H. 1998. Drug target validation and identification of secondary drug target effects using DNA microarrays. *Nature Medicine*, 4, 1293-1301.
- MASON, J. S., MORIZE, I., MENARD, P. R., CHENEY, D. L., HULME, C. & LABAUDINIERE, R. F. 1999. New 4-point pharmacophore method for molecular similarity and diversity applications: overview of the method and applications, including a novel approach to the design of combinatorial libraries containing privileged substructures. *J Med Chem*, 42, 3251-64.
- MASSANO, J. & BHATIA, K. P. 2012. Clinical approach to Parkinson's disease: features, diagnosis, and principles of management. *Cold Spring Harb Perspect Med*, 2, a008870.

- MASTER, Z., MCLEOD, M. & MENDEZ, I. 2007. Benefits, risks and ethical considerations in translation of stem cell research to clinical applications in Parkinson's disease. *J Med Ethics*, 33, 169-73.
- MATIGIAN, N., ABRAHAMSEN, G., SUTHARSAN, R., COOK, A. L., VITALE, A. M., NOUWENS, A., BELLETTE, B., AN, J., ANDERSON, M., BECKHOUSE, A. G., BENNEBROEK, M., CECIL, R., CHALK, A. M., COCHRANE, J., FAN, Y., FERON, F., MCCURDY, R., MCGRATH, J. J., MURRELL, W., PERRY, C., RAJU, J., RAVISHANKAR, S., SILBURN, P. A., SUTHERLAND, G. T., MAHLER, S., MELLICK, G. D., WOOD, S. A., SUE, C. M., WELLS, C. A. & MACKAY-SIM, A. 2010a. Disease-specific, neurosphere-derived cells as models for brain disorders. *Disease models & mechanisms*, 3, 785-98.
- MATIGIAN, N., ABRAHAMSEN, G., SUTHARSAN, R., COOK, A. L., VITALE, A. M., NOUWENS, A., BELLETTE, B., AN, J. Y., ANDERSON, M., BECKHOUSE, A. G., BENNEBROEK, M., CECIL, R., CHALK, A. M., COCHRANE, J., FAN, Y. J., FERON, F., MCCURDY, R., MCGRATH, J. J., MURRELL, W., PERRY, C., RAJU, J., RAVISHANKAR, S., SILBURN, P. A., SUTHERLAND, G. T., MAHLER, S., MELLICK, G. D., WOOD, S. A., SUE, C. M., WELLS, C. A. & MACKAY-SIM, A. 2010b. Disease-specific, neurosphere-derived cells as models for brain disorders. *Disease Models & Mechanisms*, 3, 785-798.
- MAZUMDER, K., TANAKA, K. & FUKASE, K. 2013. Cytotoxic activity of ursolic acid derivatives obtained by isolation and oxidative derivatization. *Molecules*, 18, 8929-44.
- MCGREGOR, J. J. & WILLETT, P. 1981. Use of a Maximal Common Subgraph Algorithm in the Automatic Identification of the Ostensible Bond Changes

- Occurring in Chemical Reactions *Journal of Chemical Information and Computer Sciences*, 21, 137-140.
- MERIMS, D., BALAS, M., PERETZ, C., SHABTAI, H. & GILADI, N. 2006. Rater-blinded, prospective comparison: quetiapine versus clozapine for Parkinson's disease psychosis. *Clin Neuropharmacol*, 29, 331-7.
- MIDORIKAWA, K., MURATA, M., OIKAWA, S., HIRAKU, Y. & KAWANISHI, S. 2001. Protective effect of phytic acid on oxidative DNA damage with reference to cancer chemoprevention. *Biochem Biophys Res Commun*, 288, 552-7.
- MITCHISON, T. J. 2005. Small-molecule screening and profiling by using automated microscopy. *Chembiochem*, 6, 33-9.
- MIYASAKI, J. M., AL HASSAN, K., LANG, A. E. & VOON, V. 2007. Punding prevalence in Parkinson's disease. *Mov Disord*, 22, 1179-81.
- MIZUSHIMA, N., YOSHIMORI, T. & LEVINE, B. 2010. Methods in mammalian autophagy research. *Cell*, 140, 313-26.
- MOGHAL, S., RAJPUT, A. H., D'ARCY, C. & RAJPUT, R. 1994. Prevalence of movement disorders in elderly community residents. *Neuroepidemiology*, 13, 175-8.
- MOODY, S. E., SCHINZEL, A. C., SINGH, S., IZZO, F., STRICKLAND, M. R., LUO, L., THOMAS, S. R., BOEHM, J. S., KIM, S. Y., WANG, Z. C. & HAHN, W. C. 2014. PRKACA mediates resistance to HER2-targeted therapy in breast cancer cells and restores anti-apoptotic signaling. *Oncogene*, 0.
- MORELLI, M., CARTA, A. R., KACHROO, A. & SCHWARZSCHILD, M. A. 2010. Pathophysiological roles for purines: adenosine, caffeine and urate. *Prog Brain Res*, 183, 183-208.
- MORO, E., LOZANO, A. M., POLLAK, P., AGID, Y., REHNCRONA, S., VOLKMANN, J., KULISEVSKY, J., OBESO, J. A., ALBANESE, A., HARIZ,

- M. I., QUINN, N. P., SPEELMAN, J. D., BENABID, A. L., FRAIX, V., MENDES, A., WELTER, M. L., HOUETO, J. L., CORNU, P., DORMONT, D., TORNQVIST, A. L., EKBERG, R., SCHNITZLER, A., TIMMERMAN, L., WOJTECKI, L., GIRONELL, A., RODRIGUEZ-OROZ, M. C., GURIDI, J., BENTIVOGLIO, A. R., CONTARINO, M. F., ROMITO, L., SCERRATI, M., JANSSENS, M. & LANG, A. E. 2010. Long-term results of a multicenter study on subthalamic and pallidal stimulation in Parkinson's disease. *Mov Disord*, 25, 578-86.
- MUNRO, M. H., BLUNT, J. W., DUMDEI, E. J., HICKFORD, S. J., LILL, R. E., LI, S., BATTERSHILL, C. N. & DUCKWORTH, A. R. 1999. The discovery and development of marine compounds with pharmaceutical potential. *J Biotechnol*, 70, 15-25.
- MYTHRI, R. B. & BHARATH, M. M. 2012. Curcumin: a potential neuroprotective agent in Parkinson's disease. *Curr Pharm Des*, 18, 91-9.
- MYTHRI, R. B., HARISH, G. & BHARATH, M. M. 2012. Therapeutic potential of natural products in Parkinson's disease. *Recent Pat Endocr Metab Immune Drug Discov*, 6, 181-200.
- MYTHRI, R. B., HARISH, G., DUBEY, S. K., MISRA, K. & BHARATH, M. M. 2011. Glutamoyl diester of the dietary polyphenol curcumin offers improved protection against peroxynitrite-mediated nitrosative stress and damage of brain mitochondria in vitro: implications for Parkinson's disease. *Mol Cell Biochem*, 347, 135-43.
- NEWMAN, D. J. 2005. The bryostatins. In: CRAGG G.M., KINGSTON D.G.I. & NEWMAN D.J. (eds.) *Anticancer Agents from Natural Products*. Boca Raton, FL: Taylor and Francis.



- NEWMAN, D. J. 2008. Natural products as leads to potential drugs: An old process or the new hope for drug discovery? *Journal of Medicinal Chemistry*, 51, 2589-2599.
- NEWMAN, D. J. 2012. The bryostatins. *In*: CRAGG G.M., KINGSTON D.G.I. & NEWMAN D.J. (eds.) *Anticancer agents from natural products*. 2 ed. Boca Raton, FL: Taylor and Francis.
- NEWMAN, D. J. & CRAGG, G. M. 2007. Natural products as sources of new drugs over the last 25 years. *Journal of Natural Products*, 70, 461-477.
- NEWMAN, D. J., CRAGG, G. M. & SNADER, K. M. 2000. The influence of natural products upon drug discovery (Antiquity to late 1999). *Natural Product Reports*, 17, 215-234.
- NICHOLLS, D. G. & FERGUSON, S. J. 2014. The Chemiosmotic Proton Circuit. *In*: NICHOLLS, D. G. & FERGUSON, S. J. (eds.) *Bioenergetics 2*. Academic Press.
- NISWENDER, C. M. & CONN, P. J. 2010. Metabotropic glutamate receptors: physiology, pharmacology, and disease. *Annu Rev Pharmacol Toxicol*, 50, 295-322.
- ODIN, P., WOLTERS, E. & ANTONINI, A. 2008. Continuous dopaminergic stimulation achieved by duodenal levodopa infusion. *Neurol Sci*, 29 Suppl 5, S387-8.
- OLANOW, C. W., HAUSER, R. A., JANKOVIC, J., LANGSTON, W., LANG, A., POEWE, W., TOLOSA, E., STOCCHI, F., MELAMED, E., EYAL, E. & RASCOL, O. 2008. A Randomized, Double-Blind, Placebo-Controlled, Delayed Start Study to Assess Rasagiline as a Disease Modifying Therapy in Parkinson's Disease (The ADAGIO Study): Rationale, Design, and Baseline Characteristics. *Movement Disorders*, 23, 2194-2201.

- OOI, W. L., HOSSAIN, M. & LIPSITZ, L. A. 2000. The association between orthostatic hypotension and recurrent falls in nursing home residents. *American Journal of Medicine*, 108, 106-111.
- PALHAGEN, S., HEINONEN, E., HAGGLUND, J., KAUGESAAR, T., MAKI-IKOLA, O., PALM, R. & SWEDISH PARKINSON STUDY, G. 2006. Selegiline slows the progression of the symptoms of Parkinson disease. *Neurology*, 66, 1200-6.
- PALMITER, R. D. 2007. Is dopamine a physiologically relevant mediator of feeding behavior? *Trends Neurosci*, 30, 375-81.
- PAN-MONTOJO, F., ANICHTCHIK, O., DENING, Y., KNELS, L., PURSCHE, S., JUNG, R., JACKSON, S., GILLE, G., SPILLANTINI, M. G., REICHMANN, H. & FUNK, R. H. W. 2010. Progression of Parkinson's Disease Pathology Is Reproduced by Intragastric Administration of Rotenone in Mice. *Plos One*, 5.
- PANDEY, N., STRIDER, J., NOLAN, W. C., YAN, S. X. & GALVIN, J. E. 2008. Curcumin inhibits aggregation of alpha-synuclein. *Acta Neuropathol*, 115, 479-89.
- PAPAPETROPOULOS, S., PASCHALIS, C., ATHANASSIADOU, A., PAPADIMITRIOU, A., ELLUL, J., POLYMEROPOULOS, M. H. & PAPAPETROPOULOS, T. 2001. Clinical phenotype in patients with alpha-synuclein Parkinson's disease living in Greece in comparison with patients with sporadic Parkinson's disease. *J Neurol Neurosurg Psychiatry*, 70, 662-5.
- PARK, A. & STACY, M. 2009. Non-motor symptoms in Parkinson's disease. *J Neurol*, 256 Suppl 3, 293-8.
- PARK, M., BAE, J. & LEE, D. S. 2008. Antibacterial activity of [10]-gingerol and [12]-gingerol isolated from ginger rhizome against periodontal bacteria. *Phytother Res*, 22, 1446-9.

- PEDDI, P. F. & HURVITZ, S. A. 2014. Ado-trastuzumab emtansine (T-DM1) in human epidermal growth factor receptor 2 (HER2)-positive metastatic breast cancer: latest evidence and clinical potential. *Ther Adv Med Oncol*, 6, 202-9.
- PEREZ-LLORET, S. & RASCOL, O. 2010. Dopamine receptor agonists for the treatment of early or advanced Parkinson's disease. *CNS Drugs*, 24, 941-68.
- PERLMAN, Z. E., SLACK, M. D., FENG, Y., MITCHISON, T. J., WU, L. F. & ALTSCHULER, S. J. 2004. Multidimensional drug profiling by automated microscopy. *Science*, 306, 1194-8.
- POEWE, W. 2008. Non-motor symptoms in Parkinson's disease. *Eur J Neurol*, 15 Suppl 1, 14-20.
- POLLAK, L., PROHOROV, T., KUSHNIR, M. & RABEY, M. 2009. Vestibulocervical reflexes in idiopathic Parkinson disease. *Neurophysiol Clin*, 39, 235-40.
- POSTUMA, R. B., GAGNON, J. F., VENDETTE, M., FANTINI, M. L., MASSICOTTE-MARQUEZ, J. & MONTPLAISIR, J. 2009. Quantifying the risk of neurodegenerative disease in idiopathic REM sleep behavior disorder. *Neurology*, 72, 1296-300.
- POTTERAT, O. & HAMBURGER, M. 2008. Progress in Drug Research. In: PETERSEN, F. & AMSTUTZ, R. (eds.) *Natural Compounds as Drugs, Volume I*. Basel (Switzerland): Birkhäuser Verlag AG.
- PRESLEY, A. D., FULLER, K. M. & ARRIAGA, E. A. 2003. MitoTracker Green labeling of mitochondrial proteins and their subsequent analysis by capillary electrophoresis with laser-induced fluorescence detection. *Journal of Chromatography B-Analytical Technologies in the Biomedical and Life Sciences*, 793, 141-150.

- PRUDHOMME, M. 2005. Staurosporines and structurally related indolocarbazoles as antitumor agents. *In*: CRAGG G.M., KINGSTON D.G.I. & NEWMAN D.J. (eds.) *Anticancer agents from natural products*. Boca Raton: Taylor and Francis.
- PRZEDBORSKI, S., JACKSON-LEWIS, V., DJALDETTI, R., LIBERATORE, G., VILA, M., VUKOSAVIC, S. & ALMER, G. 2000. The parkinsonian toxin MPTP: action and mechanism. *Restor Neurol Neurosci*, 16, 135-142.
- PRZEDBORSKI, S. & VILA, M. 2003. The 1-methyl-4-phenyl-1,2,3,6-tetrahydropyridine mouse model: a tool to explore the pathogenesis of Parkinson's disease. *Ann N Y Acad Sci*, 991, 189-98.
- PURVES, D., AUGUSTINE, G. J., FITZPATRICK, D., KATZ, L. C., LAMANTIA, A.-S., MCNAMARA, J. O. & WILLIAMS, S. M. 2001. The Olfactory Epithelium and Olfactory Receptor Neurons. *Neuroscience*. 2nd ed. Sunderland (MA): Sinauer Associates.
- RADI, R., CASSINA, A., HODARA, R., QUIJANO, C. & CASTRO, L. 2002. Peroxynitrite reactions and formation in mitochondria. *Free Radic Biol Med*, 33, 1451-64.
- RAMANA, K. V., SINGHAL, S. S. & REDDY, A. B. 2014. Therapeutic potential of natural pharmacological agents in the treatment of human diseases. *Biomed Res Int*, 2014, 573452.
- RAUDINO, F. 2001. Non motor off in Parkinson's disease. *Acta Neurol Scand*, 104, 312-5.
- RICHARD, I. H. & KURLAN, R. 1997. A survey of antidepressant drug use in Parkinson's disease. Parkinson Study Group. *Neurology*, 49, 1168-70.
- RICHARDSON, J. R., QUAN, Y., SHERER, T. B., GREENAMYRE, J. T. & MILLER, G. W. 2005. Paraquat neurotoxicity is distinct from that of MPTP and rotenone. *Toxicological Sciences*, 88, 193-201.

- RILEY, D. E. & CHELIMSKY, T. C. 2003. Autonomic nervous system testing may not distinguish multiple system atrophy from Parkinson's disease. *J Neurol Neurosurg Psychiatry*, 74, 56-60.
- RIMBACH, G. & PALLAUF, J. 1998. Phytic acid inhibits free radical formation in vitro but does not affect liver oxidant or antioxidant status in growing rats. *J Nutr*, 128, 1950-5.
- RODRIGUEZ-OROZ, M. C., JAHANSHAHI, M., KRACK, P., LITVAN, I., MACIAS, R., BEZARD, E. & OBESO, J. A. 2009. Initial clinical manifestations of Parkinson's disease: features and pathophysiological mechanisms. *Lancet Neurol*, 8, 1128-39.
- RODRIGUEZ-OROZ, M. C., MORO, E. & KRACK, P. 2012. Long-term outcomes of surgical therapies for Parkinson's disease. *Mov Disord*, 27, 1718-28.
- ROGERS, D. & HAHN, M. 2010. Extended-Connectivity Fingerprints. *Journal of Chemical Information and Modeling*, 50, 742-754.
- ROSNER, B., GLYNN, R. J. & LEE, M. L. 2006. The Wilcoxon signed rank test for paired comparisons of clustered data. *Biometrics*, 62, 185-92.
- RYDZEWSKI, R. M. 2008. *Real world drug discovery : a chemist's guide to biotech and pharmaceutical research*, Amsterdam, Elsevier.
- SAGE, J. I. & MARK, M. H. 1995. Drenching Sweats as an Off Phenomenon in Parkinsons-Disease - Treatment and Relation to Plasma Levodopa Profile. *Annals of Neurology*, 37, 120-122.
- SAMUELSSON, G. 2004. *Drugs of Natural Origin: a Textbook of Pharmacognosy* Swedish Pharmaceutical Press: Stockholm, Sweden.
- SCHARPF, R. B., IACOBUZIO-DONAHUE, C. A., SNEDDON, J. B. & PARMIGIANI, G. 2007. When should one subtract background fluorescence in 2-color microarrays? *Biostatistics*, 8, 695-707.

- SCHENONE, M., DANCIK, V., WAGNER, B. K. & CLEMONS, P. A. 2013. Target identification and mechanism of action in chemical biology and drug discovery. *Nat Chem Biol*, 9, 232-40.
- SCHESTATSKY, P., KUMRU, H., VALLS-SOLE, J., VALLDEORIOLA, F., MARTI, M. J., TOLOSA, E. & CHAVES, M. L. 2007. Neurophysiologic study of central pain in patients with Parkinson disease. *Neurology*, 69, 2162-9.
- SCHLAFLI, A. M., ADAMS, O., GALVAN, J. A., GUGGER, M., SAVIC, S., BUBENDORF, L., SCHMID, R. A., BECKER, K. F., TSCHAN, M. P., LANGER, R. & BEREZOWSKA, S. 2016. Prognostic value of the autophagy markers LC3 and p62/SQSTM1 in early-stage non-small cell lung cancer. *Oncotarget*, 7, 39544-39555.
- SCHNEIDER, S. A. & OBESO, J. A. 2014. Clinical and Pathological Features of Parkinson's Disease. *Curr Top Behav Neurosci*.
- SCHULZE, C. J., BRAY, W. M., WOERHMANN, M. H., STUART, J., LOKEY, R. S. & LININGTON, R. G. 2013. "Function-first" lead discovery: mode of action profiling of natural product libraries using image-based screening. *Chem Biol*, 20, 285-95.
- SCHUTZENMEISTER, A. & PIEPHO, H. P. 2010. Background correction of two-colour cDNA microarray data using spatial smoothing methods. *Theoretical and Applied Genetics*, 120, 475-490.
- SENARD, J. M. & PATHAK, A. 2010. Neurogenic orthostatic hypotension of Parkinson's disease: what exploration for what treatment? *Rev Neurol (Paris)*, 166, 779-84.
- SHARMA, S., KULKARNI, S. K., AGREWALA, J. N. & CHOPRA, K. 2006. Curcumin attenuates thermal hyperalgesia in a diabetic mouse model of neuropathic pain. *European Journal of Pharmacology*, 536, 256-261.

- SHERER, T. B., RICHARDSON, J. R., TESTA, C. M., SEO, B. B., PANOV, A. V., YAGI, T., MATSUNO-YAGI, A., MILLER, G. W. & GREENAMYRE, J. T. 2007. Mechanism of toxicity of pesticides acting at complex I: relevance to environmental etiologies of Parkinson's disease. *J Neurochem*, 100, 1469-79.
- SHEU, Y. J., BARRAL, Y. & SNYDER, M. 2000. Polarized growth controls cell shape and bipolar bud site selection in *Saccharomyces cerevisiae*. *Molecular and Cellular Biology*, 20, 5235-5247.
- SHUN, T. Y., LAZO, J. S., SHARLOW, E. R. & JOHNSTON, P. A. 2011. Identifying actives from HTS data sets: practical approaches for the selection of an appropriate HTS data-processing method and quality control review. *J Biomol Screen*, 16, 1-14.
- SINGER, T. P., SALACH, J. I., CASTAGNOLI, N. & TREVOR, A. 1986. Interactions of the Neurotoxic Amine 1-Methyl-4-Phenyl-1,2,3,6-Tetrahydropyridine with Monoamine Oxidases. *Biochemical Journal*, 235, 785-789.
- SINGH, S. B. & BARRETT, J. F. 2006. Empirical antibacterial drug discovery--foundation in natural products. *Biochem Pharmacol*, 71, 1006-15.
- SMITH, Y., WICHMANN, T., FACTOR, S. A. & DELONG, M. R. 2012. Parkinson's disease therapeutics: new developments and challenges since the introduction of levodopa. *Neuropsychopharmacology*, 37, 213-46.
- SNEADER, W. 2005. Drug Discovery. In: SNEADER, W. (ed.) *Drug Discovery. A history*. England: A John Wiley & Sons Ltd.
- SOS, M. L., MICHEL, K., ZANDER, T., WEISS, J., FROMMOLT, P., PEIFER, M., LI, D., ULLRICH, R., KOKER, M., FISCHER, F., SHIMAMURA, T., RAUH, D., MERMEL, C., FISCHER, S., STUCKRATH, I., HEYNCK, S., BEROUKHIM, R., LIN, W., WINCKLER, W., SHAH, K., LAFRAMBOISE, T., MORIARTY, W. F., HANNA, M., TOLOSI, L., RAHNENFUHRER, J.,

- VERHAAK, R., CHIANG, D., GETZ, G., HELLMICH, M., WOLF, J., GIRARD, L., PEYTON, M., WEIR, B. A., CHEN, T. H., GREULICH, H., BARRETINA, J., SHAPIRO, G. I., GARRAWAY, L. A., GAZDAR, A. F., MINNA, J. D., MEYERSON, M., WONG, K. K. & THOMAS, R. K. 2009. Predicting drug susceptibility of non-small cell lung cancers based on genetic lesions. *J Clin Invest*, 119, 1727-40.
- SPELLBERG, B. 2013. New antibiotic development: Barriers and opportunities in 2012. *Alliance Prudent Use Antibiotics Newsl* 30.
- SRINIVASAN, V., CARDINALI, D. P., SRINIVASAN, U. S., KAUR, C., BROWN, G. M., SPENCE, D. W., HARDELAND, R. & PANDI-PERUMAL, S. R. 2011. Therapeutic potential of melatonin and its analogs in Parkinson's disease: focus on sleep and neuroprotection. *Ther Adv Neurol Disord*, 4, 297-317.
- STACY, M. 2002. Sleep disorders in Parkinson's disease: epidemiology and management. *Drugs Aging*, 19, 733-9.
- STAUNTON, J. E., SLONIM, D. K., COLLIER, H. A., TAMAYO, P., ANGELO, M. J., PARK, J., SCHERF, U., LEE, J. K., REINHOLD, W. O., WEINSTEIN, J. N., MESIROV, J. P., LANDER, E. S. & GOLUB, T. R. 2001. Chemosensitivity prediction by transcriptional profiling. *Proc Natl Acad Sci U S A*, 98, 10787-92.
- STEINLECHNER, S., STAHLBERG, J., VOLKEL, B., DJARMATI, A., HAGENAH, J., HILLER, A., HEDRICH, K., KONIG, I., KLEIN, C. & LENCER, R. 2007. Co-occurrence of affective and schizophrenia spectrum disorders with PINK1 mutations. *Journal of Neurology Neurosurgery and Psychiatry*, 78, 532-535.
- STRAUSS, I., KALIA, S. K. & LOZANO, A. M. 2014. Where are we with surgical therapies for Parkinson's disease? *Parkinsonism Relat Disord*, 20 Suppl 1, S187-91.



- SUEKAWA, M., ISHIGE, A., YUASA, K., SUDO, K., ABURADA, M. & HOSOYA, E. 1984. Pharmacological studies on ginger. I. Pharmacological actions of pungent constituents, (6)-gingerol and (6)-shogaol. *J Pharmacobiodyn*, 7, 836-48.
- SUFFNESS, M. & PEZZUTO, J. M. 1991. Assays related to cancer drug discovery. In: HOSTETTMANN, K. (ed.) *Methods in Plant Biochemistry*. London: Academic Press.
- SWANSON, R. N., HARDY, D. J., SHIPKOWITZ, N. L., HANSON, C. W., RAMER, N. C., FERNANDES, P. B. & CLEMENT, J. J. 1991. In vitro and in vivo evaluation of tiacumicins B and C against *Clostridium difficile*. *Antimicrob Agents Chemother*, 35, 1108-11.
- SWINN, L., SCHRAG, A., VISWANATHAN, R., BLOEM, B. R., LEES, A. & QUINN, N. 2003. Sweating dysfunction in Parkinson's disease. *Mov Disord*, 18, 1459-63.
- TAHERI, A., QUINN, R. J. & KRASAVIN, M. 2014. Naturally occurring scaffolds for compound library design: convenient access to bis-aryl 1-azaadamantanes carrying a vicinal amino alcohol motif. *Tetrahedron Letters*, 55, 5390-5393.
- TAMAOKI, T., NOMOTO, H., TAKAHASHI, I., KATO, Y., MORIMOTO, M. & TOMITA, F. 1986. Staurosporine, a potent inhibitor of phospholipid/Ca<sup>++</sup>dependent protein kinase. *Biochem Biophys Res Commun*, 135, 397-402.
- TANG, M. K., REN, D. C., ZHANG, J. T. & DU, G. H. 2002. Effect of salvianolic acids from *Radix Salviae miltiorrhizae* on regional cerebral blood flow and platelet aggregation in rats. *Phytomedicine*, 9, 405-9.
- TANNER, C. M., KAMEL, F., ROSS, G. W., HOPPIN, J. A., GOLDMAN, S. M., KORELL, M., MARRAS, C., BHUDHIKANOK, G. S., KASTEN, M.,

- CHADE, A. R., COMYNS, K., RICHARDS, M. B., MENG, C., PRIESTLEY, B., FERNANDEZ, H. H., CAMBI, F., UMBACH, D. M., BLAIR, A., SANDLER, D. P. & LANGSTON, J. W. 2011. Rotenone, paraquat, and Parkinson's disease. *Environ Health Perspect*, 119, 866-72.
- THAVARAJAH, R., MUDIMBAIMANNAR, V. K., ELIZABETH, J., RAO, U. K. & RANGANATHAN, K. 2012. Chemical and physical basics of routine formaldehyde fixation. *J Oral Maxillofac Pathol*, 16, 400-5.
- TIAN, L. L., WANG, X. J., SUN, Y. N., LI, C. R., XING, Y. L., ZHAO, H. B., DUAN, M., ZHOU, Z. & WANG, S. Q. 2008. Salvianolic acid B, an antioxidant from *Salvia miltiorrhiza*, prevents 6-hydroxydopamine induced apoptosis in SH-SY5Y cells. *Int J Biochem Cell Biol*, 40, 409-22.
- UC, E. Y., RIZZO, M., ANDERSON, S. W., QIAN, S., RODNITZKY, R. L. & DAWSON, J. D. 2005. Visual dysfunction in Parkinson disease without dementia. *Neurology*, 65, 1907-13.
- VARMA H, LO DC & BR, S. 2011. High-Throughput and High-Content Screening for Huntington's Disease Therapeutics. In: LO DC & RE, H. (eds.) *Neurobiology of Huntington's Disease: Applications to Drug Discovery*. Boca Raton (FL): CRC Press/Taylor & Francis.
- VIAL, M. L., ZENCAK, D., GRKOVIC, T., GORSE, A. D., MACKAY-SIM, A., MELLICK, G. D., WOOD, S. A. & QUINN, R. J. 2016. A Grand Challenge. 2. Phenotypic Profiling of a Natural Product Library on Parkinson's Patient-Derived Cells. *J Nat Prod*.
- VLAAR, A., HOVESTADT, A., VAN LAAR, T. & BLOEM, B. R. 2011. The treatment of early Parkinson's disease: levodopa rehabilitated. *Pract Neurol*, 11, 145-52.

- WAGNER, B. K., KITAMI, T., GILBERT, T. J., PECK, D., RAMANATHAN, A., SCHREIBER, S. L., GOLUB, T. R. & MOOTHA, V. K. 2008. Large-scale chemical dissection of mitochondrial function. *Nat Biotechnol*, 26, 343-51.
- WALLACE, M. S. 2006. Ziconotide: a new nonopioid intrathecal analgesic for the treatment of chronic pain. *Expert Rev Neurother*, 6, 1423-8.
- WALSH, C. 2003. *Antibiotics: Actions, Origin, Resistance*, Washington,DC, ASM Press.
- WANG, D., FENG, Y., MURTAZA, M., WOOD, S., MELLICK, G., HOOPER, J. N. & QUINN, R. J. 2016. A Grand Challenge: Unbiased Phenotypic Function of Metabolites from *Jaspis splendens* against Parkinson's Disease. *J Nat Prod*, 79, 353-61.
- WANG, M. S., BODDAPATI, S., EMADI, S. & SIERKS, M. R. 2010. Curcumin reduces alpha-synuclein induced cytotoxicity in Parkinson's disease cell model. *BMC Neurosci*, 11, 57.
- WANG, T. T., SATHYAMOORTHY, N. & PHANG, J. M. 1996. Molecular effects of genistein on estrogen receptor mediated pathways. *Carcinogenesis*, 17, 271-5.
- WANG, Z. S., LUO, P., DAI, S. H., LIU, Z. B., ZHENG, X. R. & CHEN, T. 2013. Salvianolic Acid B Induces Apoptosis in Human Glioma U87 Cells Through p38-Mediated ROS Generation. *Cellular and Molecular Neurobiology*, 33, 921-928.
- WEINTRAUB, D., SIDEROWF, A. D., POTENZA, M. N., GOVEAS, J., MORALES, K. H., DUDA, J. E., MOBERG, P. J. & STERN, M. B. 2006. Association of dopamine agonist use with impulse control disorders in Parkinson disease. *Arch Neurol*, 63, 969-73.

- WEISS, S. G., TIN-WA, M., PERDUE, R. E. & FARNSWORTH, N. R. 1975. Potential anticancer agents II: antitumor and cytotoxic lignans from *Linum album* (Linaceae). *J Pharm Sci*, 64, 95-8.
- WELSCH, M. E., SNYDER, S. A. & STOCKWELL, B. R. 2010. Privileged scaffolds for library design and drug discovery. *Curr Opin Chem Biol*, 14, 347-61.
- WESS, G., URMANN, M. & SICKENBERGER, B. 2001. Medicinal Chemistry: Challenges and Opportunities. *Angew Chem Int Ed Engl*, 40, 3341-3350.
- WESTIN, J., NYHOLM, D., PALHAGEN, S., WILLOWS, T., GROTH, T., DOUGHERTY, M. & KARLSSON, M. O. 2011. A pharmacokinetic-pharmacodynamic model for duodenal levodopa infusion. *Clin Neuropharmacol*, 34, 61-5.
- WICHMANN, T. & DELONG, M. R. 2003. Pathophysiology of Parkinson's disease: the MPTP primate model of the human disorder. *Ann N Y Acad Sci*, 991, 199-213.
- WICKREMARATCHI, M. M., MAJOUNIE, E., MORRIS, H. R., WILLIAMS, N. M., LEWIS, H., GILL, S. S., KHAN, S., HEYWOOD, P., HARDY, J., WILES, C. M., SINGLETON, A. B. & QUINN, N. P. 2009. Parkin-related disease clinically diagnosed as a pallido-pyramidal syndrome. *Mov Disord*, 24, 138-40.
- WILLIAMS-GRAY, C. H., FOLTYNIE, T., BRAYNE, C. E., ROBBINS, T. W. & BARKER, R. A. 2007. Evolution of cognitive dysfunction in an incident Parkinson's disease cohort. *Brain*, 130, 1787-98.
- WILLIAMS, S. C. 2014. News feature: Next-generation antibiotics. *Proc Natl Acad Sci U S A*, 111, 11227-9.
- WINGE, K., SKAU, A. M., STIMPEL, H., NIELSEN, K. K. & WERDELIN, L. 2006. Prevalence of bladder dysfunction in Parkinson's disease. *Neurology and Urodynamics*, 25, 116-122.

- WIRDEFELDT, K., ADAMI, H. O., COLE, P., TRICHOPOULOS, D. & MANDEL, J. 2011. Epidemiology and etiology of Parkinson's disease: a review of the evidence. *Eur J Epidemiol*, 26 Suppl 1, S1-58.
- WOEHRMANN, M. H., BRAY, W. M., DURBIN, J. K., NISAM, S. C., MICHAEL, A. K., GLASSEY, E., STUART, J. M. & LOKEY, R. S. 2013. Large-scale cytological profiling for functional analysis of bioactive compounds. *Mol Biosyst*, 9, 2604-17.
- WOOD, L. D. 2010. Clinical review and treatment of select adverse effects of dopamine receptor agonists in Parkinson's disease. *Drugs Aging*, 27, 295-310.
- WOOD, L. D., NEUMILLER, J. J., SETTER, S. M. & DOBBINS, E. K. 2010. Clinical review of treatment options for select nonmotor symptoms of Parkinson's disease. *Am J Geriatr Pharmacother*, 8, 294-315.
- WU, F., XU, H. D., GUAN, J. J., HOU, Y. S., GU, J. H., ZHEN, X. C. & QIN, Z. H. 2015. Rotenone impairs autophagic flux and lysosomal functions in Parkinson's disease. *Neuroscience*, 284, 900-11.
- XIE, C. L., WANG, W. W., ZHANG, S. F., GAN, J. & LIU, Z. G. 2014. Continuous dopaminergic stimulation (CDS)-based treatment in Parkinson's disease patients with motor complications: a systematic review and meta-analysis. *Sci Rep*, 4, 6027.
- XU, Q., KANTHASAMY, A. G. & REDDY, M. B. 2008. Neuroprotective effect of the natural iron chelator, phytic acid in a cell culture model of Parkinson's disease. *Toxicology*, 245, 101-8.
- XU, Q., KANTHASAMY, A. G. & REDDY, M. B. 2011. Phytic Acid Protects against 6-Hydroxydopamine-Induced Dopaminergic Neuron Apoptosis in Normal and Iron Excess Conditions in a Cell Culture Model. *Parkinsons Dis*, 2011, 431068.

- YANG, F. S., LIM, G. P., BEGUM, A. N., UBEDA, O. J., SIMMONS, M. R., AMBEGAOKAR, S. S., CHEN, P. P., KAYED, R., GLABE, C. G., FRAUTSCHY, S. A. & COLE, G. M. 2005. Curcumin inhibits formation of amyloid beta oligomers and fibrils, binds plaques, and reduces amyloid in vivo. *Journal of Biological Chemistry*, 280, 5892-5901.
- YEO, L., SINGH, R., GUNDETI, M., BARUA, J. M. & MASOOD, J. 2012. Urinary tract dysfunction in Parkinson's disease: a review. *Int Urol Nephrol*, 44, 415-24.
- YOULE, R. J. & VAN DER BLIEK, A. M. 2012. Mitochondrial fission, fusion, and stress. *Science*, 337, 1062-5.
- YOUNG, D. W., BENDER, A., HOYT, J., MCWHINNIE, E., CHIRN, G. W., TAO, C. Y., TALLARICO, J. A., LABOW, M., JENKINS, J. L., MITCHISON, T. J. & FENG, Y. 2008. Integrating high-content screening and ligand-target prediction to identify mechanism of action. *Nature Chemical Biology*, 4, 59-68.
- YU, M. J., KISHI, Y., LITTLEFIELD, B.A. 2005. Discovery of E7389, a fully synthetic macrocyclic ketone analog of halichondrin B. *In*: CRAGG, G. M., KINGSTON, D.G.I., AND NEWMAN, D.J. (ed.) *Anticancer Agents from Natural Products*. Boca Raton, FL: CRC Press.
- ZAKRZEWSKA-PNIEWSKA, B. & JAMROZIK, Z. 2003. Are electrophysiological autonomic tests useful in the assessment of dysautonomia in Parkinson's disease? *Parkinsonism Relat Disord*, 9, 179-83.
- ZENG, G., TANG, T., WU, H. J., YOU, W. H., LUO, J. K., LIN, Y., LIANG, Q. H., LI, X. Q., HUANG, X. & YANG, Q. D. 2010. Salvianolic acid B protects SH-SY5Y neuroblastoma cells from 1-methyl-4-phenylpyridinium-induced apoptosis. *Biol Pharm Bull*, 33, 1337-42.
- ZESIEWICZ, T. A., SULLIVAN, K. L., ARNULF, I., CHAUDHURI, K. R., MORGAN, J. C., GRONSETH, G. S., MIYASAKI, J., IVERSON, D. J.,

- WEINER, W. J. & QUALITY STANDARDS SUBCOMMITTEE OF THE AMERICAN ACADEMY OF, N. 2010. Practice Parameter: treatment of nonmotor symptoms of Parkinson disease: report of the Quality Standards Subcommittee of the American Academy of Neurology. *Neurology*, 74, 924-31.
- ZHANG, C. R., LIU, H. B., FENG, T., ZHU, J. Y., GENG, M. Y. & YUE, J. M. 2009a. Alkaloids from the leaves of *Daphniphyllum subverticillatum*. *J Nat Prod*, 72, 1669-72.
- ZHANG, J. H., CHUNG, T. D. Y. & OLDENBURG, K. R. 1999. A simple statistical parameter for use in evaluation and validation of high throughput screening assays. *Journal of Biomolecular Screening*, 4, 67-73.
- ZHANG, Y., DI, Y. T., MU, S. Z., LI, C. S., ZHANG, Q., TAN, C. J., ZHANG, Z., FANG, X. & HAO, X. J. 2009b. Dapholdhamines A-D, alkaloids from *Daphniphyllum oldhami*. *J Nat Prod*, 72, 1325-7.
- ZHANG, Z. X. & ROMAN, G. C. 1993. Worldwide occurrence of Parkinson's disease: an updated review. *Neuroepidemiology*, 12, 195-208.
- ZHAO, Y., GUO, Y. & GU, X. 2011. Salvianolic Acid B, a potential chemopreventive agent, for head and neck squamous cell cancer. *J Oncol*, 2011, 534548.
- ZHOU, J., QU, X. D., LI, Z. Y., WEI, J., LIU, Q., MA, Y. H. & HE, J. J. 2014. Salvianolic acid B attenuates toxin-induced neuronal damage via Nrf2-dependent glial cells-mediated protective activity in Parkinson's disease models. *PLoS One*, 9, e101668.

